Characterisation of human dental pulp stem cells in an animal model of multiple sclerosis

Kerrie Foyle, B.Sc. (Mol bio) (Hons)

Department of Molecular & Cellular Biology

School of Biological Sciences

The University of Adelaide

A thesis submitted to the University of Adelaide in fulfilment of the requirements for the degree of Doctor of Philosophy.

2019

Declaration

I certify that this work contains no material which has been accepted for the award of any other degree or diploma in my name, in any university or other tertiary institution and, to the best of my knowledge and belief, contains no material previously published or written by another person, except where due reference has been made in the text. In addition, I certify that no part of this work will, in the future, be used in a submission in my name, for any other degree or diploma in any university or other tertiary institution without the prior approval of the University of Adelaide and where applicable, any partner institution responsible for the joint-award of this degree.

I give permission for the digital version of my thesis to be made available on the web, via the University's digital research repository, the Library Search and also through web search engines, unless permission has been granted by the University to restrict access for a period of time.

I acknowledge the support I have received for my research through the provision of an Australian Government Research Training Program Scholarship.

Signed,

Kerrie Foyle, B.Sc. (Mol bio) (Hons)
February 2020

Acknowledgements

First, I must thank Iain for taking me on as a PhD student on this project and guiding me on my journey to being scientist for these last few years. You have taught me how to design experiments, I've learned so much and your keen knowledge of immunology has been an invaluable source. Also, thank you for reading through a stack of drafts for this thesis and in such a timely manner. I absolutely could not have put all of this together without the ongoing support and feedback.

I also thank Shaun for having me in the lab, supervising my Honours degree and co-supervising my PhD degree. You have also taught me lots about science and being scientist. Also, it has been a privilege to work as a research associate in the lab which has been a wonderful experience and has also taught me lots.

Next, a thank you to Professor Simon Koblar for co-supervising my PhD and providing me with expertise on DPSCs. Also Dr Karlea Kremer and Maria Gancheva from the Koblar laboratory for providing me with some of the DPSC samples for this study and help with DPSC culture protocols.

To past and present members of the lab, thank you for your smiling faces, the laughs and the banter. It is a privilege to learn in an environment with so many intelligent students and all of you have taught me lots! Special mentions go to Jaz for being there with me through the entire process and being the only other MSC person in the lab. Thank you just for everything! We have shared a great many chats, laughs, tears and big experiment days. Also Maleika, I could not have asked for a better person to work alongside this past year and a half. Thank you for sharing the huge workload and for being a friend! For everyone who helped me with big experiments; Jaz, Todd, Tim, Maleika, Caity, Jade, Aaron and Maddie. Adriana, also, for keeping the lab running smoothly and being a lovely smiling face. Thank you also to past members of the lab who have also helped me throughout my journey and been wonderful to work with; Carly, Cameron, Kevin, Duncan, Ervin, Yuka, Michelle, Jess, Caitlin, and Mark.

Additional thank yous to Dr Natalie Payne for providing me with Ad-MSCs and additional expertise in MSCs and also to everyone who donated their wisdom teeth so that I could have DPSCs for the study.

Finally, I could not have done any of this at all without my incredible family behind me. Mum, Dad and Jacqui and Lee, thank you for providing me with so much support, seeing me through every step of the process. Though you may never understand why I undertake such enormous projects in my life or continue to put myself in stressful situations, I feel so very lucky to have you there to buffer against it all. Thank you also Drew for being by my side through all of this. I'm very grateful to each of you!

Table of contents

Table of figures

List of tables

Abbreviations

ACKR	atypical chemokine receptor	Il23rΔ9	interleukin-23 receptor delta 9
ACKR2	atypical chemokine receptor 2	IL-27	interleukin-27
ACKR4	atypical chemokine receptor 4	IL-35	interleukin-35
AdMSC	adipose-derived mesenchymal stem cell	IL-4	interleukin-4
APC	antigen-presenting cell	IL-6	interleukin-6
APRIL	A Proliferation Inducing Ligand	IL-9	interleukin 9
Arm ham	armenian hamster	ILCs	innate lymphoid cells
BBB	blood-brain barrier	iLN	inguinal lymph node
BDNF	brain-derived neurotrophic factor	IMDM	Iscove's Modified Dulbecco's Medium
BLyS	B lymphocyte stimulator	iNOS	inducible nitric oxide synthase
BM-MSC	bone marrow-derived mesenchymal stem cell	iPS cell	induced pluripotent stem cell
BSA	bovine serum albumin	IRES	internal ribosome entry site
$CaCl_2$	calcium chloride	iTreg	inducible regulatory T cell
capt	capture	IVIS	*in vivo* imaging system
CCL19	CC-chemokine ligand 19	LIF	leukaemia inhibitory factor
CCL2	CC-chemokine ligand 2	LN	lymph node
CCL20	CC-chemokine ligand 20	LPS	lipopolysaccharide
CCL20	CC-chemokine ligand 20	LTα	lymphotoxin alpha
CCL3	CC-chemokine ligand 3	Ly6C	lymphocyte antigen 6
CCL5	CC-chemokine ligand 5	M1	Type 1 macrophage or microglia
CCR1	CC-chemokine receptor 1	M2	Type 2 macrophage or microglia
CCR2	CC-chemokine receptor 2	mAb	monoclonal antibody
CCR5	CC-chemokine receptor 5	mBM-MSC	mouse bone marrow-derived mesenchymal stem cell
CCR6	CC-chemokine receptor 6	MBP	myelin basic protein
CCR7	CC-chemokine receptor 7	MFI	mean fluorescence index
CFA	complete Freund's adjuvant	MHC	major histocompatibility complex
CM	conditioned medium	MHC-I	Major histocompatibility complex class 1
CMV	Cytomegalovirus	MHC-II	Major histocompatibility complex class 2
CNS	central nervous ayatem	MLR	mixed lymphocyte reaction
CO_2	carbon dioxide	MOG	myelin oligodendrocyte protein
COX2	cyclooxygenase 2	MRCLB	mouse red cell lysis buffer
CSF	cerebrospinal fluid	MRI	magnetic resonance imaging
CXCL12	CXC-chemokine ligand 12	MS	multiple sclerosis
CXCR2	CXC-chemokine receptor 2	MSC	mesenchymal stem cell
CXCR3	CXC-chemokine receptor 3	$NaHCO_3$	sodium bicarbonate
CXCR4	CXC-chemokine receptor 4	NK	natural killer
DC	dendritic cell	NK cell	natural killer cell
DEPC	Diethylpyrocarbonate	NKT cell	natural killer T cell
det	detection	NMS	normal mouse serum

DI	deionised	NO	nitric oxide
dLN	draining lymph node	Nrf2	nuclear factor (erythroid-derived 2)-like 2
DMEM	Dulbecco's Modified Eagle Medium	OPC	oligodendrocyte progenitor cell
DMSO	dimethylsulfoxide	OR	odds ratio
DMF	dimethyl fumarate	OVA	ovalbumin
DNA	deoxyribonucleic acid	P1	passage 1
DPSC	dental pulp stem cell	P2	passage 2
DPSC-CM	dental pulp stem cell conditioned medium	P3	passage 3
ds-DNA	double-stranded deoxyribonucleic acid	P4	passage 4
DTH	delayed-type hypersensitivity	P7	passage 7
EAE	experimental autoimmune encephalomyelitis	P8	passage 8
EBV	Epstein-Barr virus	PBMC	peripheral blood mononuclear cell
ECM	extracellular matrix	PBS	phosphate-buffered saline
EDSS	expanded disability status scale	PD-1	programmed death-1
EDTA	Ethylenediaminetetraacetic acid	PDL	population doubling level
EF1α	eukaryotic translation elongation factor 1 alpha 1	PD-L1	programmed death ligand-1
eGFP	enhanced green fluorescent protein	PDLSC	periodontal ligament stem cell
ELISA	enzyme-linked immunosorbent assay	PE	phycoerythrin
ES cell	embryonic stem cell	PFA	paraformaldehyde
FACS	fluorescence activated cell sorting	PGE_2	prostaglandin E2
FasL	Fas ligand	PL-MSC	placenta-derived mesenchymal stem cell
FBS	fetal bovine serum	PLP	proteolipid protein
FC	flow cytometry	PMA	phorbol 12-myristate 13-acetate
FDA	Food and Drug Administration	PPMS	primary progressive multiple sclerosis
FGF-2	fibroblast growth factor-2	PTx	pertussis toxin
FITC	fluorescein isothiocyanate	qPCR	quantitative polymerase chain reaction
FO	follicular	RNA	ribonucleic acid
FoxP3	forkhead box P3	RORgt	retanoic acid orphan receptor gamma t
GA	glatiramer acetate	RPMI	Roswell Park Memorial Institute
GFAP	glial fibrillary acidic protein	RRMS	relapsing-remitting multiple sclerosis
GFP	green fluorescent protein	RT	room temperature
GM-CSF	granulocyte-macrophage colony stimulating factor	S1P	sphingosine-1-phosphate
GWAS	genome-wide association studies	SEM	standard error of the mean
HA	haemagglutinin	SHED	stem cells from exfoliated deciduous teeth
hAd-MSC	human adipose-derived mesenchymal stem cell	sICAM-1	soluble intracellular adhesion molecule 1
hBM-MSC	human bone marrow-derived mesenchymal stem cell	SLE	systemic lupus erythamatosus
HBSS	Hank’s balanced salt solution	SLO	secondary lymphoid organ

HCl	hydrochloric acid
HEK293FT cell	human embryonic kidney 293FT cell
HGF	hepatic growth factor
HLA	human leukocyte antigen
HLA-DR	human leukocyte antigen - DR isotype
HRP	horse radish peroxidase
HSC	haematopoietic stem cell
hUC-MSC	human umbilical cord-derived mesenchymal stem cell
IDO	indoleamine oxidase
IFNγ	interferon-gamma
IFNβ	interferon-beta
Ig	immunoglobulin
IgG	immunoglobulin G
IgG1	immunoglobulin G1
IgG4	immunoglobulin G4
IgM	immunoglobulin M
IL-10	interleukin-10
IL-12	interleukin-12
IL-12p40	interleuking-12 p40 subunit
IL-17	interleukin-17
IL-1β	interleukin-1 beta
IL-2	interleukin 2
IL-23	interleukin-23
IL-23p19	interleukin-23 p19 subunit
IL-23R	interleukin-23 receptor
SNP	single-nucleotide polymorphism
SOD3	superoxide dismutase 3
SP	spleen
SPMS	secondary-progressive multiple sclerosis
TBS	tris-buffered saline
Tc1	cytoxic $CD8^+$ T cell
TCR	T cell receptor
TGF-β1	transforming growth factor-beta 1
T-bet	T-box protein expressed in T cells
Th1	T helper 1
Th17	T helper 17
Th2	T helper 2
TMB	3,3’,5,5’-tetramethylbenzidine
TNFα	tumour necrosis factor alpha
TNFRα	tumour necrosis factor receptor alpha
Treg	regulatory T cell
TSG-6	TNF-stimulated gene 6
TSU	technical services unit
UC-MSC	umbilical cord-derived mesenchymal stem cell
uncond.	unconditioned medium
VLA-4	very late antigen 4
Wnt	wingless-related integration site
WT	wild-type
γδ T cell	gamma-delta T cell

Conference proceedings arising from this work:

Foyle K, Wilson J, Koblar S, McColl SR, Comerford I. *Stem cells from dental pulp inhibit encephalitogenic T cell responses and disease in an animal model of multiple sclerosis*. Poster presentation at the 47th Annual Scientific Meeting of the Australasian Society for Immunology (Perth, 2018).

Foyle K, Wilson J, Koblar S, McColl SR, Comerford I. *Stem cells from dental pulp inhibit encephalitogenic T cell responses and disease in an animal model of multiple sclerosis*. Poster presentation at the 15th International Congress of Neuroimmunology (Brisbane, 2018).

Foyle K, Wilson J, Koblar S, McColl SR, Comerford I. *Autoimmunity of the central nervous system is suppressed by dental pulp stem cells in an animal model of multiple sclerosis.* Oral presentation at Adelaide Immunology Retreat (Victor Harbour, 2018). *Won 2nd PhD student prize.*

Foyle K, Wilson J, Koblar S, McColl SR, Comerford I. *Dental pulp stem cells inhibit encephalitogenic T cell responses and suppress disease in an animal model of multiple sclerosis*. Poster presentation at the 46th Annual Scientific Meeting of the Australasian Society for Immunology (Brisbane, 2017).

Foyle K, Wilson J, Koblar S, McColl SR, Comerford I. *Suppressing autoimmunity in a mouse model of multiple sclerosis with stem cells isolated from human dental pulp.* Oral presentation at Adelaide Immunology Retreat (Nuriootpa, 2017).

Foyle K, Wilson J, Koblar S, McColl SR, Comerford I. *Dental pulp stem cells inhibit encephalitogenic T cell responses and suppress disease in an animal model of multiple sclerosis*. Poster presentation at the International Congress of Immunology (Melbourne, 2016).

Foyle K, Wilson J, Koblar S, McColl SR, Comerford I. *Suppression of central nervous system autoimmunity with dental pulp stem cells.* Oral presentation at Adelaide Immunology Retreat (Wirrina Cove, 2016).

Foyle K, Wilson J, Koblar S, McColl SR, Comerford I. *Suppression of autoimmunity in the CNS with dental pulp stem cells.* Oral presentation at Adelaide Immunology Retreat (Lyndoch Hill, 2015).

This page intentionally left blank.

Abstract

Multiple sclerosis (MS) is a demyelinating disease of the central nervous system (CNS) in which autoimmune inflammation destroys the protective myelin sheath that insulates axons. This leads to many symptoms including paralysis, it causes severe morbidity and is one of the most common neurological diseases affecting young adults. New treatments are urgently required for MS patients as none of the currently available disease-modifying therapies support repair of the damaged CNS. Ideally, future treatments for MS would encompass both suppression of autoimmunity and facilitate repair of the damaged CNS. Mesenchymal stem cells (MSCs) have the potential to fill both these criteria and therefore represent an attractive therapy for MS. Human dental pulp stem cells (DPSCs) are a type of MSC originating from neural crest cells and therefore more closely related to neuronal cell types than MSCs from other anatomical sources. Thus, DPSCs are potentially a more suitable therapeutic candidate than other MSCs for treatment of CNS disorders including MS.

In this study the suitability of DPSCs as a therapeutic for MS was tested in a mouse model, experimental autoimmune encephalomyelitis (EAE). DPSCs were isolated from the third molars of different donors and characterised *in vitro*. All DPSCs obtained adhered to MSC classification criteria and could be maintained continuously in culture for several weeks. Effects of DPSCs on the clinical course of EAE was thoroughly tested. Donor-to-donor variability was apparent with regard to the suppressive effect of these treatments on clinical EAE. Some donor's DPSCs were potently inhibitory to clinical EAE while DPSCs from other donors showed no significant suppression of disease. No evidence was found to support DPSC recruitment to the CNS or long-term engraftment. DPSCs that inhibited EAE impaired generation of Th17 cell responses and increased the ratio of Th1:Th17 cells in the spleen and CNS. DPSC treatment of EAE mice also resulted in significantly fewer lymphocytes, infiltrating myeloid cells and fewer microglia in the CNS. Secreted factors from DPSCs were implicated in this as conditioned medium from DPSCs was able to suppress differentiation of Th17 cells *in vitro*. DPSCs also suppressed the activation of B cells and their differentiation to antibody-secreting plasmablasts *in vitro*. Collectively, the data in this study reveals some potential for DPSCs to be therapeutic for neuroinflammatory disorders, although the donor-to-donor variability in these effects warrants further investigation. Key cells of the immune system involved in MS pathogenesis have been identified to be modulated by DPSC treatment in EAE, although further investigation is required to elucidate the molecular mechanisms by which DPSCs suppress those cell subsets in EAE.

This page intentionally left blank.

Chapter 1: Introduction

This page intentionally left blank.

1. Introduction

The research in this project aimed to assess the potential of mesenchymal stem cells (MSCs) from human dental pulp as a potential therapy in multiple sclerosis (MS) using animal models, and to understand the mechanisms that underpinned their mode of action. Therefore, in this introduction a detailed overview of the molecular and cellular pathogenesis of MS and the animal models relevant to this thesis are described. In addition, the currently available MS therapies are outlined along with their proposed modes of action. Following that, current understanding of the biology of MSCs will be discussed, with particular reference to their use in inflammatory diseases.

2. Multiple Sclerosis

MS is an autoimmune disease of the central nervous system (CNS) in which inflammation destroys the protective myelin sheath surrounding neurons in a process called demyelination. Myelin is a cholesterol-rich extension of the plasma membrane of oligodendrocytes and Schwann cells which is essential for proper structural organisation and maintenance of the axonal membrane into distinct nodes to reduce energy consumption while allowing rapid signal transmission[1]. Demyelinated neurons lose the ability to function efficiently, leading to loss of function symptoms in MS patients including loss of motor control or vision, gait disturbance, paralysis and more[2]. MS causes severe morbidity and is one of the most common neurological diseases affecting young adults[3], affecting more than 25,600 Australians and incurring an economic cost of $1.75 billion per annum[4]. Furthermore the prevalence of this disease worldwide is rising[5] and in Australia alone the number of people living with MS increased 20% between 2010 and 2017[4]. The mean onset of MS is 30 years of age[6] where patients typically present with episodic neurological symptoms interspersed with periods of full or partial remission, a form of MS called relapsing-remitting MS (RRMS). RRMS generally transforms to secondary-progressive MS (SPMS) in which symptoms accumulate and remissions are absent. About 10% of patients present directly with chronic progressive disease lacking remission which is known as primary progressive MS (PPMS)[2].

Both genetic and environmental factors clearly have roles in initiating MS. The precise mechanisms of how these factors interact to contribute to MS susceptibility are unclear, although both genetic and environmental factors have been linked to inflammation[7]. Several environmental risk factors which predispose to MS have been identified and include smoking, vitamin D deficiency, Epstein-Barr Virus (EBV) or cytomegalovirus (CMV) infections and adolescent obesity. The incidence of MS is also markedly higher at extreme latitudes compared to equatorial regions in both the northern and southern hemispheres and migration from high-risk areas to low-risk areas before puberty reduces the risk of developing MS, underscoring the importance of environmental factors in MS incidence[7,8].

The importance of genetic factors for MS susceptibility is apparent from a growing body of evidence. For example, twins have an MS disease concordance of 25.3% for monozygotic or 5.4% for dizygotic twins[3],

highlighting the genetic component of the disease. MS is also three times more prevalent in females than males[9]. Genetic risk factors for MS include both HLA- and non-HLA-associated genes, and HLA-associated genes have been calculated to account for approximately 21.4% of the heritability of MS[10]. The class II *DRB1*15:01* allele, for example, increases risk of MS with an odds ratio (OR) of 3.92[11]. Additionally, genome-wide association studies (GWAS) have identified more than 200 non-HLA-associated single nucleotide polymorphisms (SNPs) conveying moderate risk to developing MS, in which there is significant enrichment for genes that are linked to immune system[10]. Significantly, there is an enrichment for SNPs in regions associated with both $CD4^+$ and $CD8^+$ T cells, B cells, NK cells and microglia.

MS is diagnosed by the presence of macroscopic lesions in the CNS which can be detected by magnetic resonance imaging (MRI) and are most commonly seen in the spinal cord, optic nerves, brainstem/cerebellum and periventricular white matter[8]. Active MS lesions contain infiltrating inflammatory cells and show areas of tissue injury with centres devoid of myelin with or without signs of remyelination, and are sometimes accompanied by loss of axons[12]. By contrast, inactive lesions lack inflammatory infiltrates as well as myelin and any signs of remyelination and no further demyelination occurs at the lesion border.

Animal models have been crucial for the development of several treatments for MS and have furthered our understanding of some of the underlying causes of the illness. One of the commonly used models for the autoimmune aspects of MS is discussed below.

2.1 Experimental Autoimmune Encephalomyelitis (EAE)

An MS-like pathology can be induced in rodents by subcutaneous immunisation with neuropeptides emulsified in complete Freund's adjuvant (CFA) together with systemic administration of pertussis toxin (PTx)[13]. Immunisation with CNS peptides causes activation of autoreactive T cells to initiate disease, and the symptoms diverge depending on the peptides used and genetic background. Immunisation of C57Bl/6 mice with the myelin oligodendrocyte protein (MOG) peptide MOG_{35-55} causes chronic paralysis progressing from the tail tip to hind limbs and then fore limbs. Similar symptoms are induced in SJL/J mice by immunisation with the proteolipid protein (PLP) peptide $PLP_{139-151}$ but mice recover from paralysis for a short period before relapsing. These two forms of EAE are widely used to mimic autoimmune aspects of chronic and relapsing MS respectively.

Strong evidence points to a major role for autoimmunity in MS pathogenesis, and EAE has been used extensively for studying these immunological aspects of MS. Demyelination is also observed in the CNS of rodents with EAE as well as acute axonal damage, although lesions predominantly occur in the spinal cord in contrast to MS where lesions are often in the brain as well as the spinal cord[14]. Multiple therapies currently used for MS were first tested in these models which have been invaluable to our understanding of the primary immunological events which might initiate MS, especially relapsing MS[15]. Despite this, there are some aspects of MS that are not modelled by EAE. Diffuse white matter injury and grey matter injury are two other lesion

types which occur in MS and progress independently of inflammation[14]. These neurodegenerative processes may underpin progressive MS in which treatments targeting inflammation are ineffective[16].

2.2 Immunopathology of EAE

A prevalence of risk factors associated with immune system function and the inflammation which can be observed in active demyelinating lesions in the CNS point to an autoimmune component to MS pathology. The immunopathology of MS is complex and only partially understood and appears to be driven by multiple cell types including autoreactive T cells. Much of the current understanding of the immunopathology of MS has been based on studies in EAE which was thought to have many similarities to MS. In this section, a description of the major molecular and cellular drivers of the pathogenesis of EAE will be outlined.

Figure 1.1 depicts a simplified version of the current understanding of some of the main immunological events that occur in the pathogenesis of MOG_{35-55}-induced EAE in C57Bl/6 mice. Immunisation with CNS antigen with appropriate adjuvant results in antigen presentation by dendritic cells (DCs) in secondary lymphoid organs (SLOs). DCs activate $CD4^+$ T cells which migrate to the CNS and initiate an inflammatory cascade there, and B cells, $CD8^+$ T cells and regulatory T cells (Tregs) are also activated and recruited to the CNS. There is activation of local CNS antigen-presenting cells (APCs) called microglia and secondary recruitment of large numbers of infiltrating myeloid cells including monocytes, macrophages and neutrophils to the CNS whereupon downstream damage the CNS occurs including loss of oligodendrocytes and axons. The precise role of each of these infiltrating cells in the pathology of EAE is still being elucidated but our current understanding of their contributions is described in more detail in the remainder of this section.

Initially, EAE was thought to be driven by the T helper 1 (Th1) subset of $CD4^+$ T cells. The canonical role of Th1 cells is orchestrating cell-mediated immune responses against intracellular bacterial and viral infections. Adoptive transfer of MOG_{35-55} -reactive Th1 cells restimulated *in vitro* confers clinical signs of EAE to naïve mice[17]. In order to differentiate from naïve precursors, Th1 cells require the cytokine IL-12, which is a heterodimer of two subunits IL-12p35 and IL-12p40, while the main effector cytokine of Th1 cells is interferon gamma (IFNγ)[18]. However, *Il12rb2*$^{-/-}$ mice, which cannot make Th1 cells, are still susceptible to EAE[19], as are *Ifng*$^{-/-}$ and *Ifngr*$^{-/-}$ mice[20-23], demonstrating that canonical Th1 cells are actually dispensable for disease. Confusion arose from the discovery that while *Il12p35*$^{-/-}$ mice are susceptible to EAE, *Il12p40*$^{-/-}$ mice were protected from disease[24,25]. This was clarified when Oppmann *et al.* discovered in 2000 that the IL-12p40 subunit also dimerises with IL-23p19 to form the pro-inflammatory cytokine IL-23[26]. Cua *et al.*,[27] subsequently showed that IL-23, not IL-12, is critical for EAE. They also went on to find that IL-23 promoted expansion of a subset of $CD4^+$ T cells that produced IL-17 (now called Th17 cells)[28].

Following the discovery of Th17 cells, there was a shift in focus to the disease-initiating effects of these cells in EAE. Like Th1 cells, adoptive transfer of myelin-specific Th17 cells induces EAE[17] while *Il23r*$^{-/-}$ mice are protected from disease[27]. Also, the ratio of Th1:Th17 cells can affect Th17 cell infiltration of the CNS and

severity of EAE. Stromnes *et al.*,[29] found that Th17 cells can infiltrate the spinal cord of EAE mice at a range of Th1:Th17 ratios, yet at low Th1:Th17 cell ratios (≤1) Th17 cells can also enter the brain and cause severe EAE. The effector molecule of Th17 cells, IL-17, exists as several variants including IL-17A and IL-17F, and treatment with an IL-17A-neutralising antibody suppresses EAE[28,30], although IL-17-deficient mice are only partially protected from EAE indicating that IL-17A has a partially redundant role in disease pathogenesis[31,32]. More recently, it has been found that Th17 cells also produce the pro-inflammatory cytokine granulocyte-macrophage colony-stimulating factor (GM-CSF) and mice deficient for the gene for GM-CSF (*Csf2*$^{-/-}$) are protected from EAE[33] indicating that GM-CSF is critical for development of the disease. T cells that come through a Th17 developmental pathway are major producers of GM-CSF in EAE, and IL-23 signalling is required for these cells to express GM-CSF[33,34].

Current understanding of Th cell subsets and lineage stability in immunology is evolving rapidly through use of fate-mapping and cytokine reporter models, and it is clear now that Th1 and Th17 phenotypes are not necessarily stable end-differentiation states. Rather, it appears a degree of fluidity exists between these subsets and in EAE, Th17 have been shown to convert to a Th1-like "ex-Th17" phenotype in the CNS[35,36]. Hirota *et al.*,[36] used an IL-17A fate reporter mouse to show that the vast majority of IFN-γ-secreting cells in the CNS of EAE mice are in fact ex-Th17 cells. This transition is accomplished by down-regulation of the Th17 transcription factor RAR-related orphan receptor gamma t (RORγt) and up-regulation of the Th1 transcription factor T-box protein expressed by T cells (T-bet). These ex-Th17 cells produce large quantities of GM-CSF to drive CNS pathogenesis. T-bet-deficient Th17 cells are also encephalitogenic, however, demonstrating that they do not need to transition to a Th1-like phenotype to cause disease[37,38]. The fact that both Th1 and Th17 cells acquire expression of GM-CSF, which is a critical factor for EAE, might also explain how both are able to independently induce EAE[33,34].

$CD8^+$ T cells also play a role in EAE pathogenesis although they are not strictly required for disease since C57Bl/6 mice lacking $CD8^+$ T cells still develop EAE[39]. The role of $CD8^+$ T cells in EAE is debated with both pathogenic and regulatory described[39]. Adoptive transfer of MOG-reactive $CD8^+$ T cells into naïve C57Bl/6 mice can induce EAE[40,41] as can $CD8^+$ T cells that are reactive to a peptide of myelin basic protein (MBP_{79-87}) in C3H mice[42]. Although transgenic systems have demonstrated an ability of $CD8^+$ T cells to elicit cytotoxicity to neurons or astrocytes expressing their cognate antigens *in vitro* and *in vivo*[43], this has not been definitively shown to be a mechanism of $CD8^+$ T cell pathogenicity in EAE. Transfer of haemagglutinin (HA)-specific $CD8^+$ T cells into mice expressing HA specifically in oligodendrocytes also led to an MS-like pathology with inflammation of the CNS and demyelination in which the $CD8^+$ T cells were shown to localise next to oligodendrocytes[44]. Mice with $CD8^+$ T cells that express a transgenic glial fibrillary acidic protein (GFAP)-specific T cell receptor (TCR) also develop spontaneous CNS autoimmunity[45]. Conversely, CD8-deficient mice have exacerbated EAE symptoms suggesting that $CD8^+$ T cells can also have regulatory functions in EAE[46]. Supporting this, Qa-1-restricted $CD8^+$ T cells are suppressive in EAE[47-49] and can kill MBP-reactive

$CD4^+$ T cells[49]. Suppressing $CD4^+$ T cell proliferation is another way in which $CD8^+$ T cells may regulate inflammation in EAE[47].

A role for B cells in EAE is also demonstrated by the observation that B cell-specific MHC-II-deficient mice are resistant to EAE induced by immunisation with whole MOG protein[50], highlighting the importance of B cells for processing and presenting MOG protein to T cells for disease in that model. However, μMT mice, which lack B cells, are susceptible to MOG_{35-55} peptide-induced EAE on a C57Bl/6 background[51-53] and to MBP Ac1-11 peptide-induced EAE on a B10.PL background[54], indicating B cells are not required for presenting some CNS peptides. Although B cells produce antibodies in EAE, this also does not appear to be important for disease and does not correlate with severity of symptoms[55]. Secretion of cytokines may be an important function of B cells in EAE instead. B cell-derived IL-6 also contributes to EAE pathogenesis and the disease is less severe with a diminished Th17 cell response in mice which lack IL-6 specifically in B cells[56]. On the other hand, some regulatory functions have also been ascribed to subsets of B cells in EAE[55]. Anti-inflammatory IL-35^+ B cells and IL-10^+ B cells may be important for limiting CNS inflammation[57]. Mice lacking IL-10 specifically in B cells develop more severe EAE[58], while transfer of purified IL-10-secreting regulatory B cells into EAE mice limits pathology[55]. B cells can also produce TGF-β1 to limit CNS inflammation in EAE and mice lacking TGF-β1 specifically in B cells show an earlier onset of disease[59]. Thus, the role of B cells in EAE depends on the subset and the immunisation protocol that is used.

Microglia are CNS-resident antigen-presenting cells with similarities to macrophages and, amongst other functions, are important for regulating inflammation in the brain. Like macrophages, microglia can become polarised toward M1 or M2 phenotypes which are generally considered to be pro-inflammatory and anti-inflammatory respectively[60]. Ablation of microglia in EAE mice suppressed disease, indicating a pro-inflammatory role for these cells in EAE pathogenesis[61]. M1 microglia secrete pro-inflammatory cytokines, present antigen to lymphocytes and can be cytotoxic[60]. Pro-inflammatory microglia can also impede oligodendrogenesis *in vitro* and this can be rectified by treatment of the microglia with IL-4 which promotes an M2 phenotype[62]. M2 microglia, on the other hand, are important for phagocytosis and clearance of myelin debris that inhibits oligodendrocyte progenitor cell (OPC) differentiation and maturation and the production of anti-inflammatory cytokines such as IL-10 in mice[63,64]. A switch from M1 to M2 occurs during remyelination in mice, where M2 microglia support differentiation and maturation of OPCs into myelinating oligodendrocytes[64]. In that study, secretory factors were found to be important for M2 function as supernatants from cultured M2 microglia enhanced differentiation of OPCs *in vitro*. The role of microglia in EAE is therefore multifactorial and may depend on the stage of disease.

Cytokines are important signalling molecules which orchestrate immune responses and can have pro-inflammatory or anti-inflammatory effects. Cytokines which have a predominantly pro-inflammatory role in MS or EAE include the aforementioned GM-CSF, IL-17A and IL-23 as well as IL-6 and IL-1β. IL-6 and IL-1β contribute to Th17 development among other effects and deficiency in either of these cytokines confers

resistance to EAE[65-68], while IL-1β increases the encephalitogenicity of T cells[34,69,70] and activates CNS endothelial cells. Although IFNγ and tumour necrosis factor alpha (TNFα) are generally classed as pro-inflammatory cytokines, their role in EAE and MS is less clear and they appear to have both pro-inflammatory and anti-inflammatory effects which may depend on the stage of disease and the cell types producing or receptive to them[71]. Delivery of IFNγ before onset of EAE exacerbated symptoms while treatment after onset reduced the severity of disease, suggesting the effects of IFNγ in EAE are dependent on the stage of disease[23]. TNFα is produced by macrophages, Th1 cells and microglia in EAE[72,73] and while early TNFα blockade partially protected rats from EAE[74], mice deficient for TNFα or one of its receptors, TNFR1, exhibit delayed but ultimately worse symptoms of EAE[75]. Therefore like IFNγ, TNFα may have pro-inflammatory functions in the early stage of EAE but anti-inflammatory functions in the later stages of disease[73,75,76]. In contrast, the cytokine IL-10 plays an anti-inflammatory role in EAE, suppressing production of pro-inflammatory cytokines and promoting regulatory immune responses[72]. IL-27 is also anti-inflammatory and suppresses Th17 cell development[77] and increases production of IL-10 by Tregs[78].

To summarise, autoimmune Th17 cells in EAE infiltrate the CNS and produce GM-CSF among other pro-inflammatory cytokines. These cytokines recruit monocytes into the CNS and they mediate damage to oligodendrocytes. While other leukocytes including $CD8^+$ T cells and B cells have also been implicated in EAE pathogenesis their roles in the pathogenic cascade are less clear. There are other cell types which are also involved in the pathogenesis of EAE including Tregs, innate lymphoid cells (ILCs) and T follicular cells which are not discussed in detail here. Next, evidence for roles of these different leukocytes in MS is discussed.

2.3 Immunopathology of MS

Research into understanding of the immunopathology of MS is limited by the difficulty in studying the human brain and so derives from MRI analysis, and study of peripheral blood, CSF and autopsy material as well as the responses of patients to different treatments. An autoimmune aspect to MS is strongly suggested by the heavy infiltration of lesions with leukocytes, primarily myeloid cells and T cells[79]. Furthermore, the high degree of genetic risk for MS associated with immune system function[80], particularly HLA-DR, suggests that the role of inflammation may be causative of MS rather than a consequence of neurodegeneration that occurs in the disease[16]. It is thought that early in MS disease development, an inflammatory insult triggers demyelinating events from which patients can recover through spontaneous remyelination (Figure 1.2, parts 1-3)[1]. Further inflammation and demyelination causes symptom relapse, and then in later stages of disease exhaustion of remyelinating mechanisms as well as axonal transection may result in irreversible functional damage and progressive disease (Figure 1.2, parts 4, 5). Evidence implicating various subsets of leukocytes in the pathogenesis of MS is given below along with possible mechanisms of action.

Genes conferring the highest risk for MS include several MHC-II alleles, pointing to a role for $CD4^+$ T cells in MS pathogenesis[81]. Similar to EAE, Th17 cells are thought to play a pro-inflammatory role in MS. The blood of MS patients has a higher frequency of Th17 than healthy controls[82,83] suggesting that, like in EAE,

Th17 cells may be important in MS pathogenesis. IL-17 is additionally more abundant in the blood of MS patients[84] although it is produced by $CD8^+$ T cells and astrocytes in MS as well as $CD4^+$ T cells[85]. A longitudinal analysis showed increased Th17 cells but not Th1 cells during active phases of MS compared with inactive MS within the same patients[86].

In MS patients, GM-CSF expression is more abundant in Th1 cells than Th17 cells, but it is actually mostly expressed by a third subset of $CD4^+$ T cells which do not produce IL-17A or IFNγ and rather co-express other highly pro-inflammatory cytokines TNFα and IL-6[87]. GM-CSF activates and expands myeloid cells and DCs, which are also abundant in MS lesions[79,88]. Antigen presentation, expression of co-stimulatory molecules, and secretion of pro-inflammatory cytokines by myeloid cells and DCs are also all increased by GM-CSF[89], and microglia and astrocytes in acute and chronic MS lesions have increased expression of its receptor[90,91]. The frequency of total GM-CSF-producing $CD4^+$ T cells is increased in the blood of RRMS patients compared with healthy controls[92], and GM-CSF-expressing $CD4^+CD45RO^+$ memory T cells have also been found to be more frequent in the CSF of patients with MS compared with other neurological diseases[93]. Of note, $CD4^+$ T cells were identified to have the most significant increase in expression of GM-CSF associated with MS compared with other cellular sources of this cytokine[87], highlighting $CD4^+$ T cells as an important source of pro-inflammatory molecules in MS.

The frequencies of Treg cells do not appear to be altered in MS patients compared to healthy controls, unlike other $CD4^+$ T cell subsets that have been studied[94]. However, there is evidence that Tregs from MS patients are functionally defective. FoxP3 expression is reduced in RRMS[95] and Tregs isolated from MS patients are less capable of suppressing $CD4^+$ T cell proliferation *in vitro*[94]. FoxP3 expression and suppressive capacity of Tregs is restored with treatment with glatiramer acetate (GA) and IFN-β[94,96]. Interestingly, the deficit in Treg suppressive capacity in RRMS appears to return to normal by SPMS stage[97]. Furthermore, the ratio of Treg/Th17 in peripheral blood of RRMS patients negatively correlates with expanded disability status scale (EDSS), suggesting Treg control of Th17 cell responses may be an important protective mechanism against MS[95].

Like in EAE, the role of $CD8^+$ T cells in MS is controversial, with both pro- and anti-inflammatory subsets being described. $CD8^+$ T cells outnumber $CD4^+$ T cells in the perivascular cuffs of active MS lesions by up to 50:1[98], and they have been found to be clonally expanded in cerebrospinal fluid (CSF), peripheral blood and some MS lesions[99]. Despite these observations, it is unknown if these clonally expanded $CD8^+$ T cells are aggressors of CNS inflammation of if they are protective. A pro-inflammatory role for $CD8^+$ T cells is suggested by a doubling in MS risk with possession of the *HLA-A*0301* allele for MHC Class I[100]. Also, perforin-expressing $CD8^+$ T cells are more abundant in the blood of MS patients than healthy controls and this is even more apparent during relapse[101]. The CSF of MS patients is enriched for the cytotoxic molecules granzymes A and B[102] and a greater frequency of granzyme B-expressing $CD8^+$ T cells are present there, also evidence that pathological $CD8^+$ T cell subsets may be important in MS[103]. On the other hand, presence of the

HLA-A*0201 allele is associated with a 50% decrease in risk for MS[11]. $CD8^+$ T cells with specificity for neuroantigens have been found in the blood of MS patients but these are also present in healthy controls[104]. Those $CD8^+$ T cells from MS patients responded to stimulation with neuropeptides *ex vivo* by producing more IFNγ and IL-10 than healthy controls. Human $CD8^+$ T cells are capable of killing oligodendrocytes loaded with MBP peptide in a MHC Class I-dependent manner *in vitro*[105]. HLA-E-restricted $CD8^+$ T cells, which are the human equivalent of regulatory Qa1-restricted $CD8^+$ T cells that are found in mice and which can suppress $CD4^+$ effector T cells, may be impaired in MS patients. Compared with HLA-E-restricted $CD8^+$ T cells in healthy controls, those in MS patients expressed less anti-inflammatory CD122 and FoxP3 but more IFNγ, IL-17A and granzyme B, which may be indicative of a shift from a regulatory phenotype to a more inflammatory one[106].

The success of B cell-targeting monoclonal antibody therapies in MS has highlighted an important role for these cells in the pathogenesis of MS[107]. Treatment of MS patients with anti-CD20 antibodies (Rituximab and Ocrelizumab), which target CD20 which is a marker expressed by >95% of B cells, significantly reduces the frequency of new MS relapses[108,109], although the exact role of B cells in MS pathogenesis is not clear. Oligoclonal bands caused by antibody deposits can be found in the CSF of almost 90% of MS patients and these have been an important immunological diagnostic marker for MS[110]. However, Rituximab does not deplete plasma cells and it has been shown that oligoclonal bands persist in the CSF after Rituximab therapy[111], suggesting the production of autoantibodies by B cells does not play a dominant role in MS pathology. An antibody-independent role for B cells in MS pathogenesis is also supported by evidence that secretory products from B cells of RRMS patients and not healthy controls are toxic to oligodendrocytes and neurons *in vitro* even when immunoglobulin has been depleted[112]. Secretion of cytokines by B cells including TNFα, lymphotoxin-alpha (LTα) and IL-6 are important for inflammatory T cells in MS and these are also reduced by Rituximab treatment[113]. Additionally, B cells are another source of GM-CSF in MS and the frequency of GM-CSF-expressing B cells is increased in MS patient's blood[87,114]. B cells are also antigen-presenting cells, but it is not clear if this is an important function of B cells in MS. Further complicating the picture is the finding that in addition to B cells, Rituximab also depletes a small subset of $CD20^+$ T cells[115]. $CD20^+$ T cells comprise of both $CD4^+$ and $CD8^+$ T cells and express pro-inflammatory cytokines including TNFα, IL-17A and IFNγ although their function and possible contribution to MS pathogenesis is not yet known[116,117]. Therefore, B cell-depleting therapies have effects extending beyond the direct function of B cells themselves, and it is not clear to what degree the beneficial effects of B cell depletion are directly caused by reduction of cells versus other indirect effects. Interestingly, Atacicept which is a small fusion protein that targets B Lymphocyte Stimulator (BLyS) and A Proliferation-Inducing Ligand (APRIL) expressed by B cells to inhibit their maturation and survival after activation and is effective against systemic lupus erythematosus (SLE) failed in clinical trials for MS after it increased relapses in RRMS patients, perhaps due to inhibition of regulatory B cells[118,119]. Thus, although there appears to be an important role for B cells in MS pathogenesis, the mechanisms are unclear.

Another way in which B cells may contribute to MS pathogenesis is that they are a reservoir for latent EBV. EBV infects naïve B cells which then mature into memory B cells and while T cells are able to control the infection, latency is established in the memory B cell pool[120]. Approximately 90% of the general population are seropositive for EBV infection, but virtually 100% of MS patients are seropositive[121]. In fact, EBV-seronegativity has an OR for MS development of only 0.18[122], whereas seropositivity for EBV compared with EBV-seronegativity has an OR for MS of 13.5[123]. Although early childhood contraction of EBV is asymptomatic, acquiring EBV in puberty or later leads to infectious mononucleosis (IM) with fever, sore throat and fatigue[124]. A history of IM increases a person's risk for MS by 2.3 times, indicating that the stage in life in which EBV is contracted can increase MS risk[125]. In fact, EBV is one of the strongest environmental risk factors for MS[126]. A reduction in EBV-specific $CD8^+$ T cell responses has been observed in blood of MS patients, suggesting they may fail to control EBV infection[127]. Despite this, it is not known how EBV infection may cause or contribute to MS pathogenesis; there may be replication of EBV in B cells in the CNS or cross-reactive T cell responses may be elicited although evidence for these is weak[128,129]. Overall, B cell and EBV contributions to MS pathogenesis require further clarification.

Microglia are also thought to play a role in MS. MHC-II expression is up-regulated in microglia in MS lesions[130], suggesting they may be involved in antigen-presentation to T cells there. Like in EAE, a switch from M1 to M2 phenotype occurs with remyelination in brain lesions of MS patients[131]. Pro-inflammatory microglia dominate active and expanding lesions while anti-inflammatory microglia are observed at the lesion core where remyelination is attempted. In progressive MS, there is an absence of anti-inflammatory/neuroprotective microglia in the lesions which may contribute to failure to remyelinate[63]. Additionally, in that study, more activated pro-inflammatory microglia are present in normal white matter of MS patients compared with healthy controls, suggesting abnormal microglial activation may inherently contribute to MS pathology. Microglia are also thought to contribute to MS pathogenesis by the production of reactive oxygen species (ROS) which are cytotoxic to oligodendrocytes[63].

In patients with chronic progressive MS, levels of TNFα are elevated in CSF and correlates with disability[132], which initially suggested a pro-inflammatory role for TNFα for MS progression. Despite this, inhibiting TNFα in MS in two separate clinical trials exacerbated disease[133,134]. Together with mixed roles discovered in EAE (described in section 1.1.2), it appears that TNFα may play both pro- and anti-inflammatory roles in the pathogenesis of MS. After rodent studies suggested that IFNγ was protective in EAE[21,22], a clinical trial commenced to treat RRMS patients with IFNγ. However, IFNγ treatment exacerbated MS[135], and therefore IFNγ appears to be pro-inflammatory in MS.

Overall, it can be appreciated that EAE and MS are unlikely to be caused by a single cell type and the path to neuroinflammation and CNS damage can be varied. Multiple compensatory mechanisms exist which can each independently contribute to disease and the roles of various cell subsets can adapt depending on what other

signalling events are occurring. The migration of leukocytes into the CNS is also an important factor in MS pathogenesis and the chemokine signalling pathways which may be implicated in this are discussed below.

2.4 Chemokines and chemokine receptors in MS and EAE

Leukocyte trafficking is important for bringing cells into close proximity to facilitate signalling events that regulate cell activation, survival, proliferation and function. In the immune system, cell trafficking is spatially and temporally regulated by chemokines, or chemoattractant cytokines, and their receptors together with integrins and other adhesion molecules. Chemokine receptors are 7-transmembrane G protein-coupled receptors which are classified into four families based on the spacing of conserved N-terminal cysteine residues (C, CC, CXC and CX_3C). Chemokine signalling directs cell trafficking with specificity by directional migration of chemokine receptor-expressing cells toward sources of their cognate chemokine ligands.

Early in EAE, autoreactive Th17 cells have been shown to enter the CNS parenchyma via the choroid plexus using the chemokine receptor CCR6[136] (Figure 1.1A-C). Chemokine receptors bind small chemotactic cytokines (chemokines) to guide cell migration. Onset of EAE is delayed in *Ccr6*$^{-/-}$ mice but has been reported to eventually be more severe than in wild-type (WT), perhaps since Tregs also utilise CCR6 for entry to the CNS[137,138]. Once in the CNS, Th17 cells initiate an inflammatory cascade which disrupts the blood brain barrier (BBB) and facilitates secondary recruitment of other leukocytes[136]. A second wave of highly inflammatory Th17 cells then enters the CNS via expression of CCR2[138] (Figure 1D). These highly inflammatory $CCR2^+CCR6^-$ Th17 cells require IL-23 for development and produce large quantities of the pro-inflammatory cytokine GM-CSF. Mice with a deficiency of CCR2 in T cells develop less severe EAE with fewer GM-CSF-expressing Th17 cells entering the CNS[138]. GM-CSF is important for recruitment and activation of $CCR2^+Ly6C^{hi}$ pro-inflammatory monocytes from the blood to the CNS[69], whereupon infiltration of the CNS with myeloid cells results in downstream damage to the myelin sheath Figure IE-G).

There is evidence that CCR2 and CCR6 may be implicated in the pathogenesis of MS also. The sole ligand for CCR6, CCL20, is constitutively expressed by the epithelium of the choroid plexus. In MS patients and in other neuroinflammatory diseases, CCL20 is up-regulated which may increase recruitment of CCR6-expressing cells, and this is supported by the fact that T cells in the CSF of MS patients have been shown to express CCR6[139]. CCL20 has also been shown to be produced by astrocytes in MS lesions where it may direct $CCR6^+$ cells to the site of inflammation[140]. In mice, also, astrocytes produce CCL20 in response to IL-9 and this attracts CCR6-expressing cells in EAE[141]. CCR2, which was shown to be important for Th17 cell recruitment to the CNS of EAE mice[138] may also be important in MS. The major ligand for CCR2, CCL2, is expressed by glial cells and may recruit CCR2-expressing macrophages, DCs and T cells from the blood to active lesions[142].

CCR1 and CCR5 may also be important recruiting cells of the immune system to the CNS in MS or EAE pathogenesis. Relapsing MS patients have elevated levels of the CCR1 and CCR5 ligand CCL5 in the CSF compared with stable MS patients[143]. CCL5 has been shown to be required for the recruitment of peripheral

blood monocytes across the BBB during inflammation and deletion of CCR1 in mice prevents EAE[144,145]. Another of the CCR1 ligands, CCL3, has also been implicated in this process, attracting $CCR1^+$ APCs and T cells.

CCR7 and its ligands CCL19 and CCL21 have also been implicated in MS and EAE. The chemokine CCL19 is constitutively expressed at low levels in the CNS of naïve mice and healthy humans[146,147] but increases with disease progression in both chronic and relapsing EAE models[146], and is similarly increased in MS lesions and at the BBB of MS patients[147]. Another study showed no CCL19 or CCL21 protein is present in non-lesioned white matter[148]. Astrocytes and microglia in the parenchyma as well as infiltrating leukocytes accumulated in the meninges have all been shown to be sources of CCL19 in the CNS in EAE[146]. Moreover, encephalitogenic T cells have been shown to express the receptor for CCL19, CCR7, suggesting that elevated CCL19 levels may contribute to recruitment of these cells to the CNS[149]. Large numbers of $CCR7^+$ cells (T cells or maturing DCs) can be found in lesions in brain autopsy material from MS patients as well as in samples of the CSF[148].

Other chemokines and chemokine receptors which are involved in recruitment of leukocytes to the CNS include CCR5, CXCR2, and CXCR3. The T cells in the CSF of MS patients are enriched for expression of CCR5 and CXCR3[150]. CXCR3 is also used by T cells to enter the CNS during immune surveillance, leading to an enrichment of $CXCR3^+$ T cells in the CSF under steady-state conditions[151]. CXCR2, however, is important for trafficking of polymorphonuclear cells to the CNS, where the CXCR2 ligands CXCL1 and CXCL2 are induced in the spinal cord in EAE by encephalitogenic Th17 cells[152]. CXCR2 blockade inhibits EAE dependent on the trafficking of polymorphonuclear cells. As well as CCR6, CXCR3 recruits Tregs to the brain, which has been shown to be important for limiting inflammation in the perivascular space[153].

Chemokines therefore have been implicated in key aspects of MS and EAE initiation and progression, highlighting their potential as a therapeutic target for regulation or as a method for directing regulatory cells into the CNS. One mechanism by which chemokine signalling is regulated is through atypical chemokine receptors. Atypical chemokine receptors do not contain the canonical DRYLAIV motif of typical chemokine receptors that facilitates G-protein coupling and, as such, binding of chemokines to atypical chemokine receptors does not result in downstream G-protein signaling[154]. Instead, the main function of atypical chemokine receptors appears to be scavenging, sequestering, degrading or transporting their ligands in order to regulate abundance of chemokines in their biological niches[155,156]. Furthermore, the atypical chemokine receptors ACKR2 and ACKR4 have been shown to have roles in EAE[157,158].

ACKR2 has 14 ligands in the CC chemokine family, all of which are inflammatory chemokines meaning expression is induced or upregulated in inflammatory contexts[156]. These 14 chemokines encompass most of the ligands for the receptors CCR1-5 which are expressed by leukocytes including T cells, neutrophils, monocytes, macrophages, DCs and NK cells[159]. ACKR2 is itself expressed by lymphatic endothelial cells (LECs), trophoblasts of the placenta and some B cell subsets[160-163]. Expression of ACKR2 is important for regulating abundance and clearance of inflammatory chemokines in order to control leukocyte trafficking into

dLNs[164]. Failure of *Ackr2*$^{-/-}$ mice to control chemokine abundance leads to increased leukocyte entrapment in the draining lymph nodes (dLNs) and subsequent congestion of the flow of lymph and impaired leukocyte priming[165]. Subcutaneous immunisation with MOG peptide in EAE leads to formation of DC aggregates in the skin which persist there likely due to disruption of an optimal chemokine gradient for migration out of the skin to the dLN[158,165]. Additionally, T cell priming can be impaired by ACKR2-deficiency in MOG-$_{35-55}$ EAE and transfer of encephalitogenic cells from *Ackr2*$^{-/-}$ mice into WT hosts leads to less severe disease than transfer of WT cells[157]. Interestingly, immunisation with full MOG protein instead of peptide increases the severity of EAE in *Ackr2*$^{-/-}$ mice due to increased GM-CSF-expressing B cells generated in the spleen and a more potent T cell response[158]. On the other hand, ACKR2 also has important anti-inflammatory roles and ACKR2 deletion in mice abolishes their ability to control inflammation due to accumulated inflammatory CC chemokines[166-168]. Infection of *Ackr2*$^{-/-}$ mice with *Mycobacterium tuberculosis* leads to an exacerbated inflammatory response which can be reversed with blocking antibodies to the CC chemokines[167]. Also, treating the skin of *Ackr2*$^{-/-}$ mice with phorbol ester in a model which produces psoriasis-like lesions resulted in more aggravated inflammation than in WT mice due to a lack of clearance of inflammatory chemokines[166]. Some ACKR2 ligands are also important for entry of leukocytes to the CNS including CCR1 and CCR2 ligands as described above.

ACKR4 binds the homeostatic chemokines CCL19, CCL21, CCL25, and it also weakly binds human CXCL13[169], therefore potentially regulating CCR7, CCR9 and human CXCR5 respectively. ACKR4 is expressed in many tissues including the lymph node, epidermis, thymus, intestine, heart, testis and liver[170,171]. Its ligands are constitutively expressed in the SLOs, where they are important for homeostatic trafficking of naïve T cells, DCs, and B cells[169]. ACKR4 is also postulated to be important for the regulation of lymphocyte and DC trafficking in inflammatory and autoimmune responses[169,172]. ACKR4 appears to have a protective role in EAE as *Ackr4*$^{-/-}$ mice succumb to EAE more rapidly than WT mice[173]. This is coupled with a more rapid, pathological immune response, associated with an accumulation of CCL21 in the CNS. Therefore, ACKR4 may be important for limiting excessive inflammation in EAE.

2.5 MS treatments

Different treatment options are available to people living with MS and the type and stage of disease can influence which treatments are chosen. There are more than a dozen US FDA-approved and off-label treatments available for RRMS patients while no treatments were available for PPMS until March 2017 when the humanised monoclonal antibody (mAb) Ocrelizumab became the first drug to receive US FDA approval for treating PPMS[174]. Outcomes of treatment in MS are typically measured by disability status, MRI lesion activity or relapse rate. Although most current treatments produce positive outcomes in these three areas, repair of the CNS and induction of tolerance to self-antigens is lacking and these are the primary foci for recent research. Treatments for MS have focussed predominantly on reducing the inflammation which causes

demyelination, including molecules which target specific lymphocytes for depletion, inhibit T cell activation or block leukocyte infiltration of the CNS.

A schematic showing the relative safety and efficacy of the most common MS therapies is depicted in Figure 1.3. First-line therapies include subcutaneously-delivered IFN-β or GA, or orally-available dimethyl fumarate (DMF) or Teriflunomide[175]. Although treatments classed as first-line interventions are associated with fewer side effects or are more easily delivered to the patient they are also less effective than some of the other therapies available. Second-line therapies comprise many of the monoclonal antibodies which deplete certain leukocytes or target their activity or migration, as well as the orally-available Fingolimod which also targets leukocyte migration. While these therapies are more effective at treating MS, they are associated with a slightly higher risk of side effects. When first or second-line treatments have failed, third-line treatments are used. However, the side effects and risks associated with third-line therapies are significant and thus they are reserved for particularly aggressive MS. The mechanisms of action (Figure 1.4) and efficacy of some of these treatments are discussed in more detail below.

Two recombinant forms of IFN-β are available for treatment of MS; IFN-β1a and IFN-β1b. IFN-β1b was the first treatment approved by the FDA for MS in 1993. It reduces the annual rate of relapses by approximately 34%[176] and a 21-year long-term study revealed reduced mortality in MS patients that were treated with IFN-β1b early[177]. IFN-β1a also reduces the annual rate of relapses by up to 33%[178] and is associated with reduction in T2 lesion activity by MRI[179]. IFN-β increases the production of anti-inflammatory cytokines IL-4 and IL-10 by MBP-stimulated peripheral blood mononuclear cells (PBMCs) from MS patients[180] and expands IL-10-producing $CD56^{bright}$ natural killer (NK) cells and naïve Tregs[181]. It also suppress IFN-γ-induced up-regulation of some MHC-II molecules on antigen-presenting cells, reduce T cell migration into the CNS and increase apoptosis of activated T cells, although the full mechanisms of action of IFN-β in MS are not known[182,183]. IFN-β therapy is often associated with flu-like symptoms as a side effect although serious adverse events are rare[184].

Another first-line therapy, GA, is a mixture of short polypeptides of four amino acids that resemble MBP and induces proliferation of GA-specific lymphocytes including Tregs[96] (Figure 1.4 A) and Th2 cells which accumulate in the CNS and thus deviate the immune system reaction toward a less inflammatory Type 2 response there[185]. There is evidence that GA also modulates B cell responses in MS including increasing IgG4 antibodies[186-188], reduced LTα[189], IL-6 and TNF-α[190] and increased IL-10[189] production by B cells, and a reduction in $CD19^{+}$ B cells in the blood[191], although the significance of these to the clinical action of GA is not known[185]. DMF and Teriflunomide are also first-line small molecule treatments. DMF appears to increase antioxidant production through a nuclear factor (erythroid-derived 2)-like 2 (Nrf2)-dependent pathway[192] (Figure 1.4 E) and protects human astrocytes and rat cortical neurons against oxidative stress *in vitro*[193]. Taken twice daily, DMF reduced annual relapse rate by 53% in a phase III trial and also reduced lesion activity by MRI[194], whereas Teriflunomide, which suppresses proliferation of pro-inflammatory lymphocytes by

inhibiting pyrimidine synthesis (Figure 1.4 C) reduces annual relapse rate by approximately 31% and also reduces lesion activity measured by MRI[195]. These first-line therapies have many side effects and must be taken regularly. Although GA is similarly as effective as IFN-β therapy, it must be administered subcutaneously every day and is associated with pain and swelling at the injection site and lipoatrophy as well as chest-tightness, palpitations and anxiety in approximately 15% of patients[196]. Common side effects to DMF and teriflunomide, on the other hand, include nausea and diarrhoea, hair loss, infections of the respiratory tract and urinary tract, and liver function can also be affected[196].

The first mAb to receive FDA approval in 2004 was Natalizumab which binds α4-integrin, a component of very late antigen 4 (VLA-4), and blocks extravasation of leukocytes thus restricting the access of pathogenic cells to the CNS[197] (Figure 1.4 J). A series of other mAbs have since been generated targeting T or B cells, NK cells and monocytes[108,198] (Figure 1.4 F, G, H). They are generally classed as second or even third-line therapies since they can be associated with infusion-related adverse effects and many are immunogenic which limits the number of treatments a patient receives[199]. Although mAbs do not readily cross the blood-brain barrier, thus limiting their action primarily to SLOs or peripheral sites outside of the CNS, they have demonstrated good efficacy in improving disability and slowing the progression of MS. In a phase II clinical trial, Natalizumab reduced the annual relapse rate of MS by 68% and sustained progressive disability by 42% over 2 years[200]. Like Rituximab, Ocrelizumab and Ofatumumab target CD20 and thus deplete B cells. Rituximab reduced annual relapse rate by 43% over placebo in a phase II study whereas Ocrelizumab reduced the annual relapse rate by approximately 46% over IFN-β1a in two phase III clinical trials[109]. Ocrelizumab is also effective at reducing the risk for sustained progressive disability in PPMS patients by 24%[201]. The high degree of efficacy achieved with CD20-targeted monoclonal antibodies in MS have highlighted a significant role for B cells in the pathogenesis of the disease which was previously under-appreciated from rodent models. Alemtuzumab, directed against CD52 expressed by mature lymphocytes and monocytes causing their lysis after administration, is also effective in reducing annual relapse rate by 54.9% over IFN-β1a[202]. However it is also associated with significant side effects including immunosuppression and reactivation of dormant CMV infections or emergence of autoimmune conditions following off-target depletion of suppressor lymphocyte subsets[201,203]. Thus, Alemtuzumab is reserved for third-line treatment of MS.

The orally available sphingosine-1-phosphate (S1P) antagonist fingolimod prevents egress of lymphocytes from LNs and thus limits the traffic of immune effector cells to the CNS[204] (Figure 1.4 D). Fingolimod reduces the rate of relapse in MS patients[205] and is a second-line treatment for MS, although it has also been associated with increased skin cancers and herpes infections likely due to the lymphopenia which is induced in the blood of treated individuals[204]. Mitoxantrone, by contrast, is a third-line treatment for MS along with the aforementioned Alemtuzumab and autologous haematopoietic stem cell (HSC) transplant. Mitoxantrone targets DNA synthesis and repair mechanisms and suppresses lymphocyte proliferation[206]. It is highly effective in limiting the annual relapse rate of MS (63-68%) and significantly reduces EDSS deterioration[206], although cardiotoxicity has emerged as a significant side effect post-marketing[207] and it is therefore reserved for treating

patients in which several other types of therapy have failed[208]. Radiation and HSC transplant is also used to treat MS patients in which other treatment options have been exhausted[209]. Although radiation is effective in removing autoimmune cells from MS patients, HSC transfer is a highly invasive procedure exposing patients to complete immunosuppression prior to reconstitution of the immune system and is associated with a mortality risk of 2.8%[210].

Most MS patients try several different therapies over the course of their illness. Current treatments are associated with significant side effects including nausea, vomiting, alopecia, increased susceptibility to infection and certain cancers, cardiotoxicity, lymphopenia or leukopenia, infertility and many more[211]. Poor treatment response as well as needle fatigue, poor tolerability and convenience can all prompt patients to switch therapies and are also significant contributors to patients failing to adhere to treatment regimes. In fact, approximately 50% of patients on injectable therapies discontinue their treatment in the first year[211].

While current MS therapeutics have demonstrated efficacy in preventing relapses or delaying the progression of disease in RRMS, it is important to note that only a single treatment has been formally approved for progressive forms of MS. Furthermore, not all patients respond to the treatments available for relapsing MS. More importantly, no treatments are capable of reversing myelin damage in established lesions and they are therefore unable to improve accrued disability. It is clear that therapies which target inflammation only are insufficient and a therapy which combines suppression of the inflammation which causes myelin damage together with repair of the CNS is required. MSCs are promising therapeutic candidates for MS since they have demonstrated potential for both suppressing inflammation and facilitating CNS repair, possibly even regenerating new neurons or glial cells themselves.

3. MSCs

3.1 What are MSCs?

Stem cells are long-lived cells which can self-renew and differentiate into multiple different cell types[212]. Table 1.1 summarises different types of stem cells and their therapeutic advantages and limitations. MSCs have attracted a lot of interest as a source of stem cells for therapeutic uses since they are not plagued with the ethical concerns of embryonic stem (ES) cells and can be sourced directly from the patient, modified for gene delivery and have potent immunosuppressive and regenerative properties[212,213]. While pluripotent stem cells which include ES cells and induced pluripotent stem (iPS) cells have the capacity to differentiate into any cell type, multi-potent stem cells such as MSCs are more restricted in their differentiation capacity. Although this may restrict their use in some settings, MSCs are thus associated with a far lower risk of teratoma formation or ectopic tissue expression after transplantation[212].

MSCs are a reservoir of undifferentiated cells in most adult tissues which are thought to function to participate in and augment tissue renewal and repair. MSCs were first identified in bone by Friedenstein *et al*.,[214] in the

1960s as plastic-adherent colony-forming cells. Pittenger *et al*., later showed MSCs have adipogenic, osteogenic and chondrogenic potential[215]. The identification of similar plastic-adherent cells with clonogenic and multi-potent properties in most vascularised tissues since then has led to the now accepted concept that MSCs are ubiquitous within tissues[216,217]. MSCs are currently defined as multi-potent, plastic-adherent cells which express the surface markers CD105, CD73 and CD90, and lack expression of CD45, CD34, CD14 or CD11b, CD79α or CD19 and HLA-DR[218]. However, many of these markers are also shared by fibroblasts and other cell types and there are currently no unique markers to identify MSCs.

MSCs in culture represent a heterogeneous population of cells putatively consisting of *bona fide* stem cells, their progeny and probably some senescent cells[219,220]. The stem cell progeny is thought to be important for the survival and stemness of the "true" stem cells. Stemness here is defined as an undifferentiated, multi-potent state[216]. Efforts to isolate a single, unique type of stem cell from heterogeneous MSC cultures have been hampered by the absence of unique markers, artefacts introduced by culturing MSCs *in vitro* and the finding that MSCs in different tissues actually appear to be phenotypically and functionally distinct from one another[220,221]. Overall, it has been difficult to hone in on a single MSC population within the plastic-adherent stromal fraction which can be efficiently isolated and expanded *ex vivo*[221].

As previously mentioned, MSCs from different tissues may not have equivalent functional properties. A recent study by Sacchetti *et al.*,[222] challenges the perspective that MSCs in different anatomical niches are equitable sources of therapeutic value. Despite having similar *in vitro* multi-potent capacities, MSCs from different tissues proved to be highly restricted in their differentiation potential *in vivo.* Thus, the anatomical source of MSCs should be carefully considered to achieve the desired therapeutic outcome. The requirement for considering the anatomical source of MSCs for therapy is further supported by extensive research revealing that MSCs obtained from different tissues also vary in other biological characteristics. Proliferation rate, expansion potential, immunosuppressive capacity, production of growth factors and trophic molecules, migratory properties and response to pro-inflammatory stimuli are all factors which can vary with the anatomical source of MSCs[219,220,223,224]. In fact, even from the same donor, MSCs from dental pulp and periodontal ligament have been reported to have different multi-potencies, immunomodulatory parameters and responses to pro-inflammatory cytokines[225].

The following sections will describe the *in vivo* MSC niche in tissues and the role of MSCs in tissue renewal and response to injury and inflammation. The immunomodulatory functions and trophic and regenerative properties of MSCs are also discussed. An overview of MSC potential as a therapeutic agent in neurodegenerative diseases is presented including evidence from both animal studies and clinical trials. Finally, dental pulp stem cells (DPSCs) are introduced as a potential source of CNS-healing cells.

3.2 The MSC niche in tissues

In most adult tissues, MSCs reside within a perivascular niche that supports maintenance of "stemness" and quiescence[226-228]. Evidence suggests that MSCs associate with blood vessels where they are positioned to respond to both local cues and distant cues carried by the nervous system and blood (Figure 1.5)[216,227-229]. In fact, due to the expression of similar surface markers and multi-potency by both MSCs and pericytes, there is debate whether these two cell types are distinct from one another[227,230,231]. Fate-mapping has revealed MSCs *in vivo* are derived from both pericytes and adventitial cells[232] and a separate study revealed that MSCs as isolated in culture may be *ex vivo* counterparts of pericytes[233].

In stem cell niches *in vivo*, cells which support the maintenance of MSCs include endothelial cells, fibroblasts and nerves[216,234]. Direct membrane protein interactions between these other cells and MSCs as well as secreted factors and insoluble extracellular matrix (ECM) proteins collectively contribute to MSC survival, quiescence and maintenance of stemness[216]. For example, fibroblast growth factor-2 (FGF-2) and leukaemia inhibitory factor (LIF) maintain MSC stemness while Wnt signalling has been shown to be important for maintaining MSCs in a quiescent state[235]. Other signalling molecules required for MSC maintenance are still under investigation.

MSCs can be activated and respond to inflammatory cues including cytokines, growth factors and changes to the ECM[216,226]. After activation they are thought to migrate to sites of tissue damage where they can differentiate into new cell types, secrete factors which recruit and promote differentiation of other precursors, and interact with inflammatory cells to promote immune responses which facilitate tissue repair[216]. The *in vivo* cues for activation are not well known and studying the role of MSCs *in vivo* has been hampered by the lack of unique markers to identify them.

In addition to their role in providing trophic support to tissues, participating in and orchestrating repair, MSCs can also regulate inflammation in tissues. MSCs appear to functionally repress highly inflammatory immune responses and steer the response toward repair and resolution of inflammation. These immunomodulatory properties of MSCs have received a lot of attention as therapeutic devices and will be discussed in more detail below.

3.3 MSC immunomodulatory properties

MSCs have demonstrated a wide range of immunomodulatory effects on a number of cells in both innate and adaptive arms of the immune system (summarised in Figure 1.6). Several surface molecules and secreted factors have been identified as participants in MSC-dependent regulation of leukocyte function. The specific mechanisms used to modulate immune responses vary according to the species[236,237], anatomical source of the MSCs, disease model and whether they are exposed to pro-inflammatory cytokines[238,239].

The expression of surface molecules and secreted factors by MSCs from different tissues under different stimulatory or non-stimulatory conditions are listed in Tables 1.2 and 1.3 for human and mouse-derived MSCs

respectively. MSCs from both humans and mice have been shown to constitutively express IL-10. Indoleamine oxidase (IDO) has been shown to be expressed at basal levels by MSCs in some studies but can be up-regulated upon stimulation with IFNγ or TNFα. Whereas TGF-β1 is expressed constitutively by murine BM-MSCs and is unaffected by stimulation with IFNγ or TNFα, in humans those cytokines suppress expression of TGFβ1.

In autoimmune diseases such as MS, several hierarchical opportunities exist for potential MSC immuno-regulation. Broadly, these are priming of naive lymphocytes, suppressing proliferation or inducing apoptosis of pro-inflammatory cells, inhibiting differentiation of effector cells or promoting differentiation of regulatory cell subsets, and suppressing effector cell function. Following are several immune cell subsets which can be modulated by MSCs with brief discussion of the mechanisms and outcomes of MSC interactions with those cells.

1.1.1.1 MSC effects on APCs

MSC regulation of APCs can influence both priming of naïve lymphocytes and reactivation of mature effector subsets at the site of inflammation. MSCs can inhibit the differentiation of monocytes into immature DCs and the maturation of DCs after antigen encounter[240] including reducing their expression of co-stimulatory molecules including CD40, CD80, CD83 and CD86 as well as MHC-II which impairs their ability to stimulate allogeneic T cells[241-244]. When matured in the presence of MSCs, DCs also secrete more anti-inflammatory IL-10 and reduced levels of pro-inflammatory cytokines such as IL-12 and TNFα[240,244,245].

MSCs can also suppress maturation of macrophages and microglia to a pro-inflammatory M1 phenotype and promoting differentiation to a neuroprotective M2 phenotype, which is one way in which MSCs might suppress CNS inflammation and promote remyelination. MSCs skew polarisation of macrophages and microglia in this way via production of prostaglandin E2 (PGE_2) or TNF-stimulated gene-6 (TSG-6)[246]. MSCs also suppress the up-regulation of activation markers on macrophages including CD80, CD86 and MHC-II. Macrophages also demonstrate increased phagocytic activity after activation in the presence of MSCs which is associated with a regulatory M2 phenotype. Microglia stimulated with LPS in the presence of MSCs secrete lower levels of the highly inflammatory cytokines TNFα, IL-1β and IL-6[247]. Overall the suppressive capacity of MSCs toward macrophages and microglia can both promote regeneration of the CNS and disarm the inflammatory response.

1.1.1.2 MSC effects on T cells

In addition to their impact on lymphocyte priming through modifications to APCs, MSCs have been shown to directly inhibit T cell activation *in vitro*. Proliferation of both $CD4^+$ and $CD8^+$ T cells in MLRs or following stimulation with mitogens or anti-CD3 is inhibited by MSCs[237-239,248-254]. Differentiation of $CD4^+$ T cells to effector or regulatory subsets can also be regulated by MSCs. MSCs have been shown to inhibit $CD4^+$ T cell differentiation into pro-inflammatory Th1[254,255] and Th17 cells[256] and promote differentiation of

anti-inflammatory Th2 cells[257] and Tregs[256,258-260]. MSCs have also been demonstrated in some conditions to promote apoptosis of T cells[261].

A number of molecules have been shown to mediate MSC effects on T cells. Production of PGE_2 by cyclooxygenase 2 (COX2)-expressing MSCs suppresses Th17 cell differentiation[256,262] and γδ T cell proliferation, cytokine production and cytotoxicity[263]. PGE_2 and TGF-β1 expression by MSCs have conversely been shown to promote Treg expansion[258,260]. Furthermore, apoptosis of T cells is induced by Fas/Fas ligand (FasL) interactions or production of nitric oxide (NO) by murine BM-MSCs (mBM-MSCs)[261,264].

In disease settings, MSCs have been shown to induce a switch from Th1 to Th2 cells in EAE which abrogated EAE symptoms[257]. In another study of EAE, mBM-MSCs suppressed Th17 cells but induced Tregs thus attenuating disease[265]. MSCs also modulate T cells in experimental colitis. In DSS-induced colitis, mBM-MSCs produced the chemokine CCL2 to bring T cells into proximity of the MSCs for FasL-mediated apoptosis[261]. The resulting apoptotic bodies induced TGF-β expression in macrophages which promoted the expansion of Tregs. mBM-MSCs also induced apoptosis of activated T cells via production of NO in the LNs of mice with delayed-type hypersensitivity (DTH) which limited infiltration of the ears with T cells and reduced swelling[264]. From these examples it can be seen that the potential for MSCs to modulate T cell responses has been clearly identified *in vitro* and demonstrated to be important for their anti-inflammatory effects in several disease settings *in vivo*.

1.1.1.3 MSC effects on B cells

Several studies have investigated the effects of BM-MSCs on B cells *in vitro*. mBM-MSCs inhibited proliferation and differentiation of mouse B cells activated by lipopolysaccharide (LPS) via the PD-1/PD-L1 pathway[266]. In that study, expression of PD-L1 was dependent on pre-activation of the BM-MSCs with IFN-γ, while pre-activation was not required for PD-L1-mediated suppression of B cell proliferation in another study[267]. Soluble factors have also been shown to be important for MSC suppression of B cell proliferation or differentiation[268,269] Secretion of immunoglobulin (Ig) by ovalbumin (OVA)-specific plasma cells was inhibited by secretion of a truncated form of CCL2 from BM-MSCs[269]. In contrast, increased survival and IgG-secretion by OVA-specific plasma cells was reported after co-culture with mBM-MSCs[270]. Rasmusson *et al*. also reported increased Ig production by human B cells co-cultured with MSCs but only under conditions of low stimulation. Under strong stimulation Ig production by B cells was conversely inhibited by the presence of MSCs[271]. Tabera *et al*. similarly reported that the outcome of co-culturing B cells and MSCs was dependent on the strength of the stimulus. MSCs inhibited proliferation of human B cells only under highly proliferative conditions, whereas weaker stimuli resulted in promotion of B cell proliferation by the MSCs[272].

In SLE models in mice, allogeneic BM-MSCs appear to worsen disease[270], while conditioned medium from syngeneic mBM-MSCs attenuated the secretion of antigen-specific IgM and IgG1 through T cell-dependent and –independent mechanisms[273]. Early treatment of SLE with fortnightly injections of human adipose-derived

MSCs (hAd-MSCs) improved survival and reduced circulating anti-dsDNA antibodies[274], and hBM-MSCs co-administered with cyclophosphamide also reduced serum anti-dsDNA antibodies[275]. In a heart allograft model, mBM-MSCs inhibited alloreactive antibody levels and tolerance was achieved when the MSCs were co-administered with rapamycin[276].

The potential for MSCs to affect B cell proliferation, differentiation and Ig production has been clearly demonstrated *in vitro*. The outcome of interactions between MSCs and B cells appear to depend on the stimulus or model, and both contact-dependent and contact-independent mechanisms have been shown to be employed by MSCs to exert their effects. MSC effects on B cells *in vivo* are less clear although they improve disease outcome in certain circumstances such as human MSCs suppress SLE but allogeneic mouse MSCs do not.

1.1.1.4 Factors affecting the immunomodulatory properties of MSCs

In some settings the immunomodulatory capacity of MSCs has reportedly increased after stimulation with pro-inflammatory factors such as IFNγ, TNFα and IL-17A. Some studies show constitutive expression of immunomodulatory molecules by MSCs while in others pre-activation of the MSCs with pro-inflammatory cytokines is required for beneficial effects (see Tables 1.2 and 1.3). In one study, heterogeneity in expression of several immunomodulatory molecules between BM-MSC clones derived from a single mouse was abolished by treatment with IFNγ and TNFα[253]. This suggests that not all MSCs are equally immunosuppressive. Some of the variation between studies in immunosuppressive potential of MSCs or their expression of immunomodulatory molecules may also arise from different isolation and culturing methods which could affect the activation status of the MSCs.

3.4 MSCs in treatment of MS

MSCs have demonstrated good potential as a treatment for a wide range of injuries and diseases including degenerative disorders of the CNS (Figure 1.7). In MS, several studies have demonstrated marked improvement to disability after MSC treatment for a proportion of patients[277-280]. In one case study which combined intrathecal and intravenous treatment with umbilical cord-derived MSCs (UC-MSCs), improved sensory impairment and muscle strength was observed within days and was associated with reduced MS lesion load[281]. In many patients who don't show marked improvement after MSC treatment in trials, no changes in disability status or lesion activity are observed suggesting stabilisation of disease[277,278].

A summary of outcomes of MS clinical trials testing MSC treatments is given in Table 1.4. Autologous BM-MSCs delivered to MS patients intrathecally improved the mean EDSS in 3 separate clinical trials[277-279] and in another when the BM-MSCs were delivered intravenously[280]. UC-MSCs that were administered intrathecally and intravenously also improved mean EDSS and this was also associated with reduced lesion load[281]. In contrast, one study found that patients that received intrathecal BM-MSCs showed new or enhanced lesions by MRI despite having improved EDSS[279]. In a small clinical trial using placenta-derived MSCs in MS

patients, no improvements were found but there was also no worsening of disease[282]. Mohajeri *et al*. measured *FOXP3* expression in the blood of MS patients that received intrathecal autologous BM-MSC transfers and found increased transcript by qPCR, indicating that MSC therapy may increase regulatory lymphocytes in the blood[283].

While MSC clinical trials for MS and other neurodegenerative disorders have demonstrated clear therapeutic promise, questions remain over the best route of delivery, mode of action and optimal source of MSCs for treatment. Most clinical trials to date have used BM-MSCs despite animal studies showing other sources such as adipose tissue or placenta may be more effective for healing the CNS. The mode of action of MSCs in humans is relatively unknown, although some clinical trials have measured changes in PBMCs during follow-up. Studies have reported increased Tregs[277,283], reduced activated myeloid DCs[277], fewer activated $CD40^+$ cells[277] and a reduction in IL-6 production by PBMCs[278]. Together, these observations suggest MSC treatment dampens inflammation in MS patients.

3.5 Modifying MSCs to improve therapy

MSCs are proposed cellular vehicles for delivery of transgenes to patients. MSCs have been widely reported to be readily transduced and maintain long-term expression of transgenes while preserving their multi-potency, immunomodulatory and regenerative capabilities[284,285]. Their homing to inflamed sites or specific organs can be enhanced by overexpressing chemokine receptors or adhesion molecules. For example, overexpression of CCR7 in Ad-MSCs which lacked basal expression of this receptor improved homing of these cells to SLOs in mice where CCL19 and CCL21 are constitutively expressed at homeostasis[286]. CXCR5 overexpression significantly enhanced the homing of hBM-MSCs to injured tissue in a mouse model of contact hypersensitivity and improved their localisation with T cells which potentiated their suppression of the T cell function[285]. Immunomodulatory functions of MSCs can also be enhanced by overexpression of cytokines or other regulatory molecules. As an example, hBM-MSCs transduced to over-express ICOSL more effectively induced Treg differentiation than control hBM-MSCs *in vitro*[287]. Overexpression of TGF-β1 in rat BM-MSCs enhanced their induction of Tregs and suppression of Th17 cells and thus increased long-term survival of rats which received liver transplants[288]. Additionally, neuroprotective or reparative effects of MSCSs can be enhanced by overexpression of growth factors or neurotrophic molecules. hUC-MSCs expressing soluble intercellular adhesion molecule-1 (sICAM-1) reduced amyloid-β plaques in a transgenic mouse model of Alzheimer's disease after transplantation into the hippocampus[289]. Lastly, brain-derived neurotrophic factor (BDNF) overexpression has improved repair mechanisms in animal models of brain, spinal cord or nerve injury, stroke and Huntington's disease[290-296]. Periodontal ligament stem cells (PDLSCs) transduced with CXCL12 could significantly promote bone tissue repair and angiogenesis in a rat critical-sized calvarial bone defect model[297] while mAd-MSCs overexpressing FGF-2 accelerated healing of bone fractures in mice[298]. Thus, the therapeutic capacity of MSCs can readily be enhanced or tailored for specific outcomes.

3.6 Dental pulp stem cells (DPSCs)

DPSCs were first isolated more than a decade ago[299] and are of an ecto-mesenchymal lineage thought to be derived from the neural crest[300] or glial cells[301]. They have been shown to express markers of MSCs and can differentiate into adipocytes, osteocytes and chondrocytes[302,303]. To date, studies using DPSCs are relatively limited, though they are rapidly attracting interest as potential therapeutic agents like other MSCs. Research has largely focussed on their odontogenic properties although their neurogenic properties have more recently been recognised.

DPSCs readily differentiate into cells of the neural lineage including neurons[304-307] and astrocytes[308]. In addition to studies showing that DPSCs can differentiate into functional neurons *in vitro*[305,306,309,310], Gronthos *et al.* showed that DPSCs expressed neural morphology and markers after transplantation into the mesencephalon of chicken embryos[305]. Furthermore, in a rat model of stroke DPSCs injected into the brain migrated to lesions and took on astrocyte and neuronal morphologies[311]. Although only 2.3% of transplanted cells were reported to survive after 4 weeks, DPSC treatment was associated with improved neurobehavioural recovery. Thus, DPSCs have demonstrated good neurogenic potential both *in vitro* and *in vivo*.

Like other MSCs, DPSCs may also promote tissue repair through recruitment of precursors and other cells. After injection into the developing hindbrain of chicken embryos, DPSCs secrete CXCL12 causing chemoattraction of nearby axons[312]. DPSCs also have immunomodulatory properties and have been shown to inhibit proliferation and induce apoptosis of T cells *in vitro* through (FasL)[313], although other potential immunomodulatory properties remain undefined.

4. The research project

MSCs from dental pulp have strong potential for treatment of neurodegenerative disorders. DPSCs may have advantages over other stem cell populations for use as a therapy for MS. They can be isolated from the teeth of patients of many ages,[314,315] which is a less invasive procedure than harvesting bone marrow. Moreover, the origin of DPSCs from the neural crest infers they may be more suited than other types of MSCs for treatment of neural pathologies such as MS if the desired mode of action is cell replacement.

The use of DPSCs in treatment of neurodegenerative disorders is a relatively new concept with studies thus far focussing mostly on their potential for CNS repair in models of stroke. They remain poorly characterised in terms of their immunomodulatory function while their ability to treat neurodegenerative diseases of an autoimmune nature including MS is essentially unknown. Thus, whether DPSCs are suppressive in models of MS is an important question that this study aims to address. Also, whether DPSCs can modulate the immune system and have anti-inflammatory effects that can be harnessed in therapeutic settings is yet to be investigated.

Another goal of this study was to determine whether DPSCs can be manipulated to overexpress anti-inflammatory molecules and if this would affect their therapeutic properties. Anti-inflammatory molecules that were chosen to be overexpressed on DPSCs were the atypical chemokine receptors ACKR2 and ACKR4

described in Section 1.1.4. Additionally, development of a novel IL-23 antagonist was undertaken to target the generation of pathogenic Th17 cells in EAE and it was anticipated that this antagonist could also be expressed on DPSCs. Another objective of genetically modifying DPSCs in this study was to insert a reporter to facilitate tracking them *in vivo*, since it is not known if DPSCs can enter and persist the CNS after they are administered systemically.

To address these questions, human DPSCs would first be isolated from different donors and characterised *in vitro*. Human MSCs are commonly studied in animal models without apparent adverse effects. In the present study, two main considerations evoked a preference for human DPSCs. The first is that murine DPSCs are derived from incisors which are continuously growing in contrast to human molars which do not continue to grow once they are fully developed, and it is not known how these differential growth requirements may affect the stem cell populations in the teeth. Secondly, the immunomodulatory aspects of the DPSCs were to be the primary focus of their use in EAE, and species variation exists in the mechanisms of action of some other MSCs (Section 1.2.3)[236,237].

The following hypotheses and aims were developed for this study:

Hypothesis 1: Human dental pulp is a source of MSCs that will inhibit EAE.

Aim 1.1: To characterise MSCs isolated from human dental pulp.

Aim 1.2: To determine the effect of DPSC treatment in models of EAE.

Aim 1.3: To determine if DPSCs migrate to the CNS in EAE

Aim 1.4: To examine the immunomodulatory effects of DPSCs in EAE.

Hypothesis 2: DPSCs can be a useful tool for delivery of anti-inflammatory molecules in EAE.

Aim 2.1: To optimise a protocol for lentiviral transduction of DPSCs.

Aim 2.2: To generate DPSCs expressing anti-inflammatory molecules.

Aim 2.3: To determine the effect of lentiviral transduction on the MSC characteristics of DPSCs.

Aim 2.4: To test if expression of anti-inflammatory molecules by DPSCs improves their ability to suppress EAE.

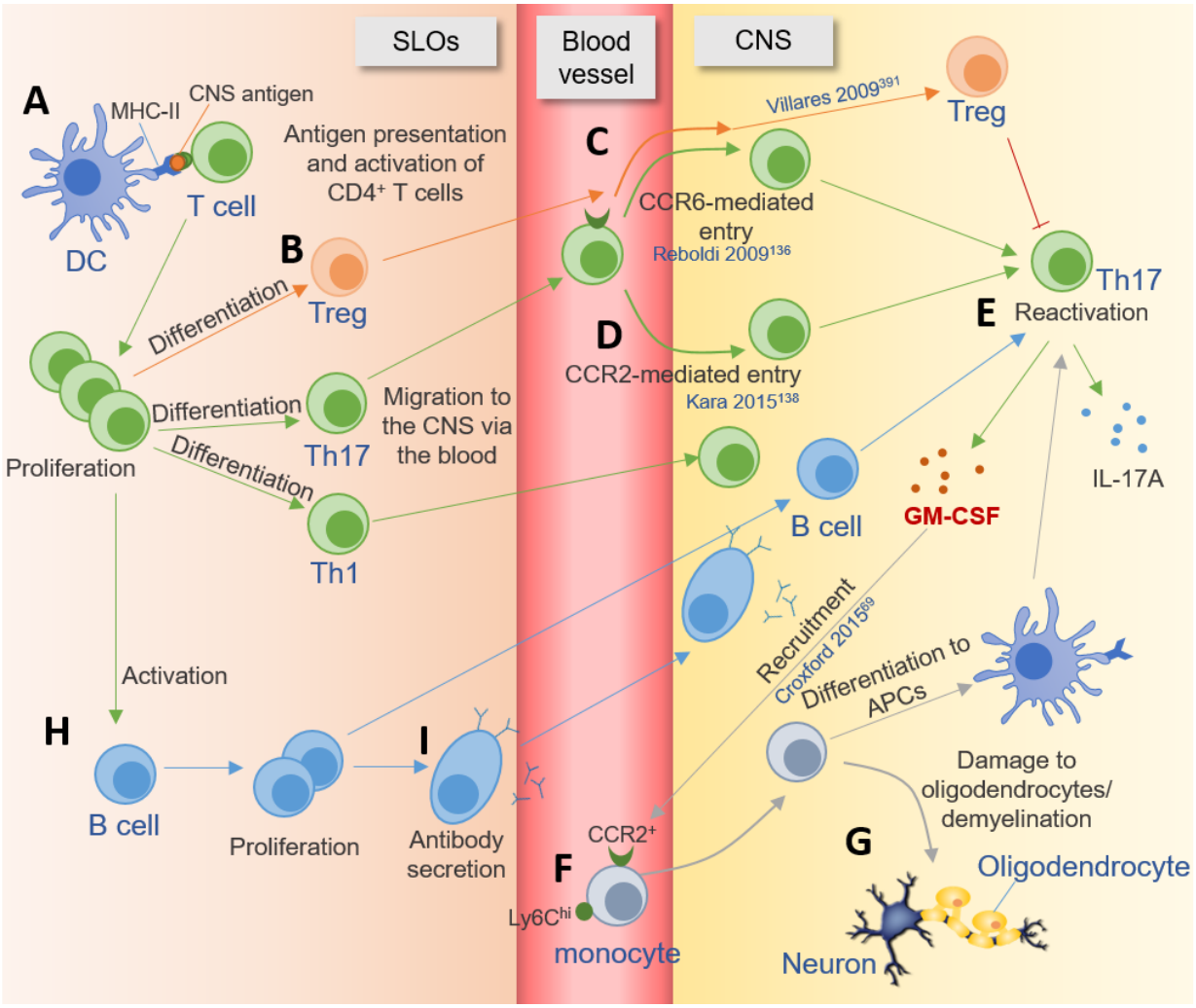

Figure 1.1. Pathogenesis of EAE.

Antigen presentation by DCs in the SLOs leads to priming of $CD4^+$ T cells **(A)** which subsequently expand and differentiate into effector T cell subsets including Th1 and Th17 cells **(B)**. Th17 cells migrate to the CNS via the blood, whereupon they enter the CNS by CCR6- (early phase; **C**) or CCR2-mediated (mid-late phase; **D**) chemotaxis. Th17 cells are reactivated the CNS by local APCs and secrete large quantities of proinflammatory cytokines **(E)**. The secretion of GM-CSF recruits $CCR2^+Ly6C^{hi}$ pro-inflammatory monocytes from the blood into the CNS **(F)**. The monocytes differentiate into APCs which further participate in reactivating and stimulating pathogenic T cells. The precise mechanisms of oligodendrocyte death and, consequently, demyelination have yet to be determined but evidence suggests products of either infiltrating myeloid cells or T cells that are reactivated by myeloid infiltrates have cytotoxic effects on oligodendrocytes **(G)**. Other leukocytes also participate in EAE pathogenesis. $CD4^+$ T cells can activate B cells **(H)** which can contribute to EAE pathology by secreting autoantibodies or presenting antigen to T cells in the CNS **(E)**. Tregs, which also enter the CNS via expression of CCR6 **(C)**, can limit inflammation in the SLOs and CNS by secreting IL-10 which is protective in EAE. Other cells which also contribute to pathogenesis of MS not depicted in this simplified immunopathological cascade include NK cells, γδ T cells, Th1 cells, $CD8^+$ T cells and neutrophils.

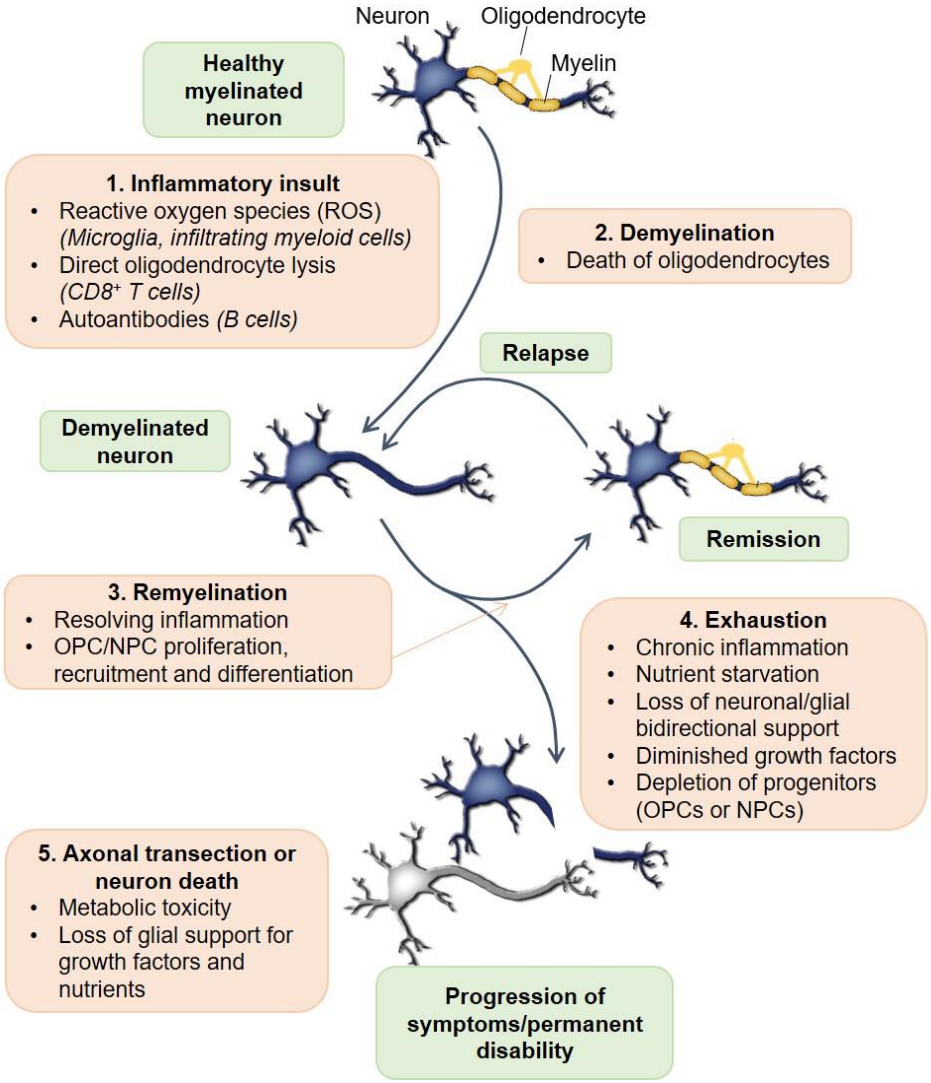

Figure 1.2. Causes and effects of demyelination in MS.

In a healthy brain, neurons are insulated by cholesterol-rich extensions of oligodendrocytes called myelin. (1,2) The initial demyelinating event in MS is unclear but is likely to be due to inflammatory insult resulting in the death of oligodendrocytes. (3) In the initial stages of MS, there are attempts to remyelinate the neurons which may or may not be successful. A patient may experience a series of demyelination and remyelination events which may reflect the relapsing and remitting course of the early stages of disease. (4) After some time, the repair process is exhausted and remyelination fails. Chronic inflammation may hinder the remyelination process, as may the gradual depletion of progenitors which differentiate into new oligodendrocytes. Since a bidirectional system exists between neurons and glial cells for nutrient and growth factor support, repeated rounds of demyelination may also result in the loss of glial cells which are no longer supported by neurons. (5) Demyelinated neurons are inefficient energy and signal transporters and are susceptible to nutrient starvation and metabolic toxicity. Eventually, the death of neurons or transection of their axons results in permanent symptoms and progression of disability.

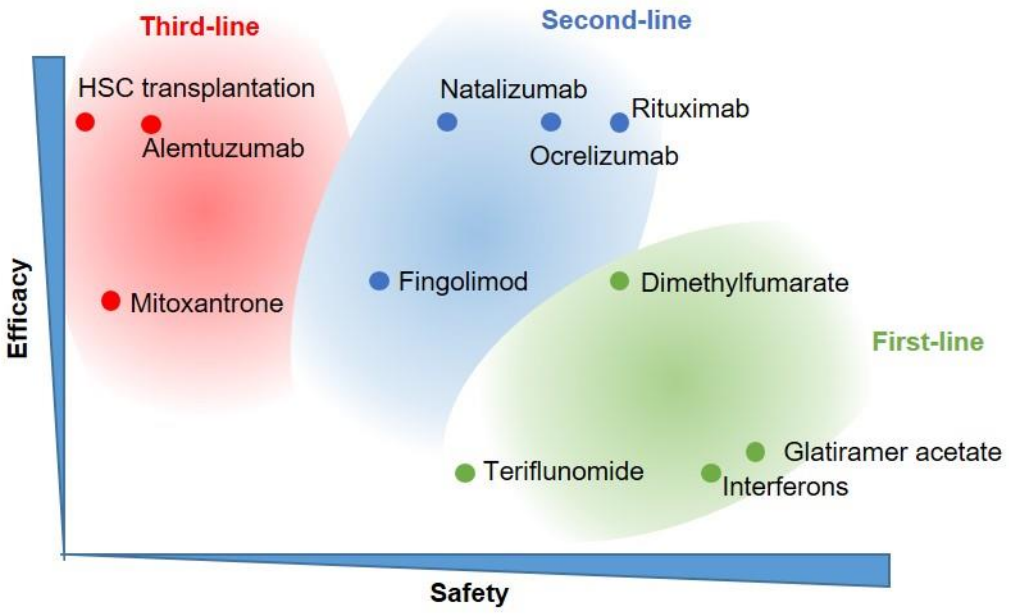

Figure based on Hauser *et al*., *Annals of Neurology* [199]

Figure 1.3. Safety and efficacy profile of various MS treatments.

Treatment options for MS vary in their efficacy and safety and thus a cost-benefit analysis is usually applied in decisions regarding which treatments are recommended to each patient. In the US, first-line therapies are generally associated with fewer side effects or are more easily administered than second and third-line therapies, although they also tend to be less effective in controlling disease. As MS progresses, patients are often switched to second or third-line therapies which have a lower safety profile but are more effective in treating highly active or advanced disease.

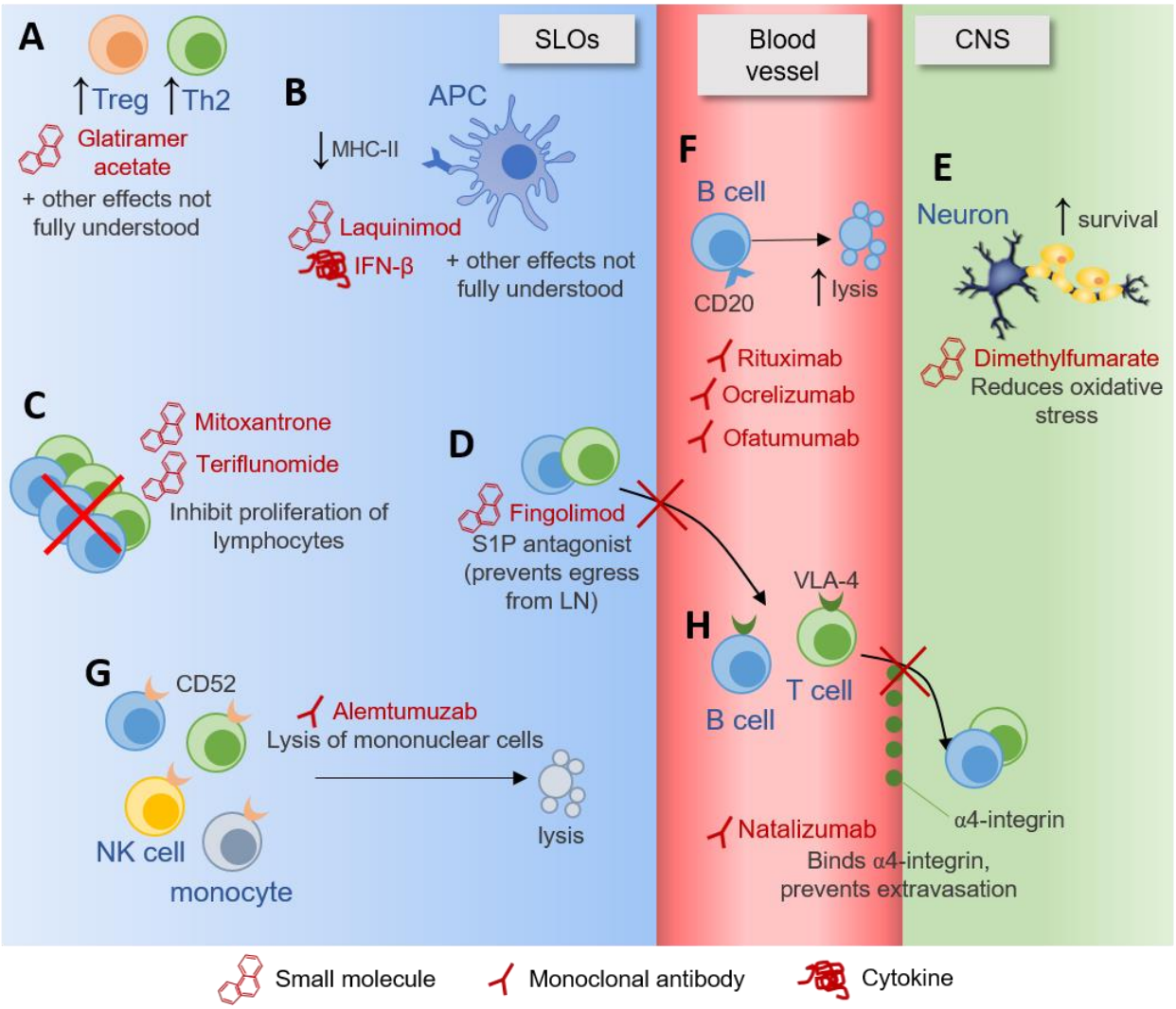

Figure 1.4. Therapeutic targets and modes of action of common treatments for MS.

Regulation of inflammation is the primary target of most current MS therapies. Treatment options include injectable GA **(A)**, IFN-β **(B)** and mitoxantrone **(C)**. The mechanisms for GA and IFN-β are not well understood but they appear to create a more regulatory environment. Fingolimod **(D)** was the first orally available treatment for relapsing MS. It is an S1P antagonist which restricts the migration of lymphocytes to the CNS by preventing their egress from the LN. Other oral treatments for MS include laquinimod **(B)**, teriflunomide **(C)** and DMF **(E)**. Since the targets of these molecules are non-specific, a multitude of off-target effects occur which have led to serious adverse events or side effects for many patients. Several mAbs have recently been developed targeting CD20 **(F)**, CD52 **(G)** and α4-integrin **(H)**. These mAbs afford a more targeted approach to suppressing autoimmunity although they are still associated with side effects including broad immunosuppression and increased susceptibility to certain cancers and infections. The effects of antibody-depletion are also transient, with some cell populations replenishing within weeks while the immunogenicity of many of the mAbs limits how many times they can be readministered. Also, since they have limited ability to enter the CNS, the effects of mAbs are also restricted to the periphery.

Type of stem cell	 Embryonic stem (ES) cells	 Induced pluritpotent stem cells (iPSCs)	 Mesenchymal stem cells (MSCs)
Source	Blastocyst	Reprogrammed from somatic cells	Reservoirs in most adult tissues
Differentiation potential	Pluripotent (unrestricted)	Pluripotent (unrestricted)	Multipotent (somewhat restricted)
Therapeutic advantages	– Unrestricted potential for differentiating into any cell type	– Can be sourced from the patient and transplanted autologously	– Can be sourced from the patient and transplanted autologously – Low risk of teratoma formation or ectopic tissue expression
Therapeutic disadvantages	– Not sourced from the patient – risk of allograft rejection or GVHD – High risk of teratoma formation or ectopic tissue expression	– High risk of teratoma formation or ectopic tissue expression	– Differentiation potential limited

Table 1.1: Characteristics of different types of stem cells.

Embryonic stem (ES) cells are harvested from embryos at the blastocyst stage of development whereas induced pluripotent stem (iPS) cells are reprogrammed to a stem-like state from somatic cells. Adult stem cells include both haematopoietic stem cells, which reside in the bone marrow and as a pool for renewal of immune system and blood cells, and MSCs which can be found in most adult tissues as a reservoir for cell replacement after tissue injury, growth or renewal. The advantages and disadvantages for using each type of stem cell depends on therapy requirements. For example, both iPS cells and MSCs can be sourced from the patient but while iPS cells have a wider differentiation potential, MSCs carry reduced risk of teratoma and ectopic tissue formation and so MSCs may be more suitable for certain applications.

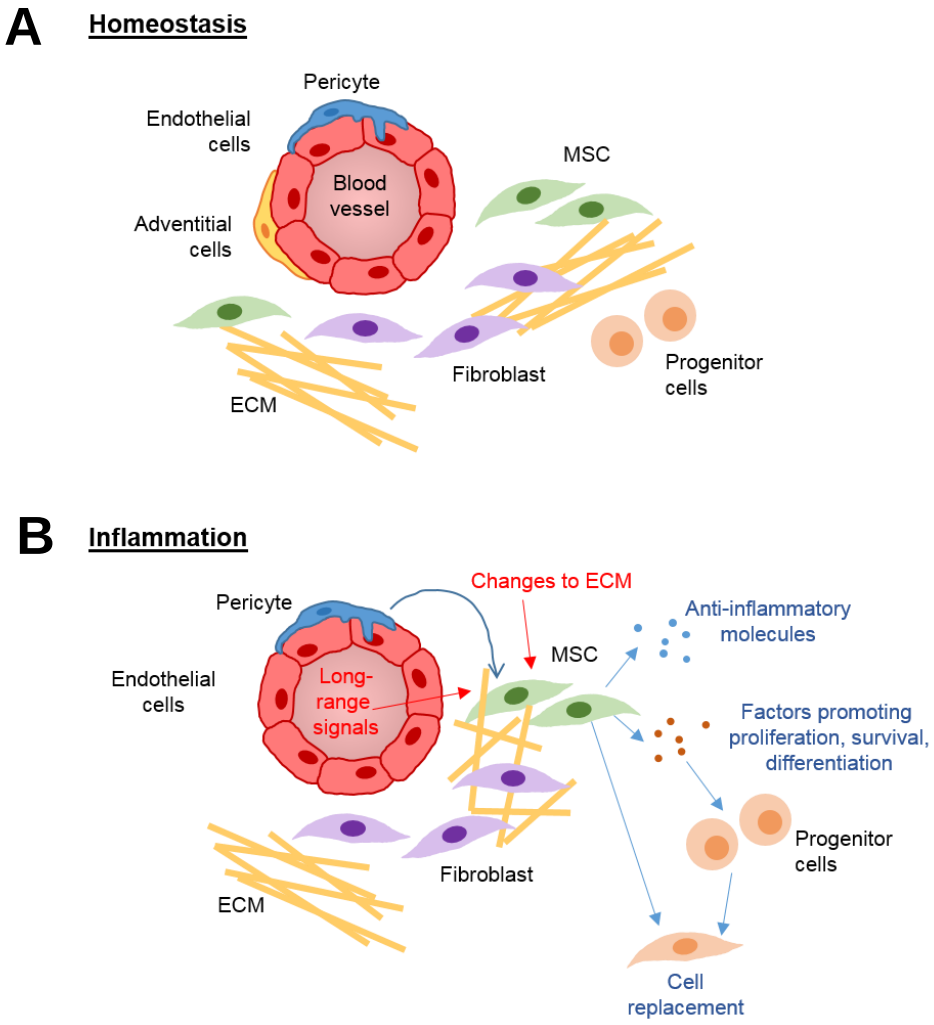

Figure 1.5. The MSC niche in tissues during homeostasis and inflammation.

(A) Homeostasis; MSCs are thought to reside in the perivascular niche. Pericytes, adventitial cells and MSCs associate closely with blood vessels. It is thought MSCs can arise from either pericytes or adventitial cells although this likely depends on the tissue[232]. MSC survival, quiescence and stemness are maintained by blood endothelial cells, fibroblasts, signals through nerves, and interactions with the ECM. **(B)** Inflammation; MSCs are activated by proximal signals through changes in the ECM or by factors produced by fibroblasts or endothelial cells. Distant inflammatory cues are carried via nerves or the blood. After activation, MSCs mobilise and proliferate and can contribute to tissue repair and regeneration through i) secretion of trophic molecules which support proliferation and differentiation of local progenitor cells; ii) production of anti-inflammatory molecules which limit further tissue damage and promote repair by fibroblasts and other cells or; iii) differentiation to replace lost or damaged cells.

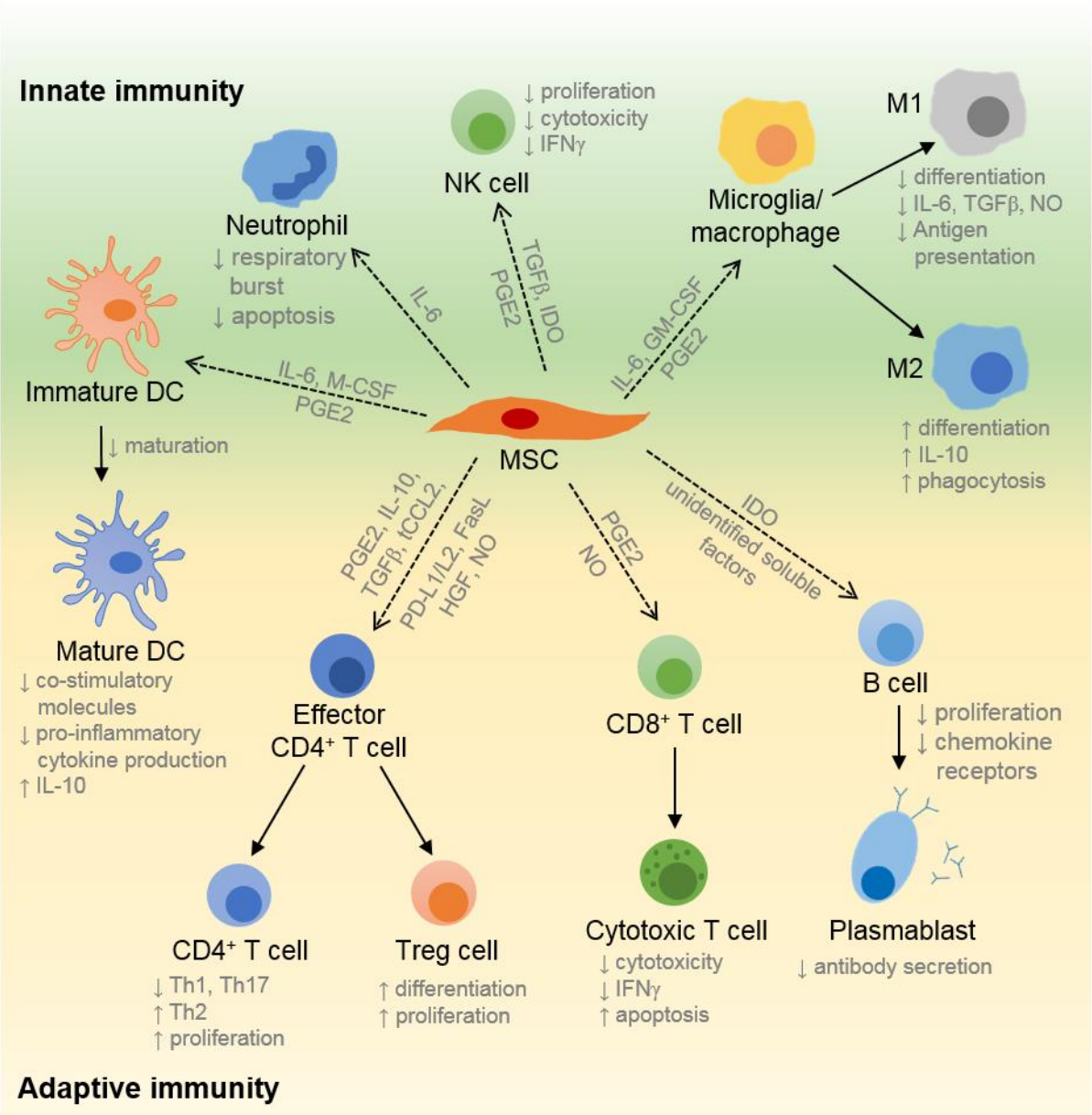

Figure 1.6. Immunomodulatory effects of MSCs.

MSCs produce a range of soluble and membrane-bound factors which modulate both innate and adaptive immune responses. MSCs inhibit the maturation of antigen-presenting cells (APCs) including DCs, macrophages, B cells and the CNS-resident microglia. Alternatively, these APCs can be matured to tolerogenic or anti-inflammatory phenotypes associated with tissue repair, such as M2 macrophages and microglia and IL-10-producing DCs. These changes in APC function modulate the activation and differentiation of effector cell subsets including lymphocytes and innate effectors. Alternatively, MSCs can directly interact with lymphocytes to inhibit their activation, proliferation and differentiation into pro-inflammatory effector cells and promote differentiation and expansion of anti-inflammatory cells including Th2 cells and Tregs.

Table 1.2: Expression of immunomodulatory factors by MSCs from humans.

Immunomodulatory factor	Anatomical source of MSCs	Expression	References
COX2/PGE2	Adipose tissue	Upregulated* (T cell co-culture)	248
	Bone marrow	Constitutive Upregulated* (IL-1β, IFNγ, TNFα or T cell contact)	249,250,316 248,252,255,256,263
	Wharton's jelly	Upregulated* (T cell co-culture)	248
IDO	Bone marrow	Induced (IFNγ) Upregulated* (IFNγ or TNFα)	239,251 237,317
TGF-β1	Bone marrow	Constitutive *(unaffected by IFNγ or TNFα)*	249,250,317
GM-CSF	Bone marrow	Upregulated* (when trapped in lung emboli)	318
M-CSF	Bone marrow	Constitutive	319
HGF	Bone marrow	Upregulated* (IFNγ) Constitutive	249 320
IL-10	Bone marrow	Constitutive *(unaffected by IFNγ + TNFα)*	317
	Bone marrow	Constitutive *(unaffected by IFNγ)*	249
IL-6	Bone marrow	Constitutive	319
SOD3	Bone marrow	Upregulated* (only by both IFNγ + TNFα combined)	321
TSG-6	Bone marrow	Upregulated* (when trapped in lung emboli, TNFα)	318
iNOS (NO)	Bone marrow	Upregulated* (IFNγ, IFNγ+TNFα or IFNγ+IL-1α synergistically)	237

**Upregulated; the molecule is expressed constitutively but upregulated further after pro-inflammatory stimulation (stimuli in parentheses).*

Table 1.3: Expression of immunomodulatory factors by MSCs from mice.

Immunomodulatory factor	Anatomical source of MSCs	Expression	References
Nos2, Ptgs2	Bone marrow	Upregulated (IFNγ + TNFα)	253
iNOS	Bone marrow	Induced (IFNγ + TNFα synergistically)	237,254
IDO	Bone marrow	Induced (IFNγ + TNFα)	253
	Bone marrow	Expressed*	259
	Bone marrow	Induced (IFNγ, much less for TNFα, IL-1β)	237
	Bone marrow	Induced (IFNγ)	238
PGE2	Bone marrow	Upregulated (T cell contact, IFNγ or TNFα)	238,262
FasL	Bone marrow	Constitutive	261
HGF	Bone marrow	Upregulated (IFNγ or TNFα)	238
TGF-β1	Bone marrow	Downregulated (IFNγ or TNFα)	238
	Bone marrow	Upregulated (PHA-stimulated splenocyte secreted factor - transwell)	267
PD-L1	Bone marrow	Induced (IFNγ)	238
	Bone marrow	Constitutive	267
PD-L2	Bone marrow	Constitutive	267
IL-10	Bone marrow	Constitutive	267
Truncated CCL2	Bone marrow	Constitutive	269

**Expressed; functionally determined to be important in model but authors did not investigate whether it is expressed constitutively or induced in their system.*

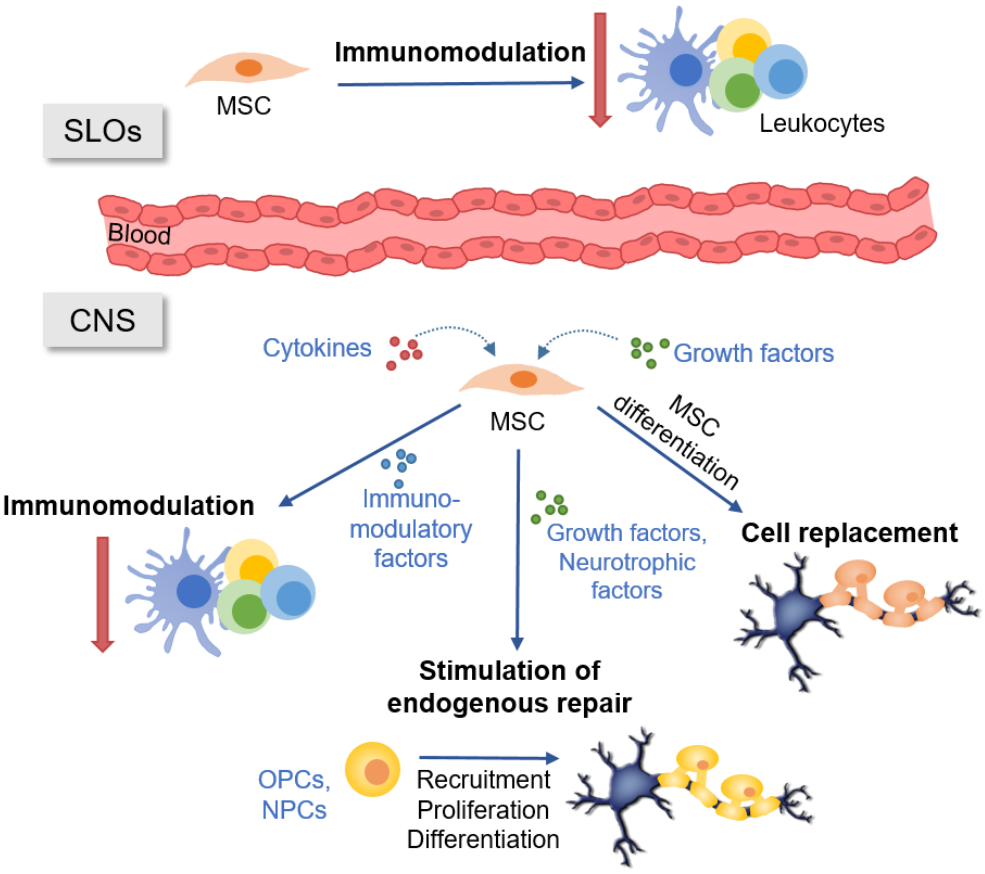

Figure 1.7. Neuroprotective and reparative effects of MSCs in neurodegenerative diseases.

MSCs are unique in their potential for both suppressing inflammation and also facilitate tissue repair in MS and other neurodegenerative diseases. In the SLOs and blood, the immunomodulatory effects of MSCs (Figure 1.5) allows them to target the generation of pro-inflammatory cells or their migration to the CNS, thus reducing the inflammatory load in the CNS. MSCs can further suppress myelin-damaging inflammation if they enter the CNS. Here, also, they can facilitate repair of the CNS through two main avenues; by the stimulation of endogenous repair mechanisms or by directly replacing cells through differentiation. MSCs produce a range of growth factors and neurotrophic factors which could stimulate endogenous remyelination by recruiting progenitor cells and supporting their proliferation and differentiation into mature, myelin-producing oligodendrocytes. Alternatively, growth factors in the CNS might stimulate the differentiation of MSCs to neurons, oligodendrocytes or other necessary glial cells. Thus, the therapeutic opportunities of MSCs are multifactorial.

Table 1.4: MS clinical trials for MSC-based therapy.

Authors	MSC source	Route of administration	Main findings	Pos/neg outcome
Karussis *et al.* 2010[277]	Bone marrow, autologous	Intrathecal +/- intravenous	Improved mean EDSS. No patients deteriorated or showed new brain lesions after 6 months.	✓
Mohajeri *et al.* 2011[283]	Bone marrow, autologous	Intrathecal	May increase $FoxP3^+$ cells in blood (qPCR).	✓
Mohyeddin Bonab *et al.* 2012[322]	Bone marrow, autologous	Intrathecal	EDSS improved or unchanged in most patients Some had new or enhanced lesions or deteriorated EDSS	✓/×
Yamout *et al.* 2010[279]	Bone marrow, autologous	Intrathecal	EDSS improved for most patients, worsened for 1. MRI showed new/enhanced lesions despite improved EDSS.	✓/×
Connick *et al.* 2012[280]	Bone marrow, autologous	Intravenous	Improved mean EDSS.	✓
Liang *et al.* 2009[281]	Umbilical cord, allogeneic	Intrathecal + intravenous	EDSS improved. Improved sensory impairment and muscle strength within days Reduced lesion load.	✓
Mohyeddin Bonab *et al.* 2007[323]	Bone marrow, autologous	Intrathecal	EDSS and lesion size/number improved for 1 patient but worsened or remained unchanged for most.	×
Li *et al.* 2014[324]	Umbilical cord, allogeneic	Intravenous	Reduced incidence of relapse, reduced EDSS.	✓
Llufriu *et al.* 2014[325]	Bone marrow, autologous	Intravenous	May reduce gadolinium-enhancing lesions but did not improve EDSS.	δ
Lublin *et al.* 2014[282]	Placenta, allogeneic	Intravenous	No worsening.	δ

✓indicates patient improvements, × indicates patients worsening, δ indicates no significant changes

This page intentionally left blank.

This page intentionally left blank.

Chapter 2: Materials and Methods

This page intentionally left blank.

2.1 **Reagents and materials**

2.1.1 Antibodies

Antibodies used in this study to detect murine or human antigens are listed in Table 2.1.

2.1.2 Peptides and recombinant proteins

Peptides and recombinant proteins used in this study are listed in Table 2.2.

2.1.3 Primers

Primers used in this study are listed in Table 2.3 and were purchased from Sigma-Aldrich (MO, USA) or Geneworks (SA, Australia). They were reconstituted to 100 µM in nucleic acid-free water (Life Technologies) and diluted to 20 µM working concentration.

2.1.4 Vectors

The expression plasmid pWPI-IRESeGFP (pWPI) was a kind gift from Dr Natalie Payne and murine ACKR2 or ACKR4 were previously cloned into pWPI by Dr Duncan Mackenzie in our laboratory. The lentiviral packaging plasmid pMD2G and psPAX2 were purchased from Addgene (MA, USA). The expression plasmid pLV-IRESmCherry was purchased from VectorBuilder (CA, USA) with inserted *Il23rΔ9* coding sequence designed as described in results section 3.4.3.1.

2.1.5 Solutions and buffers

2.1.5.1. Basic solutions

Phosphate-buffered saline (PBS), 10X Tris-buffered saline (TBS), and MilliQ water were obtained from the Technical Services Unit (TSU) at the School of Biological Sciences (SBS; University of Adelaide, SA, Australia).

2.1.5.2. DPSC complete medium

α-Modified Eagle's Medium (αMEM; Life Technologies) was supplemented with 10% FBS (Sigma-Aldrich), 100 µM L-ascorbic acid (Sigma-Aldrich) and 0.2 U/mL penicillin/streptomycin (Life Technologies).

2.1.5.3. Ad-MSC complete medium

α-Modified Eagle's Medium (αMEM; Life Technologies) was supplemented with 5% FBS (Sigma-Aldrich), 0.2 U/mL penicillin/streptomycin (Life Technologies), and 1% Mesenchymal Stem Cell Growth Supplement (MSCGS; ScienCell, CA, USA).

Table 2.1: Antibodies and streptavidin conjugates used in this study against murine antigens.

Antigen	Conjugate	Species	Application	Final working Concentration	Source
Mouse leukocyte markers					
CD3	-	Rat	*In vitro* cultures	5 µg/mL	In-house
CD3ε	PE-Cy7	Arm ham	FC	1.33 µg/mL	eBioscience
CD4	Alexa647	Rat	FC	0.83 µg/mL	BD Pharmingen
	BV786			0.67 µg/mL	BD Biosciences
CD8α	FITC	Rat	FC	2.08 µg/mL	BD Pharmingen
	PE-Cy7			0.83 µg/mL	BD Pharmingen
	BV510			0.67 µg/mL	BD Biosciences
	BUV395			0.67 µg/mL	
CD11b	PE-Cy7	Rat	FC	0.83 µg/mL	BD Pharmingen
CD28	-	Hamster	*in vitro* cultures	1 µg/mL	BD Pharmingen
CD44	BV450	Rat	FC	0.83 µg/mL	BD Biosciences
	FITC			2.08 µg/mL	BD Pharmingen
	APC-Cy7			0.67 µg/mL	BD Biosciences
	BV711			0.67 µg/mL	BD Biosciences
CD45.2	BV450	Mouse	FC	0.83 µg/mL	BD Biosciences
	APC			0.67 µg/mL	BD Biosciences
CD45R (B220)	BV510	Rat	FC	0.67 µg/mL	BD Pharmingen
	AF700			0.67 µg/mL	
	BUV496			0.67 µg/mL	
CD69	PE-Cy7	Arm ham	FC	0.67 µg/mL	BD Biosciences
CD86	PE	Rat	FC	0.83 µg/mL	Biolegends
CD138	PE	Rat	FC	0.83 µg/mL	BD Pharmingen
IgM	-	Goat	B cell stimulation	10 µg/mL	Jackson
MHC-II (IA/IE)	APC	Rat	FC	0.67 µg/mL	BD Biosciences
	biotin			0.67 µg/mL	
Mouse cytokines and intracellular antigens					
IL-17	-	Rat	ELISA capt.	1 µg/mL	BD Pharmingen
	biotin		ELISA det.	500 ng/mL	BD Pharmingen
	PE		FC	1.11 µg/mL	BD Pharmingen
	Alexa647		FC	1.11 µg/mL	BD Biosciences
IFN-γ	-	Rat	*in vitro* cultures	10 µg/mL	BioXcell
	-		ELISA capt.	1 µg/mL	BD Pharmingen
	Biotin		ELISA det.	0.5 µg/mL	BD Pharmingen
	FITC		FC	2.7 µg/mL	BD Pharmingen
	PE		FC	1.11 µg/mL	BD Pharmingen
	PE-CF594		FC	1.11 µg/mL	BD Biosciences
GM-CSF	BV421	Rat	FC	1.11 µg/mL	BD Biosciences
IL-4	-	Rat	*in vitro* cultures	10 µg/mL	BioXcell
FoxP3	FITC	Rat	FC	1.11 µg/mL	eBioscience
	Alexa647			1.11 µg/mL	

Table continued over page.

Table 2.1 continued

Antigen	Conjugate	Species	Application	Working Concentration	Source
Mouse chemokines					
CCL19	- biotin	Rat Goat	ELISA capt. ELISA det.	200 ng/mL 200 ng/mL	R&D Systems R&D Systems
CCL22	- biotin	Rat Goat	ELISA capt. ELISA det.	200 ng/mL 100 ng/mL	R&D Systems R&D Systems
Human MSC markers					
CD90	FITC	Mouse	FC	1/6	BD Biosciences
CD73	APC	Mouse	FC	1/6	BD Biosciences
CD105	PerCP-Cy5.5	Mouse	FC	1/6	BD Biosciences
CD45	PE	Mouse	FC	1/6	BD Biosciences
CD34	PE	Mouse	FC	1/6	BD Biosciences
CD11b	PE	Mouse	FC	1/6	BD Biosciences
CD19	PE	Mouse	FC	1/6	BD Biosciences
HLA-DR	PE	Mouse	FC	1/6	BD Biosciences
Other human molecules					
LIF	-	Mouse	Neutralisation	5 µg/mL	R&D Systems
Isotype controls					
IgG1	PE-Cy7	Rat	FC	1.11 µg/mL	eBioscience
Streptavidin conjugates					
-	HRP	-	ELISA	1/10000	Rockland
-	BUV395	-	FC	1/250	BD Biosciences
-	BV510	-	FC	1/100	BD Biosciences
-	Alexa647	-	FC	1/250	Biolegend

Abbreviations: Arm ham: armenian hamster; capt.: capture. det.; detection; FC: flow cytometry; HRP: horse radish peroxidase.

Table 2.2: Recombinant mouse proteins used in this study.

Recombinant protein/peptide	Application	Final working Concentration	Source
IL-1β	*in vitro* cultures	10 ng/mL	Miltenyi Biotec
IL-2	*in vitro* cultures	20 ng/mL	Thermofisher Scientific
IL-4	*in vitro* cultures	10 ng/mL	BD Pharmingen
IL-6	*in vitro* cultures	20 ng/mL	R&D Systems
IL-12	*in vitro* cultures	10 ng/mL	Biosource
IL-17A	Sandwich ELISA standards	50 ng/mL	R&D Systems
IL-23	*in vitro* cultures	10 ng/mL	R&D Systems
TGFβ1	*in vitro* cultures	5 ng/mL	R&D Systems
CCL19	Scavenging assay Sandwich ELISA standards	1-10 ng/mL 20 ng/mL	R&D Systems
CCL22	Scavenging assay Sandwich ELISA standards	1-10 ng/mL 32 ng/mL	R&D Systems
MOG_{35-55}	Immunisation for EAE *in vivo*	1 mg/mL	GM Biochem Ltd. (Shanhai)
$PLP_{139-151}$	Immunisation for EAE *in vivo*	0.5 mg/mL	Biomolecular Resource Facility, John Curtin School of Medical Research, ANU

Table 2.3: Primers used in this study.

Gene name	Protein name	Forward 5' to 3'	Reverse 5' to 3'
Human genes			
RPLP0		AATCCTCAGGGGCACCATT	CGTTGGCTCCCACTTTGT
LIF	Leukaemia inhibitory factor (LIF)	GAAAGCTTTGGTAGGTTCTTCGTT	TGCAGGTCCAGCCATCAGA
TGFB1	Transforming growth factor β1 (TGF-β1)	AAGGACCTCGGCTGGAAGTGC	CCGGGTTATGCTGGTTGTA
IL10	Interleukin 10 (IL-10)	TGAGAACAGCTGCACCCACTT	TCGGAGATCTCGAAGCATGTTA
PTGS2	Cyclooxygenase 2 (COX2)	AGGGTTGCTGGTGGTAGGAA	GGTCAATGGAAGCCTGTGATACT
VEGFA	Vascular endothelial growth factor A (VEGFA)	ATGACGAGGGCCTGGAGTGTG	CCTATGTGCTGGCCTTGGTGAG
HGF	Hepatic growth factor (HGF)	TCCACGGAAGAGGAGATGAGA	GGCCATATACCAGCTGGGAAA
TNFAIP6	TNF-stimulated gene-6 (TSG-6)	GCTGCTGGATGGATGGCTAA	GGGCCCTGGCTTCACAA
Mouse genes			
Ackr2	Atypical chemokine receptor 2 (ACKR2)	CTGCATGAGCCTGGACAAATAC	AACTGGGCCTTCGGTCTGT
Ackr4	Atypical chemokine receptor 4 (ACKR4)	AATGCTAGGTGCACTCCCATCT	CCGATTTCCAGCATCTGAATG
Other genes			
gfp	Green fluorescent protein (GFP)	TGTGATCGCGCTTCTCGTT	CTGCTGCCCGACAACCA

2.1.5.4. HEK293FT complete medium

Roswell Park Memorial Institute (RPMI; Life Technologies) was supplemented with 10% FBS (JRH Biosciences), 2 mM L-glutamine (Life Technologies) and 2 U/mL penicillin/streptomycin (TSU).

2.1.5.5. 2X HEK293FT freezing mix

Complete HEK293FT cell medium (Section 2.5.1.4) containing 20% DMSO and 50% FBS.

2.1.5.6. Complete Iscove's Modified Dulbecco's Medium (IMDM)

Powdered IMDM (Life Technologies) was made into solution (incomplete IMDM) according to the manufacturer's instructions. Complete IMDM was prepared by adding 10% FBS (Sigma-Aldrich), 0.2 U/mL penicillin/streptomycin (Life Technologies) 1X Glutamax (Life Technologies) and 54 nM β-mercaptoethanol to incomplete IMDM (all final concentrations).

2.1.5.7. B cell complete medium

RPMI (Life Technologies) was supplemented with 10% FBS (Sigma-Aldrich), 0.2 U/mL penicillin/streptomycin (Life Technologies), 1X non-essential amino acids (Life Technologies), 1X Glutamax (Life Technologies), 54 nM β-mercaptoethanol (Sigma-Aldrich), 1 mM sodium pyruvate (Life Technologies), and 10 mM HEPES (IMVS).

2.1.5.8. Adipogenic differentiation medium

Complete DPSC medium (Section 2.1.5.2) was supplemented with 0.5 µM dexamethasone (Sigma-Aldrich), 0.5 µM isobutylmethylxanthine (Sigma-Aldrich) and 50 µM indomethacin (Sigma-Aldrich) then filter-sterilised.

2.1.5.9. Osteogenic differentiation medium

Complete DPSC medium (Section 2.1.5.2) was supplemented with 10 nM dexamethasone (Sigma-Aldrich), 20 mM β-glycerol phosphate (Sigma-Aldrich) and 50 µM L-ascorbic acid 2-phosphate (Sigma-Aldrich) then filter-sterilised.

2.1.5.10. Incomplete Freund's Adjuvant (IFA)

1.8 mL of mannide manooleate (Sigma Aldrich) was added to 10.2 mL of mineral oil (Sigma Aldrich) to make a mixture of 75% mineral oil and 15% mannide manooleate.

2.1.5.11. Complete Freund's Adjuvant (CFA)

To make CFA for MOG immunisations, 100 mg of non-viable, desiccated *M. tuberculosis* H37 Ra (Becton, Dickinson and Company, USA) was mixed to 8.33 mg/mL in 12 mL of IFA (Section 2.1.5.10) and ground with a mortar and pestle. CFA was stored at 4˚C in the dark.

To make CFA for PLP immunisations, 100 mg of *M. tuberculosis* H37 Ra (Becton, Dickinson and Company, USA) and 6 mg of non-viable, desiccated *M. butyricum* (DIFCO Laboratories, USA) were mixed to 8.33 mg/mL and 0.5 mg/mL respectively in 12 mL of IFA and ground with a mortar and pestle. CFA was stored at 4˚C in the dark.

2.1.5.12. Peptide/CFA emulsions

MOG_{35-55} (GL Biochem, Shanghai) was dissolved to 2 mg/mL in PBS. The MOG/PBS solution was mixed 1:1 with CFA (Section 2.1.5.11) and emulsified by passing back and forth through a stopcock between two 3 or 5 mL syringes and incubating periodically on ice until the emulsion formed stable peaks when spotted onto paper towel. The emulsion was then loaded into 1 mL luer-lock syringes (BD Biosciences) with 25G needles for injection.

2.1.5.13. Fluorescence activated cell sorting (FACS) buffer

Bovine serum albumin (BSA; Sigma-Aldrich) and sodium azide (NaN_3) (Ajax Finechem) were added to PBS to a final concentration of 1% BSA (w/v) and 0.04% NaN_3 (w/v) and stored at 4°C.

2.1.5.14. PBS/PFA

4% paraformaldehyde (PFA) solution (w/v) was prepared by dissolving PFA in PBS overnight at 55°C and stirring. 1% PFA solution (w/v) was prepared by diluting 4% PFA in PBS. These solutions were stored at 4°C for short term storage or -20°C for long term storage.

2.1.5.15. Isotonic percoll

9 parts percoll (GE Healthcare) was added to 1 part 10X Hank's Balanced Salt Solution (HBSS) (Life Technologies) to make isotonic percoll.

2.1.5.16. Normal mouse serum (NMS)

NMS was prepared in-house by harvesting blood from naïve C57Bl/6 mice and storing in Eppendorf tubes at 4°C overnight to allow coagulation. The following day, blood was centrifuged at 300 x *g* for 5 min and the serum was carefully transferred to a fresh tube and stored at -20°C.

2.1.5.17. Mouse Red Cell Lysis Buffer (MRCLB)

155 mM NH_4Cl (AnalR) and 170 mM Tris-HCl (Biochemicals) solution (pH 7.65) were combined in a 9:1 ratio, the pH was adjusted to 7.2 with HCl and the solution was filter-sterilised before use.

2.1.5.18. Digestion buffer

Dulbecco's Modified Eagle Medium (DMEM; Life Technologies, NY, USA) was supplemented with 5% FBS (Sigma-Aldrich), 2.5 mM $CaCl_2$ (BDH Chemicals), 10 mM HEPES (IMVS) and 0.2 U/mL

penicillin/streptomycin (Life Technologies). For digestion of mouse tissues, 30 U/mL DNase I (Sigma-Aldrich) and 1 mg/mL collagenase 1A (Sigma-Aldrich) were added immediately before use. For digestion of human dental pulp, 85 µg/mL Liberase TL (Sigma-Aldrich) and 30 U/mL DNase I (Sigma-Aldrich) were added immediately before use.

2.1.5.19. Binding buffer for scavenging assay

RPMI-1640 without phenol red (Life Technologies) was supplemented with 4 mM HEPES (IMVS) and 1% BSA (Sigma-Aldrich).

2.1.5.20. PBS/Tween

Polyoxyethylene-sorbitan monolaurate (Tween 20, Sigma-Aldrich) was added to PBS to a final concentration of 0.05% (v/v) and the solution was mixed thoroughly.

2.1.5.21. Recombinant protein diluent for sequential ELISA

0.5% skim milk, 0.1% BSA (Sigma-Aldrich) and 0.005% Tween 20 (Sigma-Aldrich) were added to PBS.

2.1.5.22. Diluent for Sequential ELISA

0.01% BSA (Sigma-Aldrich) and 0.005% Tween 20 (Sigma-Aldrich) were added to PBS.

2.1.5.23. DEPC water

Diethylpyrocarbonate (DEPC, Sigma-Aldrich) was diluted in 0.1% (v/v) in MilliQ water, incubated overnight at room temperature (RT) and then autoclaved.

2.2 **Cell culture and generation of genetically modified cells**

2.2.1 Isolation of DPSCs from human molars

Unfractured, uninflamed human third molars were obtained with consent from young adults aged 21-27 according to the guidelines and consent of the University of Adelaide Human Ethics Committee (Ethics approval number H-2015-254). The molars were first sterilised by placing in 70% ethanol for 1 min before placing between two thick wads of clean paper towel and cracking them open using a hammer. The pulp was removed with tweezers from the fractured molars inside a tissue culture hood and the rest of the isolation process was carried out under aseptic conditions. The pulp was placed on the surface of a petri dish in a few drops of digestion buffer (Section 2.1.5.18). A surgical blade was used to mince the tissue into smaller pieces, then the tissue in digestion buffer was transferred to a tube containing 5 mL of digestion buffer. The pulp was digested for 1 h at 37°C, pipetting back and forth every 15 mins. After digestion, the mix was neutralised with 5 mL of complete DPSC medium (Section 2.1.5.2). The dissociated pulp was centrifuged for 5 min at 240 x *g* then resuspended in 5 mL of DPSC complete medium and transferred to a 75cm^2 vented tissue culture flask (Corning). The cells were cultured at 37°C, 5% CO_2. After one week, the supernatant containing dead cells,

non-adherent cells and debris was removed and replaced with 5 mL of fresh DPSC complete medium. The culture medium was replaced once a week until the cells reached 50% confluency then changed every 3-4 days until they reached 90% confluency.

2.2.2 DPSC culture

DPSCs were thawed at 37°C and immediately 1 mL of DPSC complete medium (Section 2.1.5.2) was added drop-wise to the cells over a period of 1 min. The cells were transferred to a tube containing 8 mL of pre-warmed DPSC complete medium and were allowed to stand for 10 min before centrifuging at 1000 x *g* and transferring to a 75 cm^2 vented tissue flask (Corning) in 8 mL of DPSC complete medium.

DPSCs were sub-cultured when they reached 90% confluency (every 3-4 days). Briefly, the culture medium was removed and the cells were rinsed with sterile PBS then incubated with trypsin/EDTA (TSU) for 3 min at 37ºC. The sides of the flask were tapped to mechanically displace remaining attached cells and the trypsin was neutralised with DPSC complete medium. The cells were counted and a new flask was seeded at 5000 cells/cm^2.

DPSCs from culture to be cryopreserved were counted and resuspended in 10% DMSO (Sigma-Aldrich) in FBS (Sigma-Aldrich) at 7.5 x 10^5 cells/mL and 0.5 mL was aliquoted into each cryovial. The cells were frozen overnight at -80°C in a cotton wool-lined poly-styrofoam container then transferred to liquid nitrogen for storage.

2.2.3 Ad-MSC culture

Ad-MSCs used in this study were either obtained from Dr Natalie Payne (Monash University) or purchased from ScienCell (clone 11537; CA, USA). Vented tissue culture flasks were pre-coated with 15 µg/cm^2 of poly-L-lysine (Sigma-Aldrich) in PBS for 1 hour at 37˚C then rinsed twice with PBS before use. Ad-MSCs in freezing medium were thawed at 37˚C and transferred to a pre-coated 75 cm^2 vented tissue culture flask containing 15 mL of Ad-MSC complete medium (Section 2.1.5.3). The cells were incubated at 37˚C, 5% CO_2 and the culture medium was changed after approximately 16 hours to remove DMSO from the freezing medium.

Ad-MSCs were sub-cultured in the same manner as DPSCs (Section 2.2.2) using poly-L-lysine coated flasks.

Ad-MSCs from culture to be cryopreserved were counted and resuspended in 5% DMSO (Sigma-Aldrich), 50% FBS (Sigma-Aldrich) and 45% Ad-MSC complete medium (Section 2.5.1.3) at 7.5 x 10^5 cells/mL and 0.5 mL was aliquoted into each cryovial. The cells were frozen overnight at -80°C in a cotton wool-lined poly-styrofoam container then transferred to liquid nitrogen for storage.

2.2.4 HEK293FT cell culture

HEK293FT cells (Invitrogen) were maintained in HEK293FT complete medium (Section 2.1.5.4) at 37°C, 5% CO_2. The cells were thawed at 37°C and transferred to a tube containing 10 mL of pre-warmed HEK293FT complete medium then centrifuged at 240 x *g* for 5 min. The cells were resuspended in HEK293FT complete medium and transferred to a 25 cm^2 vented tissue culture flask (Corning) overnight and transferred to a 75 cm^2 vented tissue culture flask in 15 mL of HEK293FT complete medium the following day.

HEK293FT cells were sub-cultured when they were ~90% confluent (every 2 days). Briefly, the adherent cells were detached by incubating with trypsin/EDTA (TSU) for 3 min at 37°C, quenching with HEK293FT complete medium and removing 9/10 of the cells.

For cryopreservation, HEK293FT cells were resuspended in HEK293FT complete medium at 2 x 10^6 cells/mL. 500 µL of cells was added to 500 µL of 2X HEK293FT freezing mix (Section 2.1.5.5) in cryovials (ThermoScientific) and frozen in a temperature rate-controlled freezing container (Mr. Frosty™; Stratagene) overnight at -80°C then transferred to liquid nitrogen for storage.

2.2.5 Transfection of HEK293FT cells

2 x 10^6 HEK293FT cells were plated in 10 cm-diameter tissue culture dishes (Corning) and the following day, when cells reached approximately 60% confluency, they were transfected with lentiviral plasmids. Four µg of each lentiviral packaging plasmid (psPAX2 and pMD2G, Addgene) and 6 µg of expression plasmid were mixed together in 1.5 mL of OptiMEM (Life Technologies). In a separate tube, 50 µL of Lipofectamine 2000 (Life Technologies) was diluted in 1.5 mL of OptiMEM. The two solutions were mixed 1:1 by inverting the tube several times then incubated at RT for 20 min. The HEK293FT cell medium was replaced with 7 mL of OptiMEM/5% FBS before adding the 3 mL of transfection mixture and mixing by gently swirling the plates. The HEK293FT cells were transfected for 6 hrs at 37˚C 5% CO_2 before replacing the medium with HEK293FT complete medium (Section 2.1.5.4). The transfected cells were cultured for two days to produce virus. The resulting virus-containing medium was harvested, centrifuged and passed through a 0.4 µm filter before use.

2.2.6 Lentiviral transduction of DPSCs

Transduction medium was prepared by diluting 1 part virus-containing medium (Section 2.2.5) in 4 parts DPSC complete medium (Section 2.5.1.2) and adding 8 µg/mL protamine sulphate (Sigma-Aldrich). DPSCs were thawed, centrifuged, resuspended in transduction medium and transferred to a 75cm^2 vented tissue culture flask (Corning). The cells were incubated in the transduction medium overnight and the medium was replaced with fresh complete DPSC medium the following morning. On the third day of culture, when the DPSCs reached approximately 80% confluency, they were expanded into 3 75 cm^2 tissue culture flasks (Corning) and the transduction procedure was repeated upon transferring the cells to the new flasks. When the double-

transduced cells reached approximately 80% confluency they were harvested and frozen for long-term storage. Transduction efficiency was measured by flow cytometry for the fluorescent reporters mCherry or eGFP.

2.2.7 Conditioned medium from DPSCs (DPSC-CM)

DPSCs were seeded into 75 cm^2 vented tissue culture flasks (Corning) at 5000 cells/cm^2 in 7 mL of complete DPSC medium and cultured for 3 days at 37°C, 5% CO_2. The supernatants were harvested, centrifuged at 1000 x *g* then passed through a 0.45 µM filter to exclude any cells or debris. The cells were also harvested and counted and the DPSC-CM was diluted with complete DPSC medium such that each 7 mL aliquot was representative of media from 2.5 x 10^6 cells. (i.e. each 50 µL aliquot of DPSC-CM came from approximately 1.8 x 10^5 cells).

2.3 **EAE induction and treatment**

2.3.1 Mice

All mice were purchased from Animal Resource Centre (ARC, Western Australia) and were housed at the University of Adelaide animal house under specific pathogen-free conditions. Experiments used aged-matched female mice (C57Bl6J, 8-12 weeks for MOG-EAE experiments; SJL/J, 7-12 weeks for PLP-EAE experiments). All experiments were conducted with the approval of the University of Adelaide Animal Ethics Committee (Ethics approval number S-2013-204).

2.3.2 Immunisation of mice for EAE

Pertussis toxin (List Biological Laboratories inc.) was diluted to 0.8 or 1.2 µg/mL in sterile PBS. 250 µL (containing either 200 or 300 ng) was injected intraperitoneally on days 0 and 2 post-immunisation using a BD Ultrafine 0.5 mL insulin syringe (BD Biosciences). The mice were then anaesthetised with isofluorane and injected with 50 µL of MOG_{35-55} or $PLP_{139-151}$ emulsion (Section 2.1.5.12) in each hind flank (total 100 µg of MOG_{35-55} or 50 µg of $PLP_{139-151}$ per mouse). EAE mice were weighed and scored for EAE symptoms daily after immunisation (Table 2.4). Day of EAE onset was the second consecutive day in which a mouse scored 0.5 or the first day in which it scored 1 or above. For cumulative disease score, the sum of all EAE scores was calculated for each mouse over time.

2.3.3 Treatment of mice with DPSCs

DPSCs were thawed and passaged once to expand sufficient cells for animal injections. DPSCs at 90% confluency were harvested from tissue culture flasks as per normal (Section 2.2.2) and rinsed twice with PBS before resuspending at 5 x 10^6 cells/mL in PBS. 200 µL (1 x 10^6 cells) was injected intraperitoneally into mice with a BD Ultrafine 0.5 mL insulin syringe (BD Biosciences).

Table 2.4: Clinical disease scoring of EAE.

EAE Score	Symptoms
0.5	Weakness when held by tail.
1	Partially flaccid tail.
1.5	Weakness when held by tail *and* partially flaccid tail.
2	Fully flaccid tail *or* difficulty up-righting when placed on back.
2.25	Fully flaccid tail *and* difficulty up-righting when placed on back.
2.5	Fully flaccid tail *and* some hind limb paralysis or troubled gait (ataxia).
3	Hind limb paralysis.
2.75	Fully flaccid tail *and* one hind limb paralysed.
3.25	Hind limb paralysis *and* some forelimb weakness.
3.5	Hind limb paralysis *and* some forelimb paralysis, moving in unidirectional circle.
4	Hind limb paralysis *and* (mostly) forelimb paralysis.
4.5	All four limbs paralysed.
5	Moribund.

2.3.4 Labelling DPSCs with tracking dye for in vivo imaging system (IVIS)

DPSCs were harvested from culture and resuspended at 3 x 10^6 cells/mL in pre-warmed complete DPSC medium (Section 2.5.1.2). 4 µM Cellbrite™ NIR790 Cytoplasmic Membrane Dye (Biotium) was added to the cells which were immediately mixed by inverting several times then incubated at 37°C for 20 min, with mixing every 5 min. The volume was made up to 10 mL with DPSC complete medium and the cells were rinsed twice with PBS before final resuspension at 5 x 10^6 cells/mL in sterile PBS for injection.

2.4 *In vitro* assays

2.4.1 Purification of naïve CD4$^+$ T cells

Naïve CD4$^+$ T cells were purified from splenocyte/inguinal LN cell mixtures using the Mouse Naïve CD4$^+$ T cell isolation kit (StemCell Technologies) according to the manufacturer's protocol. Purity was checked by flow cytometry.

2.4.2 Purification of naïve follicular (FO) B cells

Naïve follicular B cells were purified from splenocytes using the MACS naïve follicular B cell magnetic separation kit (Miltenyi Biotec) according to the manufacturer's protocol. Purity was checked by flow cytometry.

2.4.3 In vitro *T cell cultures*

96-well U bottom trays (Corning) were coated with 5 µg/mL anti-CD3ε (2F11, purified in-house) in PBS at 37˚C for 90 min. The wells were washed twice with PBS before use. 2 x 10^5 cells were cultured in 200 µL of complete IMDM (Section 2.1.52.1.5.6.) containing 1/4 conditioned medium from DPSCs (Section 2.2.7) and 1 µg/mL soluble anti-CD28. The following cytokine and antibody cocktails were used for differentiation of naïve $CD4^+$ T cells: *Th0 differentiating medium:* 10 µg/mL anti-IFNγ (XMG1.2; BioXcell) and 10 µg/mL anti-IL-4 (11B11; BioXcell); *Th1 differentiating medium:* 10 µg/mL anti-IL-4 (11B11; BioXcell) and 10 ng/mL recombinant (r) IL-12 (Biosource); *Th17 differentiating medium:* 10 µg/mL anti-IFNγ (XMG1.2; BioXcell), 10 µg/mL anti-IL-4 (11B11; BioXcell), 10 ng/mL rIL-1β (Miltenyi Biotec), 5 ng/mL rTGFβ (R&D Systems), 20 ng/mL rIL-6 (R&D Systems) and 10 ng/mL rIL-23 (R&D Systems); *iTreg differentiating medium:* 10 µg/mL anti-IFNγ (XMG1.2; BioXcell), 10 µg/mL anti-IL-4 (11B11; BioXcell), 5 ng/mL rTGFβ (R&D Systems) and 100 U/mL rIL-2 (Corning).

2.4.4 In vitro *B cell cultures*

Naïve FO B cells purified from splenocytes (Section 2.4.2) were cultured in B cell complete medium (Section 2.1.5.7) containing the following stimuli: 5 µg/mL LPS (Sigma-Aldrich-L4130), or LPS and 10 ng/mL rIL-4 (BD Pharmingen). For some experiments, the B cells were labelled with eFluor670 proliferation dye (Biolegend; Section 2.4.5). B cells were stimulated for 2-4 days at 37°C, 5% CO_2.

2.4.5 eFluor670-labelling of lymphocytes

Single cell suspensions of lymphocytes were resuspended at 2 x 10^7 cells/mL in PBS for labelling. In a separate tube, 10 µM Cell Proliferation Dye eFluor670 (eBioscience) was prepared in PBS. The two mixes were combined 1:1 and immediately vortexed for 1 second before incubating for exactly 10 min at 37˚C in the dark. eFluor670 was quenched by adding 4-5 volumes of cold complete IMDM (Section 2.1.5.5) and incubating for a further 5 min on ice in the dark. The cells were rinsed 3X in 10 mL of complete IMDM before counting and resuspending at 2 x 10^6 cells/mL for plating.

2.4.6 Differentiation of DPSCs to adipocytes and osteocytes

1 x 10^5 DPSCs were seeded in 2 mL of DPSC complete medium (Section 2.1.5.2) per well in a 6-well tray (Corning) and the cells were cultured at 37°C, 5% CO_2. When the cells became 100% confluent, the medium was replaced with 2 mL of adipogenic (Section 2.1.5.8) or osteogenic differentiation media (Section 2.1.5.9) or DPSC complete medium for control. Every 3-4 days thereafter, the medium was changed by carefully aspirating the old medium, rinsing the wells twice with 2 mL of PBS and replacing with 2 mL of fresh differentiating medium. After 21 days, the cells were ready for staining. The media was aspirated and the wells were rinsed twice with PBS before adding 2 mL of 4% PFA (Section 2.1.5.14) and incubating at RT for 1 hr. The wells were rinsed twice with 2 mL of PBS (for adipogenic wells) or deionised (DI) water (for osteogenic wells). 2 mL of Oil red O stain (Sigma-Aldrich) (for adipogenic wells) or alizarin red stain (Sigma-Aldrich)

(for osteogenic wells) were added to the relevant wells. Finally, the wells were rinsed twice with PBS (for adipogenic wells) or DI water (for osteogenic wells) then stored in 2 mL of DI water or PBS for imaging.

2.4.7 Flow cytometry of DPSCs for MSC markers

2.5 x 10^5 DPSCs in 50 µL of PBS per well in a 96-well U-bottom tray (Corning) were stained with near-infrared viability dye (1/1000; Invitrogen) for 20 min at RT. They were rinsed twice with PBS, resuspended in 50 µL of FACS buffer (Section 2.1.5.13) and stained for MSC markers using the BD Stemflow™ Human MSC Analysis kit (BD Biosciences). 10 µL of positive cocktail (containing CD44-PE, CD105-PerCP-Cy5.5, CD73-APC and CD90-FITC) or cocktail of lineage negative markers conjugated to PE was added to the relevant wells and incubated for 30 min on ice then rinsed twice with PBS and acquired with a BD LSR II flow cytometer (BD Biosciences).

2.4.8 Chemokine scavenging assays

2 x 10^5 DPSCs in Eppendorf tubes were resuspended in 200 µL of binding buffer (Section 2.1.5.19) containing recombinant 1-10 ng/mL of recombinant murine CCL19 or CCL22 (0). The cells were incubated at 37°C for 3 hr, inverting the tubes every 30 min to resuspend the cells. After incubation, the tubes were centrifuged to pellet the cells and 100 µL of the supernatant was transferred to a fresh tube with 1X protease inhibitor cocktail (Sigma-Aldrich) and stored at -20°C before measuring remaining chemokine content by ELISA (Section 2.4.10).

2.4.9 IL-23 stimulation of splenocytes

A 96-well U-bottom tray (Corning) was coated with 5 µg/mL anti-CD3ε (2F11, purified in-house) in 50 µl of PBS at 37°C for 90 min. The tray was rinsed twice with PBS before adding culture reagents. 2 x 10^5 splenocytes were cultured in 200 µL of a mixture of 1/4 conditioned medium from HEK293FT cells or DPSCs (Section 2.2.7) and 3/4 of complete IMDM (Section 2.1.5.6) containing 1 µg/mL anti-CD28 and 10 ng/mL IL-23 for 6 days at 37°C, 5% CO_2. At the end of culture, the plates were centrifuged for 1 min at 400 x *g* to pellet cells and the supernatants were transferred to fresh tubes and stored at -20°C with 1X protease inhibitor cocktail (Sigma-Aldrich) for analysis by ELISA to detect IL-17A the following day. The cells were counted, rinsed twice with PBS and stained as per normal for flow cytometric analysis (Section 2.5.2).

2.4.10 Sandwich ELISA

96-well Costar high binding trays (Sigma-Aldrich) were coated with 50 µL of capture antibodies (0) diluted in 100 mM $NaHCO_3$ (pH 9.6) overnight at 4°C. The following morning, wells were blocked with 200 µL of PBS/3% BSA at 37°C for 1 hr before adding 100 µL of samples to each well. Recombinant proteins for standards (Table 2.2) were prepared in PBS/1% BSA and serially diluted 1 in 2 before adding 100 µL per well. Samples and standards were incubated at 37°C for 90 min. 100 µL of biotinylated detection antibodies (Table 2.1) prepared in PBS were added to each well and incubated for 37°C for 1 hr before rinsing and incubating

with 100 µL of streptavidin-conjugated horseradish peroxidise (strep-HRP; Table 2.1) diluted in PBS/1% BSA for 30 min at RT. Finally, 200 µl of 3,3',5,5'-tetramethylbenzidine (TMB) substrate solution (eBioscience) was added to all wells and blue colour was allowed to develop in the dark. The reaction was stopped by addition of 50 µL of 3M HCl to each well and the absorbance at 450 nm was measured with a Biotrak II Plate Absorbance Spectrophotometer (GE Healthcare, England, UK). The wells were washed after each incubation three times with PBS/Tween (Section 2.1.5.20). The absorbance values of the standards were used to generate a standard curve from which the concentrations of the samples were calculated using GraphPad Prism software (CA, USA). The total amount of protein in the original sample was calculated by multiplying the determined concentration by the starting volume.

2.4.11 RNA isolation from frozen tissues or cultured cells

All surfaces and equipment were treated with RNaseZAP (Ambion) at the beginning of the experiment. Tissues were snap-frozen in liquid nitrogen and stored at -80°C until processing. Frozen tissues were crushed with a liquid nitrogen-cooled mortar and pestle and 1 mL of TRI Reagent (Ambion) was added immediately after the tissue thawed and then stored at -80°C. For cultured cells, cells were harvested and centrifuged and 1 mL of TRI Reagent was added to the cell pellet. RNA was extracted from the samples in TRI Reagent according to the manufacturer's instructions. Briefly, 200 µL of chloroform was added for each 1 mL of TRI Reagent and the upper aqueous phase was transferred to a fresh tube, taking care not to take any phenol. RNA was precipitated with isopropanol and washed with 75% DEPC ethanol (w/v; DEPC water, Section 2.1.5.23). The nucleic acid pellet was then resuspended in 20 µL DEPC water. RNA concentration and purity were determined by measuring the absorbance at 260 nm and 280 nm using NanoDrop 2000 (Thermo Fisher Scientific, Vic, Australia) and the samples were stored at -80°C. All samples were treated with DNase before further use, using a Turbo DNase-free kit (Ambion) according to the manufacturer's instructions. RNA concentration and purity were re-determined as described above.

2.4.12 cDNA preparation

cDNA was prepared from DNase-free RNA (Section 2.4.11) using the Transcriptor First Strand cDNA Synthesis kit (Roche) or High Capacity cDNA Reverse Transcription kit (Applied Biosciences) according to the manufacturers' instructions.

2.4.13 Real-time quantitative polymerase chain reaction (qPCR)

qPCR was conducted using SYBR Green I Master Mix (5 µL; Applied Biosciences) in 10 µL reactions containing 1 µL of cDNA and 0.3 µL of a mix of 20µM forward and reverse primers on a LightCycler-480 instrument (Roche). Relative gene expression for each gene of interest (GOI) was calculated as $2^{-(C_t(GOI)-C_t(ref))}$ where *ref* is the reference gene *Rplp0* and C_t is threshold cycle.

2.5 **Ex vivo assays**

2.5.1 Preparation of single cell suspensions for flow cytometry

Mice were humanely killed by CO_2 asphyxiation and perfused intracardially with PBS. Spleens and iLNs were homogenised to single cell suspensions in PBS on ice and passed through a 70 µM pore-sized sieve. Splenocytes were incubated in 5 mL of MRCLB (Section 2.1.5.17) and incubated for 5 min at 37˚C before rinsing twice with PBS.

Brains and spinal cords were minced in 1 mL of digestion buffer (Section 2.1.5.18) and incubated for 45 min at 37˚C, pipetting every 15 min until the cells had separated. The digestion reaction was neutralised with 1 mL of RPMI/5% FBS. The resulting suspension was passed through a 70 µM pore-sized sieve and the volume was made up to 30 mL with RPMI/5% FBS. 20 mL of isotonic percoll (Section 2.1.5.15) was added to each tube and the solution was mixed by inversion and centrifuged at 1000 x *g* for 20 min with no brake. The resulting myelin cake and supernatant were carefully aspirated and the cells were treated with MRCLB as described above. The cells were finally rinsed twice with PBS before counting in preparation for staining (Section 2.5.2).

2.5.2 Staining cells for flow cytometry

2 x 10^6 cells were stained in 96-well U-bottom trays (Corning). For intracellular cytokine staining, cells were first stimulated with 20 ng/mL phorbol 12-myristate 13-acetate (PMA) and 1 µM ionomycin in the presence of GolgiSTOP (1/1500; BD Biosciences) in complete IMDM (Section 2.1.5.6) for 4 hr at 37˚C. The cells were washed twice with PBS before resuspending in 50 µL of PBS containing near-infrared viability dye (1/1000; Invitrogen) or 575V viability dye (1/1000; BD Biosciences) and incubated for 20 min at RT. The cells were washed twice with 200 µL of PBS and resuspended in 50 µL of FACS buffer (Section 2.1.5.13) containing 200 µg/mL mouse γ globulin and incubated for 15 min at RT to block Fcγ receptors. In some stains, Brilliant Stain Buffer was included in the FACS buffer during staining (1/10; BD Biosciences). 10 µL of 6X primary antibody mixtures was added to the relevant wells and incubated for 60 min. During incubation, secondary antibody was pre-adsorbed with 2% normal mouse serum (Section 2.1.5.16) and 10 µg/mL mouse γ globulin (Rockland,USA) in FACS buffer for at least 30 min. To detect biotinylated antibodies, cells were resuspended in 50 µL of FACS buffer containing streptavidin-conjugates and incubated for 30 min.

The cells were permeabilised in 80 µL of fixation/permeabilisation solution (BD Biosciences) or 100 µL of FOXP3 nuclear permeabilisation buffer (BD Biosciences) for 20 min at RT (1 hr at RT or 4°C overnight for transcription factor staining), washed twice with perm/wash (BD Biosciences) then resuspended in 50 µL of perm/wash buffer containing antibodies against intracellular antigens. Cells were incubated with antibodies for 20 min then washed sequentially with perm/wash, PBS/0.04% Azide then finally resuspended in 200 µL of PBS or fixed in PBS/1% PFA for storage at 4°C until acquisition within a few days. Cells were washed with 200 µL of FACS buffer between each step and incubations were on ice unless otherwise specified. Centrifugations were performed at 400 x *g* for 2 min. Acquisition was performed with BD FACS LSR II, FACSAria III or BD LSRFortessa X-20 flow cytometers. Cells were gated for analysis as shown in Figure 2.1.

2.6 **Graphical and Statistical Analysis**

All graphical and statistical analysis was carried out using GraphPad Prism Software, version 7.00 for Windows (CA, USA, www.graphpad.com). Flow cytometry data were analysed with FlowJo Software, version 10.4.2 for Windows (BD, USA, flowjo.com).

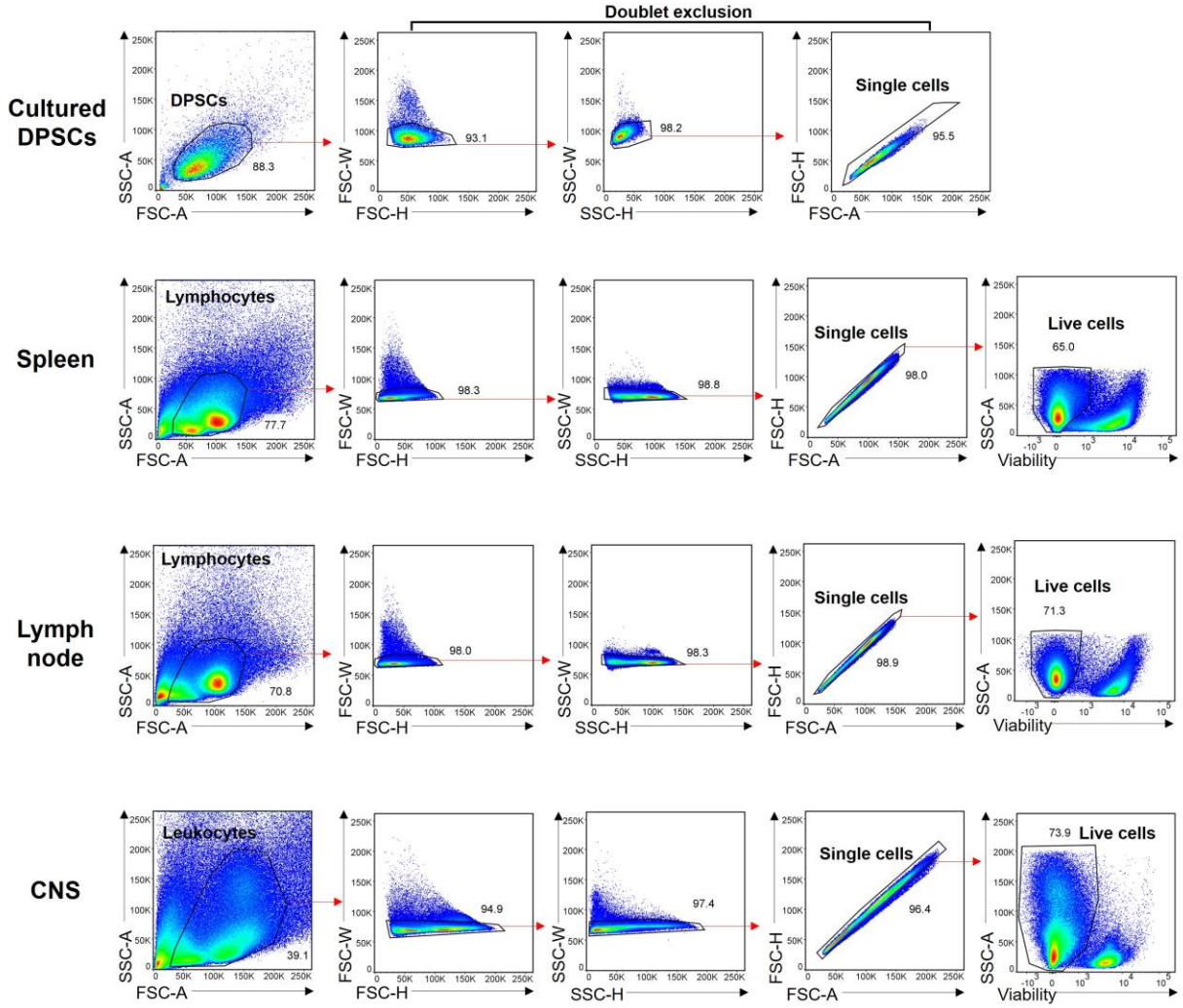

Figure 2.1: Strategy used in this study for gating DPSCs and leukocytes in flow cytometry.

For cultured DPSCs, bulk cells were first gated using FSC-A vs SSC-A, then three separate consecutive gates were used to exclude doublets and include only single cells for analysis. For cells isolated from the spleen, iLN or CNS of EAE mice, a similar gating strategy to gate bulk cells and then exclude doublets was employed. After single cells were selected, a further gate was used to include only cells which were negative for viability dye staining. Thus, all downstream analysis on cells from these organs was on live single cells.

Chapter 3: Characterisation of DPSCs

This page intentionally left blank.

3.1 Introduction

The first hypothesis in this study is that DPSCs will inhibit EAE. In addition, whether DPSCs can be a useful tool for delivery of anti-inflammatory molecules in EAE was also to be tested. Therefore, DPSCs were isolated from several different human donors and characterised extensively *in vitro*. Their adherence to MSC criteria was verified followed by a study of the effects of prolonged culture *in vitro* which included their capacity for modification by lentiviral transduction and the impact of this on the retention of MSC characteristics by the DPSCs. It was important to validate that the starting material for our study are indeed *bona fide* MSCs, and because MSCs currently require expansion to large enough numbers for therapeutic doses which may require prolonged culture time *in vitro* it was also important to ascertain effects this may have on the biology of DPSCs. Finally, if DPSCs are found to be a suitable vehicle for delivery of anti-inflammatory molecules *in vivo*, establishing that there are no negative effects on the MSC characteristics is also important for considering their therapeutic potential.

3.2 Isolation of human DPSCs and their adherence to MSC criteria

To begin, uninflamed human third molars were sourced from seven healthy male or female donors aged 20-27 (Table 3.1) who were undergoing dental surgery. In each case, the teeth extracted were cavity-free and were not inflamed or diseased. Informed consent was obtained from each donor prior to surgery and the cell lines de-identified and classified as DPSC-01-07 (University of Adelaide Human Ethics Approval number H-2015-254). The attainment of enough samples for this study occurred over a period of approximately three years and therefore the experiments in this study were performed over an extended period of time.

DPSCs were isolated from the molars by mechanical dissociation and enzymatic digestion of the pulp to a single cell suspension which was seeded into tissue culture flasks. When colonies of spindle-shaped cells were observed (typically within 1 week of culture), they were dissociated and scattered using trypsin. All cells became 70-80% confluent in a 75 cm^2 tissue culture flask within 2-3 weeks from initial harvest, at which point they were collected, frozen and stored in liquid nitrogen until further use. The DPSCs grown using this process were adherent with spindle-shaped mesenchymal cell morphology (Figure 3.1) similar to other MSC types that have been described[326,327].

Isolation of DPSC-03, 05-07 were performed in-house whereas passage 2 (P2) DPSC-01 and DPSC-02 cells and passage 1 (P1) DPSC-04 were a kind gift from Dr. Karlea Kremer (Koblar laboratory, SAHMRI, Australia). Following their isolation, a finite number of DPSCs can be generated and stored at each passage. Therefore fewer DPSC-01 and -02 cells were available for this study due to their being obtained at a higher passage than the other DPSCs.

The general method of isolating MSCs from different tissues is to harvest the bulk stromal fraction which could result in outgrowth of non-MSC cell types. Therefore, it was important to test that DPSCs used in this study strictly adhered to accepted MSC criteria. The International Society for Cellular Therapy stipulates that MSCs characteristically express the surface molecules CD90, CD73 and CD105, and do not express CD45 (a pan haematopoietic lineage marker), CD34 (a haematopoietic stem cell marker), CD14 or CD11b (macrophage markers), CD79α or CD19 (B cell markers), or HLA-DR (MHC class II)[218]. Therefore, expression of all of these surface markers was measured on DPSCs isolated from all donors in this study by flow cytometry. In line with their classification as MSCs, DPSCs from all donors used in this study were shown to uniformly express the surface molecules CD90, CD73, and CD105 and lacked expression of lineage markers CD34, CD11b, CD19, CD45 and HLA-DR (Figure 3.2).

Since MSC markers are also expressed by other cells such as fibroblasts, it was important to further characterise the DPSCs used in this study. Multi-potency is a defining feature of MSCs and the ability of isolates to differentiate into various mesenchymal lineages such as adipocytes and osteocytes should be assessed before classification as *bona fide* MSCs[218]. Hence, DPSCs isolated in this study were also tested for their adherence to this criterion.

Multi-potency of the DPSCs was assessed by culturing the DPSCs *in vitro* under conditions which promoted their differentiation toward adipocytic and osteocytic lineages. Commercially-available Ad-MSCs were included as a known multipotent positive control. First, Ad-MSCs and DPSCs were induced to differentiate to adipocytes with a combination of dexamethasone, isobutylxanthine and indomethacin added to their complete media for 3 weeks. Differentiation was confirmed by staining the monolayer of cells with Oil Red O which stains lipid deposits. Ad-MSCs cultured in their complete media showed a small degree of Oil Red O staining which greatly increased in the adipocyte-induced culture, confirming chemically-driven differentiation to adipocytes. Oil Red O staining was also apparent in DPSCs that were instructed to differentiate to adipocytes, but not in uninduced control cultures, which demonstrated potency for the adipocytic lineage for DPSCs from donors 03-07 (Figure 3.3).

DPSCs were then challenged to differentiate to osteocytes with the addition of dexamethasone, β-glycerophosphate and L-ascorbic acid 2-phosphate to their complete media for 3 weeks. Alizarin Red was used to stain calcium deposits set down in the cell monolayer of osteocyte-differentiated cells. As expected, calcium deposits were only detected in cultured AdMSCs when they were induced to undergo osteogenic differentiation but not in the presence of their complete medium alone (Figure 3.4). Likewise, DPSCs from donors 03-07 also only contained calcium deposits in wells which were induced to undergo differentiation to osteocytes.

In sum, based on the data presented above, the DPSCs used in this study clearly meet the established criteria for classification as MSCs both in surface marker expression and multi-lineage differentiation potential.

3.3 Stability and growth of human DPSCs in culture

Although self-renewal is normally a defining characteristic of stem cells, MSCs have been described to have more limited culture potential *in vitro*[328-330]. Therefore, in this study the long-term culture potential was assessed for DPSCs isolated from the different donors. Many studies indicate cell passage number to track the age of cells in culture although this can be greatly affected by differences in cell size between MSCs and different methods of re-seeding used between laboratories. To more accurately estimate how many times the DPSCs in this study had replicated the population doubling level (PDL) was calculated each time the cells were passaged.

To measure PDL, aliquots of DPSCs were thawed and cultured continuously for up to 17 weeks. The cells were passaged every 2-5 days when confluency reached approximately 90% and the number of cells was counted and used to calculate PDL based on the number of cells used to seed the flask. DPSCs from donors 01 and 02 were not included in this experiment as cells were not available at the earliest passages for those lines, thus limiting the ability to directly compare PDL with cells from the other donors.

Replicative potential *in vitro* was found to vary among DPSCs from different donors (Figure 3.5). Most DPSC lines were able to be cultured between 38-47 population doublings (17-26 passages) before reaching senescence, with the exception of cells from one donor, DPSC-06, which reached senescence around 8 doublings. Therefore, DPSC-06 was excluded from further assessment since it was not possible to expand to large enough numbers of these cells for downstream experiments.

Extended culture has been described to negatively correlate with multi-potency, expression of MSC markers and rate of proliferation of MSCs[331-333]. In the present study, it was noted that DPSCs cultured long-term increased in cell size (representative images shown in Figure 3.6). To determine if extended culture also results in loss of MSC characteristics, the expression of MSC markers and multi-potency were assessed in passage 16-18 DPSCs from each different donor. Most DPSCs retained expression of MSC markers after 16-18 passages (compare Figures 3.1 and 3.7), although in some instances expression of some markers were reduced in extended culture. This is shown in Figure 3.7 where expression of CD73 and CD105 were lost on a proportion of DPSC-03 cells after extended culture. This was not a consistent feature every time a particular DPSC line was cultured for long periods of time but indicates potential for spontaneous loss of MSC characteristics when DPSCs are cultured *ex vivo* for an extended period.

As described above, MSC markers are also expressed by a variety of other cell types. Thus, retention of expression of those markers did not suffice as a measure of maintained MSC characteristics of the DPSCs after extended culture. In light of this, DPSCs were tested for multi-potency by differentiation *in vitro* to adipocytes and osteocytes again after culture for 16 passages. All DPSCs in this study were able to differentiate to adipocytes as shown by Oil Red O staining in wells that were induced to undergo differentiation (Figure 3.8). However, the amount of Oil Red O staining was also noticeably less in passage 16 DPSCs than was observed

for the passage 3 DPSCs. The DPSC-02 uninduced control well also showed some staining for Oil Red O. Since the lowest passage DPSC-02 cells were not tested for differentiation to adipocytes, the presence of Oil Red O staining in passage 16 DPSC-02 uninduced cultures indicates either the presence of some adipocytes in the culture from isolation or some DPSCs may spontaneously differentiate to adipocytes over time in culture.

DPSCs from all donors also retained potential for osteogenic differentiation as measured by Alizarin Red staining for calcium deposits in induced cultures (Figure 3.9). However, instead of the large, darkly stained calcium deposits observed in the passage 3 DPSCs, passage 16 DPSCs formed only small deposits. Together with the reduction in Oil Red O staining seen in higher passage DPSCs, this suggests their differentiation potential may be reduced with time *ex vivo* or that the number of multipotent cells in the culture reduces over time. DPSC-05 uninduced control wells also contained some calcium deposits, again suggesting that some DPSCs may spontaneously differentiate after extended periods of time in culture.

To summarise, prolonged culture of DPSCs impacted their morphology and reduced their multi-potency, and in some cases also caused DPSCs to lose expression of surface markers or spontaneously differentiate in culture. Therefore, the passage number of DPSCs was kept as low as possible for further experiments. After establishing that our isolated DPSCs fit the current criteria for MSCs which are that they are multipotent cells and express MSC surface markers, the second aim of this study was addressed by assessing whether DPSCs retain their MSC characteristics after modification by lentiviral transduction.

3.4 Effects of modifying DPSCs by lentiviral transduction on their MSC characteristics

MSCs are proposed to have good potential as vehicles for delivery of anti-inflammatory molecules in various diseases. Whether modifying DPSCs affects their MSC characteristics is an important question in determining if they are suitable for this purpose. Ideally, DPSCs could act as vehicles for gene therapy without compromising their own therapeutic potential. Additionally, it was important in this study to generate DPSCs expressing a reporter which would facilitate tracking their fate *in vivo* later in this study. Therefore, the readiness of DPSCs to be modified by lentiviral transduction was tested and the effect of this process on the MSC characteristics of DPSCs was analysed.

3.4.1 Optimising a lentiviral transduction protocol for DPSCs

In order to generate DPSCs expressing various anti-inflammatory molecules or a reporter, the lentiviral transduction process required optimisation to find conditions which yield a high efficiency of transduction of these particular cells. To this end, different seeding densities of the DPSCs, dilutions of lentivirus and single

versus double transduction were tested using the pWPI-*gfp* vector and measuring percent of GFP^+ DPSCs to determine the best conditions for transduction.

DPSC-02 cells were seeded at three different densities, 4000, 5000 or 6000 cells/cm^2, and incubated with lentivirus made in HEK293FT cells containing pWPI-*gfp* and diluted 1/2, 1/5 or 1/10 in DPSC medium and 8ng/mL protamine sulfate. DPSCs were transduced overnight at 37˚C and 5% CO_2. DPSCs that were transduced twice were rested in complete DPSC medium for 8 hours between transductions of the same conditions. All of the conditions led to a high proportion of DPSCs being successfully transduced as determined by flow cytometry for expression of GFP (70.0-94.6%; Figure 3.10). The condition with the highest transduction efficiency was seeding DPSCs at 4000 cells/cm^2 and transducing twice at a lentivirus dilution of 1/5. Thus, DPSC-02s expressing GFP were generated to be used for tracking *in vivo* later and this transduction protocol facilitated the generation of DPSCs expressing a number of anti-inflammatory molecules as described in the sections that follow.

3.4.2 Modification of DPSCs to express atypical chemokine receptors

Since ACKR2 scavenges some inflammatory chemokines which play important roles in EAE, and ACKR4 may be important for limiting excessive inflammation in EAE[173], it was hypothesised that overexpression of ACKR2 or ACKR4 on DPSCs would enhance the capacity of DPSCs to modulate chemokine gradients that are important for leukocyte trafficking events in EAE, thereby increasing the immunosuppressive effects and therapeutic potential of DPSCs in EAE. Here, whether DPSCs can be transduced to overexpress functional ACKRs and if this affects their MSC characteristics was tested.

3.4.2.1 Transduction of DPSCs to express ACKR2

DPSC-02 cells were first transduced with pWPI-*Ackr2-gfp* vector to stably express ACKR2. This vector contains an internal ribosomal entry site (IRES) between the *Ackr2* transgene and *gfp,* resulting in separate translation of both ACKR2 and eGFP to mark cells which have successfully been transduced with the vector. At the same time, some DPSC-02 cells were transduced with pWPI-*gfp* empty vector as controls. Success of transduction was verified by flow cytometry for expression of the eGFP marker for both the empty vector and *Ackr2*-containing vector transduced cell lines. These transductions were both very efficient and approximately two-thirds of DPSCs were transduced with pWPI-*Ackr2-gfp* and almost 100% transduction efficiency was observed for the empty vector (Figure 3.11A and B). Since transduction efficiency was high, the cells were not sorted or selected to increase the percentage of DPSCs expressing ACKR2 and eGFP in order to spare the cells from further manipulation and to keep passage or time in culture as low as possible. Next, expression of the transgene was verified by qPCR. *Ackr2* mRNA was not detected by untransduced DPSC-02 cells or DPSCs

transduced with pWPI-*gfp* empty vector, but was found to be highly expressed by DPSCs transduced with pWPI-*Ackr2-gfp* (Figure 3.11C).

Transduction of cells is a process that can induce cellular stress or have off-target effects. To check that the transduced DPSCs maintained their multi-potency, they were differentiated to adipocytes of osteocytes. Both DPSC-*gfp* cells and DPSC-*Ackr2-gfp* cells showed potential for adipocytic differentiation as demonstrated by Oil Red O staining for lipid droplets cells cultured with adipogenic induction medium for 3 weeks (Figure 3.12). Similarly, both cell lines maintained osteogenic differentiation potential (Figure 3.13) as Alizarin Red staining revealed deposition of calcium in the cell cultures that were induced to differentiate to osteocytes.

After confirming retention of multi-potency, a functional assay was used to verify overexpression of ACKR2 protein and its activity. Since ACKR2 is a chemokine scavenging protein, and reliable monoclonal antibodies against this receptor are not available, a chemokine scavenging assay was used to test if DPSC-*Ackr2-gfp* cells could specifically scavenge CCL22, an ACKR2 ligand. The DPSCs were incubated with 1, 5 or 10 ng/mL CCL22 at 37˚C and remaining CCL22 in the medium after 3 hr was measured by ELISA. In controls which were incubated without any cells added, there was a reduction in the amount of CCL22 remaining in the medium which may have resulted from basal degradation of the chemokine during the period of incubation. Compared with these no cells controls, the addition of DPSC-*gfp* cells to medium with initial CCL22 concentrations of 1 or 5 ng/mL did not change the amount of CCL22 remaining in the medium. However, when the starting concentration of CCL22 was 10 ng/mL a small reduction in remaining CCL22 was observed after incubation with DPSC-*gfp* cells compared with the no cells control (Figure 3.14). Although DPSC-02 cells did not express *Ccr4* by qPCR (data not shown), it is possible that they express another unidentified receptor for CCL22. On the other hand, DPSC-*Ackr2-gfp* cells caused the amount of CCL22 to decrease in the supernatant by approximately 3-fold compared with the control samples containing no cells. Thus, DPSCs overexpressing ACKR2 functionally scavenged CCL22 *in vitro*.

3.4.2.2 Transduction of DPSCs to express ACKR4

The second candidate molecule for overexpression by DPSCs was ACKR4. DPSC-02 cells were transduced with pWPI-*Ackr4-gfp* and compared with DSPC-02 cells transduced with the pWPI-*gfp* empty vector. Transduction efficiency was checked by flow cytometry for GFP which revealed that almost all DPSCs (98.3%) were successfully transduced with pWPI-*Ackr4-gfp*, which was a similar efficiency as the empty vector (Figure 3.15A). qPCR showed *Ackr4* mRNA was highly expressed in cells transduced with pWPI-*Ackr4-gfp*, but at very low levels in DPSCs transduced with the empty vector (Figure 3.15B).

DPSC-*Ackr4-gfp* cells were then checked for multi-potency by differentiation to adipocytes and osteocytes. Adipogenic differentiation potential was maintained after transduction of the DPSC-*Ackr4-gfp* cells which

stained positive for Oil Red O lipid-staining after induction of differentiation to adipocytes for 3 weeks (Figure 3.16). DPSC-*Ackr4-gfp* cells also retained potential for osteogenic differentiation. Induction of osteogenic differentiation for 3 weeks resulted in positive Alizarin Red staining for calcium deposits confirming differentiation of the cells (Figure 3.17).

A scavenging assay was used to test the functional activity of overexpressing ACKR4 on the DPSCs. The ACKR4 ligand CCL19 was added in three different concentrations to media with or without DPSC-*Ackr4-gfp* cells or DPSC-*gfp* cells. For both 5 and 10 ng/mL starting CCL19 concentrations, DPSC-*gfp* empty vector cells had reduced CCL19 remaining in the supernatant after 3 hours incubation than controls containing no cells (Figure 3.18). This may be due to basal expression of a CCL19 receptor by DPSCs. However, when ACKR4-overexpressing DPSCs were tested, CCL19 was significantly depleted from the medium compared with DPSC-*gfp* control cells and thus, ACKR4 functionally scavenged CCL19 when expressed by DPSCs.

3.4.3 Transduction of DPSCs to express an IL-23 antagonist

In addition to overexpressing ACKRs on DPSCs to target leukocyte trafficking, another anti-inflammatory molecule was expressed in DPSC-03 cells to target the generation of pathogenic cells in EAE. The IL-23 signalling pathway was chosen to target because it is important for the development of highly pathogenic GM-CSF-expressing Th17 cells in EAE[33,34] and anti-IL-23p19 antibody treatment of EAE mice suppresses disease[334]. To target this pathway, a novel putative IL-23 antagonist was designed, tested and expressed by DPSCs.

3.4.3.1 Design of the IL-23 antagonist

A putative IL-23 antagonist was designed using a similar approach to Yu and Gallagher (2010)[335] who generated a soluble form of the human IL-23R that suppressed IL-23 signalling. The murine *Il23r* gene is structurally similar to the human *Il23r*. Both have 11 exons in which the first 8 exons encode the extracellular portion of the receptor and the IL-23 binding domain, exon 9 encodes a transmembrane-spanning portion exons 10 and 11 encode the intracellular signalling portion of the receptor. By deleting exon 9, the transmembrane-coding region of the receptor is removed (Figure 3.19). Furthermore, this deletion causes a frameshift in the downstream exons 10 and 11 which introduces a new STOP codon early in exon 10. The result of these changes is a putative truncated IL-23R which lacks the transmembrane and intracellular regions, and thus comprises only the extracellular IL-23-binding region. Also, there is a sequence change for the first 7 amino acids of exon 10 and the peptide is 270 amino acids shorter than full length *Il23r*. This putative soluble form of the receptor was proposed to bind and sequester IL-23 to inhibit cytokine signalling.

A lentiviral expression vector containing the new ORF of this putative soluble IL-23R, termed *Il23rΔ9*, was designed and purchased from VectorBuilder Inc. (Figure 3.20). This vector, pLV-*Il23rΔ9*:IRES:mCherry contains an EF1α promoter to drive expression of the *Il23rΔ9* transgene together with an mCherry reporter that can be translated separately using an internal ribosome entry site (IRES).

First, it was tested whether IL-23RΔ9 was indeed an antagonist of IL-23 signalling. To do this, HEK293FT cells were transfected with pLV-*Il23rΔ9*:IRES:mCherry then cultured in fresh culture medium for 2 days to allow the putative protein to be expressed and secreted. Some HEK293FT cells were mock transfected for a control in which they were treated in the same manner as the true transfected cells including incubation in OptiMEM containing lipofectamine transfection reagent but did not receive the expression plasmid DNA. The supernatants from Il23rΔ9-transfected and mock transfected HEK293FT cells were then used in stimulated splenocytes cultures to test if the cells had secreted a product that inhibits IL-23 signalling. IL-23 stimulation of T cells in mixed splenocyte cultures activated with anti-CD3 and anti-CD28 induces IL-17A production[336]. Splenocytes were stimulated with anti-CD3, anti-CD28 and IL-2 in the presence or absence of IL-23 and the HEK293FT supernatants and incubated at 37˚C in 5% CO_2. After 6 days, IL-17A secretion by the stimulated splenocytes was measured by enzyme-linked immunosorbent assay (ELISA). IL-23 stimulated the secretion of IL-17A by splenocytes and this was suppressed by the addition of Il23rΔ9-transfected HEK293FT cell supernatants in a dose-dependent manner but not supernatants from mock-transfected cells (Figure 3.21). Thus, it can be concluded that Il23rΔ9 encodes a soluble protein that blocks IL-23 signalling. Splenocytes that were not stimulated with IL-23 also secreted a low level of IL-17A and this was also suppressed by the supernatants of Il23rΔ9-transfected cells.

3.4.3.2 Expression of IL-23RΔ9 by DPSCs

After establishing that *Il23rΔ9* encodes a soluble IL-23 antagonist, DPSCs expressing this protein were generated. To this end, DPSC-03 cells were transduced with lentivirus containing pLV-*Il23rΔ9*:IRES:mCherry or with no expression plasmid (mock-transduced). Successful transduction of the DPSCs was verified by flow cytometry. Seventy-two percent of DPSC-03 cells were transduced with pLV-*Il23rΔ9*:IRES:mCherry as determined by positive expression of the mCherry reporter protein (Figure 3.22).

Next, it was tested if DPSCs expressing *Il23rΔ9* could suppress IL-23 signalling. Mock-transduced DPSCs or DPSC-*Il23rΔ9* cells were cultured for 3 days in DPSC culture medium to collect their secreted products. The supernatants were harvested and applied to anti-CD3 and anti-CD28-activated splenocytes that were stimulated with IL-23 and IL-2. Some of the cultures were not stimulated with IL-23. After 6 days, IL-17A production by the splenocytes was measured in their supernatants by ELISA. DPSC-conditioned medium (DPSC-CM) from mock-transduced cells suppressed IL-17A production by IL-23-stimulated splenocytes, suggesting that a secreted product of DPSCs can inhibit the production of IL-17A. However, in DPSCs which expressed *Il23rΔ9*, this ability to suppress IL-17A secretion was abolished. Thus, DPSC-*Il23rΔ9* cells appear not to be

able to suppress IL-23 signalling, which was an unexpected finding as it indicated that the IL-23RΔ9 in the context of the DPSC secretome is not capable of blocking IL-23 driven responses.

3.5 Summary

The data presented in this chapter characterised DPSCs isolated from 7 human donors. These all displayed an MSC-like immunophenotype and were multipotent *in vitro*. Six of these 7 lines could be cultured continuously for up to 17 weeks or 38-47 population doublings. However, extended culture modifies the phenotype of some DPSCs, alters their morphology by increasing cell size and appears to reduce their differentiation potential, all indications that time in culture should be minimised. DPSCs were amenable to lentiviral transduction showing high yields of up to 100% transduction efficiency. They retained expression of MSC surface markers following transduction and retained multipotent capability. DPSCs were successfully generated to overexpress functional ACKR2 or ACKR4 proteins. DPSCs expressing GFP were also generated which can facilitate tracking of the cells *in vivo*. Finally, an IL-23 antagonist was designed, expressed in HEK293FT cells and shown to functionally inhibit IL-23 signalling, but did not have this effect when expressed by DPSCs.

Table 3.1: Age and sex of the DPSC donors for this study.

DPSC cell line	Donor sex	Donor age	Source
DPSC-01	Male	20	Koblar lab
DPSC-02	Male	20	Koblar lab
DPSC-03	Male	22	In-house
DPSC-04	Male	27	Koblar lab
DPSC-05	Female	20	In-house
DPSC-06	Female	21	In-house
DPSC-07	Male	26	In-house

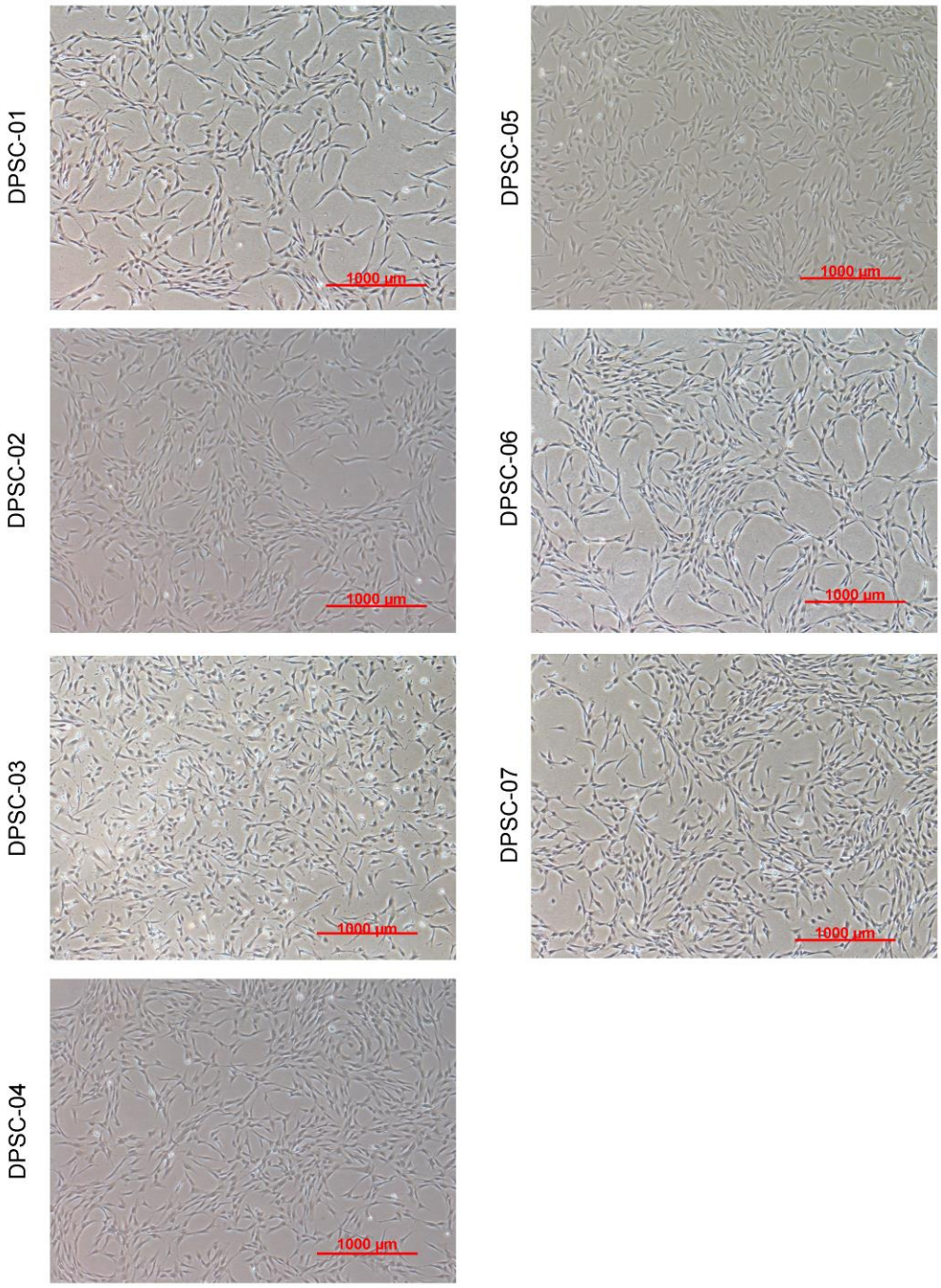

Figure 3.1: Morphology of DPSCs in culture.

DPSCs were isolated from the pulp of different human donors and cultured *in vitro*. Phase contrast images at 4X magnification were taken after 2 passages. Representative of two independent experiments.

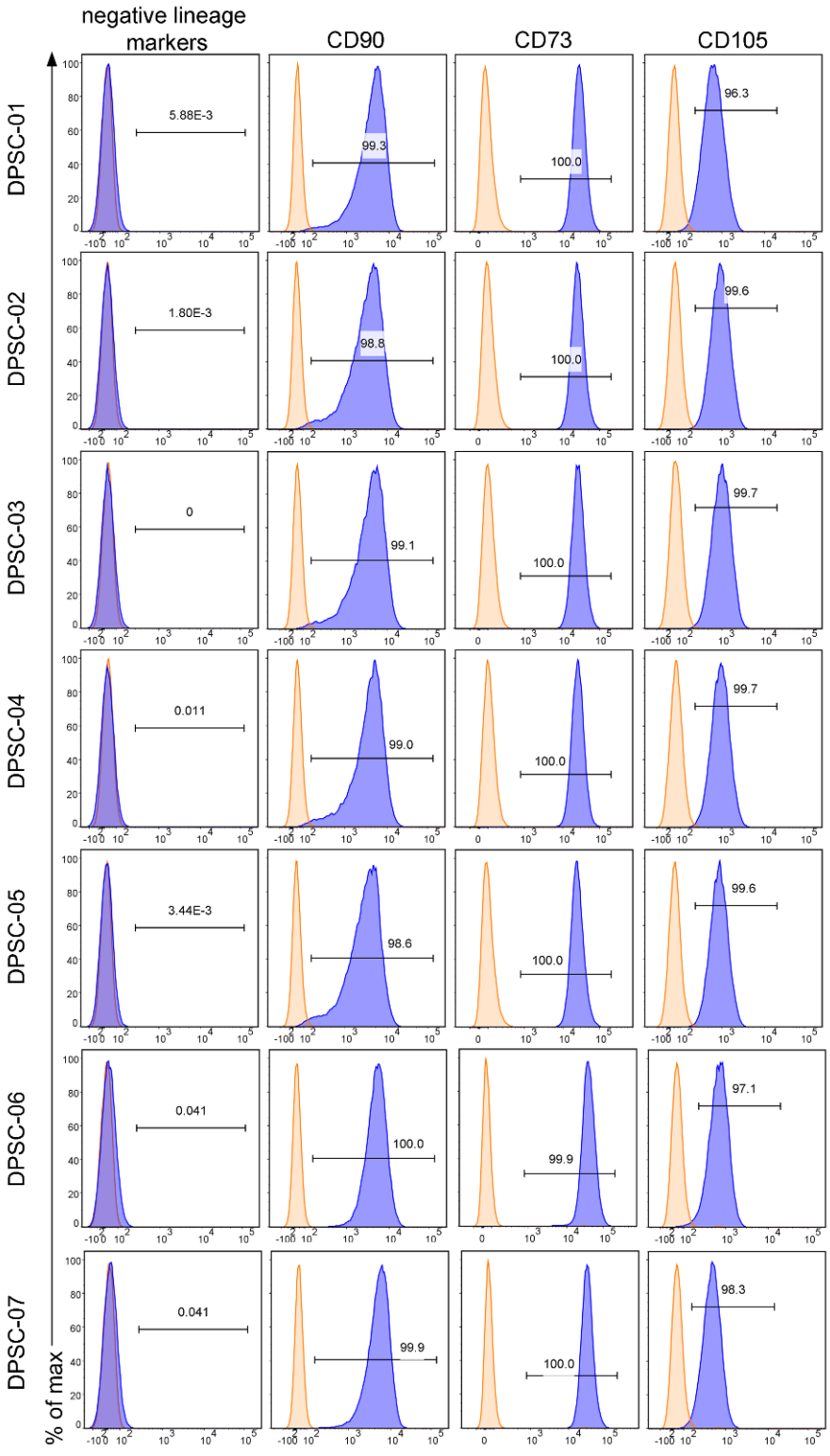

Figure 3.2: DPSCs express MSC markers.

DPSCs between passages 2-4 were assessed for expression of MSC markers by flow cytometry. The negative lineage marker cocktail contains CD34, CD11b, CD19, CD45 and HLA-DR all conjugated to PE. Orange histograms show isotype controls and blue histograms show antibody-stained samples. Representative of two independent experiments.

This page intentionally left blank.

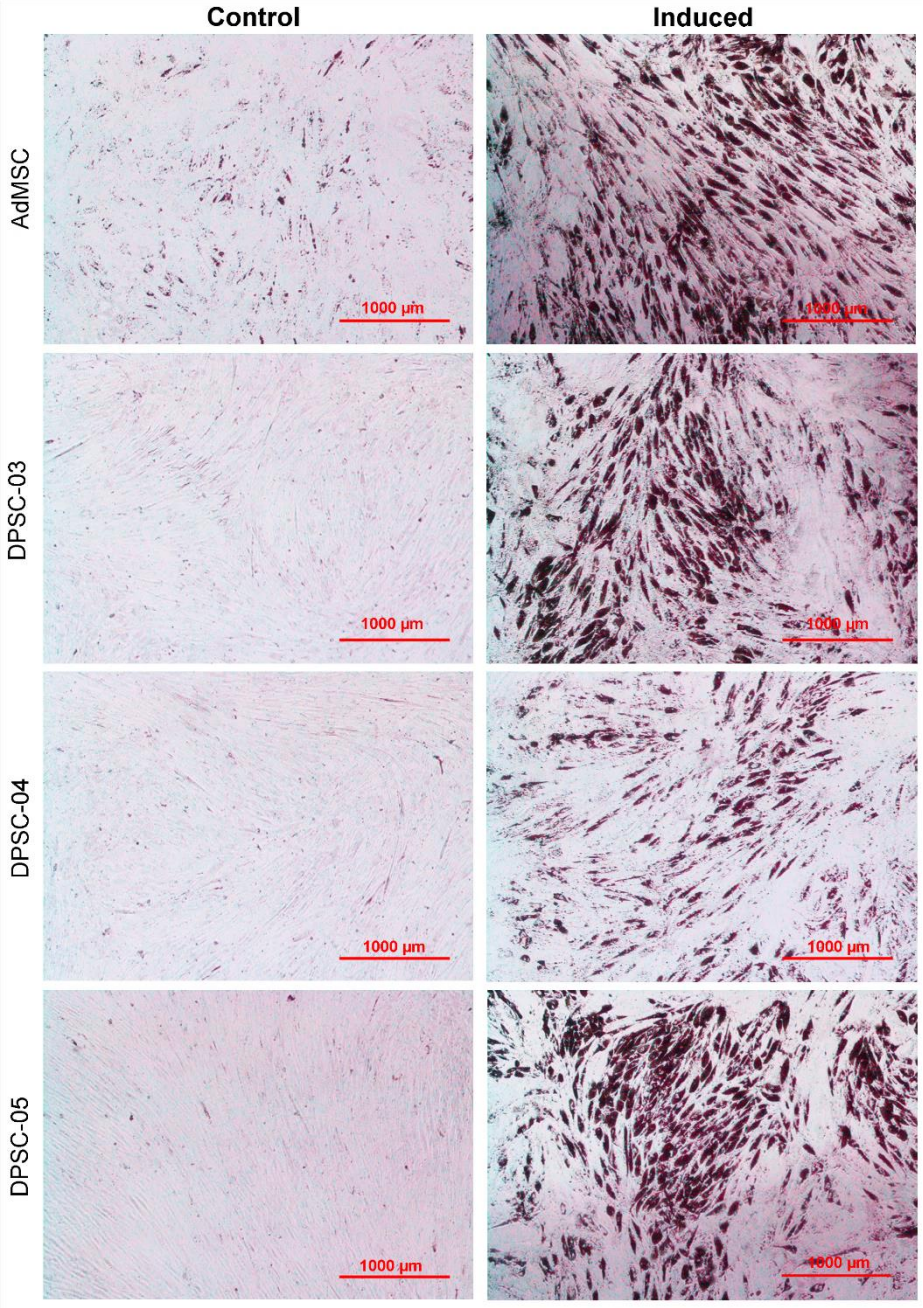
Control
Induced
AdMSC
DPSC-03
DPSC-04
DPSC-05
1000 µm

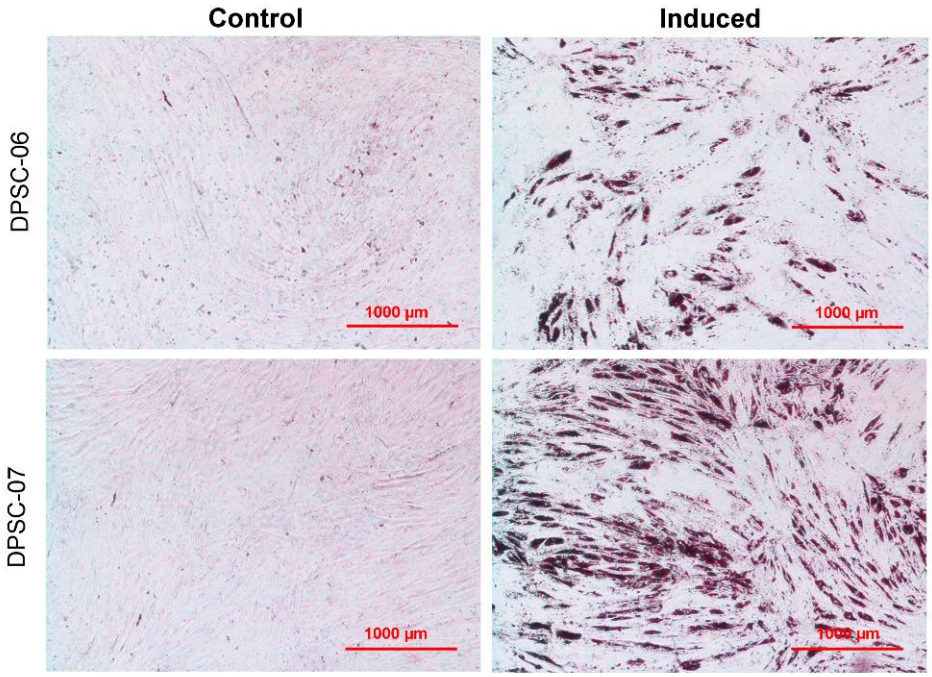

Figure 3.3: DPSCs differentiate into adipocytes *in vitro*.

Phase contrast images at 4X magnification of passage 3 DPSCs that were differentiated to adipocytes *in vitro*. AdMSCs were included as a positive control for multipotency. For non-induced controls, DPSCs were cultured for the duration of the experiment in their normal complete medium. Induced samples were cultured with complete medium supplemented with 0.5 µM dexamethasone, 0.5 µM isobutylmethylxanthine and 50 µM indomethacin for 21 days. To measure differentiation, Oil Red O was used to stain lipid droplets. 4X magnification. Representative of three independent experiments.

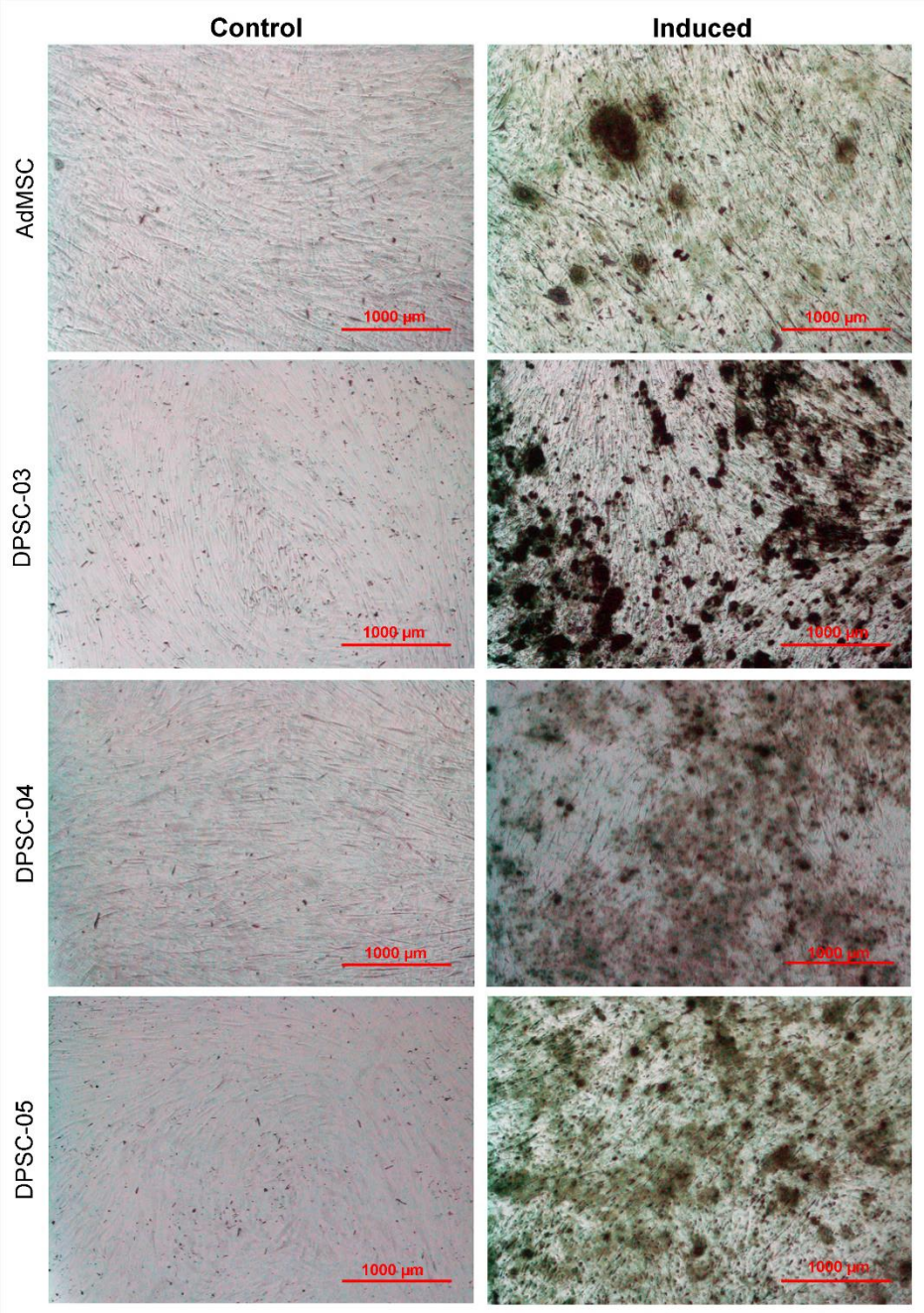
Control
Induced
AdMSC
DPSC-03
DPSC-04
DPSC-05
1000 µm

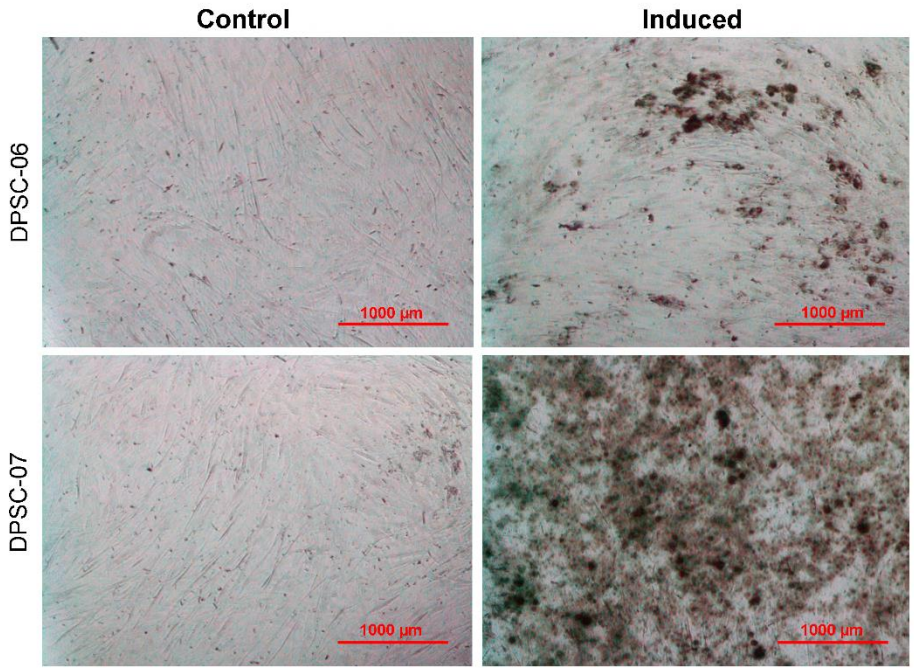

Figure 3.4: DPSCs differentiate into osteocytes *in vitro.*

Phase contrast images at 4X magnification of passage 3 DPSCs that were differentiated to osteocytes *in vitro*. AdMSCs were included as a positive control for multipotency. For non-induced controls, DPSCs were cultured for the duration of the experiment in their normal complete medium. Induced samples were cultured with complete medium supplemented with 10 nM dexamethasone, 20 mM β-glycerol phosphate and 50 µM L-ascorbic acid 2-phosphate for 21 days. To measure differentiation, Alizarin Red stain was used to identify calcium deposits. Representative of four independent experiments.

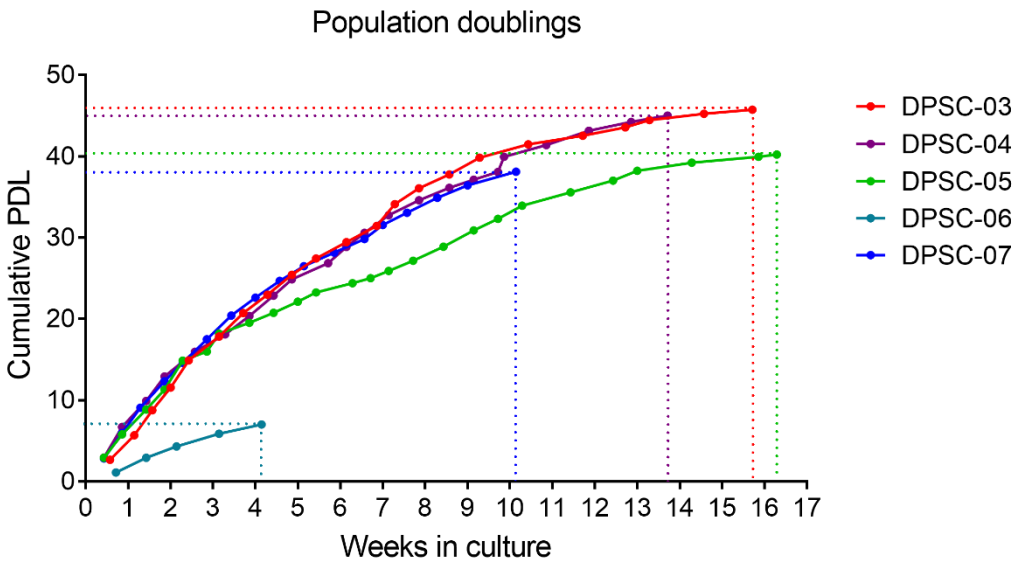

Figure 3.5: Comparison of the long-term proliferative potential of DPSCs from multiple donors.

DPSCs were cultured continuously by passaging each time the cells reached approximately 90% confluency. At each passage, the DPSCs were counted and re-seeded at 5000 cells/cm^2. Cumulative population doubling level (PDL) was calculated using the formula PDL = 3.322(log(y)-log(s)) + x, where x is the number of cells harvested, s is the number of cells initially seeded into the flask and y is the PDL from the previous passage. Each data point represents the PDL for each DPSC cell line tested. The dotted lines indicate the point where DPSCs were determined to reach senescence, which was determined by either failure of the cells to proliferate thereafter or death of the cells in culture.

This page intentionally left blank.

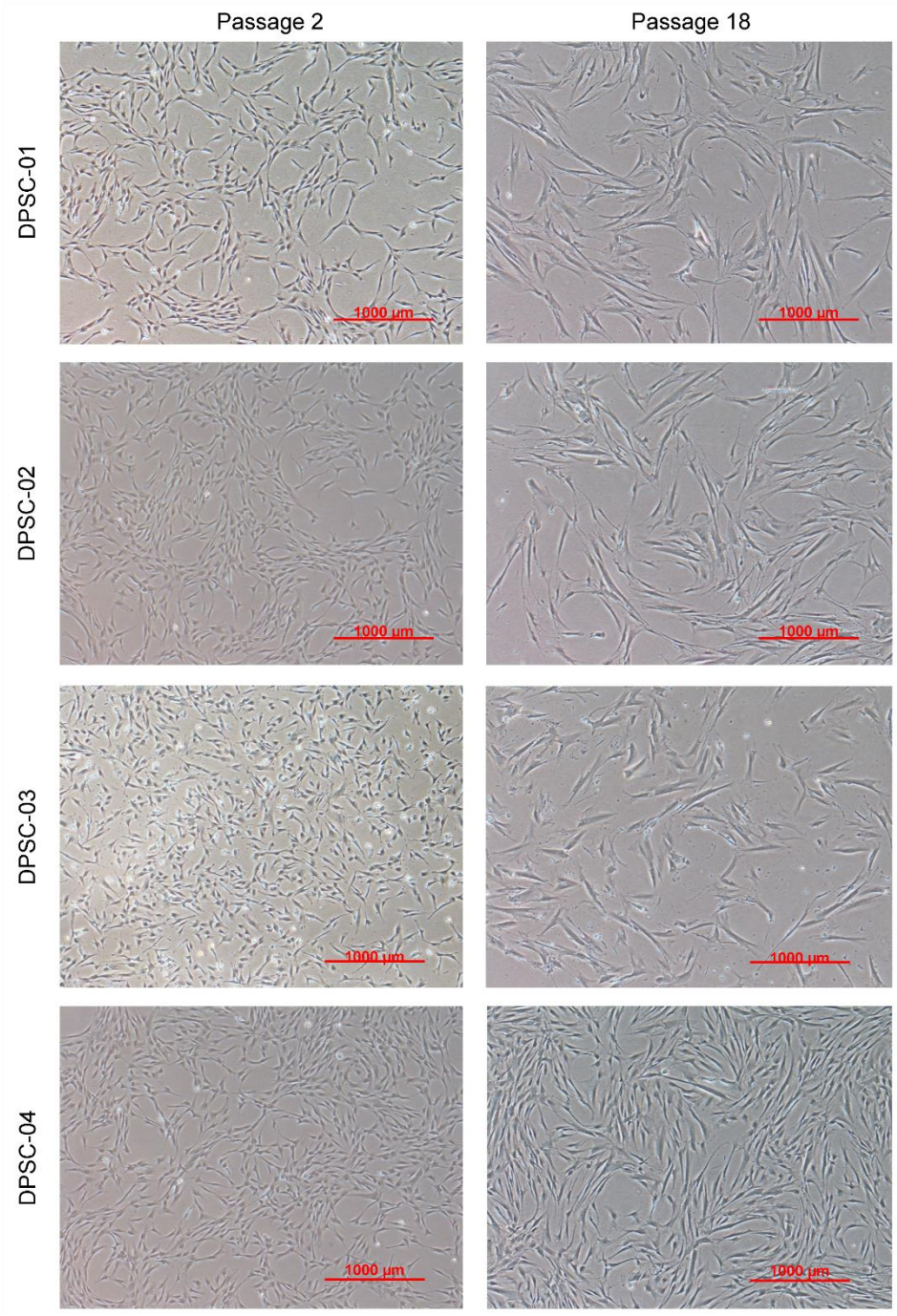
Passage 2
Passage 18
DPSC-01
DPSC-02
DPSC-03
DPSC-04
1000 µm

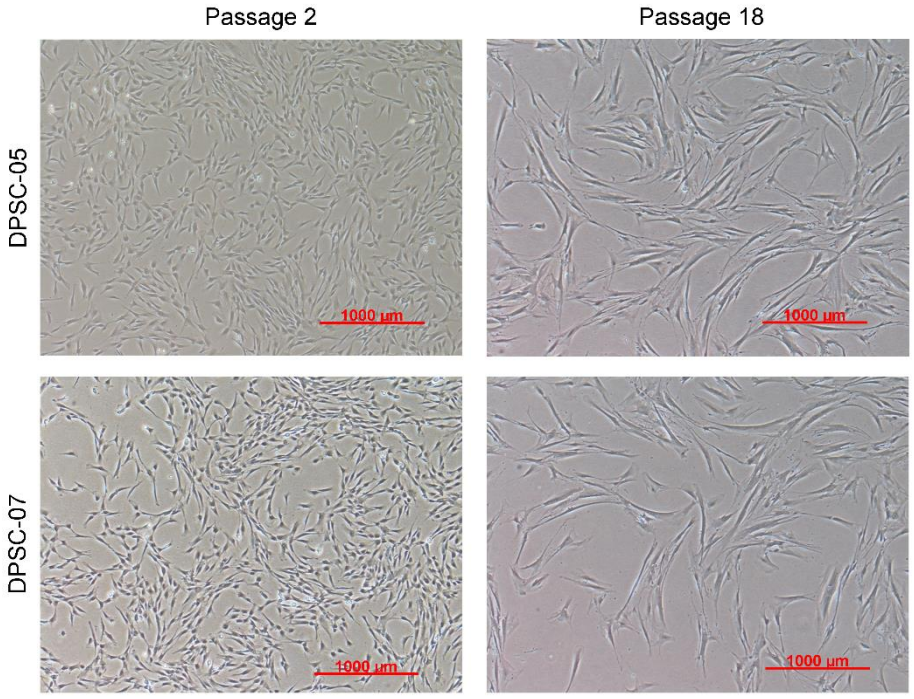

Figure 3.6: Morphology of DPSCs after extended culture.

DPSCs from different human donors (01-05, 07) were cultured continuously by passaging the cells each time they reached about 70% confluency and reseeding at 5000 cells/cm^2. Phase contrast images at 4X magnification were taken after 18 passages in culture (approximately 13 weeks). Representative of two independent experiments.

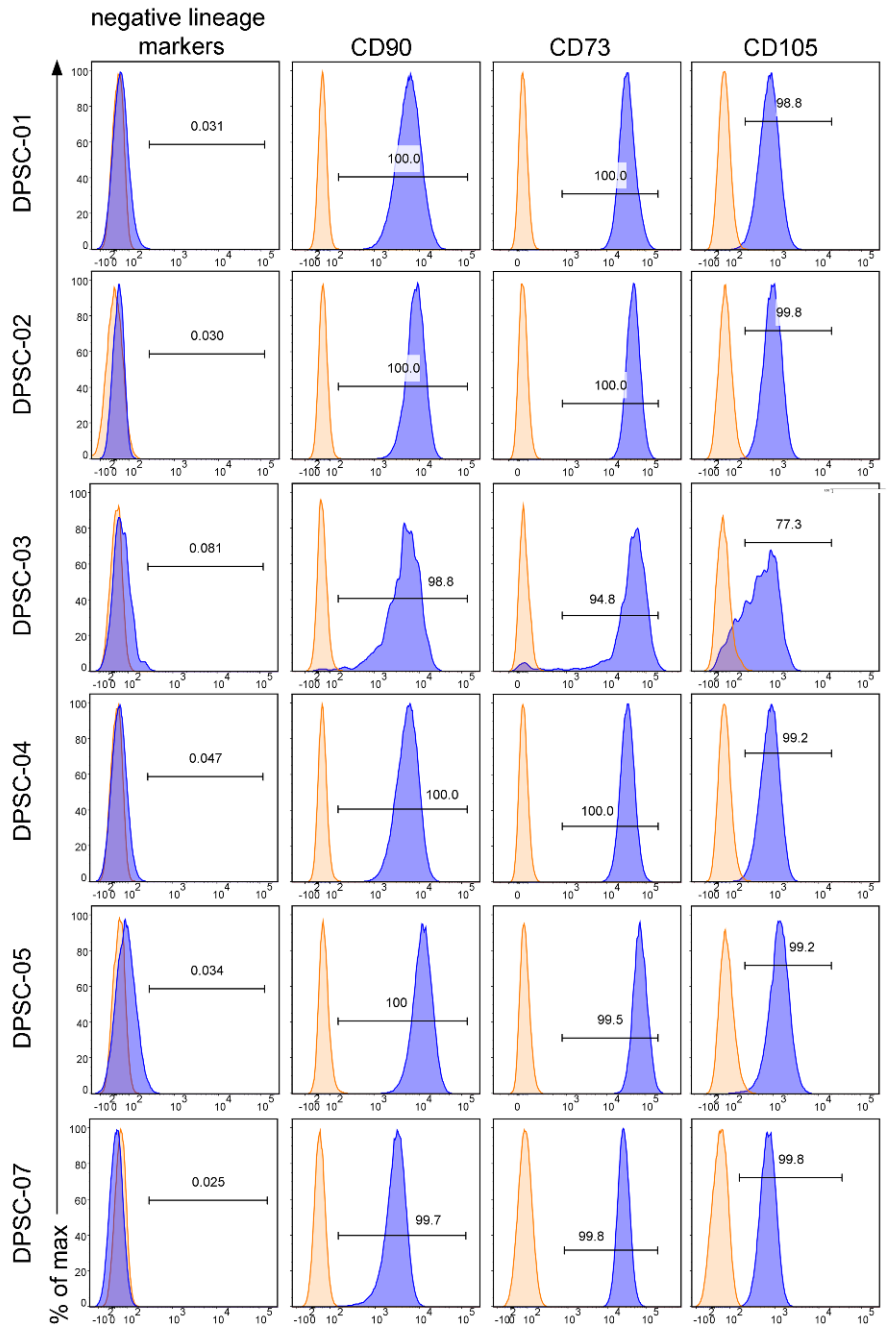

Figure 3.7: Expression of MSC markers by high-passage DPSCs.

DPSCs harvested after long-term culture (passage 16) were stained for MSC markers using the BD Stemflow™ Human MSC Analysis kit. The negative lineage marker cocktail contains CD34, CD11b, CD19, CD45 and HLA-DR all conjugated to PE. Orange histograms show isotype controls and blue histograms show antibody-stained samples. Representative of two independent experiments.

This page intentionally left blank.

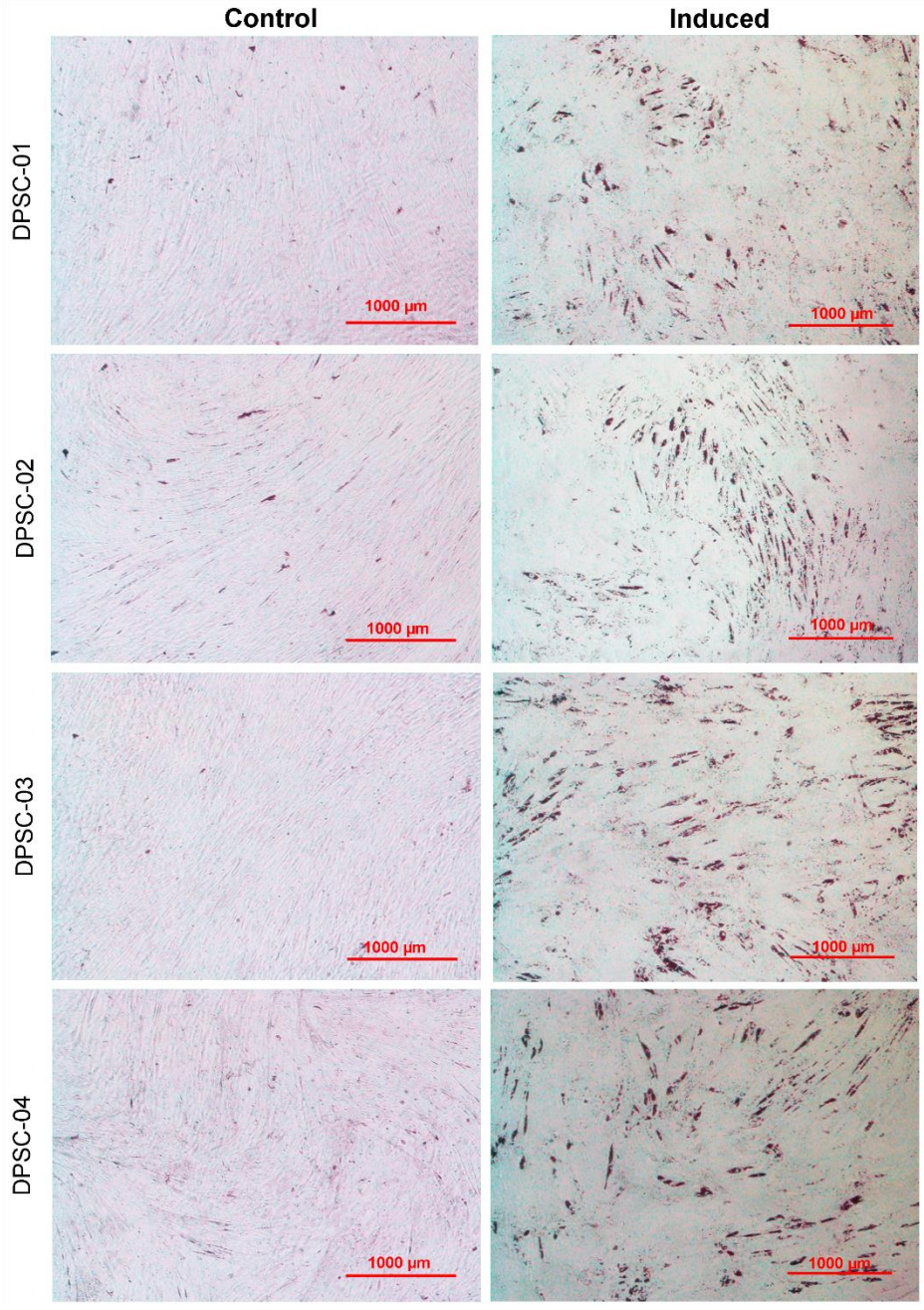
Control
Induced
DPSC-01
DPSC-02
DPSC-03
DPSC-04
1000 µm

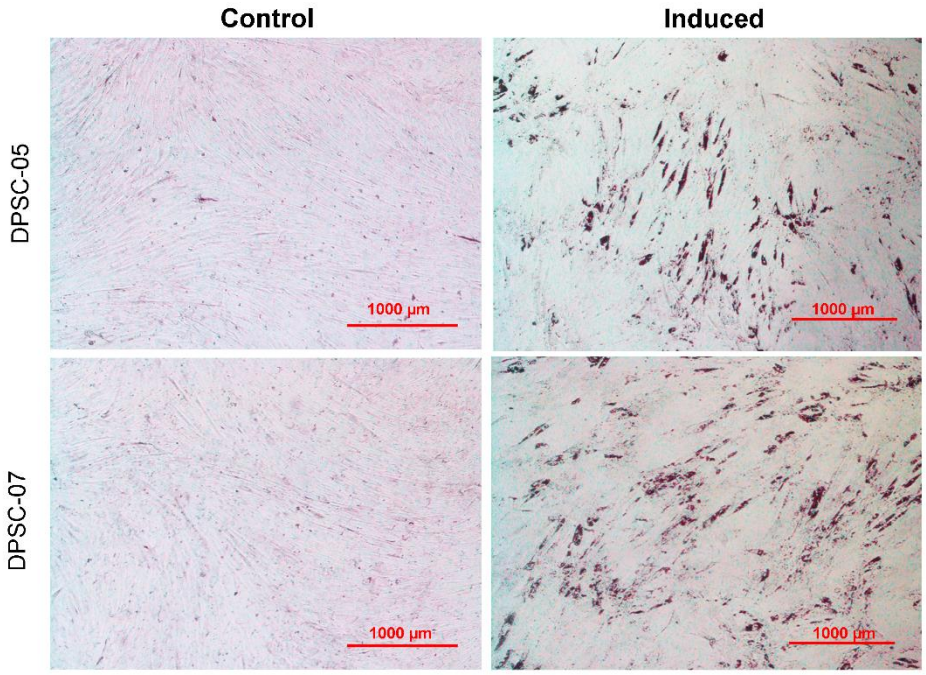

Figure 3.8: Differentiation of high passage DPSCs into adipocytes

Phase contrast images at 4X magnification of DPSCs that were differentiated to adipocytes *in vitro*. For non-induced controls, DPSCs were cultured for the duration of the experiment in their normal complete medium. Induced samples were cultured with complete medium supplemented with 0.5 µM dexamethasone, 0.5 µM isobutylmethylxanthine and 50 µM indomethacin for 21 days. To measure differentiation, Oil Red O was used to stain lipid droplets. Representative of two independent experiments.

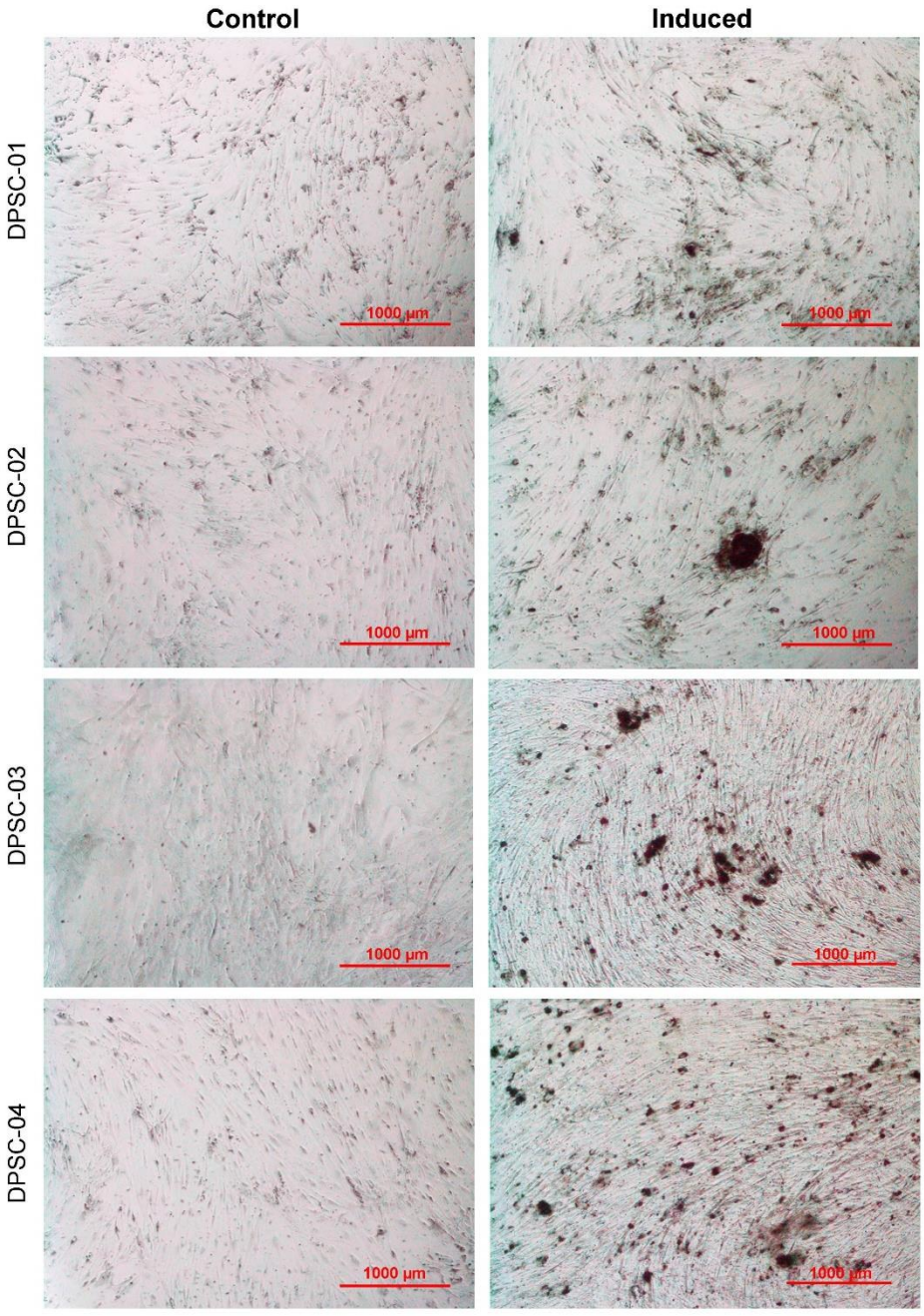
Control
Induced
DPSC-01
DPSC-02
DPSC-03
DPSC-04
1000 µm

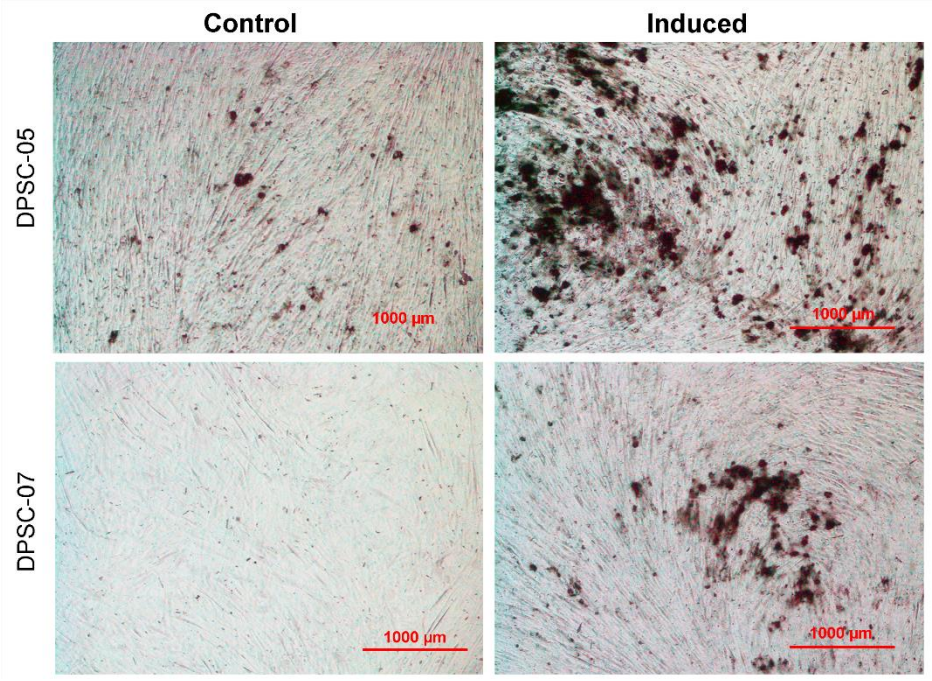

Figure 3.9: Differentiation of high passage DPSCs into osteocytes

Phase contrast images at 4X magnification of DPSCs that were differentiated to adipocytes *in vitro*. For non-induced controls, DPSCs were cultured for the duration of the experiment in their normal complete medium. Induced samples were cultured with complete medium supplemented with 10 nM dexamethasone, 20 mM β-glycerol phosphate and 50 µM L-ascorbic acid 2-phosphate for 21 days. To measure differentiation, Alizarin Red stain was used to identify calcium deposits. Representative of two independent experiments.

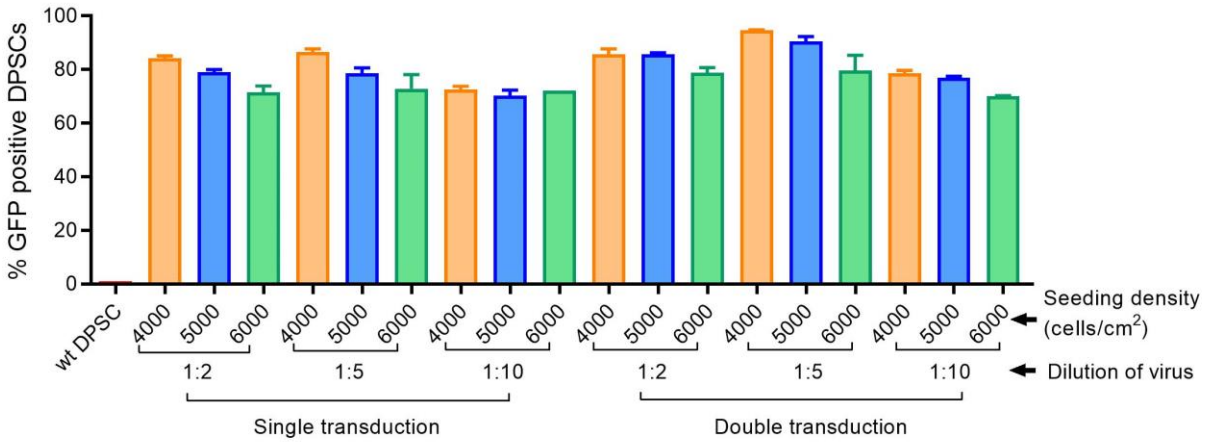

Figure 3.10: Optimising lentiviral transduction of DPSCs.

DPSCs were plated at three different seeding densities and transduced 1 or 2 times with three different dilutions of lentivirus containing pWPI-*gfp* overnight at 37˚C. Cells that were transduced twice were rested for 8 hr in complete DPSC medium in-between. Transduction efficiency was measured by flow cytometry for DPSCs which expressed GFP. Columns represent mean ± SD of each condition performed in triplicate.

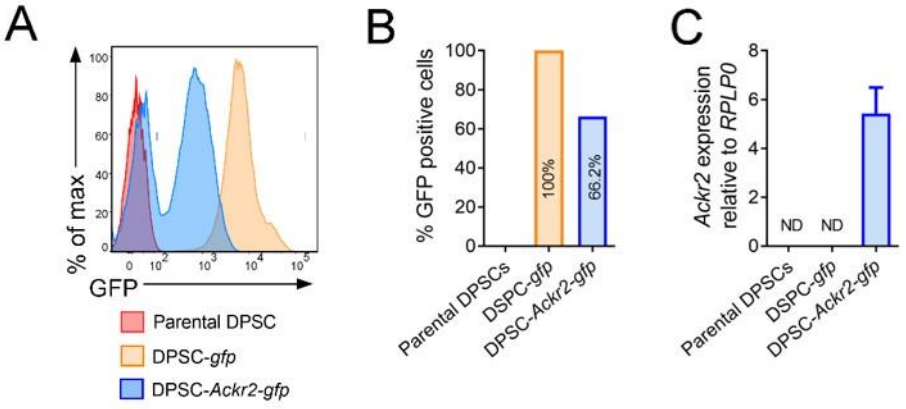

Figure 3.11: Overexpression of ACKR2 on DPSCs.

DPSCs from donor 2 were transduced with empty pWPI or pWPI-ACKR2 and successful uptake of DNA was assessed by flow cytometry for the GFP reporter contained in pWPI. **a)** Expression of GFP by transduced DPSCs (blue or orange) compared with parental DPSCs (red). **b)** Percentage of cells expressing GFP and thus successfully transduced with pWPI-*gfp* or pWPI-*Ackr2-gfp*. **c)** qPCR for expression of *Ackr2* in transduced DPSCs. The bar represents the mean ± SD of 3 technical replicates. ND = not detected.

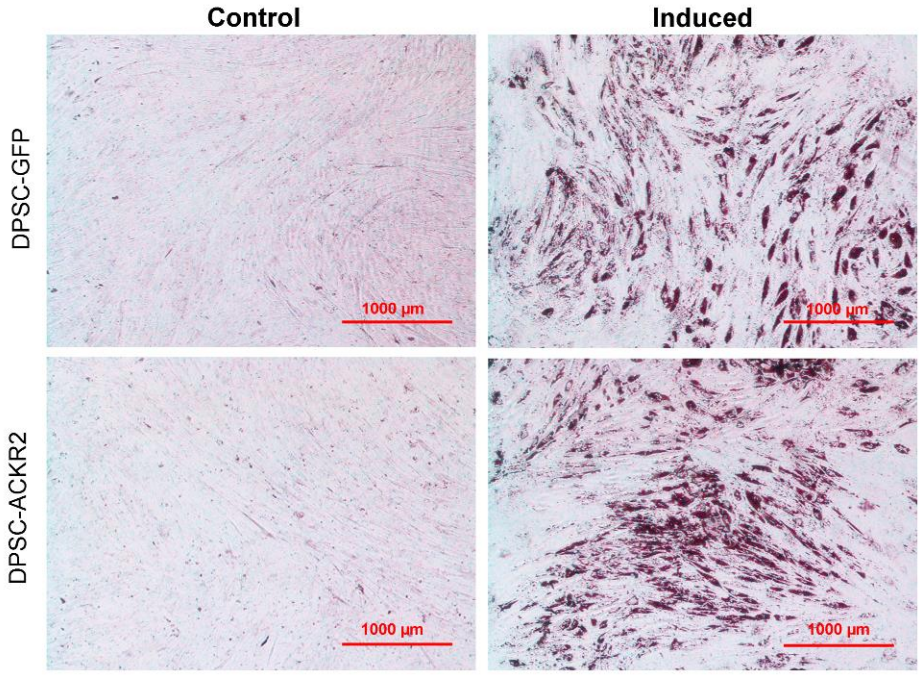

Figure 3.12: ACKR2-over-expressing DPSCs differentiate into adipocytes *in vitro*.

DPSCs transduced with empty vector (DPSC-GFP) or to express ACKR2 (DPSC-ACKR2) were differentiated to adipocytes *in vitro*. For non-induced controls, DPSCs were cultured for the duration of the experiment in their normal complete medium. Induced samples were cultured with complete medium supplemented with 0.5 µM dexamethasone, 0.5 µM isobutylmethylxanthine and 50 µM indomethacin for 21 days. To measure differentiation, Oil Red O was used to stain lipid droplets. 4X magnification. Representative of two independent experiments.

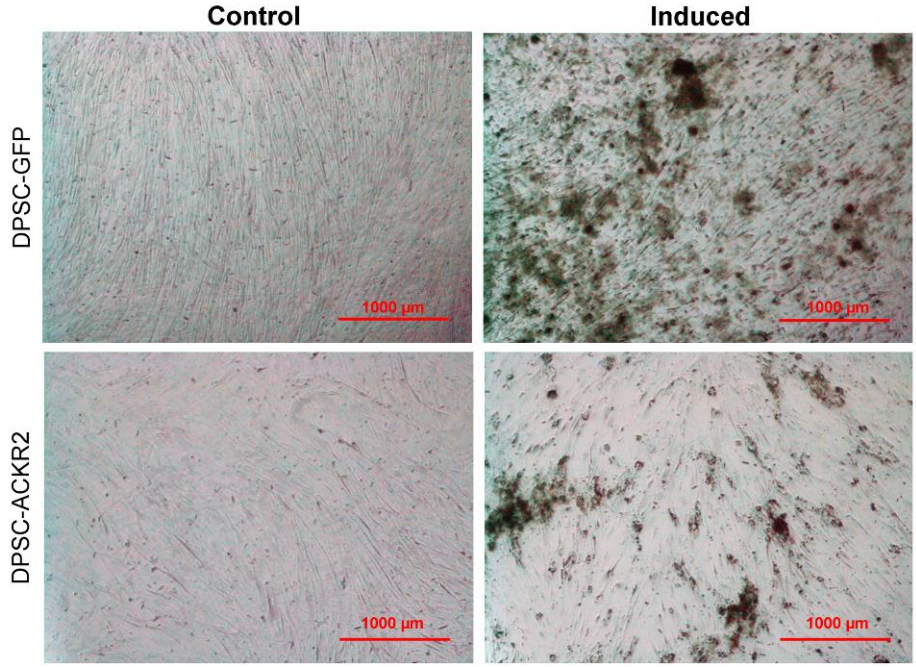

Figure 3.13: ACKR2-over-expressing DPSCs differentiate into osteocytes *in vitro*.

DPSCs transduced with empty vector (DPSC-GFP) or to express ACKR2 (DPSC-ACKR2) were differentiated to osteocytes *in vitro*. For non-induced controls, DPSCs were cultured for the duration of the experiment in their normal complete medium. Induced samples were cultured with complete medium supplemented with 10 nM dexamethasone, 20 mM β-glycerol phosphate and 50 µM L-ascorbic acid 2-phosphate for 21 days. To measure differentiation, Alizarin Red stain was used to identify calcium deposits. 4X magnification. Representative of two independent experiments.

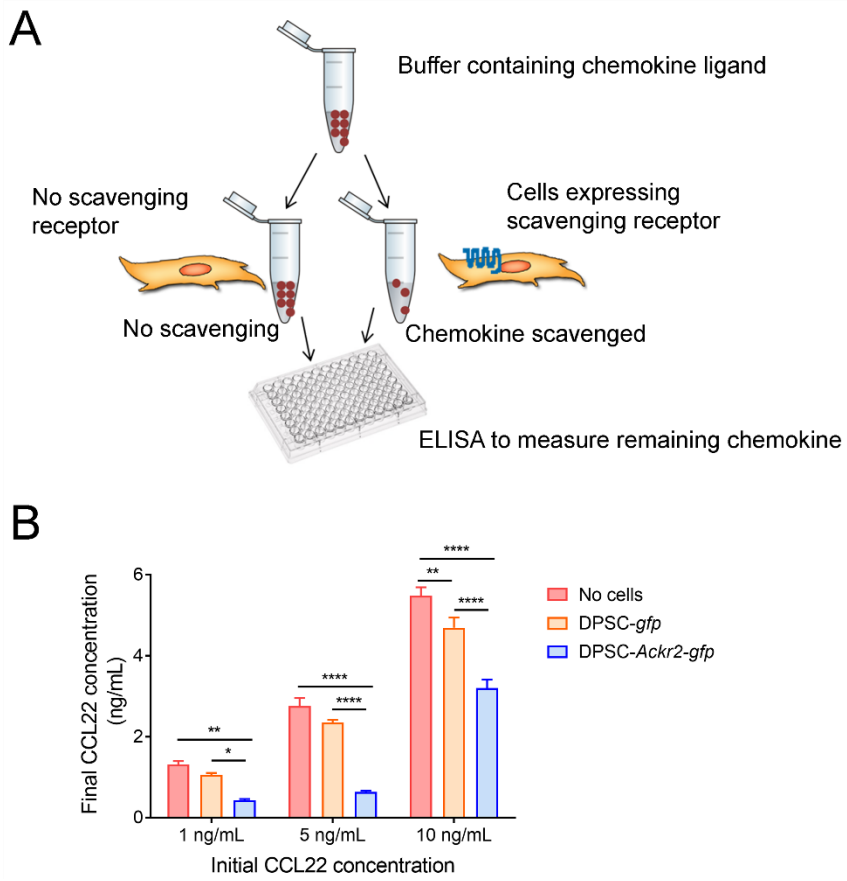

Figure 3.14: Chemokine scavenging by ACKR2-expressing DPSCs in vitro.

a) Schematic diagram of a chemokine scavenging assay. DPSCs transduced with empty vector (DPSC-*gfp*) or to express ACKR2 (DPSC-*Ackr2-gfp*) were incubated with three different starting concentrations of the ACKR2 ligand CCL22 for 3 hr at 37°C, mixing every 30 min to resuspend the cells. **b)** Remaining CCL22 in the supernatants was measured by ELISA. Each column represents mean ± SEM of each cell line performed in triplicate. *p<0.05, **p<0.01, ****p<0.001 Two-Way ANOVA with Bonferroni's multiple comparisons test. Representative of two independent experiments.

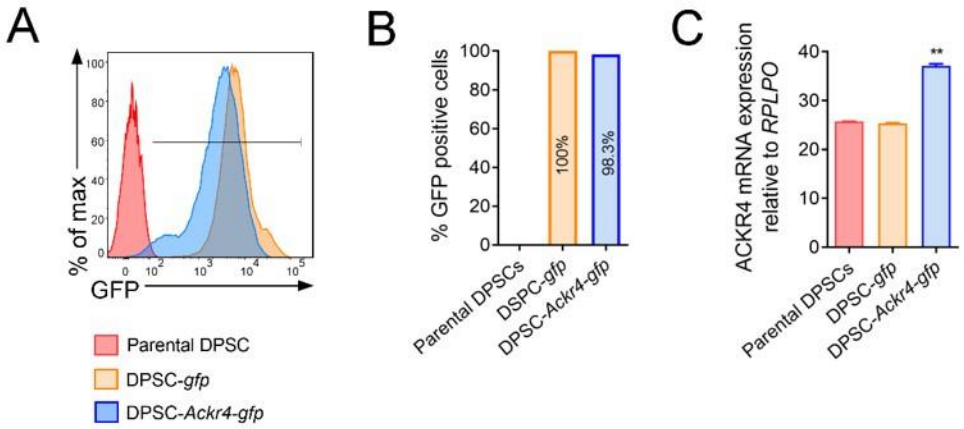

Figure 3.15: Overexpression of ACKR4 in DPSCs.

DPSCs from donor 02 were transduced with pWPI-*gfp* (empty vector control) or pWPI-*Ackr4-gfp* and successful uptake of the vectors was assessed by flow cytometry for the GFP reporter contained in pWPI. **a)** Expression of GFP by transduced DPSCs (blue or orange) compared with non-transduced parental DPSCs (red). **b)** Percentage of cells expressing GFP and thus successfully transduced with pWPI-*gfp* or pWPI-*Ackr4-gfp*. **c)** qPCR for expression of *Ackr4* in transduced DPSCs. **p<0.01 One-Way ANOVA with Bonferroni's multiple comparisons test.

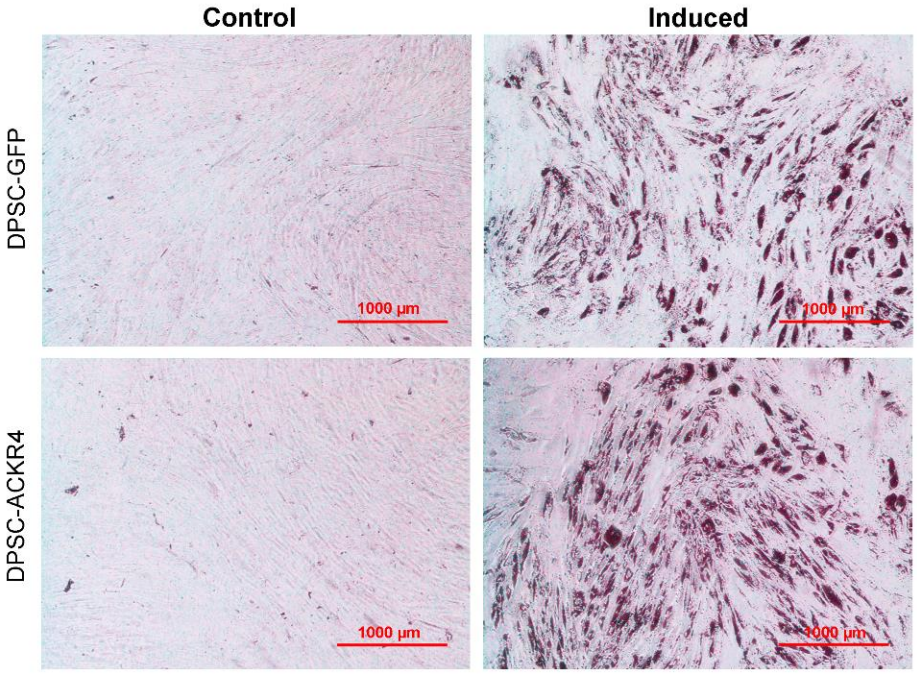

Figure 3.16: ACKR4-over-expressing DPSCs differentiate into adipocytes *in vitro.*

Phase contrast images at 4X magnification of DPSCs transduced with empty vector (DPSC-GFP) or to express ACKR4 (DPSC-ACKR4) that were differentiated to adipocytes *in vitro*. For non-induced controls, DPSCs were cultured for the duration of the experiment in their normal complete medium. Induced samples were cultured with complete medium supplemented with 0.5 µM dexamethasone, 0.5 µM isobutylmethylxanthine and 50 µM indomethacin for 21 days. To measure differentiation, Oil Red O was used to stain lipid droplets. Representative of two independent experiments.

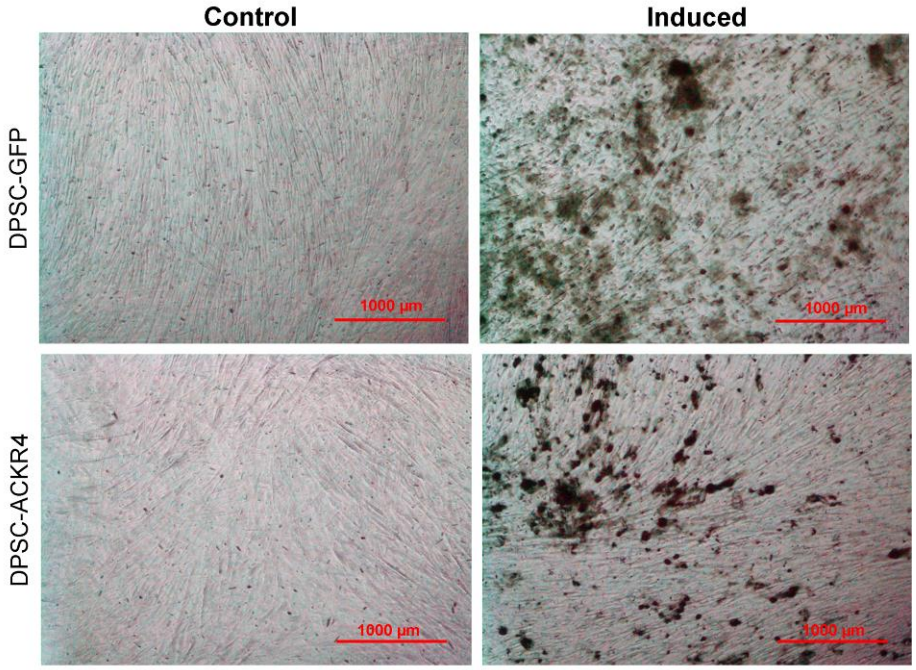

Figure 3.17: ACKR4-over-expressing DPSCs differentiate into osteocytes *in vitro*.

Phase contrast images at 4X magnification of DPSCs transduced with empty vector (DPSC-GFP) or to express ACKR4 (DPSC-ACKR4) that were differentiated to osteocytes *in vitro*. For non-induced controls, DPSCs were cultured for the duration of the experiment in their normal complete medium. Induced samples were cultured with complete medium supplemented with 10 nM dexamethasone, 20 mM β-glycerol phosphate and 50 µM L-ascorbic acid 2-phosphate for 21 days. To measure differentiation, Alizarin Red stain was used to identify calcium deposits. Representative of two independent experiments.

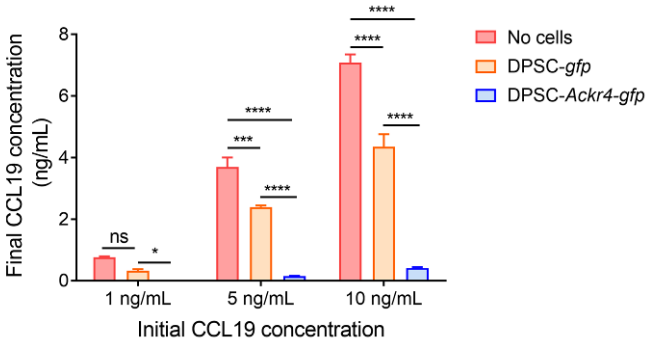

Figure 3.18: Chemokine scavenging by ACKR4-expressing DPSCs *in vitro*.

DPSCs transduced with empty vector (DPSC-*gfp*) or ACKR4 (DPSC-*Ackr4-gfp*) were incubated with three different starting concentrations of CCL19 for 3 hr at 37°C, mixing every 30 min to resuspend the cells as shown in the schematic in Figure 3.14A. Remaining CCL19 in the supernatants was measured by ELISA. Each column represents mean ± SEM of each cell line performed in triplicate. *p<0.05, ***p<0.005, ****p<0.001 Two-Way ANOVA with Bonferroni's multiple comparisons test. ns: not significant. Representative of two independent experiments.

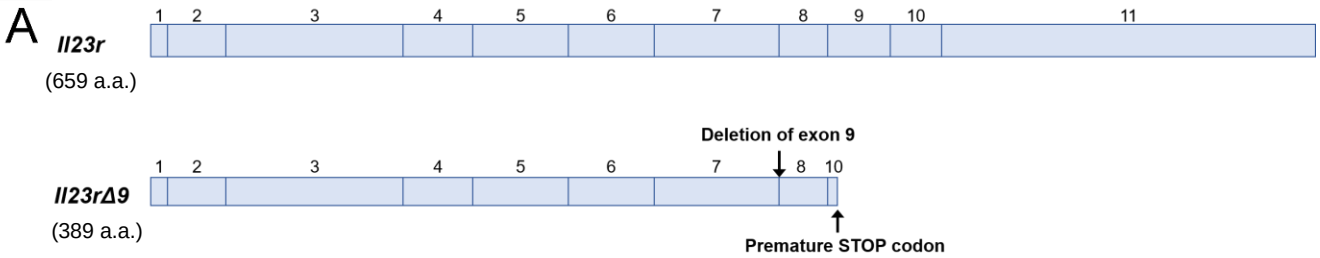

B

```
Mouse  16   MSHLTLQLHVVIALYVLFRWCHGGITSINCSGDMWVEPGEIFQMGMNVSIYCQEALKHCR  75
            M+ +T+Q   VIALY+LF WCHGGIT+INCSG +WVEP  IF+MGMN+SIYCQ A+K+C+
Human  1    MNQVTIQWDAVIALYILFSWCHGGITNINCSGHIWVEPATIFKMGMNISIYCQAAIKNCQ  60

Mouse  76   PRNLYFYKNGFKEEFDITRINRTTARIWYKGFSEPHAYMHCTAECPGHFQETLICGKDIS  135
            PR L+FYKNG KE F ITRIN+TTAR+WYK F EPHA M+CTAECP HFQETLICGKDIS
Human  61   PRKLHFYKNGIKERFQITRINKTTARLWYKNFLEPHASMYCTAECPKHFQETLICGKDIS  120

Mouse  136  SGHPPDAPSNLTCVIYEYSGNMTCTWNTGKPTYIDTKYIVHVKSLETEEEQQYLASSYVK  195
            SG+PPD P  +TCVIYEYSGNMTCTWN GK TYIDTKY+VHVKSLETEEEQQYL SSY+
Human  121  SGYPPDIPDEVTCVIYEYSGNMTCTWNAGKLTYIDTKYVVHVKSLETEEEQQYLTSSYIN  180

Mouse  196  ISTDSLQGSRKYLVWVQAVNSLGMENSQQLHVHLDDIVIPSASIISRAETTNDTVPKTIV  255
            ISTDSLQG +KYLVWVQA N+LGME S+QL +HLDDIVIPSA++ISRAET N TVPKTI+
Human  181  ISTDSLQGGKKYLVWVQAANALGMEESKQLQIHLDDIVIPSAAVISRAETINATVPKTII  240

Mouse  256  YWKSKTMIEKVFCEMRYKTTTNQTWSVKEFDANFTYVQQSEFYLEPDSKYVFQVRCQETG  315
            YW S+T IEKV CEMRYK TTNQTW+VKEFD NFTYVQQSEFYLEP+ KYVFQVRCQETG
Human  241  YWDSQTTIEKVSCEMRYKATTNQTWNVKEFDTNFTYVQQSEFYLEPNIKYVFQVRCQETG  300

Mouse  316  KRNWQPWSSPFVHQTSQETGKRNWQPWSSPFVHQTSQTVSQVTAKS-SHEPQKMEMLSAT  374
            KR WQP                    WSS F H+T +TV QVT+K+  H+     +  A+
Human  301  KRYWQP--------------------WSSLFFHKTPETVPQVTSKAFQHDTWNSGLTVAS  340

Mouse  375  IFRGHPASELKEKFY  389
            I  GH  S LKE  Y
Human  341  ISTGHLTSGLKEGSY  355
```

C

Alignment statistics					
Score	**Expect**	**Method**	**Identities**	**Positives**	**Gaps**
547 bits(1410)	0.0	Compositional matrix adjust.	262/375(70%)	298/375(79%)	21/375(5%)

Figure 3.19: Design of a soluble IL-23 antagonist *Il23rΔ9*.

a) Deletion of exon 9, which encodes a transmembrane region, from murine *Il23r* mRNA introduces a premature STOP codon in exon 10 that results in a C-terminal truncation of the product. **b)** Amino acid sequence alignment between human *Il23rd9* and the putative murine *Il23rd9*. **c)** Table of alignment statistics for the amino acid sequences in *B.*

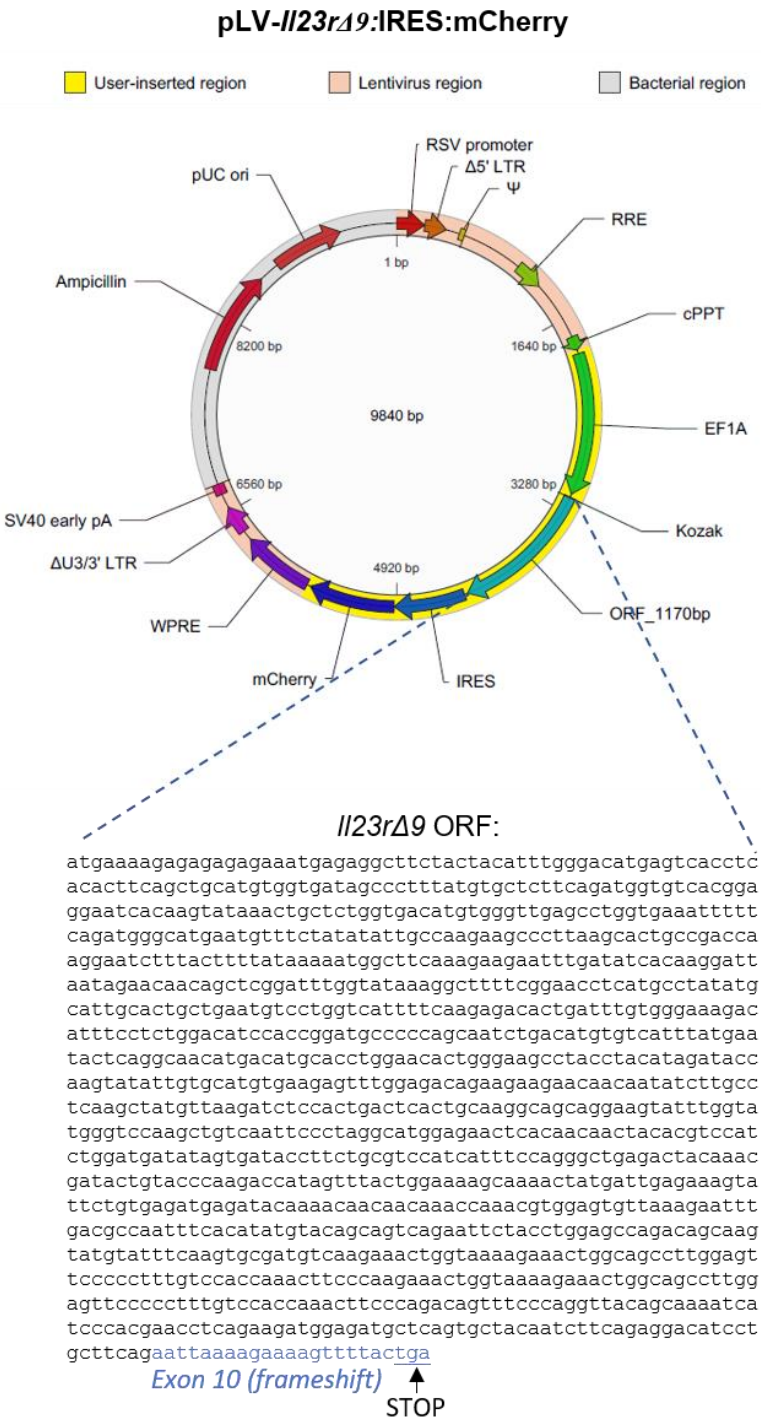

Figure 3.20: Map of pLV vector containing *Il23rΔ9* ORF.

The *Il23rΔ9* ORF sequence was generated by deleting exon 9 from the *Il23r* mRNA sequence (NCBI NM_144548.1), thus causing a frameshift in exon 10 that introduces a new STOP codon. pLV-*Il23rΔ9*:IRES:mCherry was purchased from VectorBuilder Inc.. In this vector, expression of the novel transcript is driven by an EF1α promoter and an internal ribosomal entry site (IRES) facilitates simultaneous translation of mCherry protein to mark cells with the vector.

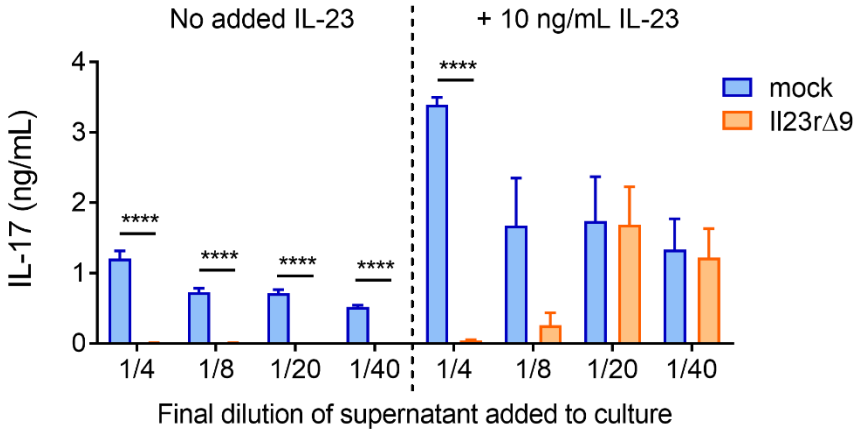

Figure 3.21: *Il23rΔ9* is a soluble antagonist of IL-23.

C57Bl/6 splenocytes were activated with anti-CD3, anti-CD28 and IL-2 *in vitro* in the presence or absence of IL-23 stimulation. Different dilutions of supernatants from mock-transfected or *Il23rΔ9*-transfected HEK293FT cells were added to the cultured splenocytes and after 6 days, IL-17A in the culture supernatants was measured by ELISA. The supernatants were measured in triplicate in the ELISA and the means were calculated to determine the concentration of IL-17 for each culture well. Each bar represents the mean ± SEM of three culture wells per condition. ****p<0.001 One-Way ANOVA with Bonferroni's multiple comparisons test. Representative of two independent experiments.

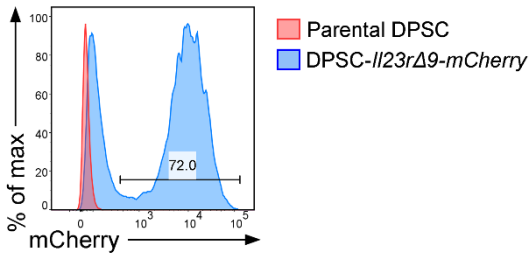

Figure 3.22: Generation of DPSCs overexpressing *Il23rΔ9*.

DPSCs from donor 03 were transduced with pLV-*Il23rΔ9*:IRES:mCherry and successful uptake of the vector was assessed by flow cytometry for the mCherry reporter contained in pLV. Shown is flow cytometry detection of mCherry by transduced cells (blue). DPSCs were also mock-transduced, in which they received empty lentivirus generated with packaging plasmids and no expression plasmid (red).

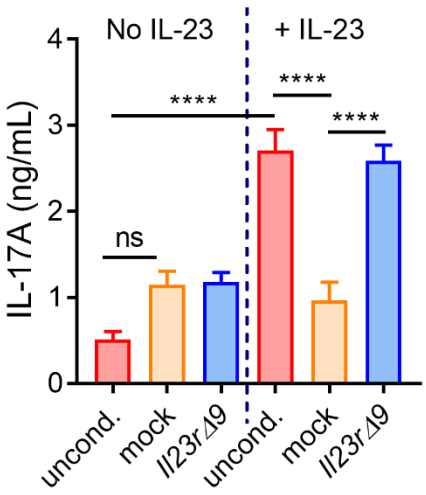

Figure 3.23: *Il23rΔ9*-expressing DPSCs do not suppress IL-23 activity *in vitro*.

C57Bl/6 splenocytes were activated with anti-CD3, anti-CD28 and IL-2 *in vitro* and in the presence of absence of IL-23 stimulation. Supernatants from mock-transduced or *Il23rΔ9*-transduced DPSC-03 cells were added to the cultured splenocytes to 1/4 of the total media volume and after 6 days, IL-17A in the culture supernatants was measured by ELISA. The supernatants were measured in duplicate in the ELISA and the means were calculated to determine the concentration of IL-17 for each culture well. Each bar represents the mean ± SEM of three culture wells per condition. ****p<0.001 One-Way ANOVA with Bonferroni's multiple comparisons test. ns, not significant; uncond., unconditioned medium. Representative of two independent experiments.

This page intentionally left blank.

Chapter 4: Effect of DPSC treatment on EAE

This page intentionally left blank.

4.1 Overview

The emerging field of DPSC research has focussed heavily on their utilisation in bone and dentin regeneration[337], although their therapeutic potential in settings beyond orthopaedic pathologies is becoming increasingly recognised[338,339]. Prior to the commencement of this study, the effect of DPSCs in MS and other autoimmune diseases was unstudied. It was unknown whether DPSCs have similar anti-inflammatory properties to other MSCs such as those isolated from bone marrow or adipose tissue. The trafficking of DPSCs after injection into mice was also completely unknown and the fate of MSCs *in vivo* in general is poorly understood. Furthermore, it has been hypothesised that DPSCs may have greater potential than other MSCs in MS due to their neurologic potential. Consequently, the DPSCs which were isolated from multiple human donors in the previous chapter were tested for their ability to suppress EAE, then their effects on the immune response in EAE were studied.

4.2 Effects of DPSCs on the clinical course of EAE

4.2.1 Prophylatic effects of DPSCs on the clinical course of chronic EAE

The principal EAE model chosen for this study was MOG_{35-55}-induced chronic EAE induced in C57Bl/6 mice since this is an established model of MS with well-characterised immunopathology and is commonly used for pre-clinical testing of MS therapies[15]. Since previous studies have shown that the therapeutic potency of some MSCs can vary from one donor to another[340], DPSCs from multiple donors were used here to test the reproducibility of the treatment. This was challenging because not all of the DPSC samples became available at the same time (indeed, they were obtained over a period of 3 years that coincided with a change in location of animal facilities and meant that the reagents used to induce EAE in this study came from different batches). In all of these experiments, C57Bl/6 mice were immunised with MOG_{35-55}/CFA and treated with 3-4 intraperitoneal injections of 1×10^6 DPSCs on alternate days from the first day after immunisation. This regime was based on a previous study treating EAE with Ad-MSCs[341] and the intraperitoneal route was selected as it has been shown to be a superior route of delivery for MSCs based on disease outcome in EAE compared to intravenous injection[342].

The development of clinical disease parameters was measured daily after immunisation for EAE and several features of disease progression were evaluated to deduce the effect of DPSC treatment on the course of disease. The day of EAE onset and the day of peak disease were assessed to compare the kinetics of the disease between control mice and DPSC-treated mice. Conversely, effects on the severity of symptoms were summarised by comparing the mean maximum scores reached by the individual mice in each treatment group. Cumulative disease score, the sum of all the disease scores exhibited by each individual mouse over the course of the experiment, was also assessed (which can be affected by both the kinetics and severity of symptoms).

The effects of treating chronic MOG_{35-55}-induced EAE with DPSCs from donors 01-05 and 07 are shown in Figures 4.1-4.6. Treatment of EAE with DPSC-01 or DPSC-03 delayed the onset of symptoms and the day of peak disease by 5.3 and 1.7 days respectively compared with controls, although the maximum clinical score reached was not significantly different from control mice (Figures 4.1 and 4.3). A trend for a delay in onset of disease and a reduction in cumulative disease score was also observed for DPSC-05, although this was not statistically significant (Figure 4.5). For all of these three DPSC lines, however, a statistically significant reduction in the course of EAE over time was apparent compared with controls when tested by repeated measures Two-Way ANOVA analysis. In addition to these DPSC lines, DPSC-02 treatment also strongly inhibited EAE symptoms in mice (Figure 4.2). Half of mice treated with DPSC-02 cells had delayed onset of symptoms and almost all DPSC-02-treated mice had a significantly reduced maximum disease score compared with control mice. In fact, 5 of 6 mice tested with these cells showed only a loss of tail tone that did not progress to hind limb paralysis (disease score of 0.5-2). By contrast, almost all control mice developed hind limb paralysis in that experiment (disease score 2.5-3). There was also a trend for a delay in time to peak disease in DPSC-02-treated mice and both the delay in EAE onset and reduction in maximum score contributed to a significant overall reduction in the cumulative disease score in those mice.

In contrast, DPSCs from donors 04 and 07 did not appear to significantly alter the outcome of disease when used to treat EAE (Figures 4.4 and 4.6). The onset of disease, maximum EAE score and time to reach peak disease was similar between mice treated with DPSC-04 or DPSC-07 and mice treated with PBS. As such, the overall cumulative EAE score for those mice also showed no change.

In those experiments, all DPSCs were at passage 5 at the time they were injected into EAE mice. However, while DPSC-02 and DPSC-03 both inhibited EAE at passage 5, at passage 7 and 8 these DPSC-02 and DPSC-03 cells no longer inhibited EAE (Figure 4.7). Thus, it appears there is a loss in therapeutic efficacy when DPSCs are passaged further *in vitro* before injection into EAE mice.

In sum, four of the six DPSC lines tested improved clinical disease scores in mice with EAE compared with controls, which is summarised in Table 4.1. These experiments revealed heterogeneity between DPSCs isolated from different donors with regard to both ability or not to improve EAE scores and whether disease was delayed or also reduced in severity. These differences between DPSC lines could not be attributed to any apparent features of the donors which were of similar age and EAE-inhibiting DPSCs originated from both males and females. Non EAE-inhibiting DPSCs-04 and -07 were also phenotypically similar to the other DPSCs *in vitro* with their regards to multi-potency and expression of surface MSC markers (Sections 3.2 and 3.3). Additionally, it appears that keeping passage number of DPSCs below 7 may be important for therapeutic effects in EAE.

4.2.2 Effect of DPSCs on established EAE

The ability of prophylactic treatment of EAE with DPSCs to suppress disease was promising. Clinically, however, treatments for MS are delivered after the development of disease. Therefore, since DPSC-02 was most potently able to both delay the onset of EAE and reduce the severity of symptoms, the ability of these cells to reverse EAE symptoms after disease onset was also tested. C57Bl/6 mice were allowed to develop EAE symptoms after immunisation before treating with either PBS or three intraperitoneal injections of 1×10^6 DPSCs on alternating days.

DPSC treatment after EAE symptoms were established in mice did not significantly alter the course of disease thereafter (Figure 4.8). The maximum disease score post-treatment was also the same for DPSC-treated mice as controls. Therefore, despite DPSC-02 being a potent inhibitor of EAE in the pre-symptomatic phase, there was no evidence that these cells were effective at treating established disease.

4.2.3 Effect of DPSCs on relapsing EAE

The MOG_{35-55}-induced chronic model of EAE is a useful tool for mimicking chronic CNS inflammation. However, most MS patients present with relapsing-remitting MS and experience intermittent inflammation of the CNS. Therefore, a relapsing-remitting model of EAE was additionally used to determine if DPSCs can prevent disease relapse.

To this end, SJL/J mice were immunised $PLP_{139-151}$ peptide in CFA on day 0 together with two intravenous injections of pertussis toxin on days 0 and 2 to induce EAE with a relapsing-remitting disease course[15]. The severity of EAE symptoms was measured daily and after mice had experienced acute paralysis (disease score > 2) and gone into remission, (disease score returns ≤ 1), they were randomly allocated to receive two intraperitoneal treatments of either PBS or 1×10^6 DPSCs from donor 02, which showed the most inhibition in the chronic model of EAE. Mice that received DPSCs were found to have a significant delay in the relapse of symptoms (as defined as an increase ≥ 1 point from the EAE score at the time of treatment) compared with control mice (Figure 4.9).

4.3 Effect of overexpressing ACKRs on the prophylactic capacity of DPSCs in EAE

In the previous chapter, DPSCs which overexpressed ACKR2 and ACKR4 were generated. Therefore, in this part of the project the effect of overexpressing ACKRs on DPSCs on their therapeutic capacity in MOG_{35-55}-induced EAE was tested. To determine if overexpression of ACKR2 improves the therapeutic capacity of DPSCs in EAE, EAE was induced in mice which were then treated with three intraperitoneal

injections of DPSC-*Ackr2-gfp* or DPSC-*gfp* cells on d1, d3 and d5 post-immunisation. Control DPSC-*gfp* cells significantly suppressed the course of EAE, however overexpression of ACKR2 on DPSCs did not improve their therapeutic capacity (Figure 4.10A). In fact, DPSC-*Ackr2-gfp* cells did not significantly affect the overall course of EAE compared with control EAE mice when analysed by Two-Way ANOVA. To further understand how ACKR2 overexpression by DPSCs modified their effect on EAE clinical parameters, disease statistics were broken down into day of onset, days to reach peak disease, maximum disease score and cumulative disease score (Figure 4.10B). DPSC-*Ackr2-gfp* cells delayed the onset of EAE compared with treatment with PBS but not DPSC-*gfp* cells. However, only DPSC-*gfp* cells significantly reduced the cumulative disease score of EAE mice suggesting ACKR2 overexpression abolishes, rather than improves, the therapeutic capacity of DPSCs. Also, despite the observation in a previous experiment that unmodified DPSC-02 cells delay onset of symptoms and reduce the mean maximum disease score in EAE mice (Figure 4.2), DPSC-*gfp* control cells did not significantly affect these parameters in the current experiments. Therefore, despite establishing in the section 3.4 of the previous chapter that DPSCs retain MSC characteristics after lentiviral transduction, this process may indeed impact their therapeutic capacity in disease settings.

Next, DPSC-*Ackr4-gfp* cells were tested for their ability to suppress EAE. Treatment of EAE mice with DPSC-*Ackr4-gfp* cells did not lead to any improvement in disease course compared with mice that received DPSC-*gfp* control cells (Figure 4.11A). The day of EAE onset was delayed in mice that received DPSC-*Ackr4-gfp* cells compared with PBS but not compared with DPSC-*gfp* treatment (Figure 4.11B). In contrast, time to reach peak disease as well as maximum and cumulative disease scores were not affected by treatment with either of the modified DPSCs. Taken together, it was concluded that overexpression of ACKR4 does not significantly improve the capacity of DPSCs to inhibit EAE.

In summary, no evidence was found to support the proposition that overexpression of atypical chemokine receptors could increase the therapeutic capacity of DPSCs in EAE as suppression of disease was not enhanced by overexpression of ACKR2 or ACKR4 on DPSCs. However, these experiments also provided evidence that lentiviral transduction of DPSCs can also interfere with their ability to suppress EAE *in vivo* despite not impairing their multi-potency *in vitro*.

4.4 DPSC distribution after injection into EAE mice

Trafficking of MSCs after injection is poorly characterised and for DPSCs in particular there is very little known about their *in vivo* migratory properties. To understand the potential for DPSCs to treat EAE, it is helpful to know where they localise after injection. Specifically, whether DPSCs enter the CNS after injection contributes to understanding how they may influence disease outcomes either at the site of inflammation and demyelination or from distant locations.

To determine if DPSCs home to organs important in EAE, DPSC-*gfp* cells (generated in the previous chapter, section 3.4.1) were used to facilitate tracking of the cells by qPCR for the *gfp* transgene. Before injection into EAE mice, the DPSCs were also additionally labelled with an infrared cytoplasmic membrane tracking dye, which enables them to be visualised by bioluminescence. EAE mice were then treated with three intraperitoneal injections of 1 x 10^6 cells on days 1, 3 and 5 post-immunisation and sacrificed 16 h after the final treatment to determine the fate of the injected DPSCs.

Bioluminescence imaging revealed strong signals in the lungs and spleen, and a small signal in some iLNs (Figure 4.12A and B). DPSCs presumably accumulate in the lungs following intravasation from the peritoneal cavity, perhaps by mechanical arrest in the capillaries. The bioluminescence observed in the spleen and iLNs and suggest DPSCs may migrate to SLOs after injection. In the SLOs, DPSCs may locate themselves in a prime position for interacting with cells of the immune system. However, the bioluminescent dye is not specific for live DPSCs; if DPSCs die or are killed after injection, phagocytosis can lead to the labelling of certain leukocytes including macrophages, monocytes, DCs or neutrophils. To confirm the presence of DPSCs in the lungs, spleen and iLNs, qPCR was performed to detect eGFP. Using the pWPI-*gfp* vector and titrating from 10^7 copies to 1 copy in a qPCR, it was determined that a minimum threshold of 10 copies of the *gfp* gene could be detected (Figure 4.12C). qPCR was then performed using cDNA prepared from mRNA isolated from the brain, spinal cord, lungs, spleen and iLNs which were collected from the bioluminescent imaging experiments. However, *gfp* could not be detected in any of these tissues (data not shown). This suggests that DPSCs may not migrate to or persist in those organs after intraperitoneal injection, and that the DPSCs may die after transfer and that the bioluminescent signals detected in the spleen, lungs and iLNs, may be carried to these organs by cells which phagocytose DPSCs. If DPSCs do migrate to those locations, then it is infrequent and below the level of detection of a sensitive qPCR assay.

Bioluminescence was not visualised in the CNS of mice receiving labelled DPSCs, although there was a trend that did not reach statistical significance for increased total bioluminescence signal measured for both the brain and spinal cord of mice that received DPSCs compared with PBS control. Since eGFP also could not be detected by qPCR in the brain or spinal cord, DPSCs either do not enter the CNS or do so only at levels that are below the limit of detection by qPCR. Despite this, DPSC-*gfp* cells suppress the course of EAE (Figure 4.10) which reveals that entry into the CNS is not necessary for DPSCs to modulate the disease. Instead, it is likely that DPSCs suppress EAE by interacting with cells in the periphery or they may secrete factors which can cross the BBB. Therefore, whether DPSCs modulate the immune response in EAE was investigated.

4.5 Effects of DPSC treatment on the immune response in EAE

In Chapter 1, immunomodulatory functions were described in detail for MSCs from multiple anatomical sources. The regulatory effects of various MSCs can extend to almost all types of leukocytes in both innate

and adaptive arms of the immune system (Figure 1.5). Furthermore, immunomodulation has been linked to favourable outcomes in a mouse model of Alzheimer's after treatment with stem cells from human exfoliated deciduous teeth (SHEDs); an MSC population similar to DPSCs. Thus, it was hypothesised that DPSC-mediated effects on the immune response in EAE mice may contribute to their disease-suppressing capability. To this end, the immunomodulatory effects of DPSCs were investigated *in vivo* and *in vitro*.

Since there was some variability between DPSCs from different donors in their ability to suppress EAE and because a limited number of low passage stocks of cells from each donor were available, cells from multiple donors were used for the enquiry that follows. DPSCs which are capable of suppressing EAE symptoms were chosen. These were DPSCs from donors 02, 03 and 05. DPSC-01, although suppressive in EAE, was not used for further study since it was obtained at a higher passage than the other DPSCs and so only few cells from that donor were available at low passage. DPSC-02 was also a gift from the Koblar laboratory meaning there were also insufficient low passage cells from this donor to use for all of the experiments in this chapter. Since DPSC-03 and 05 were isolated in-house, they represented the largest cell stocks and could therefore be used more extensively in this project.

4.5.1 Effect of DPSC treatment on leukocyte infiltration of the CNS in EAE.

The CNS, being the site of the effector phase of the EAE autoimmune response, was the first site examined for evidence that DPSCs may affect inflammation in EAE. Activation of microglia and dense infiltration of the CNS with lymphocytes and mononuclear phagocytes are hallmarks of the inflammatory presentation of EAE. Microglia also contribute to CNS inflammation through antigen presentation and reactivation of T cells and production of pro-inflammatory cytokines. The number of microglia increases in inflammatory contexts[343] and they can thus be used as an indicator of inflammation in the CNS.

To determine if DPSC treatment influences these processes, mice were immunised for EAE and treated with three intraperitoneal injections of DPSCs on days 1, 3 and 5 following immunisation. Flow cytometry was performed on the combined brain and spinal cords of the mice at peak disease for the control group. This is a time that correlates with maximum inflammation of the CNS in EAE. The expansion of microglia was measured and compared between the control mice and mice which received DPSCs from donors 03 or 05 as previously mentioned. As previously mentioned, the DPSCs from different donors were not available all at once at the beginning of the study but were rather sourced over a period of three years. The EAE experiments were performed as samples became available and in the course of this timespan, changes to the location of the animal housing facility and different batches of both MOG_{35-55} peptide and pertussis toxin led to some variation in the kinetics and severity of the disease. Thus, in order to compare across experiments that used DPSCs from different donors, all data were normalised to the control group in each experiment. Figure 4.13 shows the time

course of EAE for each experiment used for investigating DPSC effects on the immunopathology of the disease, and the individual scores of mice at each experimental endpoint.

Using flow cytometry, microglia can be identified by expression of CD11b and low to intermediate expression of CD45 (Figure 4.14A). The proportion of microglial cells in the CNS was not different between control and DPSC-treated groups. However, in terms of total cell number, fewer microglia in number were observed in the CNS of EAE mice which were treated with DPSCs from either donor 03 or 05 as compared with controls (Figure 4.14B). This indicates that microglia may not be responding and proliferating as strongly in DPSC-treated mice than in control mice. However, DPSCs were shown not to enter the CNS (Figure 4.10), suggesting that the effects of DPSC treatment on microglial cell numbers may be indirect, perhaps via the leukocytes that infiltrate the CNS. Infiltrating leukocytes, which included both lymphocytes and myeloid cells, were therefore also measured in the combined brains and spinal cords of EAE mice treated with DPSCs or PBS control. Lymphocytes ($CD45^{+}CD11b^{-}$) were significantly reduced as a proportion of cells in the CNS of mice that were treated with DPSC-03 cells treatment but not for DPSC-05. However, the total number of lymphocytes which infiltrated the CNS was reduced after treatment with DPSCs from both of these donors. Infiltrating myeloid cells ($CD45^{hi}CD11b^{+}$), which encompass DCs, monocytes, macrophages and granulocytes, were also measured in the CNS. Treatment with DPSCs led to reduced recruitment of myeloid cells for both DPSC-03 and 05. Furthermore, a positive correlation between number of infiltrating leukocytes (including both lymphocytes and myeloid cells) and microglia in the CNS for all groups of EAE mice (Figure 4.14C). This suggests that microglia cell numbers are indeed reduced in the CNS of DPSC-treated EAE mice as a result of DPSC-mediated effects on leukocytes prior to their infiltration of the CNS.

These observations that expansion of microglia appears suppressed and recruitment of both lymphocytes and myeloid cells is also significantly reduced provide evidence that DPSC treatment reduces the level of inflammation in the CNS of EAE mice which is most likely to result from effects of DPSCs on leukocytes outside of the CNS. As such, a more detailed analysis followed on the types of cells in the immune system that are affected by DPSC treatment in EAE.

4.5.2 Effect of DPSC treatment on $CD4^{+}$ and $CD8^{+}$ T cell responses in EAE.

T cells are a major subset of cells involved in initiating and perpetuating the inflammation that is characteristic of EAE. $CD4^{+}$ T cells are primed in the draining LN and the spleen after immunisation with MOG/CFA after which they expand and differentiate into various T helper subsets which contribute in different ways to EAE pathogenesis. T helper cells then migrate to the CNS whereupon they are reactivated and elicit an autoimmune response. The significant reduction in lymphocyte recruitment to the CNS of EAE mice that were treated with DPSCs prompted an investigation into whether $CD4^{+}$ T cells are suppressed in those mice.

To this end, EAE mice were treated with three injections of PBS or DPSCs and $CD4^+$ T cells were measured in the iLN, spleen and CNS at peak disease by flow cytometry. At that time-point $CD4^+$ T cells have densely infiltrated the CNS. No differences in the proportion or number of $CD4^+$ T cells were observed in the SLOs for any of the three DPSC treatments (Figure 4.15). In the CNS, however, treatment of EAE mice with DPSC-02 cells led to a significant increase in proportion of $CD4^+$ T cells although the total number of $CD4^+$ T cells in the CNS was unchanged. Thus, the increase in proportion of $CD4^+$ T cells in the CNS after DPSC treatment may be a reflection of reductions in other cell populations there including other lymphocytes as well as microglia and infiltrating myeloid cells which was noted in section 4.5.1.

Next, $CD8^+$ T cells were also enumerated in the SLOs and CNS of PBS versus DPSC-treated EAE mice. No differences were observed in proportion or number of $CD8^+$ T cells in the iLN (Figure 4.16). In the spleen, while $CD8^+$ T cells were not changed as a proportion of live cells, the total number of $CD8^+$ T cells was significantly reduced following treatment with DPSCs from one of the donors, DPSC-03. DPSC treatment also caused a significant reduction in the number of $CD8^+$ T cells in the CNS and they were also decreased as a proportion of the live cells there. Therefore, DPSCs may reduce proliferation or increase apoptosis of $CD8^+$ T cells.

4.5.3 Effect of DPSCs on B cells in EAE

The significance of B cells in MS is strongly implicated by the success of anti-CD20 monoclonal antibody therapy which depletes B cells and produces a good protective effect against relapse. In the pathogenesis of MOG-$_{35-55}$-induced EAE, however, the role of B cells is less dominant than other lymphocytes, although they can still contribute to clinical outcomes. Based on the influential role of B cells in MS, whether DPSCs can affect the B cell response was tested in EAE.

To this end, EAE mice were treated with DPSCs and B cells were quantified in the SLOs and CNS by flow cytometry and compared with control mice. The frequency and number of B cells in the SLOs remained unaffected by treatment with DPSCs from donors 03 or 05. While B cells in the CNS were not changed in proportion of cells there, the total number of B cells in the CNS was significantly reduced following DPSC treatment (Figure 4.17). Thus, by reducing infiltration of B cells into the CNS is potentially another way in which DPSCs may suppress EAE.

4.5.4 Effect of DPSC treatment on the polarisation of T helper cell responses in EAE.

As shown above, the effect of DPSC treatment on the magnitude of $CD4^+$ T cell responses overall in EAE was minimal, but it is possible that DPSCs affect the types of $CD4^+$ T cells present in EAE since they can be divided into various functional helper subsets. Both Th1 and Th17 subsets of $CD4^+$ T cells have well-described pathogenic roles in EAE although the latter is generally considered more aggressive. Therefore, Th1 and Th17 cell responses were compared in EAE mice treated with PBS or DPSCs.

Th1 cells are defined by expression of IFNγ, so to determine if DPSC treatment affects the induction of Th1 cells in EAE, IFNγ-expressing $CD4^+$ T cells were enumerated in the CNS and SLOs at peak disease following treatment with PBS or DPSCs. (Figure 4.18). There were statistically significant increases in Th1 cell proportions of activated $CD4^+$ T cells in both SLOs for mice that were treated with DPSC-02 cells but not for DPSCs from donors 03 or 05. Although the total number of Th1 cells was not different in the iLNs of any DPSC-treated groups, the spleen held a greater total number of Th1 cells after treatment with DPSCs from both donors 02 and 03 compared with control mice. In fact, the mean increase in Th1 cells across all groups was 2.17-fold over controls. Mice treated with DPSC-05 cells also trended toward this increase in number in the spleen although this was not statistically significant. No differences in proportion or number of Th1 cells was found in the CNS between control and DPSC-treated mice.

Next, Th17 cells which are defined by expression of the cytokine IL-17A were also enumerated by flow cytometry of the SLOs and CNS of EAE mice that were treated with DPSCs or PBS. In the iLN, there was no difference in the proportion or number of Th17 cells after treatment with DPSCs from any of the donors (Figure 4.19A and B). However, in stark contrast to Th1 cells, DPSC treatment significantly reduced Th17 cells as a proportion of activated $CD4^+$ T cells in the spleens of DPSC-02 and -05 treated EAE mice, and DPSC-03-treated mice also showed a non-statistically significant trend toward Th17 suppression. For DPSC-02-treated mice, but not others, this reduction in the Th17 cell response in the spleen also extended to cell number. In the CNS, Th17 cells were decreased as a proportion of activated $CD4^+$ T cells following DPSC-treatment but there was no difference in the total number of these cells.

As DPSC treatment generally led to increased Th1 cells and a suppressed Th17 cell response, the ratio of Th1 cells to Th17 cells was compared between all groups to find if there was a bias toward Th1 responses and not Th17 cell responses in mice that were treated with DPSCs. The skewing of $CD4^+$ T helper responses from Th17 to Th1 has been associated with reduced EAE pathology in another study[173]. The Th1 to Th17 cell ratio was not altered in the iLNs, however it was significantly increased in favour of Th1 cells in the spleens of EAE mice that were treated with DPSCs from any of the three donors (Figure 4.20). Also, the Th1:Th17 ratio was significantly increased in the CNS following DPSC-treatment (from all donors). Thus, a bias for differentiation

of $CD4^+$ T cells to Th1 instead of Th17 appears to be induced by treatment of EAE mice with DPSCs which may contribute to their suppressive effects on disease.

To further assess the effects of DPSC treatment on T helper cells in EAE, expression of pro-inflammatory GM-CSF by Th17 cells and all $CD4^+$ effector T cells was also measured by flow cytometry. There was a significant increase in GM-CSF-expressing $CD4^+CD44^+$ T cells (Th-GM cells) in the iLNs of DPSC-02-treated mice but not for other donors, and no difference was observed for any of the donors with respect to total number of Th-GM cells in the iLN (Figure 4.21). Also, in the spleen there was no difference in the proportion of Th-GM cells but DPSC-05-treatment significantly increased their number. No differences in Th-GM cell proportion or number were observed for the CNS. Homing more specifically on $GM\text{-}CSF^+$ cells from the Th17 population revealed no differences in the proportion of Th17-GM in either of the SLOs or the CNS for DPSCs from any of the three donors (Figure 4.22). The total number of Th17-GM cells was also unaffected in the iLNs and CNS although a statistically significant reduction was seen in the spleens of DPSC-02-treated mice but not DPSC-03 or -05. Thus, DPSC-treatment does not appear to specifically target pathogenic Th17-GM cells, and the reduction in number of these cells in the spleen after DPSC-02-treatment is likely to be due to the overall reduction in Th17 cells in those mice which was not seen for the other two donors.

4.5.5 Effect of DPSC treatment on Tregs in EAE

Another subset of $CD4^+$ T cells which play a role in EAE are Tregs. Several studies report MSCs from anatomical sources such as bone marrow can modulate inflammatory responses by expanding Tregs, so it was rationalised that DPSCs may behave in a similar fashion in EAE. Since Tregs are known to have the capacity to suppress the course of EAE, an expansion of Tregs could further explain why mice which are treated with DPSCs have less severe disease.

To this end, Tregs were measured in the SLOs of EAE mice treated with DPSCs or PBS by enumerating FoxP3-expressing $CD4^+$ T cells by flow cytometry. Treatment of EAE mice with DPSC-03 showed no significant changes in proportion or number of Tregs in the SLOs (Figure 4.23). However, treatment with DPSC-05 cells showed significantly reduced Tregs as a proportion of $CD4^+$ T cells but the total number of Tregs was unaffected.

In brief, it has been demonstrated thus far that in EAE, DPSCs from some donors increased Th1 cells and some decreased Th17, all consistently increased the Th1:Th17 ratio in the spleen. This Th1:Th17 ratio was also increased in the CNS. Tregs do not seem to be important for their suppressive effect in EAE and specifically targeting GM-CSF-expressing T cells also does not seem to be important. After establishing that T cells may be targeted for immunomodulation by DPSCs to increase Th1 output and reduce Th17 cells, the next question asked was how DPSCs may mediate their immunomodulatory effects on T cells.

4.5.6 Effect of DPSCs on CD8$^+$ T cell production of IFNγ

DPSC treatment reduced CD8$^+$ T cells in the spleen and CNS of EAE mice (Section 4.5.2, Figure 4.16). CD8$^+$ T cells are a source of IFNγ in EAE and although these CD8$^+$IFNγ$^+$ T (Tc1) cells can have cytotoxic functions their role in EAE and MS is controversial with both pathogenic and regulatory functions described[344,345] (Chapter 1, Sections 1.1.2 and 1.1.3).

To test if DPSC treatment also affects Tc1 cells in EAE, IFNγ expression by CD8$^+$ T cells was examined by flow cytometry. Tc1 proportions were unchanged in the spleen, iLNs and CNS of DPSC-treated EAE mice compared with controls (Figure 4.24). The number of Tc1 cells was also unchanged. Therefore, while DPSCs reduce the number of CD8$^+$ T cells they do not affect their expression of IFNγ.

4.5.7 DPSC modulation of T cell differentiation *in vitro*

To interrogate the mechanism by which DPSCs increase Th1 cells while suppressing Th17 cells, the ability of DPSCs to directly signal to T cells and alter their differentiation phenotype was investigated using *in vitro* T cell culture systems.

CD4$^+$ T cells are activated through recognising their cognate antigens presented on MHC-II by APCs. During this interaction, APCs deliver secondary signals which influence the fate of the T cell. Engagement of surface co-stimulatory molecules concurrent with the delivery of specific cytokines can drive T cell proliferation and differentiation to particular phenotypes which are specialised in their effector functions, giving rise to the various T helper subsets or inducible Tregs (iTregs). In this way, opportunities for DPSCs to interfere with the T cell activation and differentiation process are multiple, including signalling directly to T cells or indirectly by modifying APCs. In both scenarios, the signals may be provided either by cell-cell contact or via soluble molecules and both modes of signalling have been demonstrated by MSCs from a range of anatomical sources as described in chapter 1. A role for soluble factors was first tested by harvesting and testing CM from cultured DPSCs which contains their secreted soluble products.

First, the effect of DPSC-CM on T cell activation *in vitro* was tested by stimulating purified naïve CD4$^+$ T cells with anti-CD3 and anti-CD28 in the presence of unconditioned DPSC medium or CM from DPSCs from donors 03 or 05. DPSCs themselves were not added to the cultures because they are large adherent cells which would mask the plate-bound anti-CD3 T cell stimulus. Expression of the T cell activation marker CD44 was measured by flow cytometry 3 days later. Activation of the CD4$^+$ T cells in this culture system was highly efficient, approximately 95-98% of live T cells were CD44^{hi} under all culture conditions (Figure 4.25). However, the presence of DPSC-CM did not affect the percentage of T cells expressing CD44 or the mean

fluorescence of the CD44 staining, suggesting DPSCs do not secrete factors which affect the activation program of $CD4^+$ T cells.

To find if a DPSC-secreted factor affects $CD4^+$ T cell proliferation, naïve $CD4^+$ T cells were labelled with a plasma membrane proliferation dye to track cell divisions. They were activated with anti-CD3 and anti-CD28 and cultured with unconditioned DPSC medium or DPSC-CM from donors 03 or 05 in the presence of IL-2. After 3 days, dilution of the proliferation dye was measured by flow cytometry. The presence of DPSC-CM did not affect $CD4^+$ T cell proliferation *in vitro* since it did not change the division index of the T cells (Figure 4.26). Therefore, soluble factors produced by DPSCs do not appear to directly impact $CD4^+$ T cell proliferation.

To determine if DPSCs produce soluble factors that directly influence Th1 differentiation, naïve $CD4^+$ T cells were purified and stimulated with plate-bound anti-CD3 and soluble anti-CD28 *in vitro* with the addition of IL-12 to induce Th1 differentiation (Figure 4.27A). To control for the differentiation process, antibodies neutralising IFN-γ and IL-4 were included in some wells without IL-12 to leave the activated cells in a non-polarised (Th0) state. Unconditioned DPSC medium or DPSC-CM from donors 03 or 05 were tested for effects on Th1 differentiation. After three days in culture, IFN-γ-expressing Th1 cells were quantified by flow cytometry. DPSC-CM showed no significant effects on Th1 differentiation *in vitro*, indicating membrane factors or indirect effects such as signalling via APCs are likely required for the increased Th1 cells observed in EAE mice treated with DPSCs (Figure 4.27B and C).

Next, the effect of DPSC-CM on Th17 cell differentiation was tested. Th17 cells were induced *in vitro* by addition of anti-IFNγ, anti-IL-4, IL-6, TGF-β1, IL-1β and IL-23 to the anti-CD3 and anti-CD28-activated $CD4^+$ T cells (Figure 4.28A). Unconditioned medium or DPSC-CM was added to the T cells and the generation of Th17 cells was measured by flow cytometry three days later for cells expressing the signature cytokine IL-17A. Notably, DPSC-CM from donor 03 potently and selectively inhibited Th17 differentiation *in vitro* (Figure 4.28B and C). Both the frequency and number of Th17 cells after 3 days in culture with DPSC-03-CM were significantly reduced. In contrast, CM from DPSC-05 cells did not affect Th17 cell differentiation. From this, it was concluded that DPSC-03 produces a soluble molecule which can suppress Th17 cell differentiation. Other factors may also be required for inhibition of Th17 cells *in vivo* that is mediated by DPSC-05.

The potential for DPSC-CM to influence Treg differentiation was also tested. Again, naïve $CD4^+$ T cells were activated *in vitro* by stimulation with anti-CD3 and anti-CD28 with neutralisation of IFNγ and IL-4, this time in the presence or absence of Treg-inducing cytokines TGF-β and IL-2 (Figure 4.29a). CM from DPSC-03 or DPSC-05 cells was added to the Treg cultures to test if DPSCs produce soluble factors which influence Treg development. Tregs that were produced in culture after three days were measured by flow cytometry. These experiments revealed that DPSC-CM does not affect Treg differentiation (Figure 4.29b).

Taken together, these data indicate that DPSC-CM–does not affect Th1 or Treg differentiation *in vitro*. However, Th17 differentiation was potently inhibited by a soluble factor produced by DPSCs from one of the donors tested. Therefore, next, an attempt was made to identify soluble factors produced by DPSC-03 which inhibited Th17 cell differentiation *in vitro*.

4.5.8 Expression of secreted immunomodulatory molecules by DPSCs

Several anti-inflammatory molecules have been described in the scientific literature to be expressed by various types of MSCs (see Tables 1.2 and 1.3). Thus, DPSCs from donors 03 and 05 were screened by qPCR for expression of various genes for these MSC anti-inflammatory molecules which have soluble products. cDNA from Ad-MSCs was included as a reference for another type of MSC that expresses immunomodulatory molecules[346].

DPSCs from both donors expressed all of the immunomodulatory genes that were tested (Figure 4.30A). Among these genes, *LIF*, *TGFB1*, *HGF* and *VEGFA* were consistently expressed at higher levels in DPSCs compared with Ad-MSCs, which may suggest that DPSCs have more immunosuppressive capacity than Ad-MSCs. *PTGS2*, *TNFAIP6* and *IL10*, which encode COX2, TSG-6 and IL-10 respectively, were also found to be expressed by both DPSCs and Ad-MSCs. The immunomodulatory genes that were expressed at the highest levels in DPSCs were *TGFB1*, *VEGFA* and *LIF*. Of these three genes, *LIF* was identified as the most promising candidate molecule that might be suppressing Th17 cell differentiation. LIF is a member of the interleukin 6 class of cytokines and is classically involved in inhibiting cell differentiation. It is important for maintaining stem cells in an undifferentiated state but also has anti-inflammatory properties and is known to suppress Th17 cell differentiation[347]. TGFβ1, on the other hand, is required for Th17 cell differentiation and therefore is an unlikely candidate, whereas VEGFA increases IFNγ production by $CD4^+$ T cells[348] and suppresses their proliferation[349] but its direct effect on Th17 cell differentiation is unknown.

To test if LIF is important for DPSC-mediated suppression of Th17 differentiation, naïve $CD4^+$ T cells were activated and differentiated *in vitro* with DPSC-03 CM with the inclusion of an antibody to neutralise LIF. Th17 cells were enumerated in the cultures after 3 days by flow cytometry. Additionally, IL-17A secretion into the supernatants of the Th17 cultures was measured by ELISA. LIF neutralisation did not affect the suppression of Th17 differentiation by DPSC-03-CM, as shown by an equivalent reduction in Th17 cells between cultures that contained anti-LIF and those that did not (Figure 4.31A and B). Similarly, the Th17 culture supernatants showed no change in the level of IL-17A when anti-LIF was added with DPSC-03-CM (Figure 4.31C). Therefore, signalling via secretion of LIF is not likely to be a mechanism by which DPSCs regulate Th17 cells and further investigation is required to identify the secreted factor(s) present in DPSC-03 CM which suppresses Th17 cell differentiation.

4.5.9 Effect of DPSCs on B cell activation, maturation and differentiation *in vitro*

Based on the changes to B cell abundance detected *in vivo*, the potential for DPSCs to directly interact with and modulate B cell biology was investigated *in vitro*. Other MSC types, Ad-MSCs and BM-MSCs, have been shown to modulate different aspects of B cell biology including B cell activation, proliferation and plasmablast differentiation as discussed in Chapter 1. In this study, both contact-dependent and contact-independent interactions were tested by co-culturing B cells with DPSCs or with isolated CM from DPSCs.

Firstly, the effect of DPSCs on B cell activation and maturation was investigated. B cells upregulate a number of molecules as they mature following activation including CD69, CD86 and MHC-II. Therefore, to test if DPSCs or their soluble products affect activation of B cells, naïve FO B cells were isolated from the spleens of C57Bl/6 mice then stimulated with LPS and cultured for 2 days before measuring expression of CD69, CD86 and MHC-II by flow cytometry (Figure 4.32A). The different culture conditions tested were the inclusion of DPSCs or DPSC-CM. The inclusion of DPSC-03 cells did not affect expression of activation markers by B cells (Figure 4.32B-D). While CD86 expression increased on B cells co-cultured with DPSC-05 cells after LPS stimulation, the presence of DPSC-05 cells suppressed up-regulation of both MHC-II and the early activation marker CD69. CD69 up-regulation was also suppressed when CM from either DPSC-03 or DPSC-05 was used in place of DPSCs themselves, indicating DPSCs produce soluble factors which are sufficient to block early B cell activation and maturation. Since DPSC-03 CM suppressed CD69 expression by B cells but co-culture of DPSC-03 cells with B cells had no effect, it is possible that the soluble mediator produced by DPSC-03 cells is expressed at low levels and insufficient quantities were present at the beginning of the co-culture to robustly suppress CD69 up-regulation. Alternatively, cross-talk with B cells may cause some DPSCs to switch off expression of certain molecules.

Secondly, an investigation into whether or not DPSCs can directly affect B cell proliferation was prompted by the increased number of B cells observed in the spleen of EAE mice treated with DPSCs. Naïve FO B cells were first labelled with a membrane proliferation dye. The labelled B cells were then stimulated with LPS in the presence or absence of DPSCs or DPSC-CM from donors 03 or 05 and proliferation of the B cells was measured by dilution of the proliferation dye after culturing for 2 days. Co-culture of the B cells with DPSCs or addition of DPSC-CM did not significantly affect B cell proliferation (Figure 4.33). Thus, DPSCs do not appear to directly affect B cell proliferation.

The effect of DPSCs on B cell differentiation was also tested. Purified naïve FO B cells were induced to differentiate to plasmablasts by culture with LPS and IL-4 for 4 days and then the number of IgG1-secreting $B220^{lo}CD138^{+}$ cells was measured by flow cytometry (Figure 4.34A). Previous reports have cited differences in the response of B cells to the presence of DPSCs depending on the ratio of DPSC:B cells. Therefore, three

different ratios of B cells:DPSCs were tested here, ranging from 10:1 to 80:1. B cell differentiation was significantly inhibited by co-culture with DPSC-03 cells in a dose-dependent manner (Figure 4.34B and C). Moreover, the addition of DPSC-CM to the cultures was sufficient to mediate the effect, showing soluble factors are at least one way in which DPSCs can inhibit B cell differentiation.

In conclusion, DPSCs can directly suppress B cell activation and differentiation. Furthermore, production of soluble factors are at least in part responsible for the effects of DPSCs on B cells *in vitro*.

4.6 Summary

The data in this study support the hypothesis that dental pulp is a source of MSCs that can inhibit EAE. However, differences were identified in the therapeutic efficacy of DPSCs isolated from different donors which do not appear to be due to age, gender, or *in vitro* characteristics and for which the cause could not be readily recognised. Importantly, however, 4 of 6 DPSC cell lines were able to significantly suppress the course of EAE in mice when the cells were administered in the early, pre-symptomatic phase of disease. Although there was no definitive evidence that DPSCs can reverse symptoms in established disease, DPSCs were found to be additionally capable of delaying relapse in a relapsing-remitting model of EAE. Overexpression of ACKR2 and ACKR4 by DPSCs were postulated to increase their ability to suppress EAE but this was not supported by the data.

Tracking of DPSCs *in vivo* revealed they may localise to lungs, spleen and iLNs after intraperitoneal injection although live cells did not appear to persist *in vivo*. The immunomodulatory effects of DPSCs in EAE were also investigated and DPSC treatment led to reduced infiltration of the CNS with both lymphocytes and mononuclear phagocytes, and there were fewer microglia which are all indicative of less inflammation. Although there were some differences in which types of T cells were affected by each DPSC donors, all increased the Th1:Th17 cell ratio in the spleen which may favour better clinical outcome in EAE. Additionally, DPSCs reduced the number of B cells that infiltrated the CNS of EAE mice. DPSCs were shown to express genes for various immunomodulatory factors and *in vitro* experiments highlighted the production of soluble immunomodulatory factors to be one way in which some DPSCs can directly influence activation of B cells and differentiation of Th17 cells and plasmablasts.

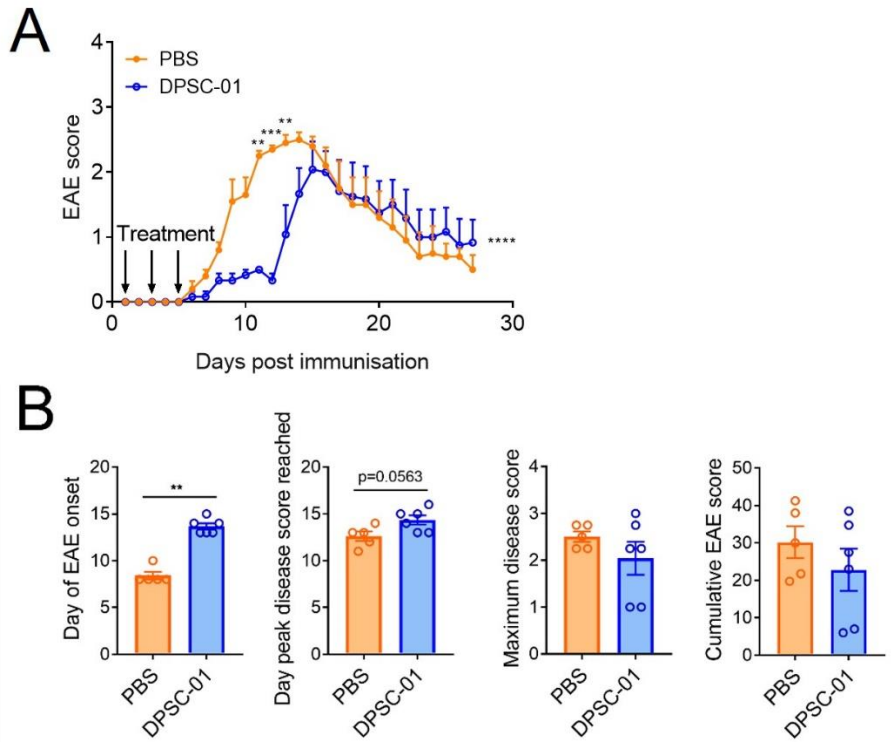

Figure 4.1: Effect of DPSC-01 treatment on course of MOG_{35-55}-EAE.

C57Bl/6 mice were immunised for EAE by subcutaneous injection of 100 µg of MOG_{35-55} emulsified in CFA on day 0 (d0) and two doses of 300 ng of pertussis toxin intravenously on days 0 and 2. Mice were treated intraperitoneally with 1 x 10^6 DPSCs or PBS for control on days 0, 1, 3 and 5. Clinical signs of EAE were measured daily after immunisation. **a)** Time-course of severity of EAE clinical signs. **b)** Graphical summary of disease parameters from the experiment in (a). For a) each point represents the mean ± SEM of each group. **p<0.01, ***p<0.005, ****p<0.001; asterisks at the end of the time-course indicate time-points that are statistically significant by Two-Way repeated measures ANOVA whereas asterisks above and below each day on the graph are indicative of Bonferroni's multiple comparisons post-test statistics. For b) each point represents one mouse and columns represent mean ± SEM of each group. n=5-6 mice. *p<0.05, ****p<0.001 Mann-Whitney U test.

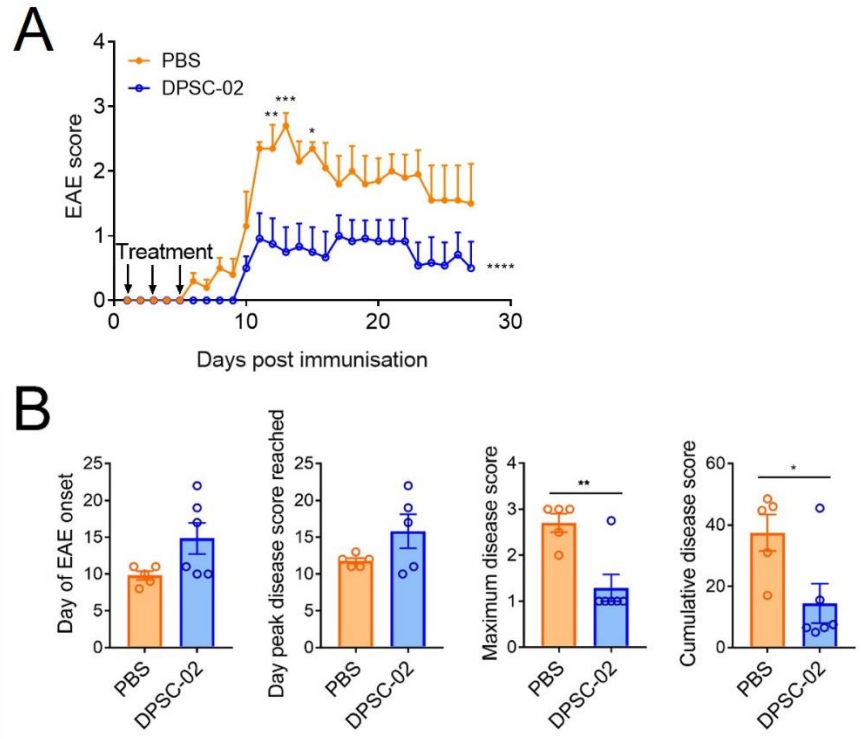

Figure 4.2: Effect of DPSC-02 treatment on course of MOG_{35-55}-EAE.

C57Bl/6 mice were immunised for EAE by subcutaneous injection of 100 µg of MOG_{35-55} emulsified in CFA on day 0 (d0) and two doses of 300 ng of pertussis toxin intravenously on days 0 and 2. Mice were treated intraperitoneally with 1 x 10^6 DPSCs or PBS for control on days 0, 1, 3 and 5. Clinical signs of EAE were measured daily after immunisation. **a)** Time-course of severity of EAE clinical signs. **b)** Graphical summary of disease parameters from the experiment in (a). For a) each point represents the mean ± SEM of each group. *p<0.05, **p<0.01, ***p<0.005 ****p<0.001; asterisks at the end of the time-course indicate time-points that are statistically significant by Two-Way repeated measures ANOVA whereas asterisks above and below each day on the graph are indicative of Bonferroni's multiple comparisons post-test statistics. For b) each point represents one mouse and columns represent mean ± SEM of each group. n=5-6 mice. *p<0.05, **p<0.01 Mann-Whitney U test.

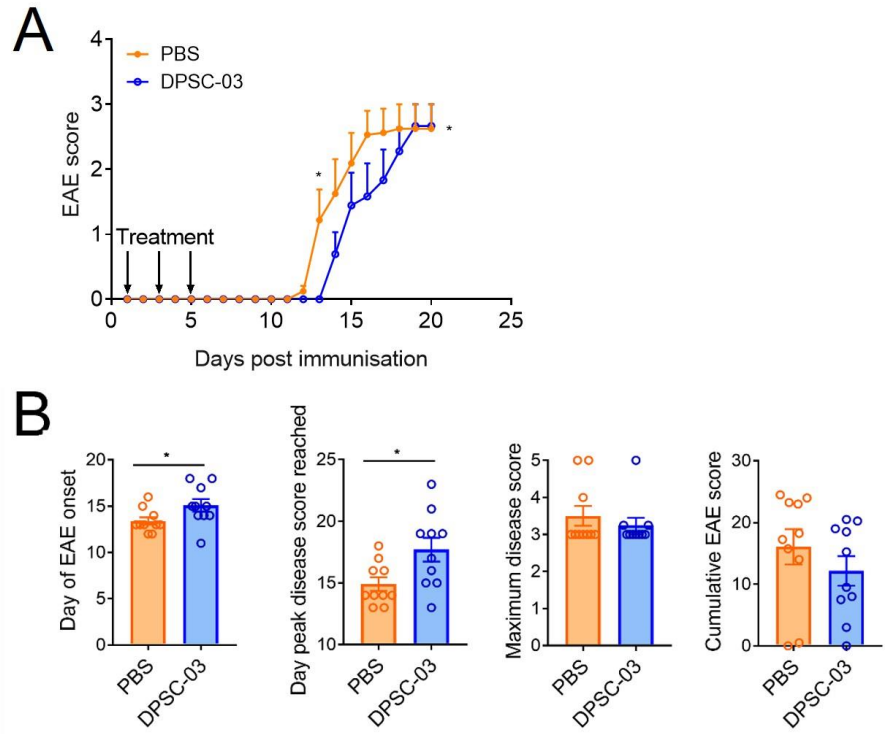

Figure 4.3: Effect of DPSC-03 treatment on course of MOG_{35-55}-EAE.

C57Bl/6 mice were immunised for EAE by subcutaneous injection of 100 µg of MOG_{35-55} emulsified in CFA on day 0 (d0) and two doses of 300 ng of pertussis toxin intravenously on days 0 and 2. Mice were treated intraperitoneally with 1 x 10^6 DPSCs or PBS for control on days 1, 3 and 5. Clinical signs of EAE were measured daily after immunisation. **a)** Time-course of severity of EAE clinical signs. **b)** Graphical summary of disease parameters from the experiment in (a). For a) each point represents the mean ± SEM of each group. *p<0.05; asterisks at the end of the time-course indicate time-points that are statistically significant by Two-Way repeated measures ANOVA whereas asterisks above and below each day on the graph are indicative of Bonferroni's multiple comparisons post-test statistics. For b) each point represents one mouse and columns represent mean ± SEM of each group. n=10 mice per group, pooled from two independent experiments. *p<0.05 Mann-Whitney U test.

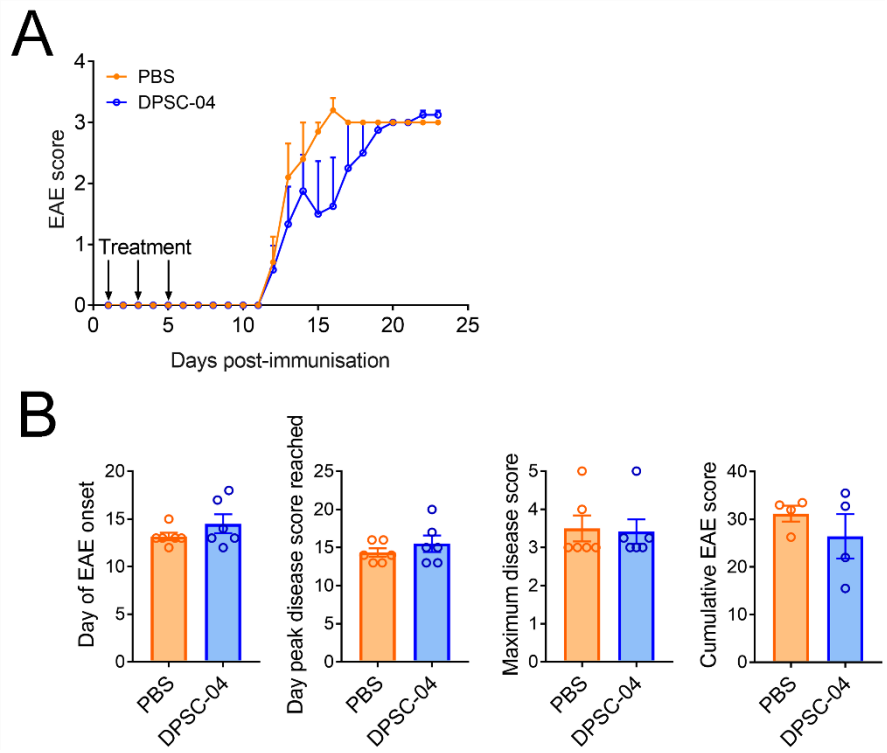

Figure 4.4: Effect of DPSC-04 treatment on course of MOG_{35-55}-EAE.

C57Bl/6 mice were immunised for EAE by subcutaneous injection of 100 µg of MOG_{35-55} emulsified in CFA on day 0 (d0) and two doses of 300 ng of pertussis toxin intravenously on days 0 and 2. Mice were treated intraperitoneally with 1 x 10^6 DPSCs or PBS for control on days 1, 3 and 5. Clinical signs of EAE were measured daily after immunisation. **a)** Time-course of severity of EAE clinical signs. **b)** Graphical summary of disease parameters from the experiment in (a). For a) each point represents the mean ± SEM of each group. For b) each point represents one mouse and columns represent mean ± SEM of each group. n=6 mice.

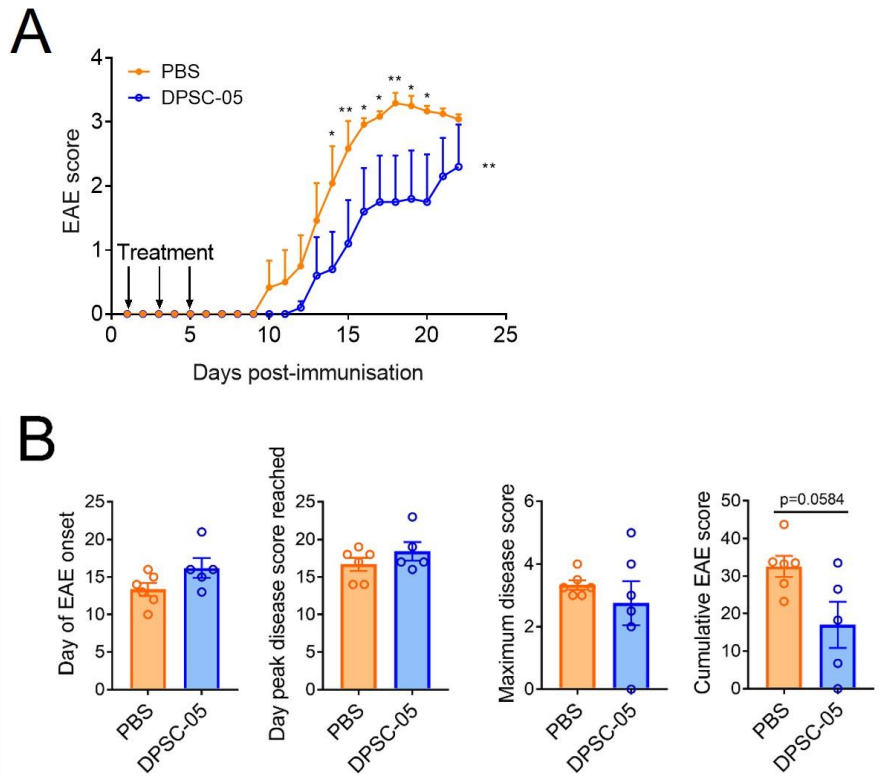

Figure 4.5: Effect of DPSC-05 treatment on course of MOG_{35-55}-EAE.

C57Bl/6 mice were immunised for EAE by subcutaneous injection of 100 µg of MOG_{35-55} emulsified in CFA on day 0 (d0) and two doses of 200 ng of pertussis toxin intravenously on days 0 and 2. Mice were treated intraperitoneally with 1 x 10^6 DPSCs or PBS for control on days 1, 3 and 5. Clinical signs of EAE were measured daily after immunisation. **a)** Time-course of severity of EAE clinical signs. **b)** Graphical summary of disease parameters from the experiment in (a). For a) Each point represents the mean ± SEM of each group. *p<0.05, **p<0.01; asterisks at the end of the time-course indicate time-points that are statistically significant by Two-Way repeated measures ANOVA whereas asterisks above and below each day on the graph are indicative of Bonferroni's multiple comparisons post-test statistics. For b) each point represents one mouse and columns represent mean ± SEM of each group. n=5-6 mice.

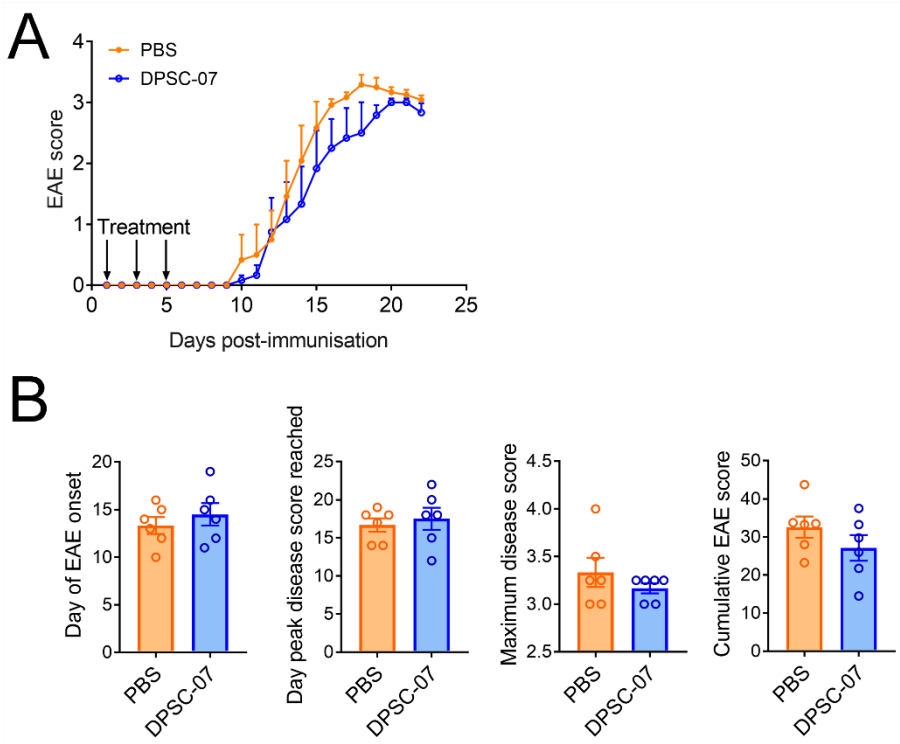

Figure 4.6: Effect of DPSC-07 treatment on course of MOG_{35-55}-EAE.

C57Bl/6 mice were immunised for EAE by subcutaneous injection of 100 µg of MOG_{35-55} emulsified in CFA on day 0 (d0) and two doses of 200 ng of pertussis toxin intravenously on days 0 and 2. Mice were treated intraperitoneally with 1 x 10^6 DPSCs or PBS for control on days 1, 3 and 5. Clinical signs of EAE were measured daily after immunisation. **a)** Time-course of severity of EAE clinical signs. **b)** Graphical summary of disease parameters from the experiment in (a). For a) each point represents the mean ± SEM of each group. For b) each point represents one mouse and columns represent mean ± SEM of each group. n=6 mice.

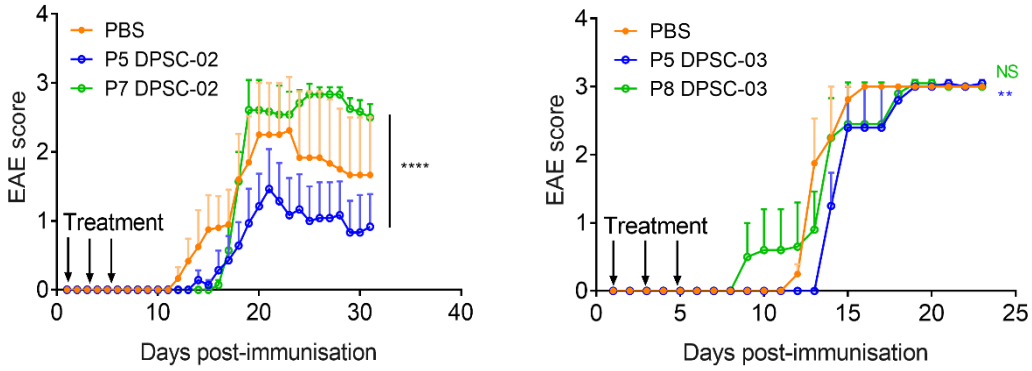

Figure 4.7: Higher passage DPSCs have reduced ability to suppress the course of MOG_{35-55}-EAE.

C57Bl/6 mice were immunised for EAE by subcutaneous injection of 100 µg of MOG_{35-55} emulsified in CFA on day 0 (d0) and two doses of 200 ng or 300 ng of pertussis toxin intravenously on days 0 and 2. Mice were treated intraperitoneally with 1 x 10^6 DPSCs or PBS for control on days 1, 3 and 5. Clinical signs of EAE were measured daily after immunisation. Time-course of severity of EAE clinical symptoms. Each point represents the mean ± SEM of 6-7 mice per group. ****$p<0.0001$ P5 DPSC compared with P7 DPSC, ** $p<0.01$ P5 DPSC compared with PBS by Two-Way ANOVA. NS; not statistically significant.

Table 4.1: Summary of disease statistics for EAE mice treated with PBS or DPSCs from different donors.

DPSC donor	Incidence		Day of onset		Day of peak disease		Maximum score		Cumulative Score	
	Control	Treated	Control	Treated	Control	Treated	Control	Treated	Control	Treated
DPSC-01 ****	5/5	6/6	8 (8-10)	13.5 (13-15)**	13 (11-14)	14.5 (13-16)	2.5 (2.25-2.75)	2.25 (1-3)	30 (19.8-41.3)	25.3 (6-38.5)
DPSC-02 ****	5/5	6/6	10 (8-11)	14 (10-22)	12 (11-13)	17 (10-22)	3 (2-3)	1 (1-2.75)	44.8 (17-48.5)	7 (5-45)*
DPSC-03 *	9/10	9/10	13 (12-16)	15 (11-18)*	14 (13-18)	18 (13-23)	3 (3-5)	3 (3-5)	17.8 (0-24.5)	12.4 (0-20.5)
DPSC-04	6/6	6/6	13 (12-15)	13.5 (12-18)	14 (13-16)	15 (13-20)	3 (3-5)	3.13 (3-5)	32.5 (26.3-33.5)	27.4 (15.5-27.4)
DPSC-05 **	6/6	5/6	13.5 (10-16)	16 (13-21)	17.5 (14-19)	17 (16-23)	3.25 (3-4)	2.75 (0-5)	33.4 (43.8)	18.3 (0-33.5)
DPSC-07	6/6	6/6	13.5 (10-16)	14.5 (11-19)	17.5 (14-19)	18 (12-22)	3.25 (3-4)	3.25 (3-3.25)	33.4 (23.3)	18.3 (0-33.5)

Medians are given for each parameter and range of the data in brackets. *p<0.05, **p<0.01, ****p<0,0001. For the DPSC donor column, statistics are indicative of Two-Way ANOVA test of the time-course of EAE. For all other columns, comparisons were made using the Mann-Whitney U test.

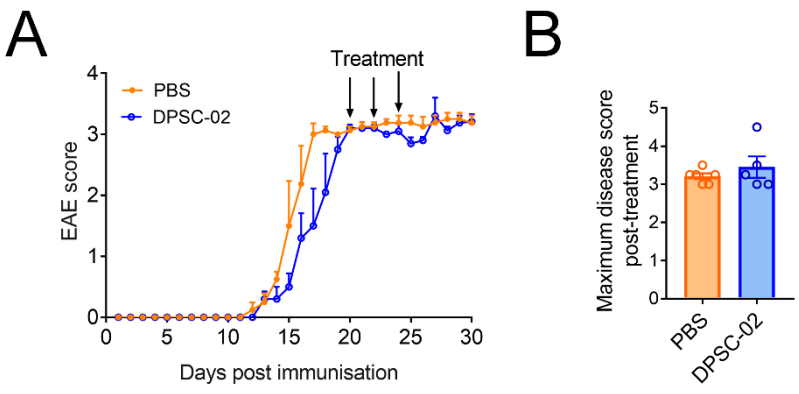

Figure 4.8: Effect of treating MOG$_{35-55}$-EAE with DPSCs after the onset of clinical signs.

C57Bl/6 mice were immunised for EAE by subcutaneous injection of 100 µg of MOG$_{35-55}$ emulsified in CFA on day 0 (d0) and two doses of 300 ng of pertussis toxin intravenously on days 0 and 2. After peak disease was reached, the mice were split into two treatment groups and treated intraperitoneally with 1 x 10^6 DPSCs or PBS for control three times on alternate days (d21, d23 and d25). This graph is representative of two independent experiments with similar results. Each point represents mean EAE score ± SEM of n=5-6 mice per group.

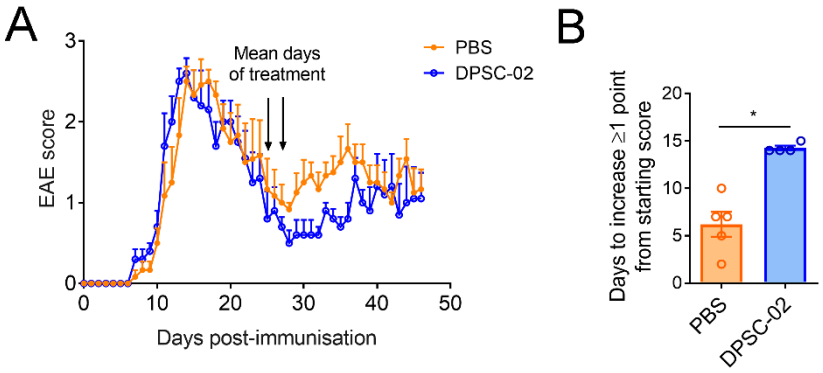

Figure 4.9: Effect of treating relapsing EAE with DPSCs.

SJL/J mice were immunised for EAE by subcutaneous injection of 50 µg of $PLP_{139-151}$ emulsified in CFA on day 0 (d0) and two doses of 300 ng of pertussis toxin intravenously on days 0 and 2. Mice were treated with two intraperitoneal injections of DPSCs (1 x 10^6 cells) or PBS on an individual basis when EAE went into remission. **a)** Time-course of the severity of EAE clinical signs measured daily. Each point represents the mean ± SEM of each group. **b)** Time until relapse of clinical signs as determined by an increase ≥1 point from the EAE score at the time of treatment. For b) each point represents one mouse and columns represent mean ± SEM of each group of n=4-5 mice. *$p<0.05$ Mann-Whitney U test.

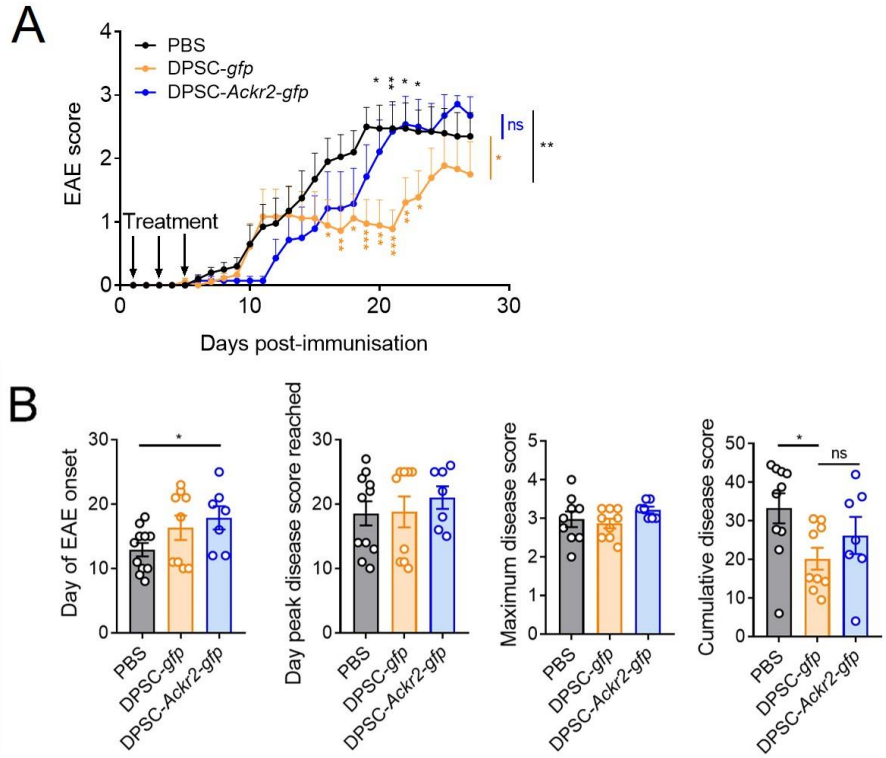

Figure 4.10: Effect of ACKR2 expression on DPSC ability to suppress EAE.

C57Bl/6 mice were immunised for EAE by subcutaneous injection of 100 µg of MOG_{35-55} emulsified in CFA on day 0 (d0) and two doses of 200 ng of pertussis toxin intravenously on days 0 and 2. Mice were treated on days 1, 3 and 5 with intraperitoneal injection of PBS or 1 x 10^6 DPSCs overexpressing ACKR2 (DPSC-*Ackr2-gfp*) or transduced with empty vector (DPSC-*gfp*). **a)** Time-course of the severity of EAE clinical signs. **b)** Graphical summary of disease parameters for the experiments in (a). For a) each point represents mean ± SEM of the group. Statistics in black compare DPSC-*gfp* vs DPSC-*Ackr2-gfp*. Statistics in orange compare PBS vs DPSC-*gfp*. Asterisks at the end of the time-course indicate time-points that are statistically significant by Two-Way repeated measures ANOVA whereas asterisks above and below each day on the graph are indicative of Bonferroni's multiple comparisons post-test statistics. *p<0.05, **p<0.01, ***p<0.005, ns: not significant. For b) each point represents one mouse and columns represent mean ± SEM of each group. *p<0.05 Kruskal-Wallis test with Dunn's multiple comparisons post-test. Data are pooled from two independent experiments with total 7-10 mice per group.

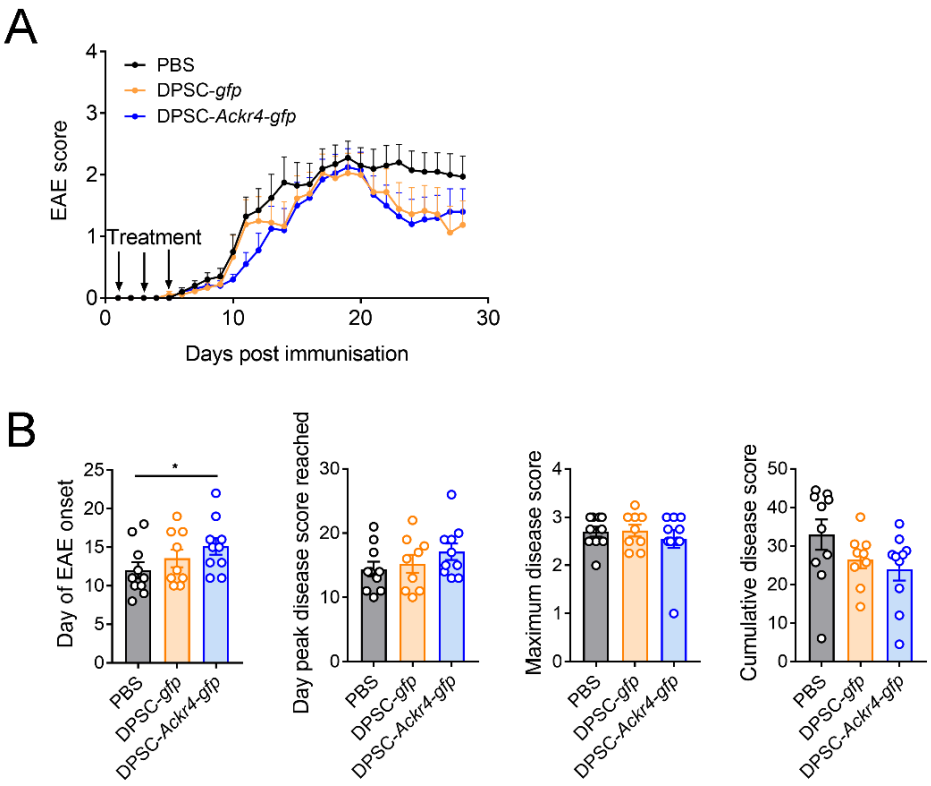

Figure 4.11: Effect of ACKR4 expression on DPSC ability to suppress EAE.

C57Bl/6 mice were immunised for EAE by subcutaneous injection of 100 µg of MOG_{35-55} emulsified in CFA on day 0 (d0) and two doses of 200 ng of pertussis toxin intravenously on days 0 and 2. Mice were treated on days 1, 3 and 5 with intraperitoneal injections of PBS or 1 x 10^6 DPSCs overexpressing ACKR4 or DPSCs transduced with empty vector. **a)** Time-course of the severity of EAE clinical signs. **b)** Graphical summary of disease parameters for the experiments in (a). For a) each point represents mean ± SEM of the group. For b) each point represents one mouse and columns represent mean ± SEM of each group. *p<0.05 Kruskal-Wallis test with Dunn's multiple comparisons post-test. Data are pooled from two independent experiments with total 9-10 mice per group.

This page intentionally left blank.

Figure 4.12: Homing of DPSCs after multiple injections in EAE mice.

GFP-expressing DPSCs were labelled with Cellbrite™ NIR790 Cytoplasmic Membrane Dye (Biotium) and EAE mice received three intraperitoneal injections of 1 x 10^6 DPSCs or PBS on days 1, 3 and 5 post-immunisation. Approximately 18 hours after the final injection, mice were humanely killed and perfused intracardially to remove circulating leukocytes. The organs of interest were excised and imaged whole by *in vivo* imaging system (IVIS). **a)** Organs from three representative DPSC-treated EAE mice showing bioluminescence imaged by IVIS. **b)** Quantification of the bioluminescent signal detected in each organ in PBS or DPSC-treated EAE mice by IVIS. *$p<0.05$ Mann-Whitney U test. n=3-7 mice pooled from two independent experiments. **c)** Titration of pWPI-*gfp* vector from 10^7 copies to 1 copy and detection of the *gfp* gene by qPCR. Each dot represents mean ± SEM of each dilution of pWPI performed in triplicate and is representative of two independent experiments.

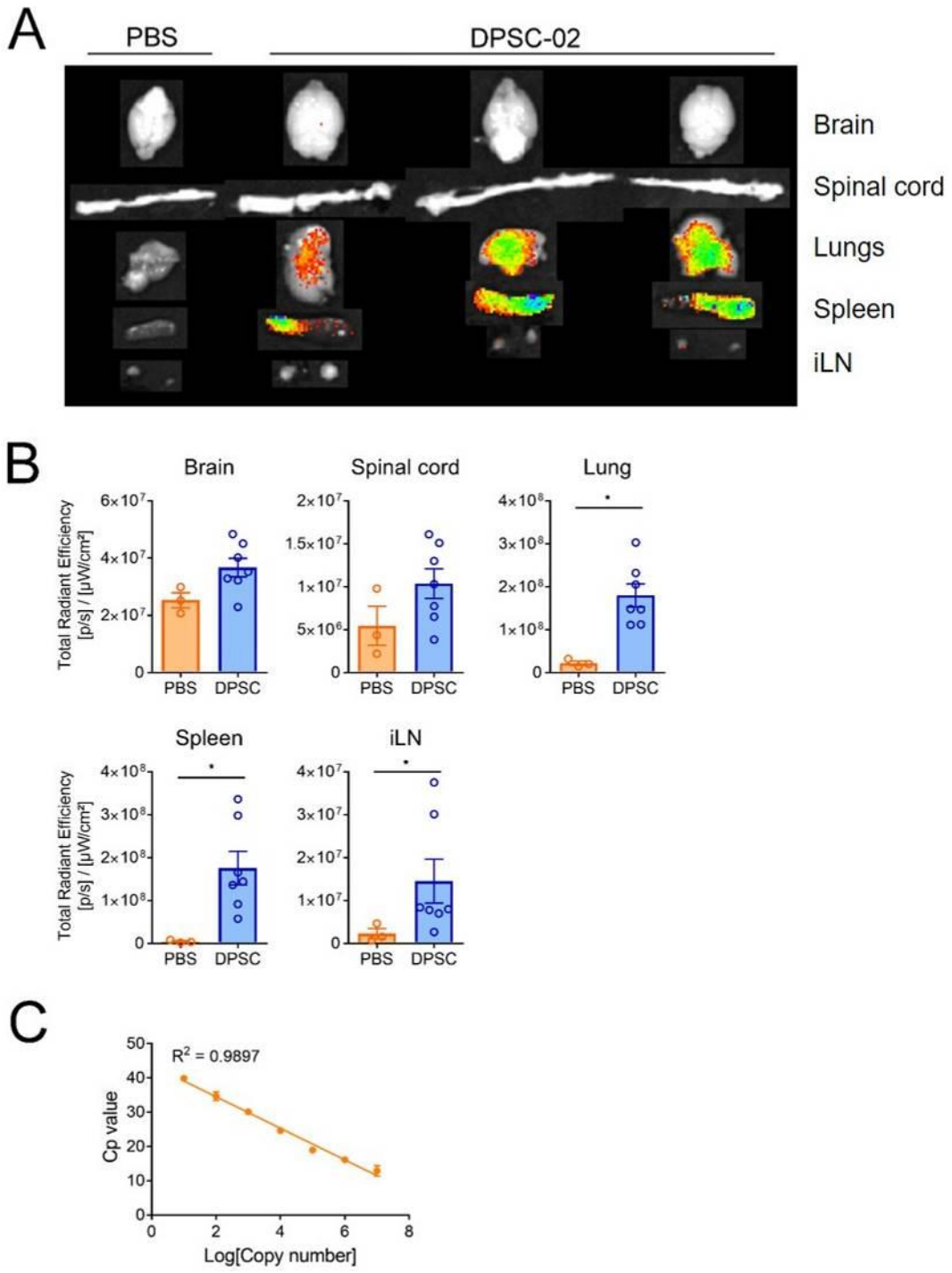
A
PBS
DPSC-02
Brain
Spinal cord
Lungs
Spleen
iLN
B
Brain
Spinal cord
Lung
Spleen
iLN
Total Radiant Efficiency [p/s] / [µW/cm²]
PBS
DPSC
C
R² = 0.9897
Cp value
Log[Copy number]

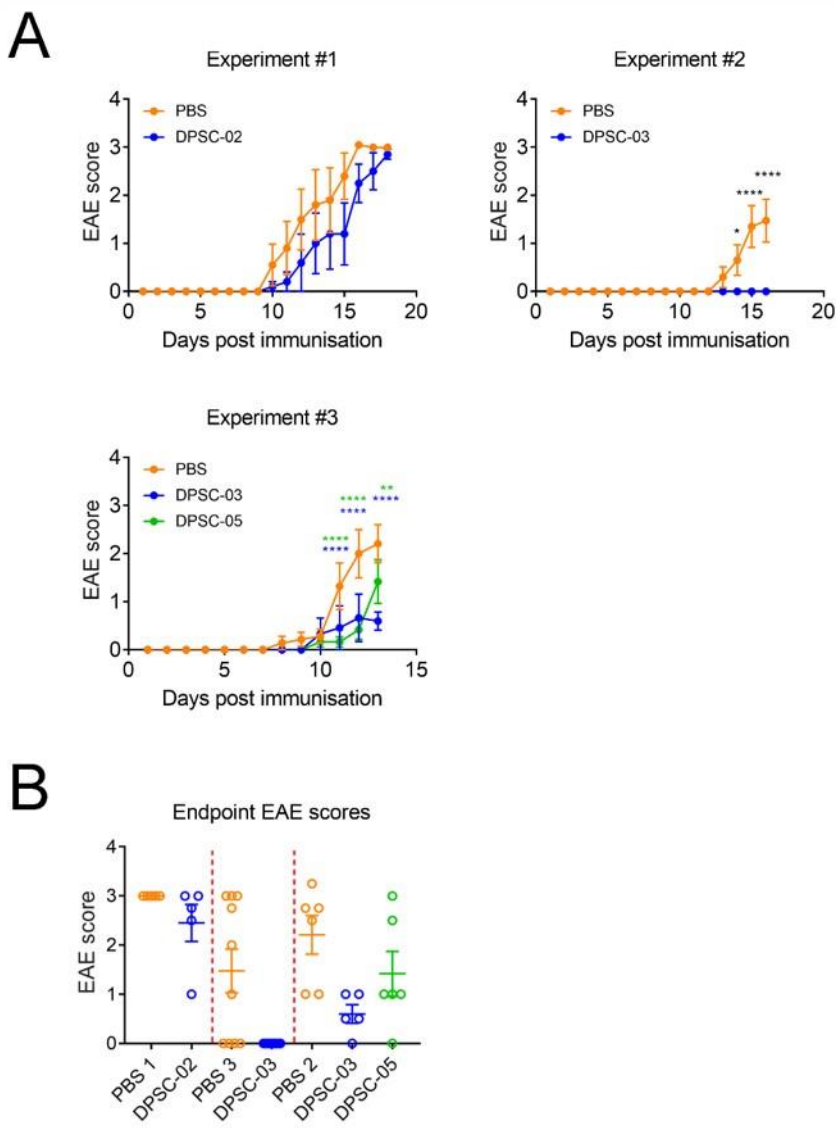

Figure 4.13: EAE time-courses and endpoint disease scores for experiments investigating DPSC effects on the immune response.

C57Bl/6 mice were immunised for EAE by subcutaneous injection of 100 µg of MOG_{35-55} emulsified in CFA on day 0 (d0) and two doses of 200 ng[§] (#1) or 300 ng[§] of pertussis toxin (#2 and #3) intravenously on days 0 and 2. Mice were treated intraperitoneally with 1 x 10^6 DPSCs from donors 02, 03 or 05 or PBS for control on days 1, 3 and 5. Symptoms of EAE were measured daily after immunisation. **a)** Time-courses of severity of EAE symptoms. **b)** EAE disease scores of individual mice from the experiments in (a) at the experimental endpoint for analysis. For a) each point represents the mean ± SEM of each group. For b) each point represents one mouse and bars represent mean ± SEM of each group. n=5-8 mice. *p<0.05, **p<0.01, ****p<0.001 Two-Way ANOVA with Bonferroni's multiple comparisons test.

[§]*Pertussis toxin from different lots between experiments led to different amounts required to initiate disease.*

This page intentionally left blank.

Figure 4.14: Leukocyte populations in the CNS of DPSC-treated EAE mice.

EAE mice were treated with three intraperitoneal injections of PBS or 1 x 10^6 DPSCs on days 1, 3 and 5 post-immunisation. When the control group reached peak disease, microglia and infiltrating leukocytes in the CNS (brain and spinal cord combined) were quantified by flow cytometry. **a)** Representative flow cytometry showing gating for infiltrating lymphocytes ($CD45^+CD11b^-$), infiltrating myeloid cells ($CD45^{hi}CD11b^+$) and microglia ($CD45^{lo/int}CD11b^+$) in PBS- or DPSC-treated mice after pre-gating on live single cells. **b)** Proportion and total number of each leukocyte population in the CNS. Each point represents one mouse and bars represent mean ± SEM of each group (n=5-12 mice). **c)** Correlation between the number of infiltrating leukocytes (sum of infiltrating lymphocytes and myeloid cells) relative to control and the number of microglia relative to control. A linear regression was fitted using all of the data points combined. The data for PBS and DPSC-03 for all panels are pooled from two independent experiments and DPSC-05 was performed once. The means of the PBS group were calculated and set to 100% (for proportion) or 1 cell (for number) and all data points were normalised to these values; proportion (P) was calculated as ($P = \frac{Sample\ \%}{Mean\ of\ PBS\ group}\ x\ 100\%$); number was normalised as ($N = \frac{Number\ in\ sample}{Mean\ number\ in\ PBS}$). *p<0.05, **p<0.01 Kruskal-Wallis test with multiple comparisons.

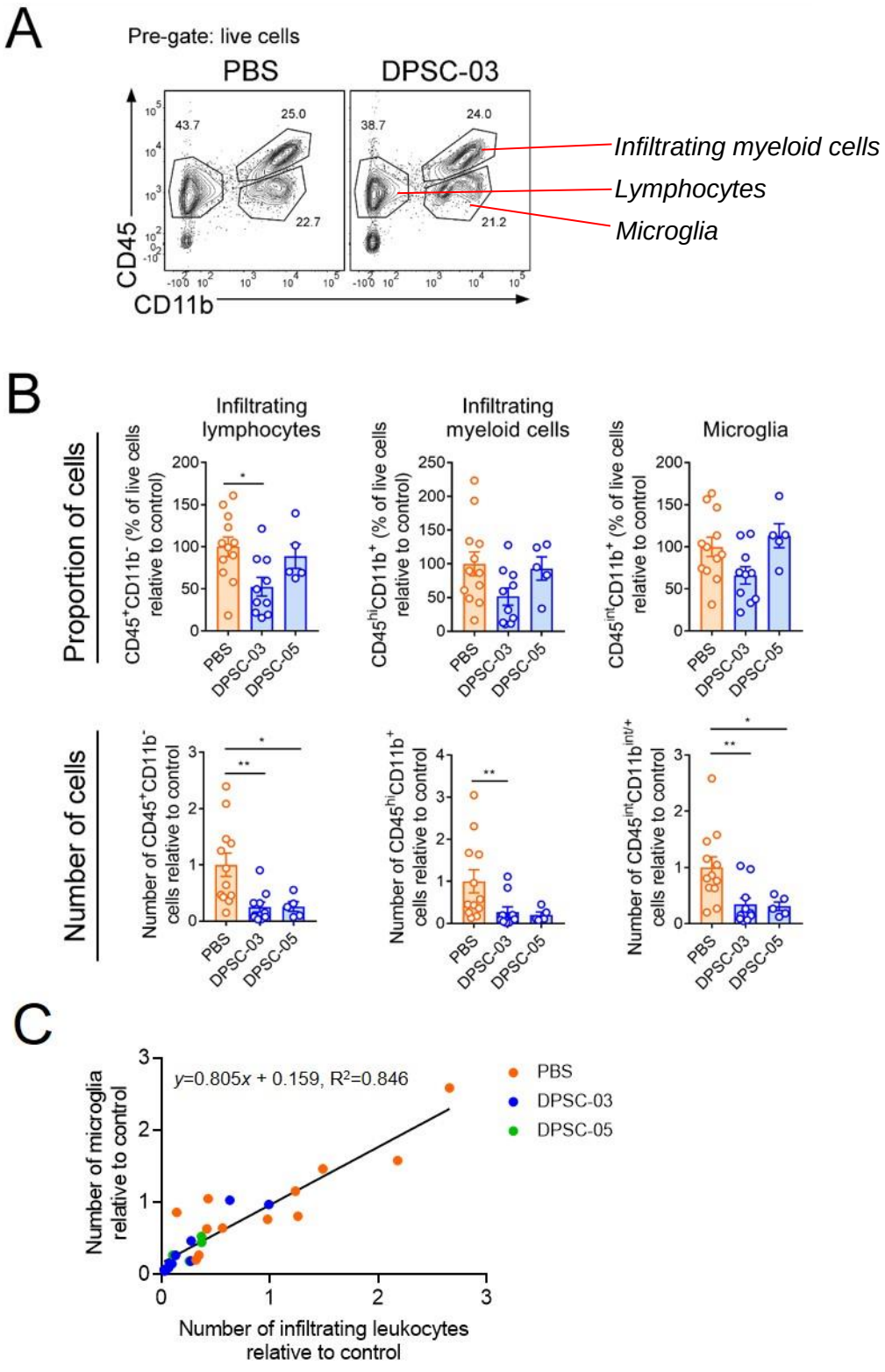
A
Pre-gate: live cells
PBS
DPSC-03
43.7
25.0
22.7
38.7
24.0
21.2
CD45
CD11b
Infiltrating myeloid cells
Lymphocytes
Microglia
B
Proportion of cells
Number of cells
Infiltrating lymphocytes
Infiltrating myeloid cells
Microglia
CD45+CD11b- (% of live cells relative to control)
CD45hiCD11b+ (% of live cells relative to control)
CD45intCD11b+ (% of live cells relative to control)
Number of CD45+CD11b- cells relative to control
Number of CD45hiCD11b+ cells relative to control
Number of CD45intCD11bint/+ cells relative to control
PBS
DPSC-03
DPSC-05
C
y=0.805x + 0.159, R²=0.846
Number of microglia relative to control
Number of infiltrating leukocytes relative to control
PBS
DPSC-03
DPSC-05

Figure 4.15: CD4$^+$ T cells in EAE mice treated with DPSCs.

EAE mice were treated with three intraperitoneal injections of PBS or 1 x 10^6 DPSCs on days 1, 3 and 5 post-immunisation. When mean peak disease scores were reached in the PBS control group, CD4$^+$ T cells were quantified in inguinal LNs (iLNs), spleen (SP) and CNS (brain and spinal cord combined). **a)** Representative flow cytometry showing CD4$^+$ T cells vs CD8$^+$ T cells after pre-gating on B220$^-$ cells. **b)** Proportion (top) and total number (bottom) of CD4$^+$ T cells in each organ. For iLN and SP, the PBS group is pooled while DPSC-02 and DPSC-03 and -05 were performed in two independent experiments. Each point represents one mouse and bars represent mean ± SEM of each group (n=4-11 mice). For the CNS, the DPSC data are pooled from all the donors for both experiments (n=10 mice per group). For all data, the means of the PBS group were calculated and set to 100% (for proportion) or 1 cell (for number) and all data points were normalised to these values; proportion (*P*) was calculated as ($P = \frac{Sample\ \%}{Mean\ of\ PBS\ group}\ x\ 100\%$); number was normalised as ($N = \frac{Number\ in\ sample}{Mean\ number\ in\ PBS}$). **p<0.01 Mann-Whitney U test.

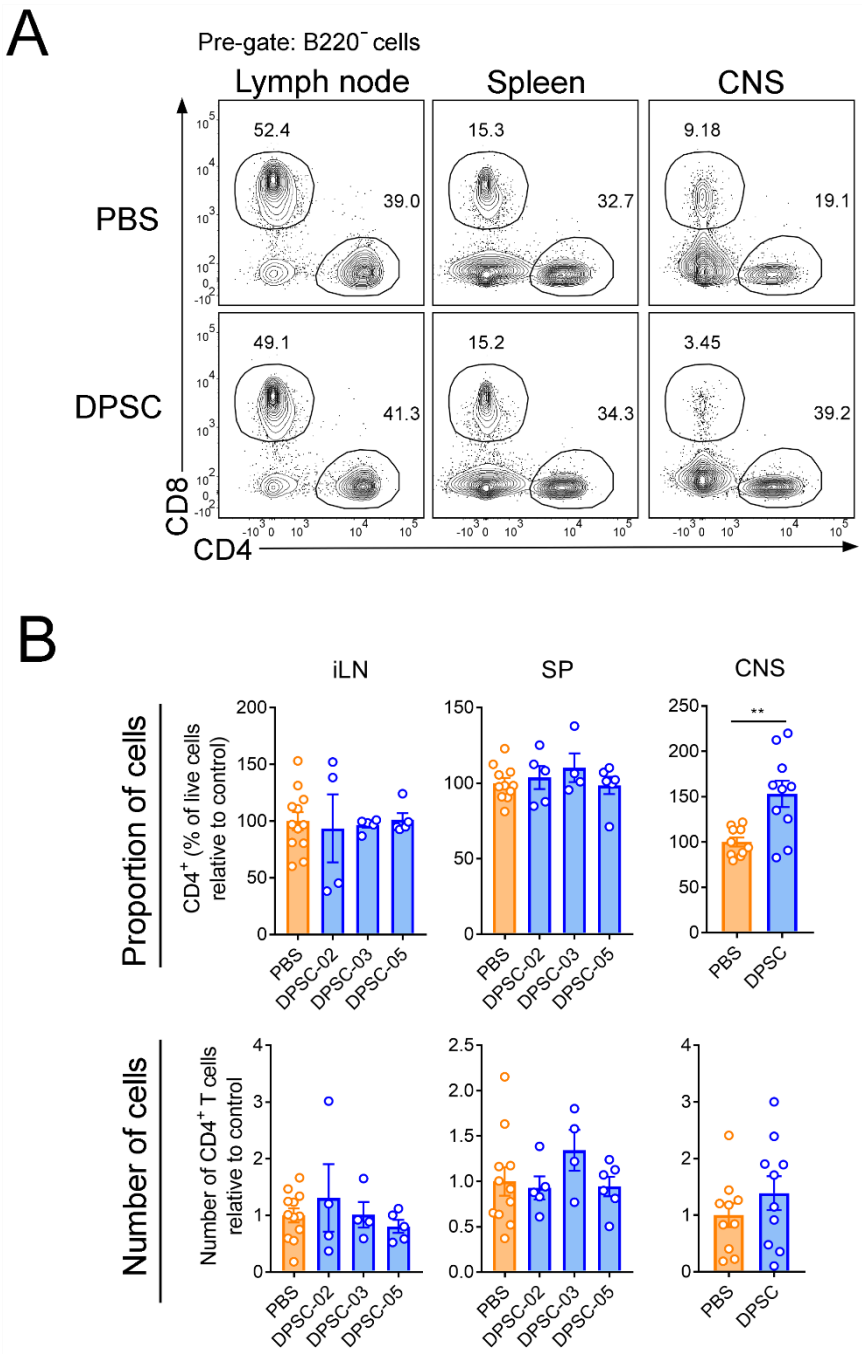
A
Pre-gate: B220⁻ cells
Lymph node
Spleen
CNS
PBS
DPSC
52.4
39.0
15.3
32.7
9.18
19.1
49.1
41.3
15.2
34.3
3.45
39.2
CD8
CD4
B
iLN
SP
CNS
Proportion of cells
CD4+ (% of live cells relative to control)
Number of cells
Number of CD4+ T cells relative to control
**
PBS
DPSC-02
DPSC-03
DPSC-05
DPSC

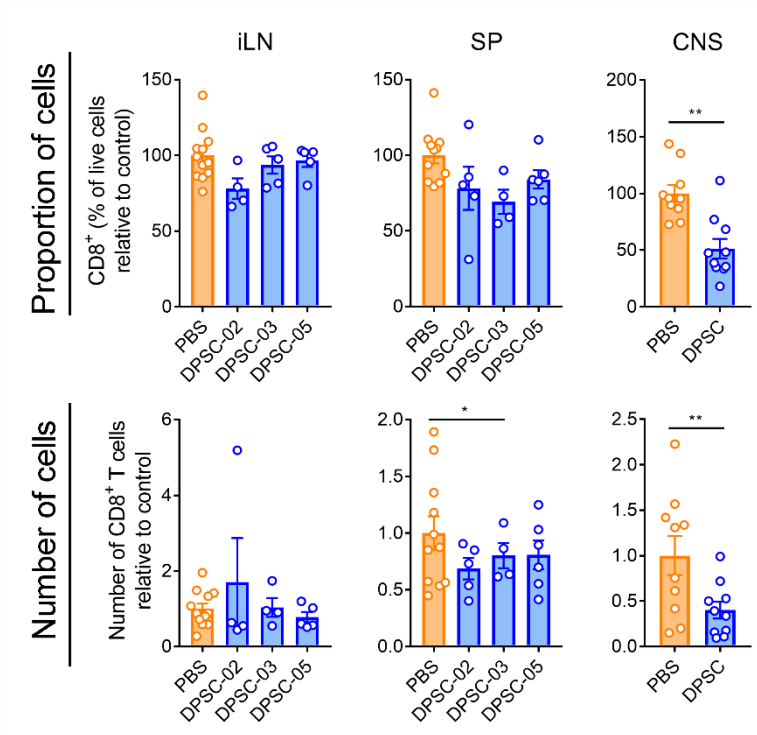

Figure 4.16: CD8⁺ T cells in EAE mice treated with DPSCs.

EAE mice were treated with three intraperitoneal injections of PBS or 1 x 10^6 DPSCs on days 1, 3 and 5 post-immunisation. When mean peak disease scores were reached in the PBS control group, CD8⁺ T cells were quantified in inguinal LNs (iLNs), spleen (SP) and CNS (brain and spinal cord combined). Proportion (top) and total number (bottom) of CD4⁺ T cells in each organ. For iLN and SP, the PBS group is pooled while DPSC-02 and DPSC-03 and -05 were performed in two independent experiments. Each point represents one mouse and bars represent mean ± SEM of each group (n=4-11 mice). For the CNS, the DPSC data are pooled from all the donors for both experiments (n=10 mice per group). For all data, the means of the PBS group were calculated and set to 100% (for proportion) or 1 cell (for number) and all data points were normalised to these values; proportion (P) was calculated as ($P = \frac{Sample\ \%}{Mean\ of\ PBS\ group}\ x\ 100\%$); number was normalised as ($N = \frac{Number\ in\ sample}{Mean\ number\ in\ PBS}$). *p<0.05, **p<0.01 Kruskal-Wallis test with multiple comparisons (for SP) or Mann-Whitney U test (for CNS). Representative flow cytometry is shown in Figure 4.15:.

This page intentionally left blank.

Figure 4.17: B cells in EAE mice treated with DPSCs.

EAE mice were treated with three intraperitoneal injections of PBS or 1 x 10^6 DPSCs on days 1, 3 and 5 post-immunisation. When mean peak disease scores were reached in the PBS control group, B cells were quantified in inguinal LNs (iLNs), spleen (SP) and CNS (brain and spinal cord combined). **a)** Representative flow cytometry showing B cells after pre-gating on live single cells. **b)** Proportion (top) and total number (bottom) of B cells in each organ. For iLN and SP, the data for PBS and DPSC-03 are pooled from two independent experiments and DPSC-05 was performed once. Each point represents one mouse and bars represent mean ± SEM of each group (n=6-11 mice). For the CNS, the DPSC data are pooled from all the donors for both experiments (n=10 mice per group). For all data, the means of the PBS group were calculated and set to 100% (for proportion) or 1 cell (for number) and all data points were normalised to these values; proportion (*P*) was calculated as ($P = \frac{Sample\ \%}{Mean\ of\ PBS\ group}\ x\ 100\%$); number was normalised as ($N = \frac{Number\ in\ sample}{Mean\ number\ in\ PBS}$). *p<0.05 Mann-Whitney U test.

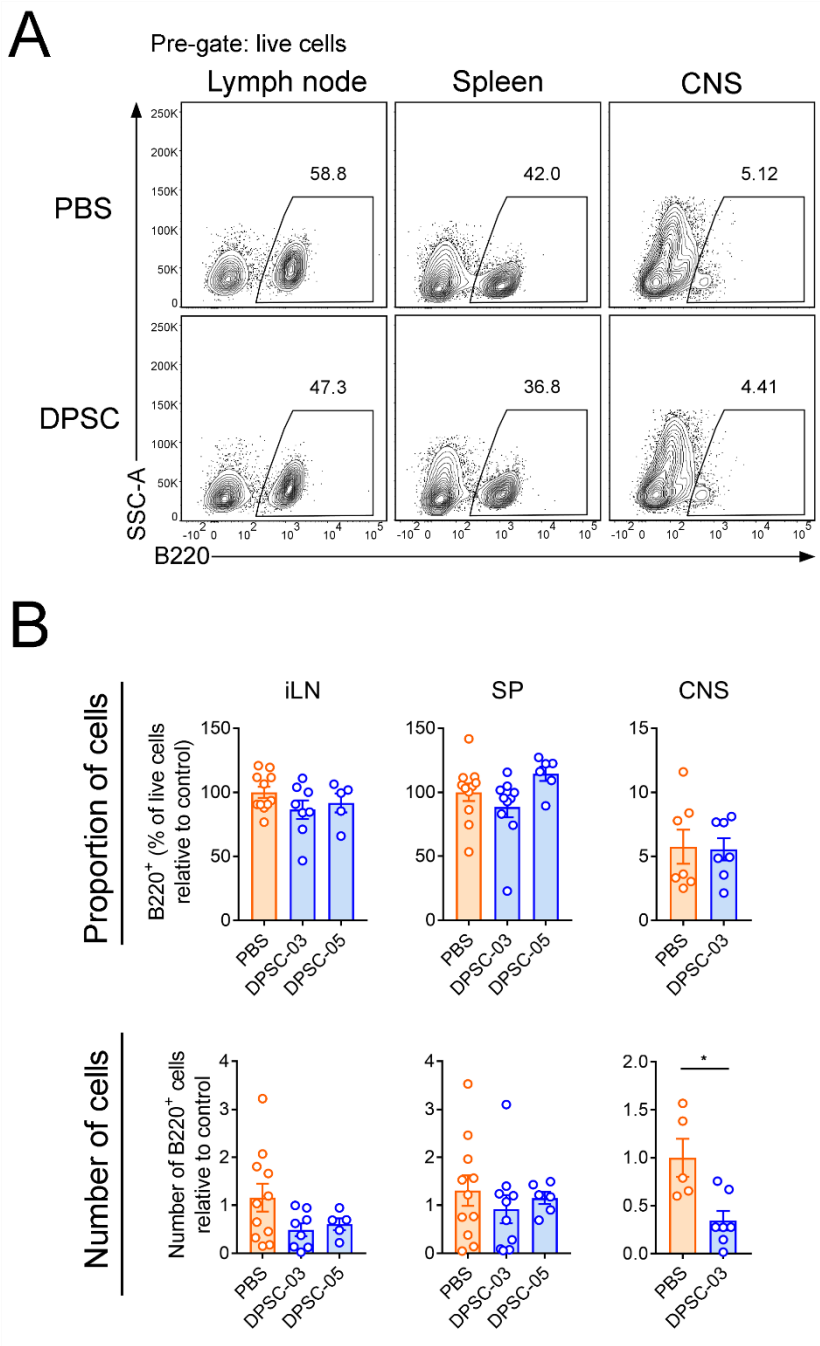
A
Pre-gate: live cells
Lymph node
Spleen
CNS
PBS
DPSC
58.8
42.0
5.12
47.3
36.8
4.41
SSC-A
B220
B
Proportion of cells
B220+ (% of live cells relative to control)
iLN
SP
CNS
PBS
DPSC-03
DPSC-05
Number of cells
Number of B220+ cells relative to control
*

Figure 4.18: Th1 cells in EAE mice treated with DPSCs.

EAE mice were treated with three intraperitoneal injections of PBS or 1 x 10^6 DPSCs on days 1, 3 and 5 post-immunisation. When mean peak disease scores were reached in the PBS control group, Th1 cells were quantified in inguinal LNs (iLNs), spleen (SP) and CNS (brain and spinal cord combined). **a)** Representative flow cytometry showing IFNγ-expressing $CD4^+$ T cells (Th1). **b)** Proportion (top) and total number (bottom) of Th1 cells in each organ. For iLN and SP, the PBS group is pooled while DPSC-02 and DPSC-03 and -05 were performed in two independent experiments. Each point represents one mouse and bars represent mean ± SEM of each group (n=4-11 mice). For the CNS, the DPSC data are pooled from all the donors for both experiments (n=10 mice per group). For all data, the means of the PBS group were calculated and set to 100% (for proportion) or 1 cell (for number) and all data points were normalised to these values; proportion (*P*) was calculated as ($P = \frac{Sample\ \%}{Mean\ of\ PBS\ group}\ x\ 100\%$); number was normalised as ($N = \frac{Number\ in\ sample}{Mean\ number\ in\ PBS}$). *p<0.05, **p<0.01 Kruskal-Wallis test with multiple comparisons.

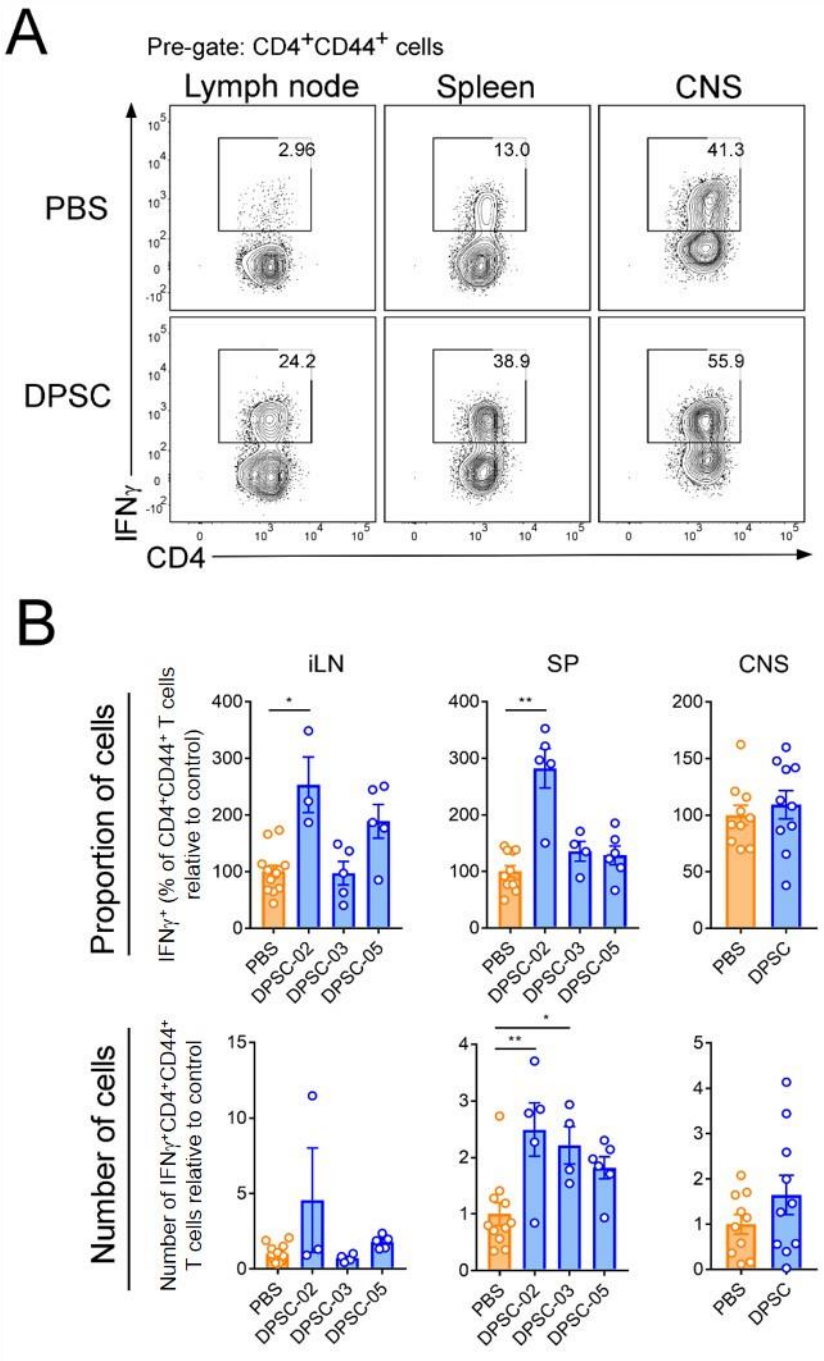
A
Pre-gate: CD4+CD44+ cells
Lymph node
Spleen
CNS
PBS
DPSC
2.96
13.0
41.3
24.2
38.9
55.9
IFNγ
CD4
B
Proportion of cells
IFNγ+ (% of CD4+CD44+ T cells relative to control)
iLN
SP
CNS
PBS
DPSC-02
DPSC-03
DPSC-05
DPSC
Number of cells
Number of IFNγ+CD4+CD44+ T cells relative to control

Figure 4.19: Th17 cells in EAE mice treated with DPSCs.

EAE mice were treated with three intraperitoneal injections of PBS or 1 x 10^6 DPSCs on days 1, 3 and 5 post-immunisation. When mean peak disease scores were reached in the PBS control group, Th17 cells were quantified in inguinal LNs (iLNs), spleen (SP) and CNS (brain and spinal cord combined). **a)** Representative flow cytometry showing IL-17A-expressing $CD4^+$ T cells (Th17). **b)** Proportion (top) and total number (bottom) of Th1 cells in each organ. For iLN and SP, the PBS group is pooled while DPSC-02 and DPSC-03 and -05 were performed in two independent experiments. Each point represents one mouse and bars represent mean ± SEM of each group (n=4-11 mice). For the CNS, the DPSC data are pooled from all the donors for both experiments (n=10 mice per group). For all data, the means of the PBS group were calculated and set to 100% (for proportion) or 1 cell (for number) and all data points were normalised to these values; proportion (P) was calculated as ($P = \frac{Sample\ \%}{Mean\ of\ PBS\ group}\ x\ 100\%$); number was normalised as ($N = \frac{Number\ in\ sample}{Mean\ number\ in\ PBS}$). *p<0.05, **p<0.01 Kruskal-Wallis test with multiple comparisons (for SP) or Mann-Whitney U test (for CNS).

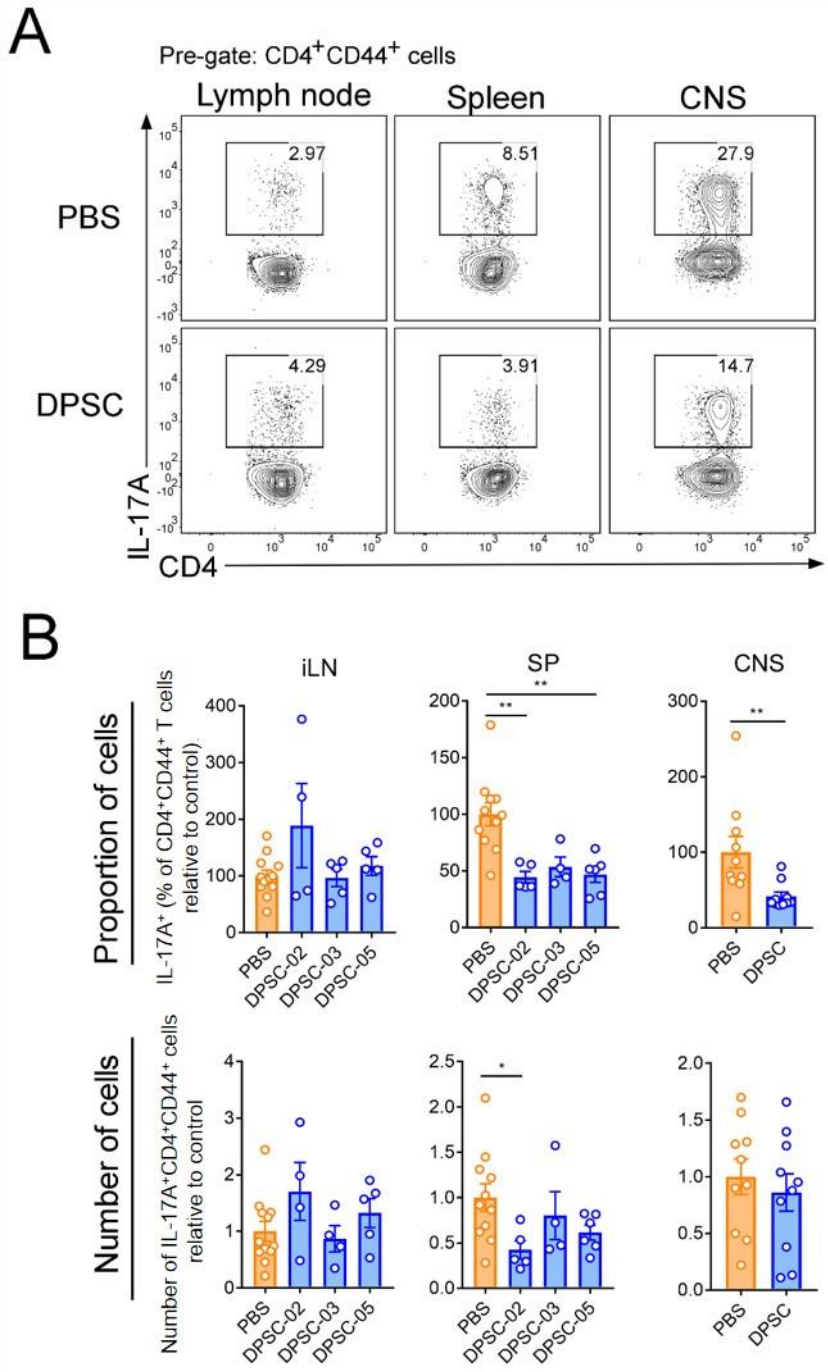
A
Pre-gate: CD4+CD44+ cells
Lymph node
Spleen
CNS
PBS
DPSC
2.97
8.51
27.9
4.29
3.91
14.7
IL-17A
CD4
B
Proportion of cells
IL-17A+ (% of CD4+CD44+ T cells relative to control)
iLN
SP
CNS
PBS
DPSC-02
DPSC-03
DPSC-05
DPSC
Number of cells
Number of IL-17A+CD4+CD44+ cells relative to control

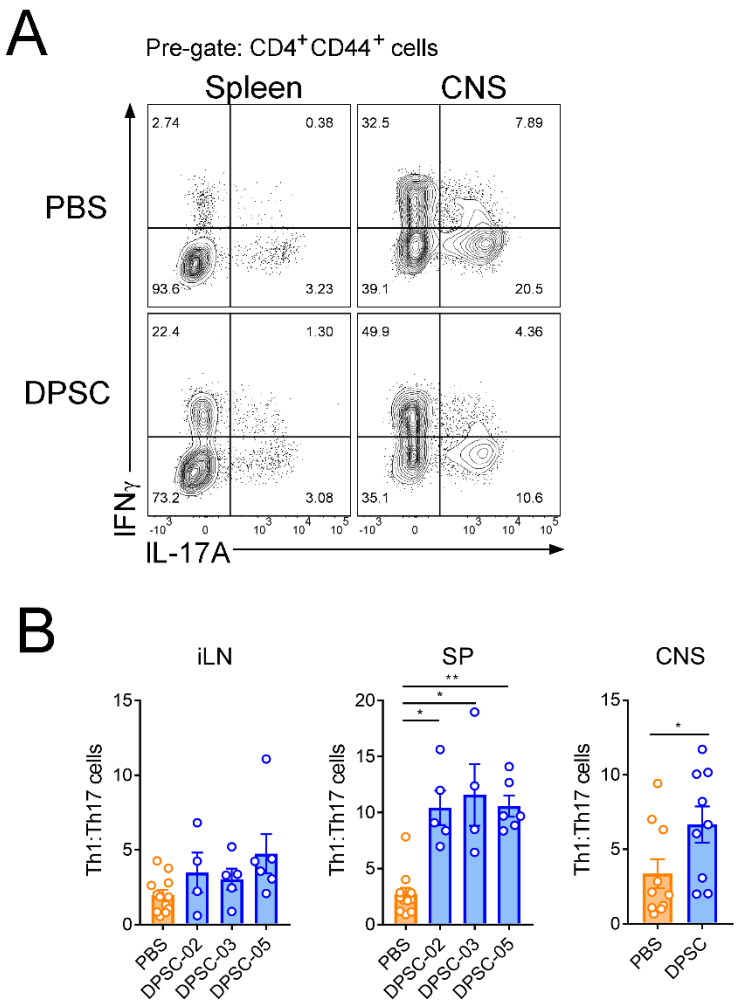

Figure 4.20: Th1:Th17 cells in EAE mice treated with DPSCs.

EAE mice were treated with three intraperitoneal injections of PBS or 1 x 10^6 DPSCs on days 1, 3 and 5 post-immunisation. When mean peak disease scores were reached in PBS control group Th1 and Th17 cells were quantified in inguinal LNs (iLN), spleen (SP) and CNS (brain and spinal cord combined) (Refer to Figures 3.4 and 3.5). The number of Th1 cells was divided by the number of Th17 cells to obtain Th1:Th17. For iLN and SP, the PBS group is pooled while DPSC-02 and DPSC-03 and -05 were performed in two independent experiments. Each point represents one mouse and bars represent mean ± SEM of each group (n=4-11 mice). For the CNS, the DPSC data are pooled from all the donors for both experiments (n=10 mice per group) since insufficient cells were isolated from some of the samples to stain more than one flow cytometry panel. Each point represents one mouse and bars represent mean ± SEM of each group (n=5-6 mice). *p<0.05, **p<0.01 Kruskall-Wallis test for iLN, SP and Mann-Whitney U test for CNS.

This page intentionally left blank.

Figure 4.21: Th-GM cells in EAE mice treated with DPSCs.

EAE mice were treated with three intraperitoneal injections of PBS or 1 x 10^6 DPSCs on days 1, 3 and 5 post-immunisation. When mean peak disease scores were reached in the PBS control group, Th-GM cells were quantified in inguinal LNs (iLNs), spleen (SP) and CNS (brain and spinal cord combined). **a)** Representative flow cytometry showing GM-CSF-expressing $CD4^+$ T cells (Th-GM). **b)** Proportion (top) and total number (bottom) of Th-GM cells in each organ. For iLN and SP, the PBS group is pooled while DPSC-02 and DPSC-03 and -05 were performed in two independent experiments. Each point represents one mouse and bars represent mean ± SEM of each group (n=4-11 mice). For the CNS, the DPSC data are pooled from all the donors for both experiments (n=10 mice per group). For all data, the means of the PBS group were calculated and set to 100% (for proportion) or 1 cell (for number) and all data points were normalised to these values; proportion (P) was calculated as ($P = \frac{Sample\ \%}{Mean\ of\ PBS\ group}\ x\ 100\%$); number was normalised as ($N = \frac{Number\ in\ sample}{Mean\ number\ in\ PBS}$). *p<0.05 Kruskal-Wallis test with multiple comparisons.

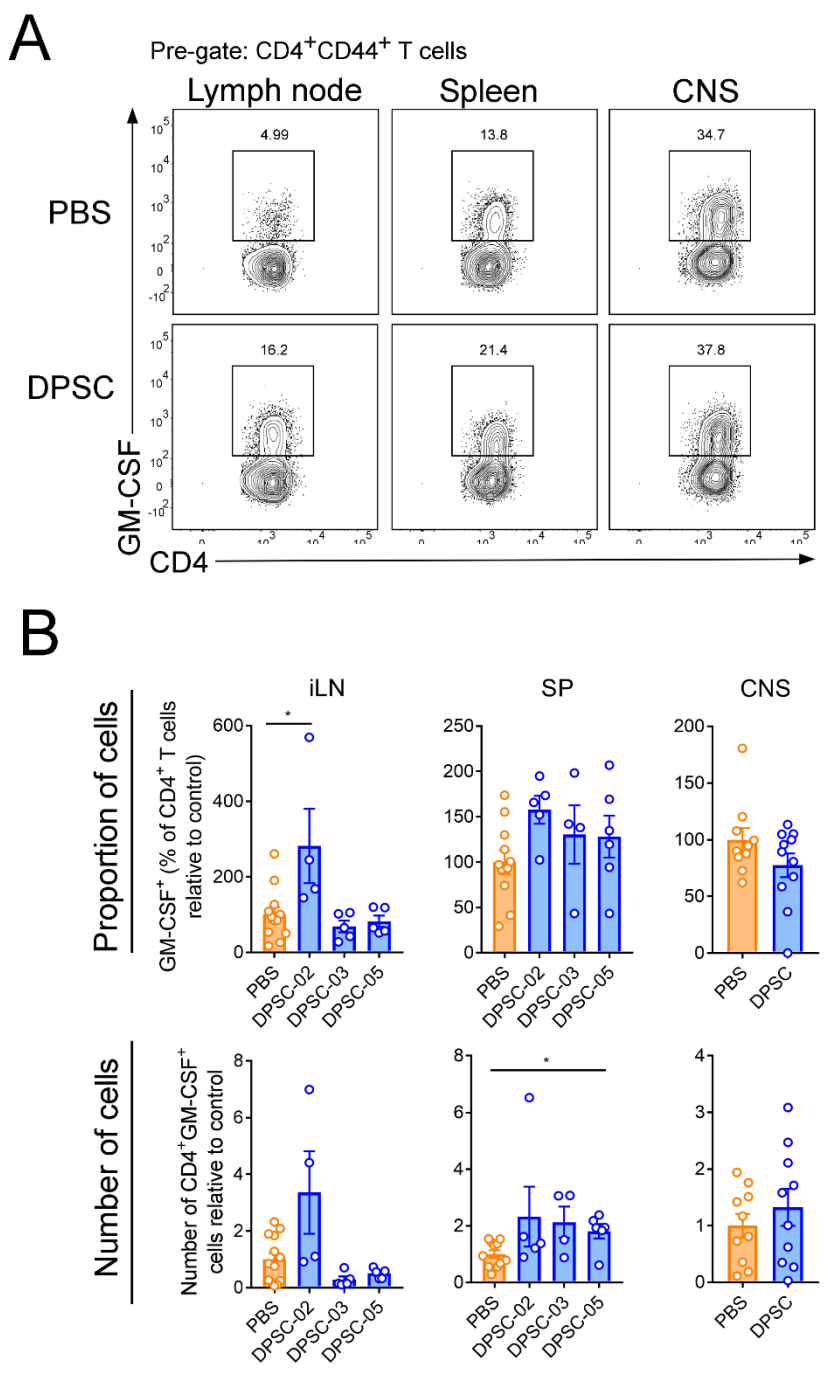
A
Pre-gate: CD4+CD44+ T cells
Lymph node
Spleen
CNS
PBS
DPSC
4.99
13.8
34.7
16.2
21.4
37.8
GM-CSF
CD4
B
Proportion of cells
GM-CSF+ (% of CD4+ T cells relative to control)
iLN
SP
CNS
PBS
DPSC-02
DPSC-03
DPSC-05
DPSC
Number of cells
Number of CD4+GM-CSF+ cells relative to control

Figure 4.22: Th17-GM cells in EAE mice treated with DPSCs.

EAE mice were treated with three intraperitoneal injections of PBS or 1 x 10^6 DPSCs on days 1, 3 and 5 post-immunisation. When mean peak disease scores were reached in the PBS control group, Th17-GM cells were quantified in inguinal LNs (iLNs), spleen (SP) and CNS (brain and spinal cord combined). **a)** Representative flow cytometry showing GM-CSF-expressing Th17 cells (Th17-GM). **b)** Proportion (top) and total number (bottom) of Th17-GM cells in each organ. For iLN and SP, the PBS group is pooled while DPSC-02 and DPSC-03 and -05 were performed in two independent experiments. Each point represents one mouse and bars represent mean ± SEM of each group (n=4-11 mice). For the CNS, the DPSC data are pooled from all the donors for both experiments (n=10 mice per group). For all data, the means of the PBS group were calculated and set to 100% (for proportion) or 1 cell (for number) and all data points were normalised to these values; proportion (P) was calculated as ($P = \frac{Sample\ \%}{Mean\ of\ PBS\ group}\ x\ 100\%$); number was normalised as ($N = \frac{Number\ in\ sample}{Mean\ number\ in\ PBS}$). *p<0.05 Kruskal-Wallis test with multiple comparisons.

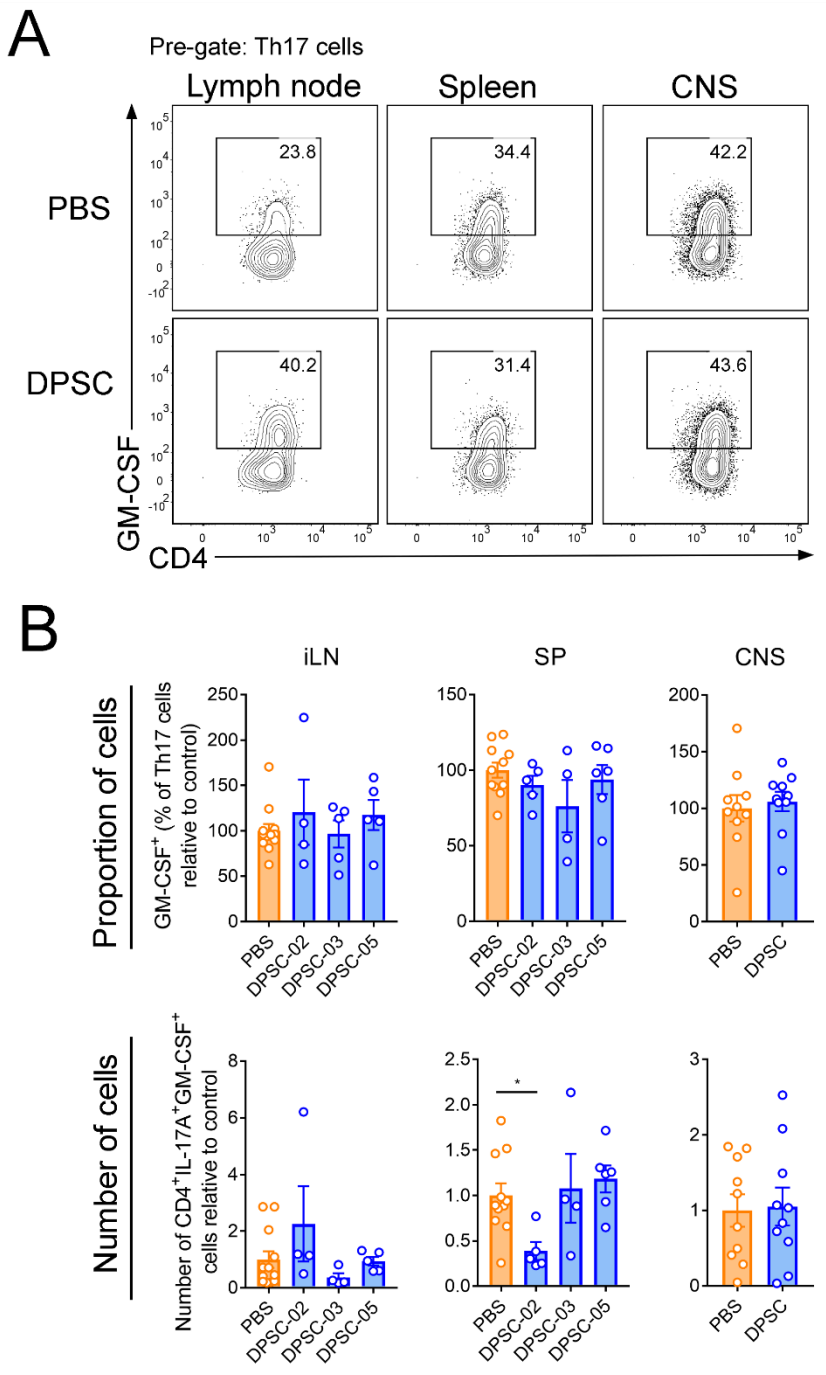
A
Pre-gate: Th17 cells
Lymph node
Spleen
CNS
PBS
DPSC
23.8
34.4
42.2
40.2
31.4
43.6
GM-CSF
CD4
B
iLN
SP
CNS
Proportion of cells
GM-CSF+ (% of Th17 cells relative to control)
Number of cells
Number of CD4+IL-17A+GM-CSF+ cells relative to control
PBS
DPSC-02
DPSC-03
DPSC-05
DPSC
*

Figure 4.23: Regulatory T cells in EAE mice treated with DPSCs.

EAE mice were treated with three intraperitoneal injections of PBS or 1 x 10^6 DPSCs on days 1, 3 and 5 post-immunisation. When mean peak disease scores were reached in the PBS control group, Tregs were quantified in inguinal LNs (iLNs), spleen (SP) and CNS (brain and spinal cord combined). **a)** Representative flow cytometry showing FoxP3-expressing $CD4^+$ T cells (Treg). **b)** Proportion (top) and total number (bottom) of Tregs in each organ. For iLN and SP, the PBS group is pooled while DPSC-02 and DPSC-03 and -05 were performed in two independent experiments. Each point represents one mouse and bars represent mean ± SEM of each group (n=4-11 mice). For the CNS, the DPSC data are pooled from all the donors for both experiments (n=10 mice per group). For all data, the means of the PBS group were calculated and set to 100% (for proportion) or 1 cell (for number) and all data points were normalised to these values; proportion (P) was calculated as ($P = \frac{Sample\ \%}{Mean\ of\ PBS\ group}\ x\ 100\%$); number was normalised as ($N = \frac{Number\ in\ sample}{Mean\ number\ in\ PBS}$). *p<0.05, **p<0.01 Kruskal-Wallis test with multiple comparisons.

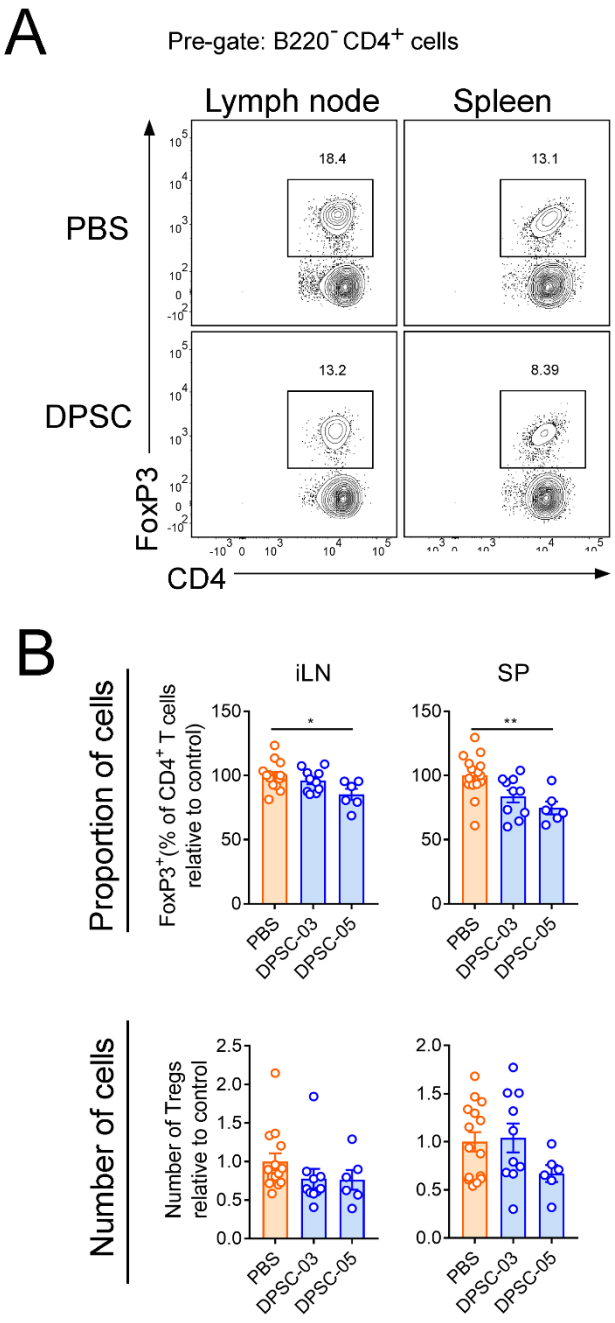
A
Pre-gate: B220⁻ CD4⁺ cells
Lymph node
Spleen
PBS
DPSC
18.4
13.1
13.2
8.39
FoxP3
CD4
B
Proportion of cells
FoxP3⁺(% of CD4⁺ T cells relative to control)
iLN
SP
*
**
PBS
DPSC-03
DPSC-05
Number of cells
Number of Tregs relative to control

Figure 4.24: Tc1 cells in EAE mice treated with DPSCs.

EAE mice were treated with three intraperitoneal injections of PBS or 1 x 10^6 DPSCs on days 1, 3 and 5 post-immunisation. When mean peak disease scores were reached in the PBS control group, Tc1 cells were quantified in inguinal LNs (iLNs), spleen (SP) and CNS (brain and spinal cord combined). **a)** Representative flow cytometry showing IFNγ-expressing $CD8^+$ T cells (Tc1). **b)** Proportion (top) and total number (bottom) of Tc1 cells in each organ. For iLN and SP, the PBS group is pooled while DPSC-02 and DPSC-03 and -05 were performed in two independent experiments. Each point represents one mouse and bars represent mean ± SEM of each group (n=4-11 mice). For the CNS, the DPSC data are pooled from all the donors for both experiments (n=10 mice per group). For all data, the means of the PBS group were calculated and set to 100% (for proportion) or 1 cell (for number) and all data points were normalised to these values; proportion (*P*) was calculated as ($P = \frac{Sample\ \%}{Mean\ of\ PBS\ group}\ x\ 100\%$); number was normalised as ($N = \frac{Number\ in\ sample}{Mean\ number\ in\ PBS}$). *p<0.05, **p<0.01 Kruskal-Wallis test with multiple comparisons.

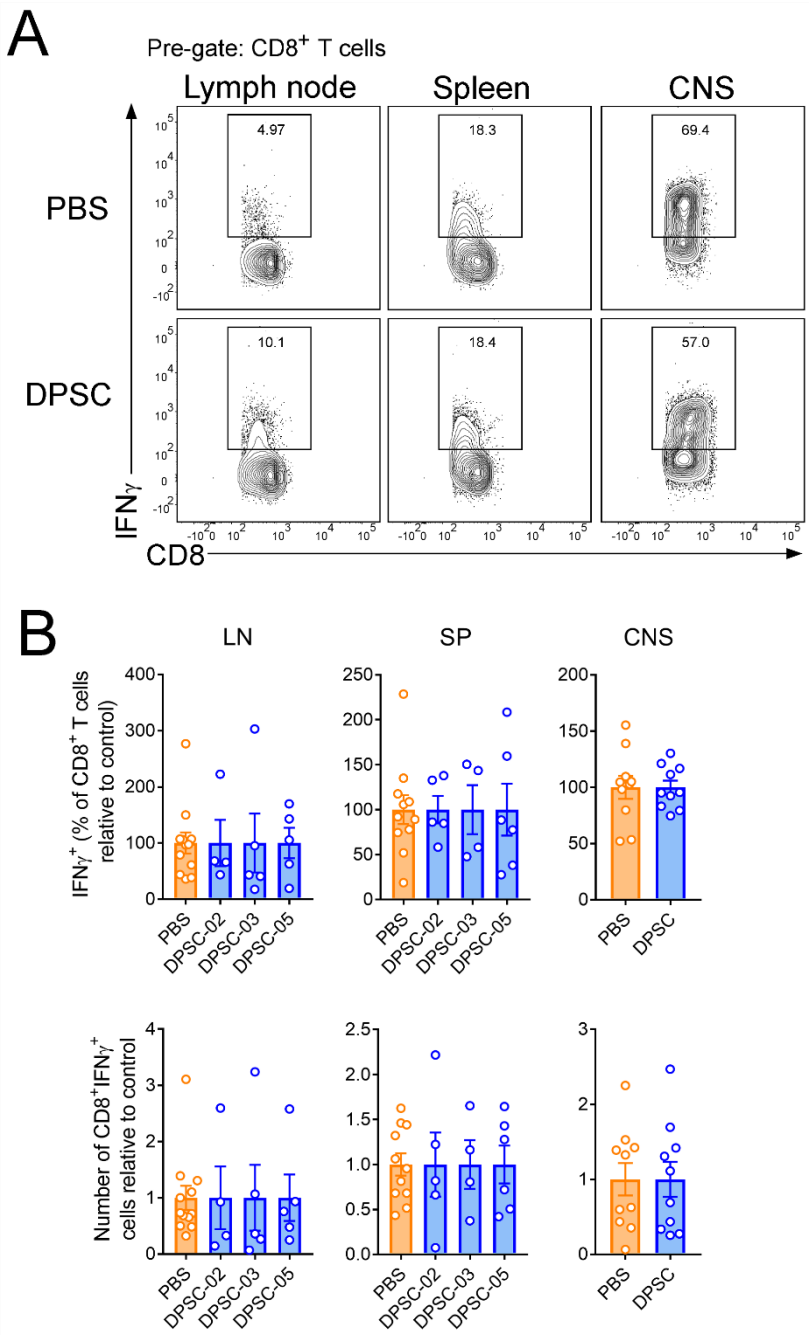
A
Pre-gate: CD8+ T cells
Lymph node
Spleen
CNS
PBS
DPSC
4.97
18.3
69.4
10.1
18.4
57.0
IFNγ
CD8
B
LN
SP
CNS
IFNγ+ (% of CD8+ T cells relative to control)
Number of CD8+IFNγ+ cells relative to control
PBS
DPSC-02
DPSC-03
DPSC-05
DPSC

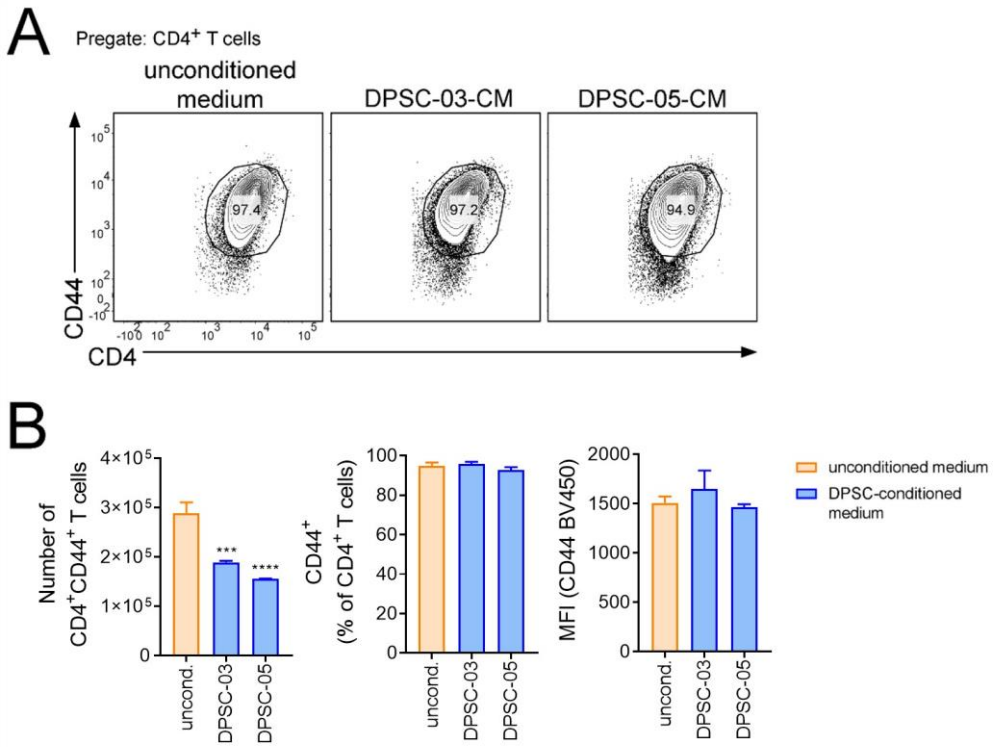

Figure 4.25: Effect of DPSC-conditioned medium on CD4⁺ T cell activation *in vitro*.

Purified naïve CD4⁺ T cells were activated *in vitro* with anti-CD3 and anti-CD28 in the presence of anti-IFNγ and anti-IL-4. Conditioned medium (CM) from DPSCs from donors 03 and 05 was added to the cultures at 1/4 final volume. Unconditioned DPSC medium (uncond.) was included as a control. **a)** Representative flow cytometry and **b)** frequency and number of CD44⁺ (activated) T cells in the cultures after 3 days culture. Columns represent mean ± SEM of each condition of 6 technical replicates pooled from three independent experiments. ***p<0.005, ****p<0.001 One-Way ANOVA with Bonferroni's multiple comparisons test.

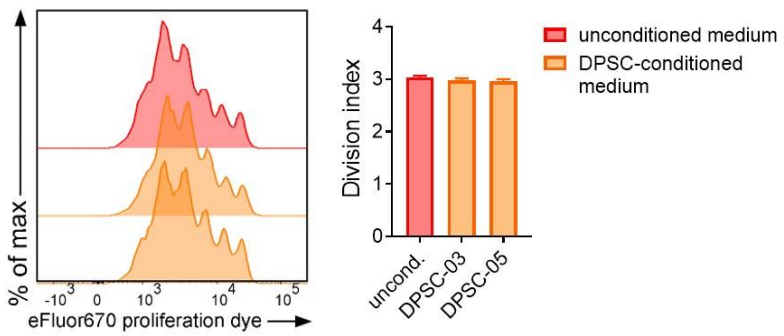

Figure 4.26: Effect of DPSC-conditioned medium on CD4⁺ T cell proliferation *in vitro*.

Purified naïve CD4⁺ T cells were activated *in vitro* with anti-CD3 and anti-CD28 in the presence of IL-2. Conditioned medium (CM) from DPSCs from donors 03 and 05 was added to the cultures at 1/4 final volume. Unconditioned DPSC medium (uncond.) was included as a control. **a)** Representative flow cytometry and **b)** division index of proliferating T cells in the cultures after 3 days culture. Division index is the average number of divisions across all cells in culture including non-dividing cells. Columns represent mean ± SEM of each condition performed in quadruplicate, pooled from two independent experiments.

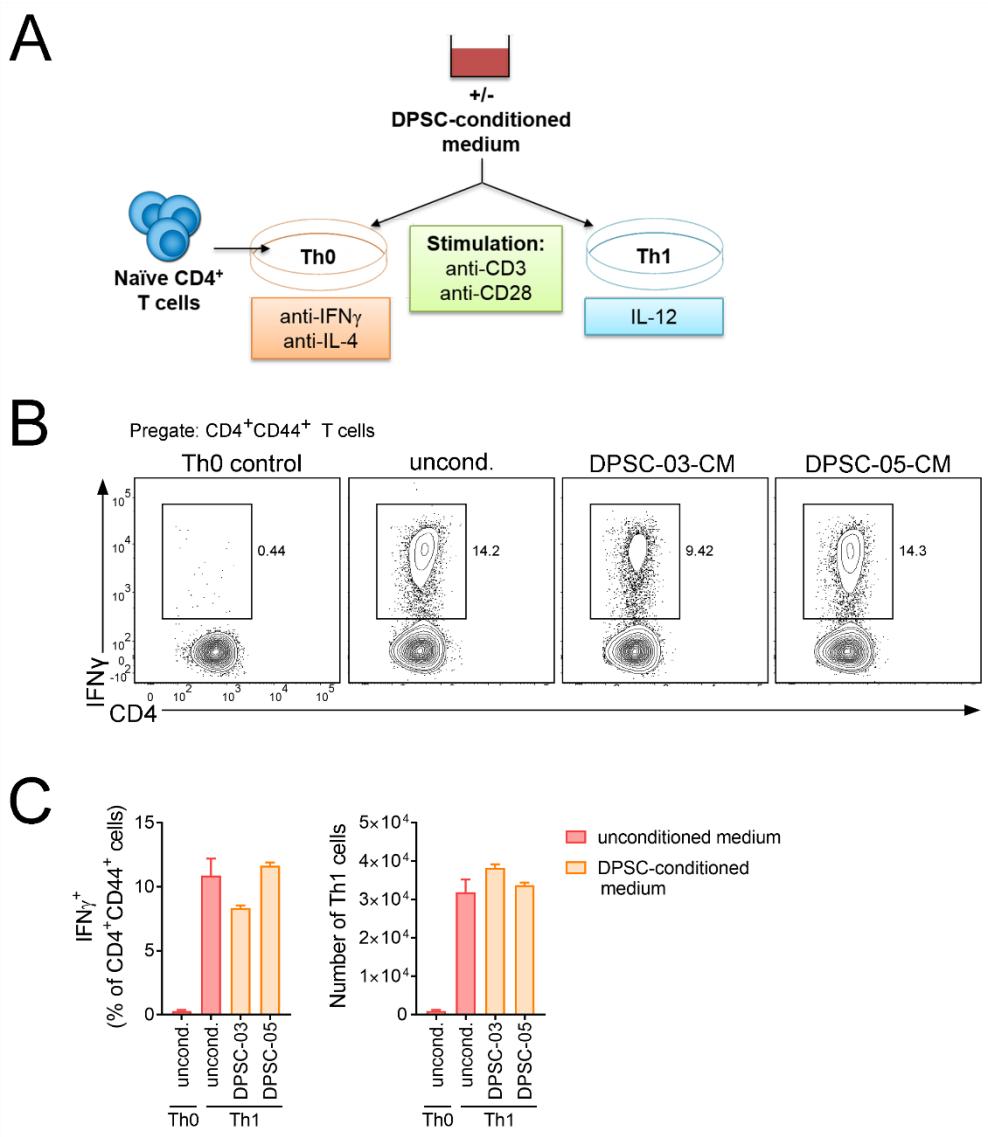

Figure 4.27: Effect of DPSC-conditioned medium on Th1 cell differentiation *in vitro*.

a) Experimental strategy for testing the effect of soluble factors produced by DPSCs on Th1 cell differentiation. Briefly, purified naïve $CD4^+$ T cells were activated *in vitro* with anti-CD3 and anti-CD28 and polarised to Th0 or Th1 cells with neutralising antibodies or cytokines as indicated. Conditioned medium (CM) from DPSCs from donors 03 or 05 was added to the cultures at 1/4 final volume. Unconditioned DPSC medium (uncond.) was included as a control. **b)** Representative flow cytometry showing IFN-γ^+ Th1 cells after gating on $CD4^+CD44^+$ T cells. **c)** Frequency and number of Th1 cells in the cultures after 3 days. Columns represent mean ± SEM of each condition performed in triplicate.

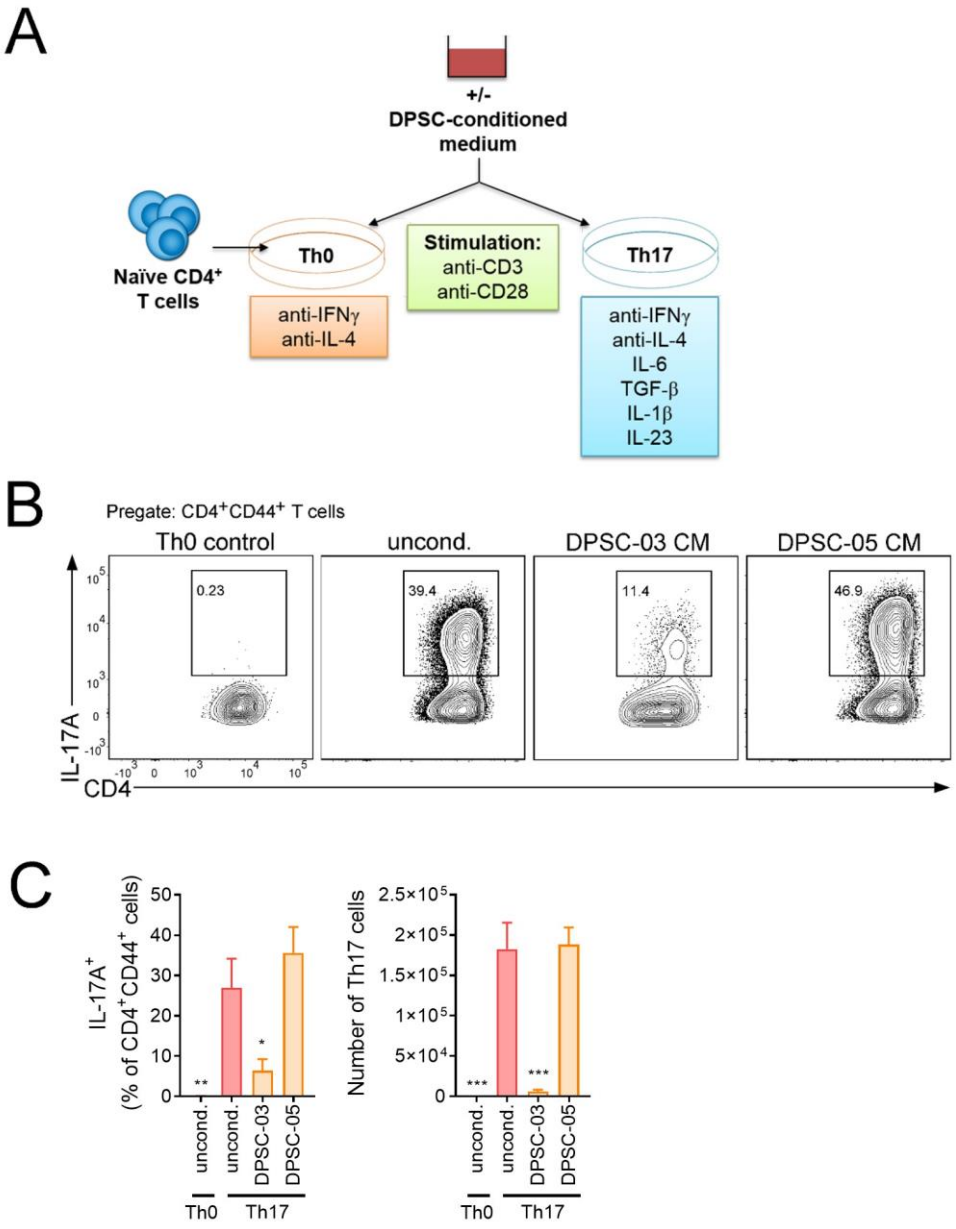

Figure 4.28: Effect of DPSC-conditioned medium on Th17 cell differentiation *in vitro*.

a) Experimental strategy for testing the effect of soluble factors produced by DPSCs on Th17 cell differentiation. Briefly, purified naïve $CD4^+$ T cells were activated *in vitro* with anti-CD3 and anti-CD28 and polarised to Th0 or Th17 cells with neutralising antibodies or cytokines as indicated. Conditioned medium (CM) from DPSCs from donors 03 or 05 was added to the cultures at 1/4 final volume. Unconditioned DPSC medium (uncond.) was included as a control. **b)** Representative flow cytometry showing $IL\text{-}17A^+$ Th17 cells after gating on $CD4^+CD44^+$ T cells. **c)** Frequency and number of Th17 cells in the cultures after 3 days. Columns represent mean ± SEM of each condition performed in quadruplicate pooled from two independent experiments. *p<0.05, **p<0.01, *p<0.005 One-way ANOVA with Bonferroni's multiple comparisons test all compared with Th17-induced unconditioned medium control.

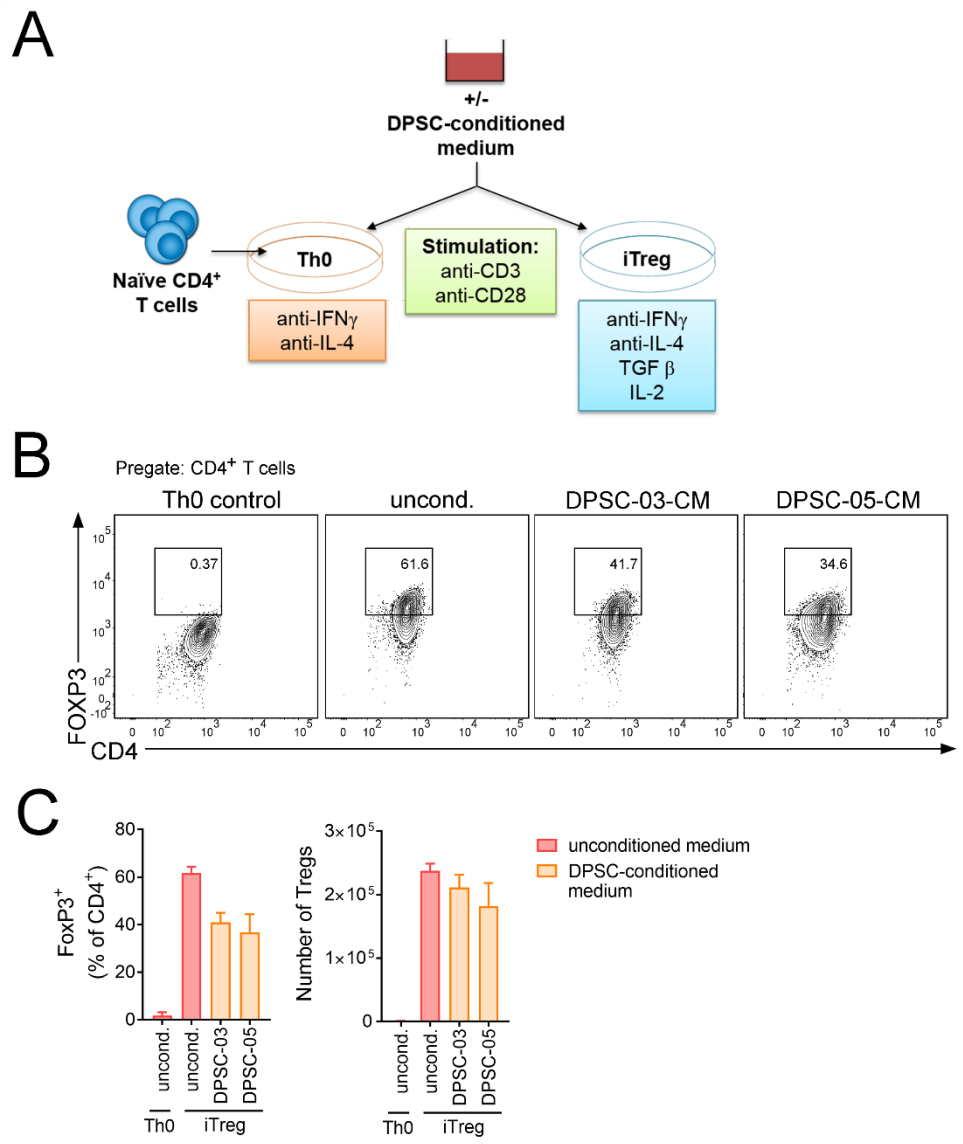

Figure 4.29: Effect of DPSC-conditioned medium on Treg cell differentiation *in vitro*.

a) Experimental strategy for testing the effect of soluble factors produced by DPSCs on Treg cell differentiation. Briefly, purified naïve $CD4^+$ T cells were activated *in vitro* with anti-CD3 and anti-CD28 and polarised to Th0 or Treg cells with neutralising antibodies or cytokines as indicated. Conditioned medium (CM) from DPSCs from donors 03 or 05 was added to the cultures at 1/4 final volume. Unconditioned DPSC medium (uncond.) was included as a control. **b)** Representative flow cytometry showing $FoxP3^+$ Tregs after gating on $CD4^+$ T cells. **c)** Frequency and number of Tregs in the cultures after 3 days. Columns represent mean ± SEM of each condition performed in triplicate. *p<0.05, **p<0.01 One-way ANOVA with Bonferroni's multiple comparisons test all compared with Treg-induced unconditioned medium control.

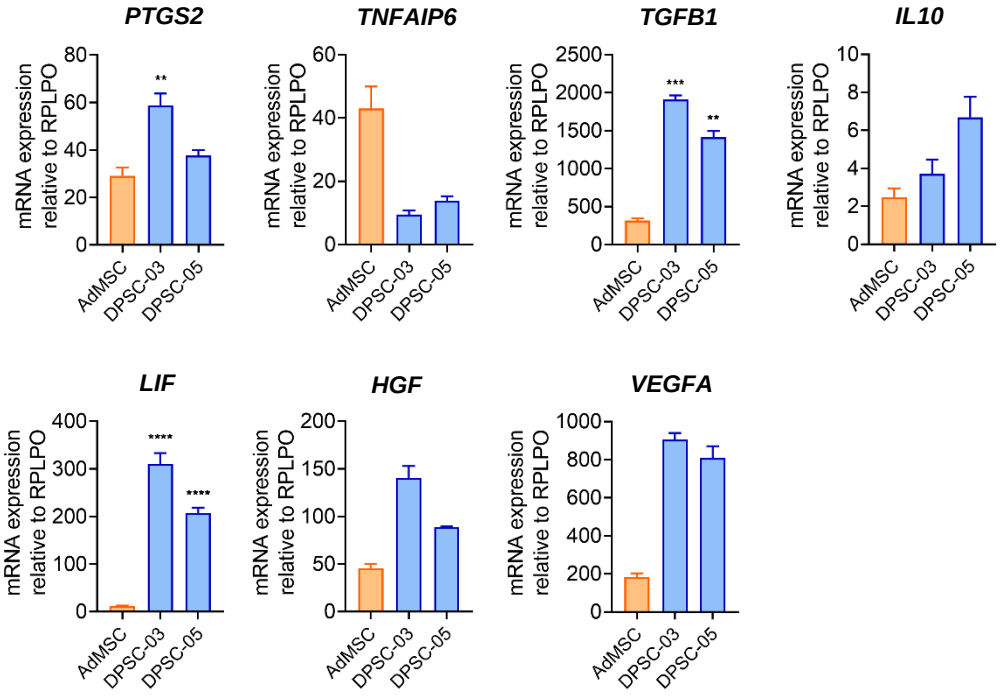

Figure 4.30: DPSCs express immunomodulatory molecules.

RNA was isolated from passage 3 cultured DPSCs from different donors and converted to cDNA before measuring the levels of gene expression of various immunomodulatory molecules by real-time qPCR. The level of mRNA expression for each gene was normalised to the expression of *Rplp0*. Each column represents mean ± SEM of 3 technical replicates for sample. *p<0.05, **p<0.01, ****p<0.001. One-way ANOVA with Bonferroni's multiple comparisons test all compared with Ad-MSC.

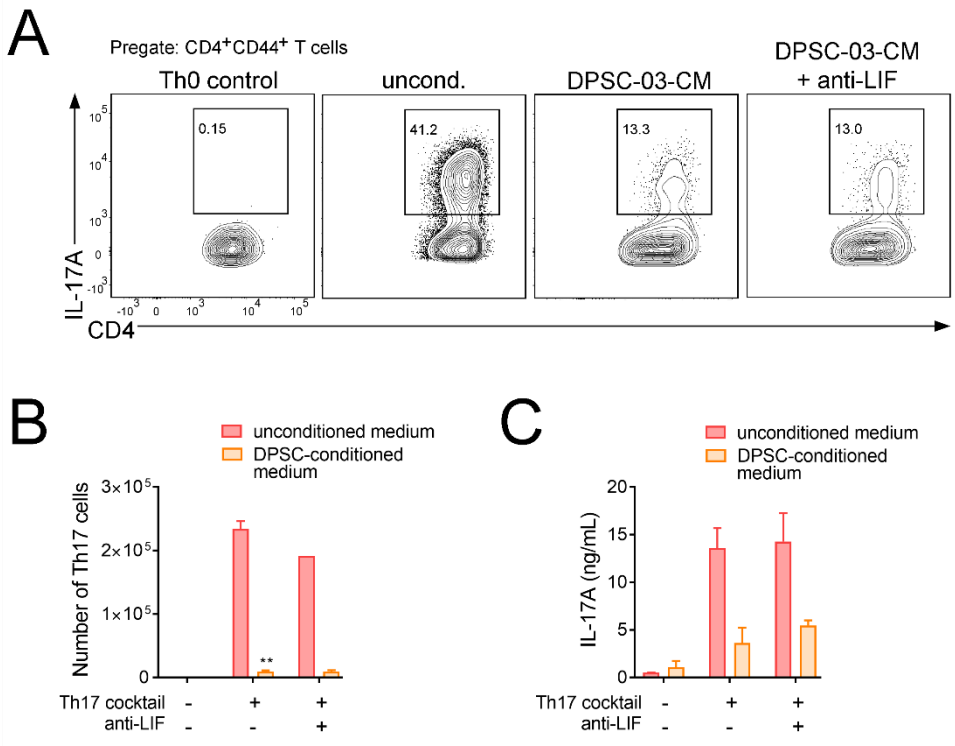

Figure 4.31: Effect of neutralising LIF on suppression of Th17 cell differentiation by DPSC-conditioned medium.

Purified naïve $CD4^+$ T cells were activated *in vitro* with anti-CD3 and anti-CD28 and polarised to Th0 or Th17 cells with neutralising antibodies and cytokines as shown in Figure 4.28:. The T cells were cultured in the presence or absence of conditioned medium (CM) from DPSCs and a LIF-neutralising antibody. **a)** Representative flow cytometry showing the generation of Th17 cells in each culture. **b)** Number of Th17 cells in the cultures after 3 days. **c)** IL-17A in the culture supernatants as measured by ELISA. **b and c)** Columns represent mean ± SEM of each condition performed in triplicate. **p<0.01 unpaired *t*-test.

This page intentionally left blank.

Figure 4.32: DPSC effects on B cell activation *in vitro.*

a) Purified naïve follicular (FO) B cells were activated *in vitro* with LPS in the presence or absence of DPSCs from donors 03 or 05 or DPSC-conditioned medium (CM; 1/4 of final culture volume). **b)** Representative histograms and **c)** mean fluorescence index (MFI) of activation markers and MHC-II measured by flow cytometry after 2 days in culture. ***p<0.005, ****p<0.001 **p<0.01 One-way ANOVA with Bonferroni's multiple comparisons test all compared with stimulated unconditioned medium control.

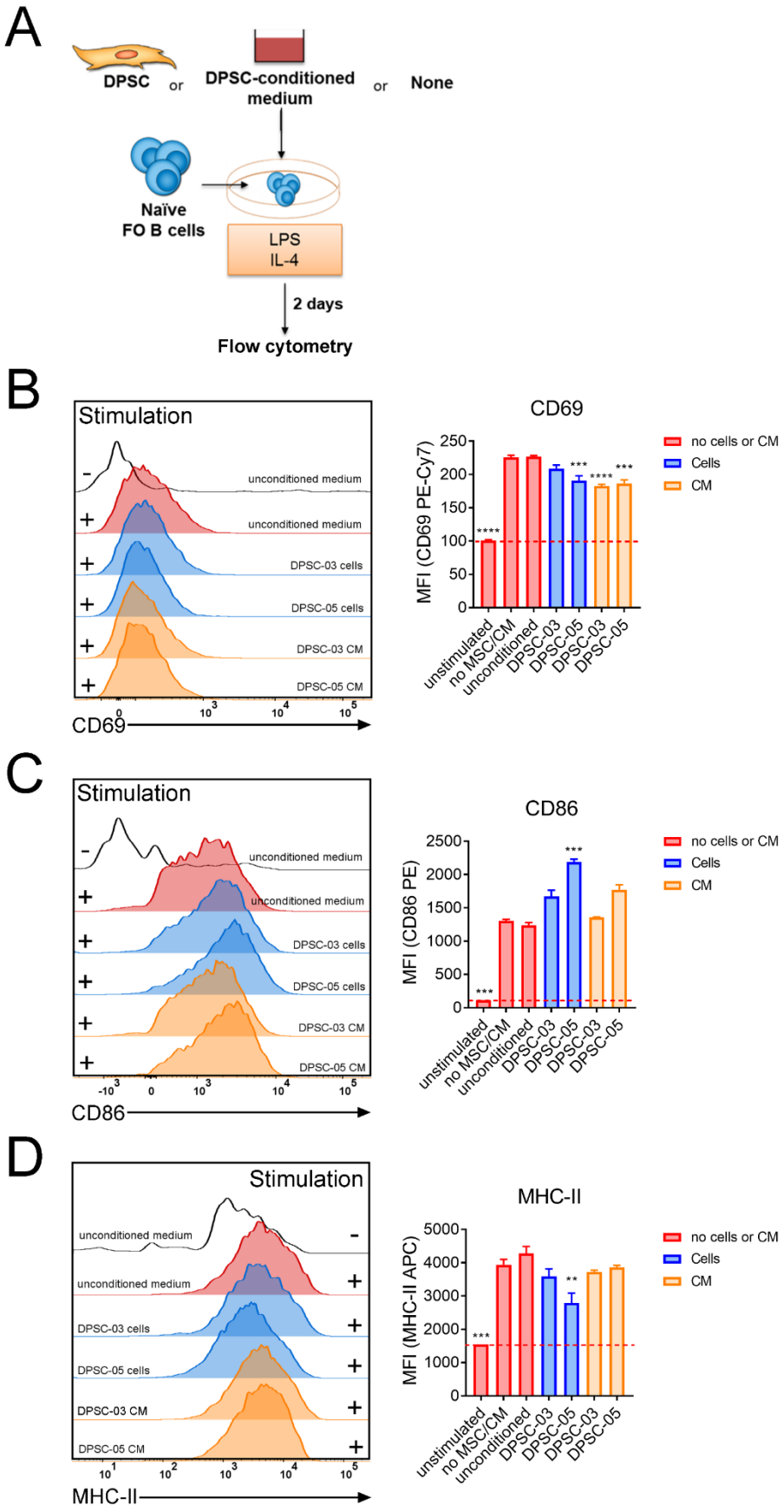
A
DPSC
or
DPSC-conditioned medium
or
None
Naïve FO B cells
LPS
IL-4
2 days
Flow cytometry
B
Stimulation
unconditioned medium
unconditioned medium
DPSC-03 cells
DPSC-05 cells
DPSC-03 CM
DPSC-05 CM
CD69
CD69
MFI (CD69 PE-Cy7)
no cells or CM
Cells
CM
unstimulated
no MSC/CM
unconditioned
DPSC-03
DPSC-05
DPSC-03
DPSC-05
C
Stimulation
CD86
CD86
MFI (CD86 PE)
D
Stimulation
MHC-II
MHC-II
MFI (MHC-II APC)

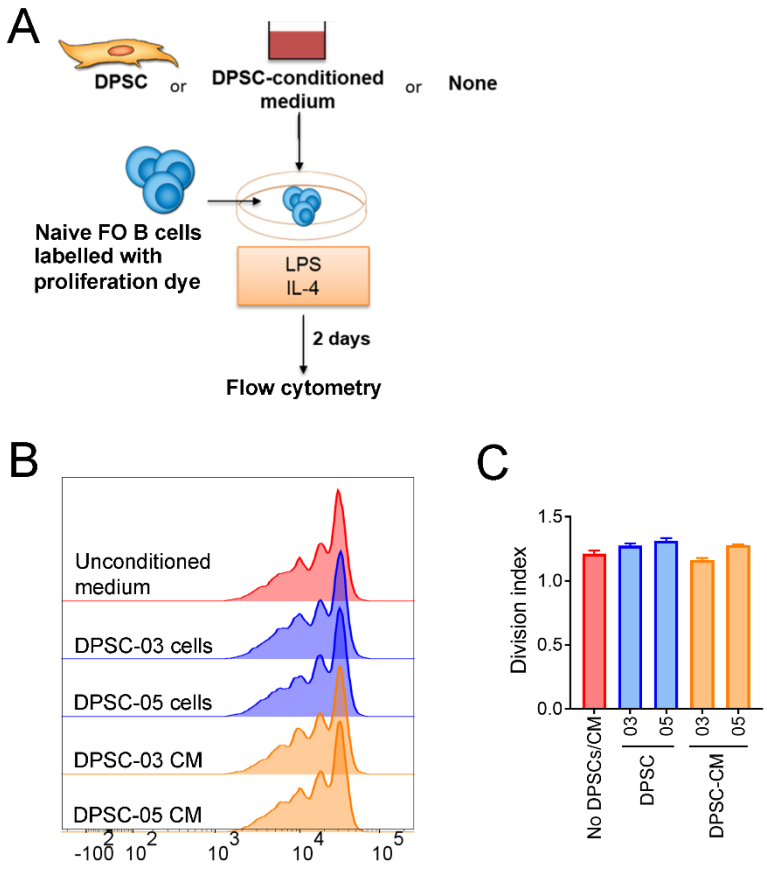

Figure 4.33: DPSC effects on B cell proliferation *in vitro*.

a) Purified naïve follicular (FO) B cells were labelled with eFlour-670 proliferation dye (Biolegend) and activated *in vitro* with LPS in the presence or absence of DPSCs from different human donors or DPSC-conditioned medium (CM; 1/4 of final culture volume). After 2 days, eFlour-670 dilution was measured by flow cytometry. **b)** Representative histograms showing the dilution of eFlour670. **c)** Graph of the division index of the proliferating cells.

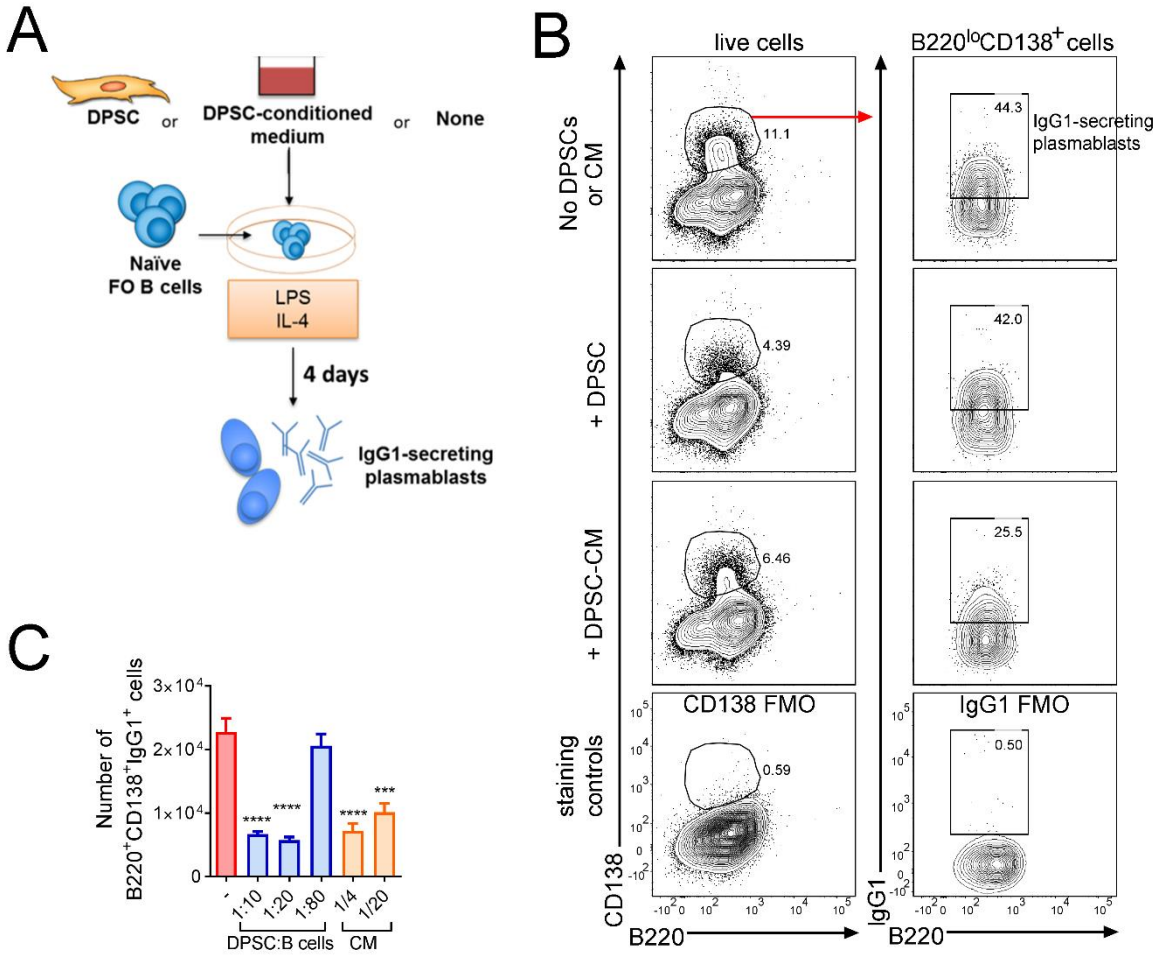

Figure 4.34: DPSC effects on B cell differentiation *in vitro.*

a) Experimental setup for measuring effect of DPSCs on B cell differentiation *in vitro*. Purified naïve follicular (FO) B cells were activated *in vitro* with LPS and IL-4 in the presence or absence of DPSCs or DPSC-conditioned medium (CM; 1/4 of 1/20 of final culture volume) from donor 03. After 4 days, IgG1-secreting plasmablasts ($B220^{lo}CD138^{+}IgG1^{+}$) cells were quantified by flow cytometry. **b)** Representative plots pre-gated on live cells (left) or $B220^{lo}CD138^{hi}$ cells (right) showing effects of DPSC co-culture or DPSC-CM on plasmablast generation. **c)** Graph of **b** showing number of IgG1-secreting plasmablasts at the end of culture. Tests were performed in triplicate and the data are representative of two independent experiments. ***p<0.005, ****p<0.001 unpaired *t* test.

This page intentionally left blank.

Chapter 5: Discussion

This page intentionally left blank.

5.1 Overview

The main aims of this project were to isolate and characterise MSCs from human third molars and to investigate their potential as a cell-based therapeutic in MS in models of EAE. Furthermore, the immunomodulatory effects of DPSCs *in vitro* and *in vivo* were investigated in detail. To summarise the main findings of the study, all of the DPSCs isolated in this study met MSC classification criteria at low passage, although they went on to exhibit signs of aging *in vitro* which corroborates with other studies which were published using DPSCs during the course of this research[350,351]. Importantly, this study revealed that DPSCs have the capacity to inhibit EAE, yet also identified that different donors yield DPSCs which vary in their ability to modulate the disease. Among the main findings were that treatment of EAE with DPSCs consistently caused an increased Th1:Th17 cell ratio and suppressed B cell responses in those mice. This is a significant finding since both Th17 cells and B cells have pathological roles in EAE and are also implicated in pathogenesis of MS. While the molecular mechanisms causing these changes in EAE immunopathology remain to be fully elucidated, the production of soluble factors by DPSCs was identified to modulate both T cells and B cells *in vitro.*

5.2 Suppression of EAE by treatment with DPSCs

DPSCs have been shown to have therapeutic action in animal models of stroke[311], spinal cord injury[352], ocular diseases[353], oral reconstruction[354], and myocardial infarction[355], but this current study is one of very few to address if DPSCs treatment may have beneficial effects in the context of an autoimmune disease. To this end, MOG_{35-55}-induced EAE was used as a model for inflammatory MS to find evidence if DPSCs might be a useful therapeutic tool for suppressing the disease. The data in this study provide evidence that DPSCs suppress immune responses that are relevant to MS. Significantly, DPSCs suppressed the symptoms of chronic EAE or delayed the onset of disease and this was associated with a reduction of some indicators of inflammation in this model. This study also demonstrated that DPSC treatment can suppress re-emergence of symptoms in relapsing EAE, although this was tested only once and requires future more detailed investigation. Thus, in two different rodent models of MS with CNS inflammation, DPSCs showed significant therapeutic benefit.

An important question for the development of MSCs as a potential therapy of MS is to identify the source of MSCs that have the most potent therapeutic effects. Early treatment of EAE with BM-MSCs, Ad-MSCs and UC-MSCs can all delay the onset or suppress the severity of ensuing disease[342,356,357]. Some studies have attempted to directly compare MSCs isolated from two or more different tissues, however strong conclusions are difficult to draw from these studies so far due to using non-age-matched donors[358] or using few or only a single donor for each MSC type[342]. In addition, other factors including variable doses of MSCs, different treatment regimens and routes of administration also make it difficult to compare across studies and conclude

which source of MSCs best suppress EAE. Payne *et al.*,[342] showed that three IV injections of 1 x 10^6 BM-MSCs or UC-MSCs beginning 3 days before onset of symptoms significantly delayed disease by 3.3-3.4 days, while Ad-MSCs used in this manner reduced the mean maximum clinical disease score by 20-25%. In that study, none of the MSCs were able to suppress disease when treatment was administered only after the onset of symptoms. Constantin *et al.*,[359] instead used 2 IV injections of 0.5 x 10^6 Ad-MSCs prior to symptom onset which both delayed disease and reduced the maximum score. A single IV dose of 1 x 10^6 BM-MSCs 3 days post-immunisation was also effective at delaying onset of EAE in a study by Guo *et al.*,[356]. The maximum disease score was additionally suppressed in that study and an even greater suppression was achieved when treatment occurred on the day of symptom onset, although the severity of EAE was less compared with both the current study and the other studies discussed here. Thus, although some DPSCs tested in this study were able to prevent development of full hind limb paralysis in EAE mice, which is a similar therapeutic efficacy as other types of MSCs, a robust comparison is required which ideally compares DPSCs with MSCs from other tissue sources that are isolated from the same donor. Also, one of the significant potential advantages of using DPSCs instead of other types of MSCs is that originating from the neural crest may cause them to be more amenable to regenerating the CNS. Although DPSCs were not found to enter the CNS in the current study, engraftment and potential cell replacement mechanisms of EAE suppression warrant future investigation in a more appropriate setting such as isolating and using allogeneic rodent DPSCs to avoid immune rejection.

During the course of this investigation, three studies from other investigators which explored the use of two other types of dental-derived MSCs in EAE; PDLSCs and SHEDs. SHEDs, like DPSCs, are derived from human dental pulp, except that instead of adult third molars, the source of SHEDs are infant molars naturally shed during early childhood. Rossato *et al*.[360] found that although SHED-treatment did not delay onset of EAE, the progression of symptoms was slower than in control mice. Since their experiment ended while the progression of disease was still increasing in SHED-treated mice, it is not known whether SHED-treated mice would have eventually become as ill as control mice if the experiment were continued longer. This, together with differences in the number and timing of treatments in their study compared with the present study, make it difficult to compare the efficacy of SHEDs versus DPSCs in suppressing EAE. A preceding study by Shimojima *et al.*,[361] showed that a single intravenous dose of SHED-CM alone delivered at peak disease was effective in reducing the severity of EAE compared with DMEM, and suppression of EAE symptoms was associated with a reduction in demyelination and leukocyte infiltration of the CNS. In light of this and the findings in this study that DPSC-CM has potent immunomodulatory properties *in vitro*, it would be interesting to test if DPSC-CM delivered to EAE mice also suppresses disease in future.

The second type of dental-derived MSC which was published in the context of EAE during the course of the present study was PDLSCs, which are MSCs isolated from the periodontal ligament of the tooth instead of the pulp. Trubiani *et al.* treated MOG_{35-55}-induced EAE mice with a single intravenous injection of 1 x 10^6 PDLSCs at the onset of disease symptoms and this suppressed the severity of disease compared with controls which did

not receive an injection. Like SHEDs, suppression of EAE was associated with reduced demyelination and leukocyte infiltration of the CNS. The treatment strategy is, again, different from the one employed in this current study which hinders direct comparison of efficacy. Furthermore, although PDLSCs were isolated from five separate donors, the mice in Trubiani *et al.*'s PDLSC-treated EAE group each received randomly allocated PDLSCs from those different donors. Thus, it is not clear if all PDLSCs were suppressive or if variation was observed between donors as was noted in this study with DPSCs.

While the protracted nature of this study in terms of obtaining human dental samples over a period of 3 years caused significant technical challenges, a major strength of the current study is that DPSCs from multiple different donors were tested for their effects as a therapeutic agent in EAE. The outcome of testing DPSCs from many donors was that variability in their efficacy for inhibiting EAE was identified. DPSCs from 4 of the 7 different donors that were tested in this study significantly suppressed the course of MOG_{35-55}-induced EAE by delaying the onset of symptoms or reducing the severity of disease. However, even the DPSCs that were most potent at inhibition of EAE in prophylactic settings in this study did not reverse disease when delivered after the onset of symptoms. However, future experimentation should also test if direct delivery of DPSCs to the CNS via intracerebral injection is more effective in suppressing disease, particularly after the onset of symptoms when inflammation is established in the CNS. Intracerebral injection of DPSCs may increase their efficacy through local delivery of DPSC-derived neurotrophic factors and may also facilitate DPSC engraftment and cell replacement which do not appear to be achieved through IP delivery of the cells.

Currently, one proposed benefit of using MSCs instead of other types of stem cells such as ES cells is the potential for autologous cell transfer. However, an important factor to consider is whether DPSCs from different individuals are equally effective in their therapeutic capacity. Comparing DPSCs from different donors was a challenge in this study because not all of the samples were available at once. Indeed, almost 3 years passed between obtaining the first and last samples. This comparison revealed that even among healthy individuals in a relatively small age-bracket, there were major differences in the therapeutic efficacy of the DPSCs that were obtained. The heterogeneity in efficacy that was observed in this present study among healthy individuals firstly highlights an important requirement for testing the efficacy of each patient's DPSCs before use, and secondly suggests that there is room to improve the therapeutic quality of DPSCs from some individuals. Future studies could compare the transcriptome of DPSCs that suppress EAE with DPSCs that are not suppressive by RNA sequencing (RNAseq) to identify factors that are required for DPSCs to inhibit EAE, which could be used to develop a highly potent cellular therapy or to design novel therapies that do not require cell transplantation. Further experiments with DPSCs from additional donors in the SJL/J relapsing model of EAE would also be beneficial to establish whether the suppressive capacity of DPSCs displays a similar heterogeneity amongst donors for relapsing EAE as was observed for the C57Bl/6 chronic EAE model in the present.

DPSCs have also been proposed to be a more suitable source of MSCs for treatment of CNS injury or disease because they are derived from the neural crest. DPSCs were not found to enter the CNS in the present study and also appeared not to persist a day after injection into EAE mice, thus cell replacement mechanisms of EAE inhibition were not explored. Although the main focus of this study was on the immunosuppressive properties of DPSCs, it is important for future studies to also test their potential effects on CNS repair. Other investigators have shown that DPSCs can differentiate into functional neurons *in vitro*[305,306,309,310] and this would need to be tested for the DPSCs in the current study before exploring possible engraftment and cell replacement effects of DPSCs in EAE. In addition to the growth factors *VEGFA* and *LIF* which were detected in the current study, Koblar *et al.,*[362] showed that DPSCs also express *BDNF, GDNF, NGF* and *ANGPT1*, suggesting that provision of neurotrophic support may be another remedial action of DPSCs in EAE. The cuprizone model of chemically-induced demyelination may be a more suitable model for this, since autoimmune T cell responses are not required for demyelination in that model[363].

One potential hurdle for DPSCs as a clinical tool that also presented a significant limitation in this study was that prolonged culture *in vitro* appeared to negatively affect the morphology of DPSCs, the degree of differentiation of the cells to adipocyte and osteocyte lineages and their therapeutic capacity in EAE. The use of DPSCs was therefore limited in this study because passage number was kept as low as possible for all of the *in vivo* experiments. The effects of aging *in vitro* are important to consider in the development of MSC therapies since all MSCs currently require significant expansion to generate large enough numbers of cells for therapeutic doses. Additional considerations would also need to be made for aging patients for whom DPSC yield could be negatively affected by mass of dental pulp decreasing with age[364] and increased senescent cells among their DPSC populations, and these factors may contribute to earlier senescence *in vitro*. Clinical trials for MSCs in MS have thus far employed doses of $>10^8$ total MSCs for treatment[280,282,322]. It is possible to expand DPSCs to these numbers which would require an estimated minimum of 4-5 passages *in vitro*. This falls within the limits of passaging that maintain DPSCs that are capable of suppressing EAE, which was <P7 or P8 for DPSC-02 and DPSC-03 cells used in this study. Thus, expanding sufficient DPSCs for use in humans is feasible.

The effects of aging *in vitro* are not limited to DPSCs, and Chrisostomo *et al.,*[365] found that the ability of mBM-MSCs to improve recovery of myocardial ischemia/reperfusion in rats was lost with increased passaging *in vitro*. Salkin *et al.,*[366] transduced DPSCs to express TGF-β1 which increased their proliferation and delayed senescence *in vitro*. Although the effect of modifying DPSCs to delay senescence on their therapeutic efficacy is also yet to be tested, this may facilitate more extensive expansion of DPSCs *in vitro* for transplantation.

5.3 Effects of DPSCs on the immune system

Treatment of EAE with DPSCs that inhibited the course of disease led to modified immune responses both in the CNS and the SLOs. Again, variability was discovered between DPSCs from different donors in terms of their effects on cells of the immune system both *in vitro* and *in vivo*. $CD8^+$ T cells, Th1 cells, Th17 cells, B cells, microglia and infiltrating myeloid cells in the CNS were all found to be significantly affected by treatment with DPSCs from at least one donor, although the effects on each of these cell types was not equal among DPSCs from different individuals. In addition to the research on MSCs as cellular therapies, there is increasing interest in MSC-derived products such as CM or purified extracellular vesicles[367]. This study highlights that in addition to variability amongst responses of EAE mice to whole DPSCs, not all DPSC-derived soluble products are equal across individuals either. In this section the effect of DPSCs on various cells of the immune system in the context of EAE will be discussed.

5.3.1 $CD4^+$ T cell responses

$CD4^+$ T cell polarisation is a critical feature of the autoimmune response in EAE and the production of Th17 cells and T cells that produce GM-CSF is strongly correlated with disease severity[33,34,368]. In contrast, production of Tregs in EAE is associated with less severe pathology[369]. A consistent feature of DPSC treatment of EAE mice was that it led to an increased Th1:Th17 cell ratio both in the spleen and CNS, without appearing to impact on Tregs. The inverse situation of tipping the ratio of Th1:Th17 cells in favour of Th17 cells has been shown to increase the severity of EAE[173]. Additionally, Stromnes *et al.,*[29] showed that the ratio of Th1:Th17 cells also affects the migration of Th17 cells into the CNS. At a range of Th1:Th17 cell ratios in EAE, Th17 cells infiltrated the spinal cord, whereas only low Th1:Th17 cell ratio facilitated the entry of Th17 cells into the brain parenchyma. In that study, low Th1 to Th17 cell ratio was also associated with more severe EAE. Thus, increasing the ratio of Th1:Th17 cells may contribute to DPSC suppression of EAE, which is the first time this effect has been noted for any MSC type. IFNγ and IL-17A double-producing $CD4^+$ T cells were not independently investigated in the current study and would fall into both Th1 and Th17 cell populations in the data which have been presented. In future, $IFN\gamma^+IL\text{-}17A^+$ cells could be separated from bulk Th1 and Th17 and also be compared between DPSC-treated mice and controls. The mechanisms of how DPSCs may influence Th1 and Th17 frequencies in EAE will next be considered.

Here in the present study DPSCs appear to have a Th1-promoting effect *in vivo*, whereas some studies have found MSCs to suppress Th1 cell responses. Luz-Crawford *et al.,*[370] and Ohshima *et al.,*[370] showed that mBM-MSCs and fetal membrane-derived MSCs suppress both Th1 and Th17 cell differentiation *in vitro* and mBM-MSCs were additionally shown by Luz-Crawford *et al.,* to reduce the percent of Th1 and Th17 cells in the LNs of EAE mice which was associated with suppressed disease scores. Percent of Th1 and Th17 cells in the LNs of mice were also suppressed by gingiva-derived MSCs in collagen-induced arthritis[371]. Despite these findings, but like in the present study, Goodwin *et al.,*[372] found that MSCs can promote Th1 responses *in vivo*. They showed increased Th1 in allergic airways inflammation after treatment with mBM-MSCs which led to

increased IFNγ production and balanced the Th2 response which was sufficient to ameliorate disease. In another study, Th1 cells were also increased by the addition of cord blood-derived MSCs to alloantigen-stimulated PBMCs, and these Th1 cells co-expressed the regulatory cytokine IL-10[373]. Although many of these reports have observed that MSCs can increase Th1 cell responses, the ratio of Th1:Th17 cells has not been looked at in other studies of MSCs, and the increased Th1:Th17 cell ratio seen here using DPSCs merits further investigation as another potential mechanism of MSC immunomodulation.

One possibility is that DPSCs produce a secreted factor that either promotes Th1 cell development or impairs Th17 cells. However, DPSC-CM did not affect Th1 differentiation *in vitro*, which may indicate that the increase in Th1 cells that was observed in the spleens of EAE mice is due to direct contact signalling or via indirect mechanisms such as via APCs. Production of a soluble factor was sufficient, however, for potent suppression of Th17 cell differentiation *in vitro* by DPSCs, although this was only seen from one of the donors tested. As the *in vivo* alteration in the Th1:Th17 ratio was a consistent feature across all donors tested, together these findings indicate that the DPSC-mediated influence on Th1 and Th17 cells generally involves additional contact-mediated factors or interactions that occur in the *in vivo* microenvironment. The nature of any putative contact-dependent mechanisms used by DPSCs to affect T cell activation, proliferation and differentiation remains an open question. Co-culture experiments that may have addressed this involving both DPSCs and T cells proved to be challenging as plate-bound anti-CD3 would be blocked by the adherent DPSCs. Unfortunately, stimulation of naïve $CD4^+$ T cells with soluble instead of plate-bound anti-CD3 did not lead to robust Th1 or Th17 generation in this study (data not shown) and therefore direct co-cultures with DPSCs to interrogate the effect of cell-contact mechanisms of communication between these cells was not able to be tested, but should be tested in future studies using alternative T cell activation platforms.

The identity of the soluble factor(s) that some DPSCs produce to suppress Th17 cell production is also an interesting open question. Previously, PGE2 and IL-10 have been shown to be soluble mediators of MSCs modulating Th17 cell responses. Qu *et al.*,[374] used RNA interference to demonstrate that hBM-MSCs suppress Th17 cell differentiation using IL-10. Two other studies have implicated PGE_2, a product of COX2, in effects of MSCs on Th17 cell differentiation *in vitro* although its role in MSC effects on Th17 cells is somewhat controversial. Duffy *et al.*,[262] found that mBM-MSC production of PGE_2 inhibited Th17 cell differentiation from mouse naïve $CD4^+$ T cells whereas Rozenberg *et al.*,[255] found a pro-Th17 differentiating role using human PBMCs for hBM-MSC-derived PGE_2. Variation between human and murine MSCs and T cells may contribute to these discrepancies here. While LIF is an antagonist of Th17 cell differentiation and was expressed by DPSCs tested in this study, neutralisation of LIF did not affect the ability of DPSCs to suppress Th17 cell differentiation. While this may appear to rule out LIF as the secreted factor produced by these DPSCs that inhibits Th17 cells, a positive control for the neutralising activity of the anti-LIF antibody was not available. Therefore, although a neutralising concentration of antibody to block LIF activity[375,376], it is still possible that this was insufficient to entirely suppress LIF activity in this assay. Therefore, although it cannot be completely ruled out that DPSC-derived LIF plays some role in suppressing Th17 cells in the context of EAE, it appears

that other secreted factors must also be involved. The investigation of other factors is clearly warranted but was not able to be performed in depth in the present study due to time constraints.

5.3.2 $CD8^+$ T cells

Although $CD8^+$ T cells are not required for EAE pathogenesis in the C57Bl/6 model of EAE[39], they are thought to be important in MS and do expand and infiltrate the CNS in EAE. The finding in the present study that $CD8^+$ T cells were reduced in the CNS of EAE mice treated with DPSCs concurs with two recently published studies using other types of dental-derived MSCs. Rossato *et al.,*[360] found that SHED-treatment of EAE reduced total $CD8^+$ T cells as well as the number of $CD8^+$ T cells that expressed IFNγ or IL-4 in the CNS. By contrast, the number of IFNγ-expressing $CD8^+$ T cells in the present study were unchanged by DPSC treatment, suggesting DPSCs may function differently to SHEDs in their effects on $CD8^+$ T cell cytokine production. $CD8^+$ T cells were also found to be reduced in the CNS by Trubiani *et al.* following PD-LSC treatment. Although these two studies did not quantify $CD8^+$ T cells in the SLOs, the fact that the number of $CD8^+$ T cells was reduced in the spleen in the present study suggests that DPSCs may suppress $CD8^+$ T cell proliferation or induce their apoptosis. $CD8^+$ T cells may have pro-inflammatory functions in MS due to the increased risk associated with carrying the MHC Class I *HLA-A*0301* allele[100], they are clonally expanded in MS patients[99] and can be pathogenic in EAE[40], in which case suppressing their proliferation or inducing their apoptosis may be beneficial in reducing the pathology of MS, although this is controversial[46]. On the other hand, these studies contrast with the findings of Glenn *et al.,*[377] in which mBM-MSCs increased infiltration of the CNS with $CD8^+$ T cells and exacerbated EAE induced with MOG_{37-50} which is an MHC-I-targeted peptide. Whether this difference is due to the nature of DPSCs versus BM-MSCs or if DPSCs might also promote $CD8^+$ T cell responses in the CNS under different conditions should be tested in future studies.

5.3.3 B cells

In contrast to the findings with $CD8^+$ T cells, B cells may actually proliferate more in EAE mice after DPSC treatment as they were found to be increased in frequency in the spleen of DPSC-treated mice, although decreased in the CNS. This suggests that DPSCs either alter the migration of B cell recruitment to the CNS or induce a change in kinetics of B cell proliferation/apoptosis and/or egress from the spleen. Notably, DPSCs did not affect B cell proliferation *in vitro*. A report from Tabera *et al.,*[272] showed that hBM-MSCs suppressed B cell proliferation under a strong stimulatory condition using phorbol ester (12-o-tetradodecanoyl-phorbol-13-acetate; TPA) but when CpG-C and anti-Ig were used to activate the B cells instead, which is a weaker stimulus, hBM-MSCs promoted B cell proliferation. Differences in the B cell stimulus and the use of DPSCs and murine B cells in the present study versus hBM-MSCs and human B cells by Tabera *et al.,* could help to explain this difference.

The present study also revealed complexity and donor-to-donor heterogeneity in respect to the effects on B cell activation that resulted from either co-culture or exposure to CM *in vitro*. One donor's DPSCs apparently produced a secreted factor that suppressed up-regulation of CD69 on B cells but did not affect CD86 expression. Surprisingly however, co-culture of these same DPSCs did not have the same effect. One possible explanation for this is that these cells may indeed produce an inhibitory secreted factor but that in the context of a co-culture it is not produced in sufficient quantities at the appropriate time to inhibit CD69 expression. By contrast, DPSCs from another donor suppressed up-regulation of CD69 regardless of whether this was tested in co-culture or using CM. This clearly further indicates that there is heterogeneity in terms of immunomodulatory gene expression by DPSCs from different donors that results in profoundly distinct effects on B cells.

The ability of DPSCs to modulate B cells is potentially significant for MS since some of the most successful treatments for MS to date target B cells, including the anti-CD20 monoclonal antibodies Rituximab and Ocrelizumab. EAE induced by immunisation with full-length MOG protein is dependent on B cells processing and presenting MOG antigen to T cells, although they are not required for this function in EAE induced by immunisation with MOG peptides and thus the full effect of suppressing B cells may be underappreciated in the MOG_{35-55} model used in the current study. Testing DPSC treatment of full-length MOG-induced EAE may reveal further contributions of DPSCs to suppression of the disease through B cells.

5.3.4 Other cell types

Myeloid cells including microglia, monocytes and macrophages play an important role in EAE and are abundant in MS lesions[61,69,79]. Suppressing the activation and expansion of microglia may be beneficial because microglia can reactivate T cells in the CNS, and microglia can also have other detrimental functions such as producing pro-inflammatory cytokines and ROS[63]. On the other hand, some microglia also dampen inflammation and promote repair of the CNS including remyelination[64]. In a study by Ma *et al.*,[286], Ad-MSCs delivered intracerebrally increased activation of microglia but promoted their maturation to a regenerative phenotype. The microglia expressed less pro-inflammatory TNFα and IL-1β and more IL-4 and ARG1 which are associated with alternatively activated M2 microglia. M2 microglia have been associated with remyelination[64] and therefore, promoting activation of M2 microglia can be a favourable outcome of MSC treatment. In the present study, however, it appeared that DPSCs may have suppressed the activation of microglia in EAE as they were less abundant in the CNS compared with controls. Liu *et al.*, found that mBM-MSCs suppressed expression genes of pro-inflammatory cytokines TNFα, IL-1β, and IL-6 as well as *iNOS* which is an M1 marker following stimulation of a microglial cell line *in vitro* with LPS, and this was mediated by secretion of TSG-6. It was shown in the present study that DPSCs also express the gene for TSG-6 indicating they might regulate microglial function in a similar manner. Thus, testing if DPSCs have the potential to regulate microglial functions can be carried out using a microglial cell line or isolating primary

microglia and culturing them with DPSCs or their CM under LPS-stimulation and using qPCR to measure gene expression for *iNOS* and *Arg1* which demarcate M1 and M2 microglia respectively. Additionally, gene silencing such as the introduction of short interfering RNA (siRNA) to downregulate TSG-6 production in DPSCs could determine if TSG-6 mediates any potential direct effects of DPSCs on microglia in the same type of experiment. Also, further characterising the activation status and expression of M1/M2 markers by microglia in DPSC-treated mice may reveal if suppression of a pro-inflammatory microglial response is a mechanism of DPSC immunomodulation in EAE. This could be achieved by sorting microglia from DPSC-treated mice and control mice by FACS and testing for *iNOS* and *Arg1* expression by qPCR.

Reduced infiltration of the CNS of EAE mice with myeloid cells, which can include monocytes, macrophages and granulocytes, particularly neutrophils, was another effect of DPSC treatment in the present study. Peron *et al.*,[378] also found fewer myeloid infiltrates in EAE mice that were treated with human endometrial-derived MSCs which was associated with delayed disease. However, there was also a reduction in Th1 and Th17 cells in that study and thus, like in the present study it is difficult to separate the effects of MSCs on T cells versus myeloid cells and other cells in EAE. It is possible that changing the Th1:Th17 cell ratio and suppressing B cells by DPSC treatment altered the cytokine milieu in the CNS which could affect myeloid cell activation and recruitment, and further investigation measuring levels of cytokines and chemokines in the CNS as well as the expression of chemokine receptors, adhesion molecules and activation markers on the myeloid cells is warranted to determine if DPSCs dampen inflammation in the CNS overall. Furthermore, whether DPSCs can directly affect the activation or maturation of myeloid cells is an outstanding question that should be addressed in future studies.

Overall, several immunomodulatory functions of DPSCs in EAE may be beneficial to MS, including the ability of some DPSCs to secrete immunomodulatory molecules that suppress production of Th17 cells. However, variation exists amongst DPSCs from different donors in the ways in which they regulate Th17 cells and B cells which may impact how they could be used clinically. In particular, some DPSCs may be more suitable than others for production of soluble factors that could be isolated and harnessed as a therapy in itself. Identifying sources of variation in DPSCs can be helpful for screening to transplant cells with the most beneficial features, such as ability to suppress B cell activation or Th17 cell production and may also reveal ways in which to improve other DPSCs. Since co-cultures of DPSCs with T cells was not able to be explored in the current study, it is still possible that EAE-supressing DPSCs share common surface molecules that can modulate changes to Th cell differentiation. RNAseq could be used to compare DPSCs which are capable of suppressing EAE with those that are not in order to identify surface markers that demarcate suppressive DPSCs and to potentially elucidate new mechanisms of DPSC immunomodulation. However, it also suggests that the use of autologous DPSCs for treating MS may not the most beneficial option compared with banking DPSCs with superior immunomodulatory functions for general use.

5.4 DPSCs as a tool for delivery of therapeutic molecules

Several strategies to enhance the immunomodulatory capacity of DPSCs were employed in this study. It was hypothesised that this would boost the capacity of DPSCs to control autoimmune inflammation in EAE and ultimately lead to the development of novel strategies to treat MS. Other researchers have successfully used transduction to overexpress immunomodulatory molecules on other types of and did not report any adverse effects on the MSCs and were able to improve therapeutic benefit of the cellular therapy[287,289]. For example, Payne *et al.*,[341] increased the potency of Ad-MSCs to inhibit the symptoms of EAE by lentiviral expression of IL-4. Also, Cobo *et al.*,[379] retrovirally-expressed vasoactive intestinal protein (VIP) on mAd-MSCs to improve their ability to suppress EAE and reduce astrogliosis and neurodegeneration marked by β-amyloid as well as reducing pro-inflammatory cytokine levels in the CNS. Thus, genetically modifying MSCs to deliver therapeutic molecules and improve EAE is possible.

Unfortunately, none of the strategies to enhance the immunomodulatory capacity of DPSCs in this study resulted in the desired outcome. There are a number of potential explanations for this. First, the choice of molecules used to inhibit encephalitogenic immune responses may need to be refined in future. Expression of a putative antagonist of mIL-23 (IL-23RΔ9), of which a human isoform has previously been reported to inhibit hIL-23 activity[335], in the context of expression by DPSCs did not result in suppression of IL-23-driven elicitation of IL-17A despite having this effect when expressed by HEK293T cells. The reasons for this have not been elucidated but are likely to be due to the effect of the IL-23RΔ9 molecule in the context of the diverse array of immunomodulatory factors produced by DPSCs. The IL-23RΔ9 molecule may also act on DPSCs themselves to repress their secretion of immunomodulatory molecules. qPCR for expression of *Il23r* by DPSCs could reveal if this is the case although DPSCs would then require additional modifications if the IL-23RΔ9 molecule were to remain a candidate for expression. Likewise, while ACKR2 and ACKR4 are scavenging receptors that mediate effective removal of multiple chemokines relevant for cell migration in EAE, such as CCL2, CCL3, CCL5 and CCL21[136,144,145,156], it now seems unlikely that DPSCs that carry these receptors are able to reach and persist at the site where they would be required. Inflammatory chemokines that recruit leukocytes to the CNS are produced locally, so it is likely that DPSCs expressing these atypical chemokine receptors would only be useful if the DPSCs were able to populate the CNS. It is possible that delivery of the DPSCs at a later timepoint in the disease course such as immediately prior to the onset of symptoms may permit their entry to the inflamed CNS which expresses different chemokines. The data in this thesis does not support the idea that DPSCs have this capacity following intraperitoneal transfer into EAE mice however. In addition, overexpressing ACKR2 and ACKR4 on DPSCs from donors which did not suppress EAE instead of using DPSC-02 cells which were capable of inhibiting EAE prior to modification may have more clearly demonstrated whether these molecules could be of therapeutic benefit.

While transduction of DPSCs did not affect their multi-potency *in vitro*, it did negatively affect their therapeutic capacity in EAE. It is possible that the double transduction that was used in this study to achieve a highly efficient level of transduction caused changes to immunomodulatory gene expression without affecting expression of MSC surface markers or multi-potency. Perhaps using a single round of transduction with a low multiplicity of infection then cell sorting for successfully transduced cells and expanding those may reduce cellular stress. However, this would also introduce potential problems as the cell sorting process is also likely to modify the biology of these cells, placing additional stress from shear forces on the cells and also require increased passaging of the cells to expand them, which the data also suggests negatively affects their therapeutic capacity. Thus, while DPSCs were not shown in this study to be suitable vehicles for delivery of immunomodulatory transgenes in EAE, other molecular targets such as antagonising GM-CSF or delivering anti-inflammatory IL-10 and alternative methods of gene delivery such as retroviral transduction could be tested in future.

5.5 The fate of DPSCs in EAE

MSCs have been proposed to be able to engraft in injured tissues and potentially partake in tissue repair there, perhaps even differentiating and persisting to replace damaged cells[311,380]. There are data which both supports and refutes this possibility. For example, Zhao et al.,[380] found that rat BM-MSCs which significantly improved recovery from lung injury were found to engraft in injured lungs and expressed pan-cytokeratin, indicating they may have differentiated to alveolar epithelial cells. On the other hand, Tögel *et al.*,[381] located rat BM-MSCs attached to the peritubular capillaries in the rat kidneys in a model of acute renal failure and although the BM-MSCs significantly improved renal recovery, the MSCs did not take on endothelial cell morphology. Ezquer *et al.*,[382] also found no evidence of cell replacement or engraftment in the pancreas of mice with type 1 diabetes treated with mBM-MSCs, but the MSCs were located in the SLOs up to 65 days post-transplantation in that study and recovery was associated with modulation of Th1 and Th2 responses. In the present study, the data do not strongly support a model whereby DPSCs engraft in the CNS. Although a very low level of bioluminescence was detected in the brains and spinal cords of EAE mice treated with labelled DPSCs, qPCR of these organs did not detect the presence of DPSCs and thus suggests that live DPSCs were not present there. The demonstrated sensitivity of the qPCR assay used suggested that less than 10 copies of the DPSC genetic material were present in the CNS in the samples tested. It is possible that DPSCs enter the CNS transiently and then rapidly die or, alternatively but not mutually exclusively, phagocytic cells may carry internalised bioluminescent membrane dye from the DPSCs to the CNS. Nevertheless, it appears that early intraperitoneal delivery of DPSCs in EAE does not facilitate engraftment in the CNS. Notwithstanding the capacity of DPSCs to enter the CNS at all, which would be largely dependent on expression of adhesion molecules and migratory signals perhaps including chemokine receptors, other factors which may have affected the ability of DPSCs to

enter the CNS include a lack of long-term survival of DPSCs after delivery, the route of injection and the stage of EAE. For experiments where DPSCs were tracked in the current study, the DPSCs were delivered during the priming phase of disease when there is only limited inflammation in the CNS. However, it has been suggested that MSCs migrate to sites of tissue injury or inflammation[383], and thus delivery of DPSCs at a later stage of EAE when inflammation in the CNS is at its peak may facilitate their migration into the CNS if survival after delivery is not an issue.

Whether DPSCs have the potential to engraft and differentiate to replace cells of the damaged CNS would be better studied in a syngeneic system, such as transplanting murine-derived DPSCs in the same mouse strain to avoid rejection. Additionally, direct delivery to the CNS via intracerebral injection may enhance the rate of engraftment and thus more easily facilitate studying its effects. Despite this, Leong *et al.*,[311] demonstrated that human DPSCs have the potential to engraft in rodent brains using a rat model of ischemic stroke. In that study, DPSCs were delivered intracerebrally and the rate of engraftment was low (2.3% after 4 weeks). However, it has also become increasingly evident in the field of MSC research that perhaps the greatest contribution of MSCs therapeutically has not been through engraftment but through alternative actions of dampening inflammation or secretion of molecules that contribute to endogenous repair[261,320,382,384]. For example, Akiyama *et al.*,[261] found that BM-MSCs induced T cell apoptosis in experimental colitis in mice which in turn tolerised macrophages that phagocytosed the T cells, resulting in secondary expansion of Tregs. Fas/FasL interactions were found to be important for the ability of the BM-MSCs to induce T cell apoptosis and suppress disease in that model. Also a study by Bai *et al.*,[320] showed that a single dose of CM from BM-MSCs at peak disease abrogated EAE, indicating that soluble products of BM-MSCs alone are sufficient for significant therapeutic benefit and HGF was found to be mediate suppression of disease in that study.

With regard to the long-term persistence of DPSCs in the present study, the fact that the membrane dye which was used to label DPSCs was detected in the spleens and iLNs of EAE mice, but qPCR did not show the presence of DPSCs themselves there, suggests that DPSCs may die soon after transfer and either drain to the SLOs or be carried there by phagocytic cells that may take up dead DPSCs. Recent evidence shows that long-term survival of MSCs may not be required to induce immunosuppressive effects. De Witte *et al.*,[384] tracked the fate of IV-infused UC-MSCs in healthy mice and revealed that the cells localised primarily to the lungs and some (mostly dead cells) to the liver. In that study, the dead MSCs were phagocytosed by monocytes and neutrophils, and this led to an anti-inflammatory prolife in those monocytes which enabled them to induce Tregs. Since DPSCs in the current study do not appear to survive in large numbers for a long period of time after injection into EAE mice, their immunosuppressive effects could be elicited by transient interactions with leukocytes or secretion of anti-inflammatory molecules before their death. This seems likely given that both the donor and extent of passaging of DPSCs affects their therapeutic capacity and it is difficult to discern how these factors could affect EAE outcome in the absence of the DPSCs eliciting signals to other cells before death. Alternatively, phagocytosis of dead DPSCs may also have immunomodulatory outcomes on APCs.

Migration of APCs to the SLOs after phagocytosis of DPSCs would place them in a prime location for further modulating inflammatory responses in those mice.

Another important factor for consideration is the potential immunogenicity of MSCs, which has important implications for translation of MSC-based therapies to the clinic. Early studies in which MSCs failed to activate T cells in mixed lymphocytes reactions (MLRs) led to the idea that MSCs are immune-privileged and not targeted by the adaptive immune system[250,252]. A lack of immunogenicity of MSCs might permit the development of MSC "banks" where patients can receive MSCs from other donors. MSC banks would greatly reduce treatment costs, facilitate efficient quality control procedures and allow patients whose own MSCs have low therapeutic capacity to receive more suitable MSCs from other donors. However, if MSCs are even mildly immunogenic this may affect treatment outcomes including failure of the cells to engraft efficiently due to clearance by the recipient's immune response or generation of an inflammatory environment.

A large proportion of MSC studies, including the present study, utilise xenogeneic systems where human MSCs are transplanted into other species including rodents and primates. This is important for our understanding of species-specific effects, such as mechanisms of immunomodulation which can vary between humans and rodents[236,237]. However, these systems may not be ideal for studying cell engraftment since more recent studies have determined that MSCs can indeed elicit immune responses in the host[385-388]. MSCs express ligands that are recognised by NK cells and are susceptible to NK cell-mediated lysis *in vitro*[316,389]. Interestingly, treating MSCs with IFNγ caused upregulation of MHC-I and reduced their susceptibility to NK-mediated lysis[316]. Immune responses against transferred MSCs have also been described *in vivo*. Eliopoulos *et al* reported increased NK, NKT and $CD8^+$ T cell infiltration of mBM-MSC grafts in allogeneic hosts compared with syngeneic hosts in mice[388]. In another study, Nauta *et al* primed Balb/c mice with allogeneic C57Bl/6 MSCs or syngeneic Balb/c MSCs and then challenged the mice with a transfer of C57Bl/6 splenocytes. Mice which received allogeneic but not syngeneic MSCs rapidly rejected the transferred allogeneic splenocytes, demonstrating that the host is capable of generating immunological memory against allogeneic MSCs[387]. Some studies also report induction of alloantibodies against MSCs after transplantation[385,390] although this is disputed by other investigators[391].

Notably, and as discussed above, in the present study Th1 cells were consistently found to be expanded in the spleens of DPSC-treated EAE mice. While this may result from DPSC-mediated immunomodulation of Th1:Th17 differentiation as discussed above, it is also possible that the increase in Th1 cells results from an expansion of these cells in response to the DPSCs. In this case, the increased Th1 cells may still contribute to altering the autoimmune response against the CNS through a bystander effect, producing IFNγ that suppresses disease. It is difficult to study MSC immunogenicity in isolation because of their immunosuppressive effects but administering DPSCs to otherwise naïve mice then measuring changes in the immune system of those mice may show whether DPSC-specific immune responses occur in C57Bl/6 mice. Overall, despite allogeneic and xenogeneic MSC transfers having therapeutic benefits in a range of disease models, immunogenicity should

not be ignored and more research into the immunogenicity of MSCs will inform the future direction of MSC-based treatment platforms.

5.6 Conclusion

To conclude, DPSCs are shown here in this study to be a possible candidate for development of a future therapy for MS, since many DPSCs were shown to inhibit the course of EAE and had anti-inflammatory effects *in vitro* and *in vivo*. DPSCs significantly dampened inflammation in the CNS of treated EAE mice and appeared to target multiple arms of the immune system including increasing the ratio of Th1:Th17 cells, reducing $CD8^+$ T cells, B cells and infiltrating myeloid cells in the CNS and also reducing the number of microglia.

The capacity of DPSCs to modulate immune responses means they may be beneficial for treating MS as well as other inflammatory conditions. However, the evidence of this study that DPSCs from different donors are not equally suppressive in EAE and that prolonged culture *in vitro* negatively affects their therapeutic efficacy highlight two significant hurdles to bringing DPSCs to the clinic. Further investigations should bring a focus to identifying differences between suppressive and non-suppressive DPSCs, improving the quality of DPSCs that are not suppressive in EAE and development of protocols which better maintain DPSCs during expansion *in vitro* to ensure their effectiveness *in vivo*. Since DPSCs did not appear to survive for long after injection into EAE mice, this may be a limiting factor for MS therapy if long-term engraftment is desired or multiple rounds of therapy may be required for optimal responses.

This page intentionally left blank.

References

1 Kremer, D., Göttle, P., Hartung, H.-P. & Küry, P. Pushing Forward: Remyelination as the New Frontier in CNS Diseases. *Trends in Neurosciences* **39**, 246-263.

2 Milo, R. & Miller, A. Revised diagnostic criteria of multiple sclerosis. *Autoimmunity reviews* **13**, 518-524 (2014).

3 Willer, C. J., Dyment, D. A., Risch, N. J., Sadovnick, A. D., Ebers, G. C., The Canadian Collaborative Study GroupWellcome Trust Centre for Human Genetics, U. o. O. R. D. O. O. X. B. N. U. K., Department of Genetics, S. U. M. A. S. C. A., Department of Medical, G., Faculty of Medicine, U. o. B. C. V. B. C. C. V. T. B. & Department of Clinical Neurology, R. I. O. U. W. R. O. O. X. H. E. U. K. Twin concordance and sibling recurrence rates in multiple sclerosis. *Proceedings of the National Academy of Sciences of the United States of America* **100**, 12877-12882 (2003).

4 Ahmad, H., Palmer, A. J., Campbell, J. A., Mei, I. v. d. & Taylor, B. Health Economic Impact of Multiple Sclerosis in Australia in 2017. *Multiple Sclerosis Research Australia* (2018).

5 Wallin, M. T., Culpepper, W. J., Nichols, E., Bhutta, Z. A., Gebrehiwot, T. T., Hay, S. I., Khalil, I. A., Krohn, K. J., Liang, X., Naghavi, M., Mokdad, A. H., Nixon, M. R., Reiner, R. C., Sartorius, B., Smith, M., Topor-Madry, R., Werdecker, A., Vos, T., Feigin, V. L. & Murray, C. J. L. Global, regional, and national burden of multiple sclerosis 1990–2016: a systematic analysis for the Global Burden of Disease Study 2016. *The Lancet Neurology* **18**, 269-285 (2019).

6 Confavreux, C. & Vukusic, S. Age at disability milestones in multiple sclerosis. *Brain : a journal of neurology* **129**, 595-605 (2006).

7 Olsson, T., Barcellos, L. F. & Alfredsson, L. Interactions between genetic, lifestyle and environmental risk factors for multiple sclerosis. *Nature reviews. Neurology* **13**, 25-36 (2017).

8 Rejdak, K., Jackson, S. & Giovannoni, G. Multiple sclerosis: a practical overview for clinicians. *British medical bulletin* **95**, 79-104 (2010).

9 Ysrraelit, M. C. & Correale, J. Impact of sex hormones on immune function and multiple sclerosis development. *Immunology* **0**.

10 Multiple sclerosis genomic map implicates peripheral immune cells and microglia in susceptibility. *Science (New York, N.Y.)* **365**, eaav7188 (2019).

11 Moutsianas, L., Jostins, L., Beecham, A. H., Dilthey, A. T., Xifara, D. K., Ban, M., Shah, T. S., Patsopoulos, N. A., Alfredsson, L., Anderson, C. A., Attfield, K. E., Baranzini, S. E., Barrett, J., Binder, T. M. C., Booth, D., Buck, D., Celius, E. G., Cotsapas, C., D'Alfonso, S., Dendrou, C. A., Donnelly, P., Dubois, B., Fontaine, B., Fugger, L., Goris, A., Gourraud, P. A., Graetz, C., Hemmer, B., Hillert, J., Kockum, I., Leslie, S., Lill, C. M., Martinelli-Boneschi, F., Oksenberg, J. R., Olsson, T., Oturai, A., Saarela, J., Sondergaard, H. B., Spurkland, A., Taylor, B., Winkelmann, J., Zipp, F., Haines, J. L., Pericak-Vance, M. A., Spencer, C. C. A., Stewart, G., Hafler, D. A., Ivinson, A. J., Harbo, H. F., Hauser, S. L., De Jager, P. L., Compston, A., McCauley, J. L., Sawcer, S. & McVean, G. Class II HLA interactions modulate genetic risk for multiple sclerosis. *Nat Genet* **47**, 1107-1113 (2015).

12 Lassmann, H., van Horssen, J. & Mahad, D. Progressive multiple sclerosis: pathology and pathogenesis. *Nature reviews. Neurology* **8**, 647-656 (2012).

13 Mix, E., Meyer-Rienecker, H., Hartung, H.-P. & Zettl, U. K. Animal models of multiple sclerosis—Potentials and limitations. *Progress in Neurobiology* **92**, 386-404 (2010).

14 Kipp, M., Nyamoya, S., Hochstrasser, T. & Amor, S. Multiple sclerosis animal models: a clinical and histopathological perspective. *Brain pathology (Zurich, Switzerland)* **27**, 123-137 (2017).

15 Robinson, A. P., Harp, C. T., Noronha, A. & Miller, S. D. The experimental autoimmune encephalomyelitis (EAE) model of MS: utility for understanding disease pathophysiology and treatment. *Handbook of clinical neurology* **122**, 173-189 (2014).

16 Mahad, D. H., Trapp, B. D. & Lassmann, H. Pathological mechanisms in progressive multiple sclerosis. *The Lancet Neurology* **14**, 183-193 (2015).

17 Kroenke, M. A., Carlson, T. J., Andjelkovic, A. V. & Segal, B. M. IL-12– and IL-23–modulated T cells induce distinct types of EAE based on histology, CNS chemokine profile, and response to cytokine inhibition. *The Journal of experimental medicine* **205**, 1535-1541 (2008).

18 Athie-Morales, V., Smits, H. H., Cantrell, D. A. & Hilkens, C. M. U. Sustained IL-12 Signaling Is Required for Th1 Development. *The Journal of Immunology* **172**, 61-69 (2004).

19 Zhang, G. X., Gran, B., Yu, S., Li, J., Siglienti, I., Chen, X., Kamoun, M. & Rostami, A. Induction of experimental autoimmune encephalomyelitis in IL-12 receptor-beta 2-deficient mice: IL-12 responsiveness is not required in the pathogenesis of inflammatory demyelination in the central nervous system. *Journal of immunology (Baltimore, Md. : 1950)* **170**, 2153-2160 (2003).

20 Ferber, I. A., Brocke, S., Taylor-Edwards, C., Ridgway, W., Dinisco, C., Steinman, L., Dalton, D. & Fathman, C. G. Mice with a disrupted IFN-gamma gene are susceptible to the induction of experimental autoimmune encephalomyelitis (EAE). *Journal of immunology (Baltimore, Md. : 1950)* **156**, 5-7 (1996).

21 Chu, C.-Q., Wittmer, S. & Dalton, D. K. Failure to Suppress the Expansion of the Activated Cd4 T Cell Population in Interferon γ–Deficient Mice Leads to Exacerbation of Experimental Autoimmune Encephalomyelitis. *The Journal of experimental medicine* **192**, 123-128 (2000).

22 Willenborg, D. O., Fordham, S., Bernard, C. C., Cowden, W. B. & Ramshaw, I. A. IFN-gamma plays a critical down-regulatory role in the induction and effector phase of myelin oligodendrocyte glycoprotein-induced autoimmune encephalomyelitis. *The Journal of Immunology* **157**, 3223-3227 (1996).

23 Naves, R., Singh, S. P., Cashman, K. S., Rowse, A. L., Axtell, R. C., Steinman, L., Mountz, J. D., Steele, C., De Sarno, P. & Raman, C. The Interdependent, Overlapping, and Differential Roles of Type I and II IFNs in the Pathogenesis of Experimental Autoimmune Encephalomyelitis. *The Journal of Immunology* **191**, 2967-2977 (2013).

24 Gran, B., Zhang, G. X., Yu, S., Li, J., Chen, X. H., Ventura, E. S., Kamoun, M. & Rostami, A. IL-12p35-deficient mice are susceptible to experimental autoimmune encephalomyelitis: evidence for redundancy in the IL-12 system in the induction of central nervous system autoimmune demyelination. *Journal of immunology (Baltimore, Md. : 1950)* **169**, 7104-7110 (2002).

25 Becher, B., Durell, B. G. & Noelle, R. J. Experimental autoimmune encephalitis and inflammation in the absence of interleukin-12. *The Journal of clinical investigation* **110**, 493-497 (2002).

26 Oppmann, B., Lesley, R., Blom, B., Timans, J. C., Xu, Y., Hunte, B., Vega, F., Yu, N., Wang, J., Singh, K., Zonin, F., Vaisberg, E., Churakova, T., Liu, M., Gorman, D., Wagner, J., Zurawski, S., Liu, Y., Abrams, J. S., Moore, K. W., Rennick, D., de Waal-Malefyt, R., Hannum, C., Bazan, J. F. & Kastelein, R. A. Novel p19 protein engages IL-12p40 to form a cytokine, IL-23, with biological activities similar as well as distinct from IL-12. *Immunity* **13**, 715-725 (2000).

27 Cua, D. J., Sherlock, J., Chen, Y., Murphy, C. A., Joyce, B., Seymour, B., Lucian, L., To, W., Kwan, S., Churakova, T., Zurawski, S., Wiekowski, M., Lira, S. A., Gorman, D., Kastelein, R. A. & Sedgwick, J. D. Interleukin-23 rather than interleukin-12 is the critical cytokine for autoimmune inflammation of the brain. *Nature* **421**, 744-748 (2003).

28 Langrish, C. L., Chen, Y., Blumenschein, W. M., Mattson, J., Basham, B., Sedgwick, J. D., McClanahan, T., Kastelein, R. A. & Cua, D. J. IL-23 drives a pathogenic T cell population that induces autoimmune inflammation. *The Journal of experimental medicine* **201**, 233-240 (2005).

29 Stromnes, I. M., Cerretti, L. M., Liggitt, D., Harris, R. A. & Goverman, J. M. Differential regulation of central nervous system autoimmunity by TH1 and TH17 cells. *Nature medicine* **14**, 337-342 (2008).

30 Park, H., Li, Z., Yang, X. O., Chang, S. H., Nurieva, R., Wang, Y. H., Wang, Y., Hood, L., Zhu, Z., Tian, Q. & Dong, C. A distinct lineage of CD4 T cells regulates tissue inflammation by producing interleukin 17. *Nature immunology* **6**, 1133-1141 (2005).

31 Haak, S., Croxford, A. L., Kreymborg, K., Heppner, F. L., Pouly, S., Becher, B. & Waisman, A. IL-17A and IL-17F do not contribute vitally to autoimmune neuro-inflammation in mice. *The Journal of clinical investigation* **119**, 61-69 (2009).

32 Komiyama, Y., Nakae, S., Matsuki, T., Nambu, A., Ishigame, H., Kakuta, S., Sudo, K. & Iwakura, Y. IL-17 plays an important role in the development of experimental autoimmune encephalomyelitis. *Journal of immunology (Baltimore, Md. : 1950)* **177**, 566-573 (2006).

33 Codarri, L., Gyulveszi, G., Tosevski, V., Hesske, L., Fontana, A., Magnenat, L., Suter, T. & Becher, B. RORgammat drives production of the cytokine GM-CSF in helper T cells, which is essential for the effector phase of autoimmune neuroinflammation. *Nature immunology* **12**, 560-567 (2011).

34 El-Behi, M., Ciric, B., Dai, H., Yan, Y., Cullimore, M., Safavi, F., Zhang, G.-X., Dittel, B. N. & Rostami, A. The encephalitogenicity of TH17 cells is dependent on IL-1- and IL-23-induced production of the cytokine GM-CSF. *Nature immunology* **12**, 568-575 (2011).

35 Mukasa, R., Balasubramani, A., Lee, Y. K., Whitley, S. K., Weaver, B. T., Shibata, Y., Crawford, G. E., Hatton, R. D. & Weaver, C. T. Epigenetic Instability of Cytokine and Transcription Factor Gene Loci Underlies Plasticity of the T Helper 17 Cell Lineage. *Immunity* **32**, 616-627 (2010).

36 Hirota, K., Duarte, J. H., Veldhoen, M., Hornsby, E., Li, Y., Cua, D. J., Ahlfors, H., Wilhelm, C., Tolaini, M., Menzel, U., Garefalaki, A., Potocnik, A. J. & Stockinger, B. Fate mapping of IL-17-producing T cells in inflammatory responses. *Nature immunology* **12**, 255-263 (2011).

37 O'Connor, R. A., Cambrook, H., Huettner, K. & Anderton, S. M. T-bet is essential for Th1-mediated, but not Th17-mediated, CNS autoimmune disease. *European journal of immunology* **43**, 2818-2823 (2013).

38 Grifka-Walk, H. M., Lalor, S. J. & Segal, B. M. Highly polarized Th17 cells induce EAE via a T-bet independent mechanism. *European journal of immunology* **43**, 2824-2831 (2013).

39 Ortega, S. B., Kashi, V. P., Tyler, A. F., Cunnusamy, K., Mendoza, J. P. & Karandikar, N. J. The disease-ameliorating function of autoregulatory CD8 T cells is mediated by targeting of encephalitogenic CD4 T cells in experimental autoimmune encephalomyelitis. *Journal of immunology (Baltimore, Md. : 1950)* **191**, 117-126 (2013).

40 Sun, D., Whitaker, J. N., Huang, Z., Liu, D., Coleclough, C., Wekerle, H. & Raine, C. S. Myelin antigen-specific CD8+ T cells are encephalitogenic and produce severe disease in C57BL/6 mice. *Journal of immunology (Baltimore, Md. : 1950)* **166**, 7579-7587 (2001).

41 Ford, M. L. & Evavold, B. D. Specificity, magnitude, and kinetics of MOG-specific CD8+ T cell responses during experimental autoimmune encephalomyelitis. *European journal of immunology* **35**, 76-85 (2005).

42 Huseby, E. S., Liggitt, D., Brabb, T., Schnabel, B., Ohlen, C. & Goverman, J. A pathogenic role for myelin-specific CD8(+) T cells in a model for multiple sclerosis. *The Journal of experimental medicine* **194**, 669-676 (2001).

43 McPherson, S. W., Heuss, N. D., Roehrich, H. & Gregerson, D. S. Bystander killing of neurons by cytotoxic T cells specific for a glial antigen. *Glia* **53**, 457-466 (2006).

44 Saxena, A., Bauer, J., Scheikl, T., Zappulla, J., Audebert, M., Desbois, S., Waisman, A., Lassmann, H., Liblau, R. S. & Mars, L. T. Cutting edge: Multiple sclerosis-like lesions induced by effector CD8 T cells recognizing a sequestered antigen on oligodendrocytes. *Journal of immunology (Baltimore, Md. : 1950)* **181**, 1617-1621 (2008).

45 Sasaki, K., Bean, A., Shah, S., Schutten, E., Huseby, P. G., Peters, B., Shen, Z. T., Vanguri, V., Liggitt, D. & Huseby, E. S. Relapsing-remitting central nervous system autoimmunity mediated by GFAP-specific CD8 T cells. *Journal of immunology (Baltimore, Md. : 1950)* **192**, 3029-3042 (2014).

46 Najafian, N., Chitnis, T., Salama, A. D., Zhu, B., Benou, C., Yuan, X., Clarkson, M. R., Sayegh, M. H. & Khoury, S. J. Regulatory functions of CD8+CD28– T cells in an autoimmune disease model. *The Journal of clinical investigation* **112**, 1037-1048 (2003).

47 Tyler, A. F., Mendoza, J. P., Firan, M. & Karandikar, N. J. CD8(+) T Cells Are Required For Glatiramer Acetate Therapy in Autoimmune Demyelinating Disease. *PloS one* **8**, e66772 (2013).

48 Jiang, H., Braunstein, N. S., Yu, B., Winchester, R. & Chess, L. CD8⁺ T cells control the TH phenotype of MBP-reactive CD4⁺ T cells in EAE mice. *Proceedings of the National Academy of Sciences* **98**, 6301-6306 (2001).

49 Tang, X., Maricic, I., Purohit, N., Bakamjian, B., Reed-Loisel, L. M., Beeston, T., Jensen, P. & Kumar, V. Regulation of immunity by a novel population of Qa-1-restricted CD8alphaalpha+TCRalphabeta+ T cells. *Journal of immunology (Baltimore, Md. : 1950)* **177**, 7645-7655 (2006).

50 Molnarfi, N., Schulze-Topphoff, U., Weber, M. S., Patarroyo, J. C., Prod'homme, T., Varrin-Doyer, M., Shetty, A., Linington, C., Slavin, A. J., Hidalgo, J., Jenne, D. E., Wekerle, H., Sobel, R. A., Bernard, C. C., Shlomchik, M. J. & Zamvil, S. S. MHC class II-dependent B cell APC function is required for induction of CNS autoimmunity independent of myelin-specific antibodies. *The Journal of experimental medicine* **210**, 2921-2937 (2013).

51 Hjelmström, P., Juedes, A. E., Fjell, J. & Ruddle, N. H. Cutting Edge: B Cell-Deficient Mice Develop Experimental Allergic Encephalomyelitis with Demyelination After Myelin Oligodendrocyte Glycoprotein Sensitization. *The Journal of Immunology* **161**, 4480-4483 (1998).

52 Lyons, J.-A., San, M., Happ, M. P. & Cross, A. H. B cells are critical to induction of experimental allergic encephalomyelitis by protein but not by a short encephalitogenic peptide. *European journal of immunology* **29**, 3432-3439 (1999).
53 Svensson, L., Abdul-Majid, K.-B., Bauer, J., Lassmann, H., Harris, R. A. & Holmdahl, R. A comparative analysis of B cell-mediated myelin oligodendrocyte glycoprotein-experimental autoimmune encephalomyelitis pathogenesis in B cell-deficient mice reveals an effect on demyelination. *European journal of immunology* **32**, 1939-1946 (2002).
54 Wolf, S. D., Dittel, B. N., Hardardottir, F. & Janeway, C. A. Experimental Autoimmune Encephalomyelitis Induction in Genetically B Cell–deficient Mice. *The Journal of experimental medicine* **184**, 2271-2278 (1996).
55 Matsushita, T., Yanaba, K., Bouaziz, J. D., Fujimoto, M. & Tedder, T. F. Regulatory B cells inhibit EAE initiation in mice while other B cells promote disease progression. *The Journal of clinical investigation* **118**, 3420-3430 (2008).
56 Barr, T. A., Shen, P., Brown, S., Lampropoulou, V., Roch, T., Lawrie, S., Fan, B., O'Connor, R. A., Anderton, S. M., Bar-Or, A., Fillatreau, S. & Gray, D. B cell depletion therapy ameliorates autoimmune disease through ablation of IL-6-producing B cells. *The Journal of experimental medicine* **209**, 1001-1010 (2012).
57 Shen, P., Roch, T., Lampropoulou, V., O'Connor, R. A., Stervbo, U., Hilgenberg, E., Ries, S., Dang, V. D., Jaimes, Y., Daridon, C., Li, R., Jouneau, L., Boudinot, P., Wilantri, S., Sakwa, I., Miyazaki, Y., Leech, M. D., McPherson, R. C., Wirtz, S., Neurath, M., Hoehlig, K., Meinl, E., Grutzkau, A., Grun, J. R., Horn, K., Kuhl, A. A., Dorner, T., Bar-Or, A., Kaufmann, S. H. E., Anderton, S. M. & Fillatreau, S. IL-35-producing B cells are critical regulators of immunity during autoimmune and infectious diseases. *Nature* **507**, 366-370 (2014).
58 Fillatreau, S., Sweenie, C. H., McGeachy, M. J., Gray, D. & Anderton, S. M. B cells regulate autoimmunity by provision of IL-10. *Nature immunology* **3**, 944-950 (2002).
59 Bjarnadottir, K., Benkhoucha, M., Merkler, D., Weber, M. S., Payne, N. L., Bernard, C. C. A., Molnarfi, N. & Lalive, P. H. B cell-derived transforming growth factor-beta1 expression limits the induction phase of autoimmune neuroinflammation. *Scientific reports* **6**, 34594 (2016).
60 Miron, V. E. & Franklin, R. J. Macrophages and CNS remyelination. *Journal of neurochemistry* (2014).
61 Heppner, F. L., Greter, M., Marino, D., Falsig, J., Raivich, G., Hovelmeyer, N., Waisman, A., Rulicke, T., Prinz, M., Priller, J., Becher, B. & Aguzzi, A. Experimental autoimmune encephalomyelitis repressed by microglial paralysis. *Nature medicine* **11**, 146-152 (2005).
62 Butovsky, O., Landa, G., Kunis, G., Ziv, Y., Avidan, H., Greenberg, N., Schwartz, A., Smirnov, I., Pollack, A., Jung, S. & Schwartz, M. Induction and blockage of oligodendrogenesis by differently activated microglia in an animal model of multiple sclerosis. *The Journal of clinical investigation* **116**, 905-915 (2006).
63 Zrzavy, T., Hametner, S., Wimmer, I., Butovsky, O., Weiner, H. L. & Lassmann, H. Loss of 'homeostatic' microglia and patterns of their activation in active multiple sclerosis. *Brain : a journal of neurology* **140**, 1900-1913 (2017).
64 Miron, V. E., Boyd, A., Zhao, J.-W., Yuen, T. J., Ruckh, J. M., Shadrach, J. L., van Wijngaarden, P., Wagers, A. J., Williams, A., Franklin, R. J. M. & ffrench-Constant, C. M2 microglia/macrophages drive oligodendrocyte differentiation during CNS remyelination. *Nature neuroscience* **16**, 1211-1218 (2013).
65 Okuda, Y., Sakoda, S., Fujimura, H., Saeki, Y., Kishimoto, T. & Yanagihara, T. IL-6 plays a crucial role in the induction phase of myelin oligodendrocyte glucoprotein 35-55 induced experimental autoimmune encephalomyelitis. *Journal of neuroimmunology* **101**, 188-196 (1999).
66 Lévesque, S. A., Paré, A., Mailhot, B., Bellver-Landete, V., Kébir, H., Lécuyer, M.-A., Alvarez, J. I., Prat, A., Vaccari, J. P. d. R., Keane, R. W. & Lacroix, S. Myeloid cell transmigration across the CNS vasculature triggers IL-1β–driven neuroinflammation during autoimmune encephalomyelitis in mice. *The Journal of experimental medicine* **213**, 929-949 (2016).
67 Mufazalov, I. A., Schelmbauer, C., Regen, T., Kuschmann, J., Wanke, F., Gabriel, L. A., Hauptmann, J., Müller, W., Pinteaux, E., Kurschus, F. C. & Waisman, A. IL-1 signaling is critical for expansion but not generation of autoreactive GM-CSF⁺ Th17 cells. *The EMBO Journal* **36**, 102-115 (2017).

68 Samoilova, E. B., Horton, J. L., Hilliard, B., Liu, T. S. & Chen, Y. IL-6-deficient mice are resistant to experimental autoimmune encephalomyelitis: roles of IL-6 in the activation and differentiation of autoreactive T cells. *Journal of immunology (Baltimore, Md. : 1950)* **161**, 6480-6486 (1998).

69 Croxford, A. L., Lanzinger, M., Hartmann, F. J., Schreiner, B., Mair, F., Pelczar, P., Clausen, B. E., Jung, S., Greter, M. & Becher, B. The Cytokine GM-CSF Drives the Inflammatory Signature of CCR2+ Monocytes and Licenses Autoimmunity. *Immunity* **43**, 502-514 (2015).

70 Ronchi, F., Basso, C., Preite, S., Reboldi, A., Baumjohann, D., Perlini, L., Lanzavecchia, A. & Sallusto, F. Experimental priming of encephalitogenic Th1/Th17 cells requires pertussis toxin-driven IL-1β production by myeloid cells. *Nature Communications* **7**, 11541 (2016).

71 Arellano, G., Ottum, P. A., Reyes, L. I., Burgos, P. I. & Naves, R. Stage-Specific Role of Interferon-Gamma in Experimental Autoimmune Encephalomyelitis and Multiple Sclerosis. *Frontiers in immunology* **6**, 492-492 (2015).

72 Gobel, K., Ruck, T. & Meuth, S. G. Cytokine signaling in multiple sclerosis: Lost in translation. *Multiple sclerosis (Houndmills, Basingstoke, England)* **24**, 432-439 (2018).

73 Probert, L. TNF and its receptors in the CNS: The essential, the desirable and the deleterious effects. *Neuroscience* **302**, 2-22 (2015).

74 Körner, H., Lemckert, F. A., Chaudhri, G., Etteldorf, S. & Sedgwick, J. D. Tumor necrosis factor blockade in actively induced experimental autoimmune encephalomyelitis prevents clinical disease despite activated T cell infiltration to the central nervous system. *European journal of immunology* **27**, 1973-1981 (1997).

75 Kassiotis, G. & Kollias, G. Uncoupling the Proinflammatory from the Immunosuppressive Properties of Tumor Necrosis Factor (Tnf) at the P55 TNF Receptor Level. *Implications for Pathogenesis and Therapy of Autoimmune Demyelination* **193**, 427-434 (2001).

76 Kaltsonoudis, E., Voulgari, P. V., Konitsiotis, S. & Drosos, A. A. Demyelination and other neurological adverse events after anti-TNF therapy. *Autoimmunity reviews* **13**, 54-58 (2014).

77 Diveu, C., McGeachy, M. J., Boniface, K., Stumhofer, J. S., Sathe, M., Joyce-Shaikh, B., Chen, Y., Tato, C. M., McClanahan, T. K., de Waal Malefyt, R., Hunter, C. A., Cua, D. J. & Kastelein, R. A. IL-27 Blocks RORc Expression to Inhibit Lineage Commitment of Th17 Cells. *The Journal of Immunology* **182**, 5748-5756 (2009).

78 Fitzgerald, D. C., Ciric, B., Touil, T., Harle, H., Grammatikopolou, J., Sarma, J. D., Gran, B., Zhang, G.-X. & Rostami, A. Suppressive Effect of IL-27 on Encephalitogenic Th17 Cells and the Effector Phase of Experimental Autoimmune Encephalomyelitis. *The Journal of Immunology* **179**, 3268-3275 (2007).

79 Henderson, A. P. D., Barnett, M. H., Parratt, J. D. E. & Prineas, J. W. Multiple sclerosis: Distribution of inflammatory cells in newly forming lesions. *Annals of neurology* **66**, 739-753 (2009).

80 Sawcer, S., Hellenthal, G., Pirinen, M., Spencer, C. C. A., Patsopoulos, N. A., Moutsianas, L., Dilthey, A., Su, Z., Freeman, C., Hunt, S. E., Edkins, S., Gray, E., Booth, D. R., Potter, S. C., Goris, A., Band, G., Bang Oturai, A., Strange, A., Saarela, J., Bellenguez, C., Fontaine, B., Gillman, M., Hemmer, B., Gwilliam, R., Zipp, F., Jayakumar, A., Martin, R., Leslie, S., Hawkins, S., Giannoulatou, E., D'alfonso, S., Blackburn, H., Martinelli Boneschi, F., Liddle, J., Harbo, H. F., Perez, M. L., Spurkland, A., Waller, M. J., Mycko, M. P., Ricketts, M., Comabella, M., Hammond, N., Kockum, I., McCann, O. T., Ban, M., Whittaker, P., Kemppinen, A., Weston, P., Hawkins, C., Widaa, S., Zajicek, J., Dronov, S., Robertson, N., Bumpstead, S. J., Barcellos, L. F., Ravindrarajah, R., Abraham, R., Alfredsson, L., Ardlie, K., Aubin, C., Baker, A., Baker, K., Baranzini, S. E., Bergamaschi, L., Bergamaschi, R., Bernstein, A., Berthele, A., Boggild, M., Bradfield, J. P., Brassat, D., Broadley, S. A., Buck, D., Butzkueven, H., Capra, R., Carroll, W. M., Cavalla, P., Celius, E. G., Cepok, S., Chiavacci, R., Clerget-Darpoux, F., Clysters, K., Comi, G., Cossburn, M., Cournu-Rebeix, I., Cox, M. B., Cozen, W., Cree, B. A. C., Cross, A. H., Cusi, D., Daly, M. J., Davis, E., de Bakker, P. I. W., Debouverie, M., D'hooghe, M. B., Dixon, K., Dobosi, R., Dubois, B., Ellinghaus, D., Elovaara, I., Esposito, F., Fontenille, C., Foote, S., Franke, A., Galimberti, D., Ghezzi, A., Glessner, J., Gomez, R., Gout, O., Graham, C., Grant, S. F. A., Rosa Guerini, F., Hakonarson, H., Hall, P., Hamsten, A., Hartung, H.-P., Heard, R. N., Heath, S., Hobart, J., Hoshi, M., Infante-Duarte, C., Ingram, G., Ingram, W., Islam, T., Jagodic, M., Kabesch, M., Kermode, A. G., Kilpatrick, T. J.,

Kim, C., Klopp, N., Koivisto, K., Larsson, M., Lathrop, M., Lechner-Scott, J. S., Leone, M. A., Leppä, V., Liljedahl, U., Lima Bomfim, I., Lincoln, R. R., Link, J., Liu, J., Lorentzen, Å. R., Lupoli, S., Macciardi, F., Mack, T., Marriott, M., Martinelli, V., Mason, D., McCauley, J. L., Mentch, F., Mero, I.-L., Mihalova, T., Montalban, X., Mottershead, J., Myhr, K.-M., Naldi, P., Ollier, W., Page, A., Palotie, A., Pelletier, J., Piccio, L., Pickersgill, T., Piehl, F., Pobywajlo, S., Quach, H. L., Ramsay, P. P., Reunanen, M., Reynolds, R., Rioux, J. D., Rodegher, M., Roesner, S., Rubio, J. P., Rückert, I.-M., Salvetti, M., Salvi, E., Santaniello, A., Schaefer, C. A., Schreiber, S., Schulze, C., Scott, R. J., Sellebjerg, F., Selmaj, K. W., Sexton, D., Shen, L., Simms-Acuna, B., Skidmore, S., Sleiman, P. M. A., Smestad, C., Sørensen, P. S., Søndergaard, H. B., Stankovich, J., Strange, R. C., Sulonen, A.-M., Sundqvist, E., Syvänen, A.-C., Taddeo, F., Taylor, B., Blackwell, J. M., Tienari, P., Bramon, E., Tourbah, A., Brown, M. A., Tronczynska, E., Casas, J. P., Tubridy, N., Corvin, A., Vickery, J., Jankowski, J., Villoslada, P., Markus, H. S., Wang, K., Mathew, C. G., Wason, J., Palmer, C. N. A., Wichmann, H. E., Plomin, R., Willoughby, E., Rautanen, A., Winkelmann, J., Wittig, M., Trembath, R. C., Yaouanq, J., Viswanathan, A. C., Zhang, H., Wood, N. W., Zuvich, R., Deloukas, P., Langford, C., Duncanson, A., Oksenberg, J. R., Pericak-Vance, M. A., Haines, J. L., Olsson, T., Hillert, J., Ivinson, A. J., De Jager, P. L., Peltonen, L., Stewart, G. J., Hafler, D. A., Hauser, S. L., McVean, G., Donnelly, P., Compston, A., The International Multiple Sclerosis Genetics, C. & The Wellcome Trust Case Control, C. Genetic risk and a primary role for cell-mediated immune mechanisms in multiple sclerosis. *Nature* **476**, 214-219 (2011).

81 Consortium, T. I. M. S. G. & 2*, W. T. C. C. C. Genetic risk and a primary role for cell-mediated immune mechanisms in multiple sclerosis. *Nature* **476**, 214-219 (2011).

82 Teniente-Serra, A., Grau-López, L., Mansilla, M. J., Fernández-Sanmartín, M., Ester Condins, A., Ramo-Tello, C. & Martínez-Cáceres, E. Multiparametric flow cytometric analysis of whole blood reveals changes in minor lymphocyte subpopulations of multiple sclerosis patients. *Autoimmunity* **49**, 219-228 (2016).

83 Tang, S.-c., Fan, X.-h., Pan, Q.-m., Sun, Q.-s. & Liu, Y. Decreased expression of IL-27 and its correlation with Th1 and Th17 cells in progressive multiple sclerosis. *Journal of the neurological sciences* **348**, 174-180 (2015).

84 Lock, C., Hermans, G., Pedotti, R., Brendolan, A., Schadt, E., Garren, H., Langer-Gould, A., Strober, S., Cannella, B., Allard, J., Klonowski, P., Austin, A., Lad, N., Kaminski, N., Galli, S. J., Oksenberg, J. R., Raine, C. S., Heller, R. & Steinman, L. Gene-microarray analysis of multiple sclerosis lesions yields new targets validated in autoimmune encephalomyelitis. *Nature medicine* **8**, 500-508 (2002).

85 Tzartos, J. S., Friese, M. A., Craner, M. J., Palace, J., Newcombe, J., Esiri, M. M. & Fugger, L. Interleukin-17 production in central nervous system-infiltrating T cells and glial cells is associated with active disease in multiple sclerosis. *The American journal of pathology* **172**, 146-155 (2008).

86 Durelli, L., Conti, L., Clerico, M., Boselli, D., Contessa, G., Ripellino, P., Ferrero, B., Eid, P. & Novelli, F. T-helper 17 cells expand in multiple sclerosis and are inhibited by interferon-β. *Annals of neurology* **65**, 499-509 (2009).

87 Galli, E., Hartmann, F. J., Schreiner, B., Ingelfinger, F., Arvaniti, E., Diebold, M., Mrdjen, D., van der Meer, F., Krieg, C., Nimer, F. A., Sanderson, N., Stadelmann, C., Khademi, M., Piehl, F., Claassen, M., Derfuss, T., Olsson, T. & Becher, B. GM-CSF and CXCR4 define a T helper cell signature in multiple sclerosis. *Nature medicine* **25**, 1290-1300 (2019).

88 Lucchinetti, C., Brück, W., Parisi, J., Scheithauer, B., Rodriguez, M. & Lassmann, H. Heterogeneity of multiple sclerosis lesions: Implications for the pathogenesis of demyelination. *Annals of neurology* **47**, 707-717 (2000).

89 Croxford, A. L., Spath, S. & Becher, B. GM-CSF in Neuroinflammation: Licensing Myeloid Cells for Tissue Damage. *Trends in Immunology* **36**, 651-662 (2015).

90 Vogel, D. Y. S., Kooij, G., Heijnen, P. D. A. M., Breur, M., Peferoen, L. A. N., Valk, P., Vries, H. E., Amor, S. & Dijkstra, C. D. GM-CSF promotes migration of human monocytes across the blood brain barrier. *European journal of immunology* **45**, 1808-1819 (2015).

91 Imitola, J., Rasouli, J., Watanabe, F., Mahajan, K., Sharan, A. D., Ciric, B., Zhang, G.-X. & Rostami, A. Elevated expression of granulocyte-macrophage colony-stimulating factor receptor in multiple sclerosis lesions. *Journal of neuroimmunology* **317**, 45-54 (2018).

92 Rasouli, J., Ciric, B., Imitola, J., Gonnella, P., Hwang, D., Mahajan, K., Mari, E. R., Safavi, F., Leist, T. P., Zhang, G.-X. & Rostami, A. Expression of GM-CSF in T Cells Is Increased in Multiple Sclerosis and Suppressed by IFN-β Therapy. *The Journal of Immunology* **194**, 5085-5093 (2015).

93 Restorick, S. M., Durant, L., Kalra, S., Hassan-Smith, G., Rathbone, E., Douglas, M. R. & Curnow, S. J. CCR6+ Th cells in the cerebrospinal fluid of persons with multiple sclerosis are dominated by pathogenic non-classic Th1 cells and GM-CSF-only-secreting Th cells. *Brain, behavior, and immunity* **64**, 71-79 (2017).

94 Haas, J., Hug, A., Viehöver, A., Fritzsching, B., Falk, C. S., Filser, A., Vetter, T., Milkova, L., Korporal, M., Fritz, B., Storch-Hagenlocher, B., Krammer, P. H., Suri-Payer, E. & Wildemann, B. Reduced suppressive effect of CD4+CD25high regulatory T cells on the T cell immune response against myelin oligodendrocyte glycoprotein in patients with multiple sclerosis. *European journal of immunology* **35**, 3343-3352 (2005).

95 Jamshidian, A., Shaygannejad, V., Pourazar, A., Zarkesh-Esfahani, S.-H. & Gharagozloo, M. Biased Treg/Th17 balance away from regulatory toward inflammatory phenotype in relapsed multiple sclerosis and its correlation with severity of symptoms. *Journal of neuroimmunology* **262**, 106-112 (2013).

96 Haas, J., Korporal, M., Balint, B., Fritzsching, B., Schwarz, A. & Wildemann, B. Glatiramer acetate improves regulatory T-cell function by expansion of naive CD4+CD25+FOXP3+CD31+ T-cells in patients with multiple sclerosis. *Journal of neuroimmunology* **216**, 113-117 (2009).

97 Venken, K., Hellings, N., Hensen, K., Rummens, J.-L., Medaer, R., D'hooghe, M. B., Dubois, B., Raus, J. & Stinissen, P. Secondary progressive in contrast to relapsing-remitting multiple sclerosis patients show a normal CD4+CD25+ regulatory T-cell function and FOXP3 expression. *Journal of neuroscience research* **83**, 1432-1446 (2006).

98 Hauser, S. L., Bhan, A. K., Gilles, F., Kemp, M., Kerr, C. & Weiner, H. L. Immunohistochemical analysis of the cellular infiltrate in multiple sclerosis lesions. *Annals of neurology* **19**, 578-587 (1986).

99 Babbe, H., Roers, A., Waisman, A., Lassmann, H., Goebels, N., Hohlfeld, R., Friese, M., Schroder, R., Deckert, M., Schmidt, S., Ravid, R. & Rajewsky, K. Clonal expansions of CD8(+) T cells dominate the T cell infiltrate in active multiple sclerosis lesions as shown by micromanipulation and single cell polymerase chain reaction. *The Journal of experimental medicine* **192**, 393-404 (2000).

100 Burfoot, R. K., Jensen, C. J., Field, J., Stankovich, J., Varney, M. D., Johnson, L. J., Butzkueven, H., Booth, D., Bahlo, M., Tait, B. D., Taylor, B. V., Speed, T. P., Heard, R., Stewart, G. J., Foote, S. J., Kilpatrick, T. J. & Rubio, J. P. SNP mapping and candidate gene sequencing in the class I region of the HLA complex: Searching for multiple sclerosis susceptibility genes in Tasmanians. *Tissue Antigens* **71**, 42-50 (2008).

101 Giovanni, F., Domenico, P., Alessandro, M., Raffaele, I., Viviana, N., Katia, P. A. & Paola, B. A. Circulating CD8+CD56-perforin+ T cells are increased in multiple sclerosis patients. *Journal of neuroimmunology* **240-241**, 137-141 (2011).

102 Malmestrom, C., Lycke, J., Haghighi, S., Andersen, O., Carlsson, L., Wadenvik, H. & Olsson, B. Relapses in multiple sclerosis are associated with increased CD8+ T-cell mediated cytotoxicity in CSF. *Journal of neuroimmunology* **196**, 159-165 (2008).

103 Ifergan, I., Kebir, H., Alvarez, J. I., Marceau, G., Bernard, M., Bourbonniere, L., Poirier, J., Duquette, P., Talbot, P. J., Arbour, N. & Prat, A. Central nervous system recruitment of effector memory CD8+ T lymphocytes during neuroinflammation is dependent on alpha4 integrin. *Brain : a journal of neurology* **134**, 3560-3577 (2011).

104 Crawford, M. P., Yan, S. X., Ortega, S. B., Mehta, R. S., Hewitt, R. E., Price, D. A., Stastny, P., Douek, D. C., Koup, R. A., Racke, M. K. & Karandikar, N. J. High prevalence of autoreactive, neuroantigen-specific CD8+ T cells in multiple sclerosis revealed by novel flow cytometric assay. *Blood* **103**, 4222-4231 (2004).

105 Jurewicz, A., Biddison, W. E. & Antel, J. P. MHC Class I-Restricted Lysis of Human Oligodendrocytes by Myelin Basic Protein Peptide-Specific CD8 T Lymphocytes. *The Journal of Immunology* **160**, 3056-3059 (1998).

106 Pannemans, K., Broux, B., Goris, A., Dubois, B., Broekmans, T., Van Wijmeersch, B., Geraghty, D., Stinissen, P. & Hellings, N. HLA-E restricted CD8+ T cell subsets are phenotypically altered in multiple sclerosis patients. *Multiple sclerosis (Houndmills, Basingstoke, England)* (2013).
107 Milo, R. Therapeutic strategies targeting B-cells in multiple sclerosis. *Autoimmunity reviews* **15**, 714-718 (2016).
108 Yamout, B. I., El-Ayoubi, N. K., Nicolas, J., El Kouzi, Y., Khoury, S. J. & Zeineddine, M. M. Safety and Efficacy of Rituximab in Multiple Sclerosis: A Retrospective Observational Study. *Journal of Immunology Research* **2018**, 9 (2018).
109 Hauser, S., Arnold, D., Bar-Or, A., Comi, G., Hartung, H.-P., Lublin, F., Selmaj, K., Traboulsee, A., Klingelschmitt, G., Masterman, D., Fontoura, P., Chin, P., Garren, H. & Kappos, L. Efficacy of Ocrelizumab in Patients with Relapsing Multiple Sclerosis: Pooled Analysis of Two Identical Phase III, Double-Blind, Double-Dummy, Interferon Beta-1a-Controlled Studies (S49.003). *Neurology* **86**, S49.003 (2016).
110 Dobson, R., Ramagopalan, S., Davis, A. & Giovannoni, G. Cerebrospinal fluid oligoclonal bands in multiple sclerosis and clinically isolated syndromes: a meta-analysis of prevalence, prognosis and effect of latitude. *Journal of neurology, neurosurgery, and psychiatry* **84**, 909-914 (2013).
111 Cross, A. H., Stark, J. L., Lauber, J., Ramsbottom, M. J. & Lyons, J.-A. Rituximab reduces B cells and T cells in cerebrospinal fluid of multiple sclerosis patients. *Journal of neuroimmunology* **180**, 63-70 (2006).
112 Lisak, R. P., Nedelkoska, L., Benjamins, J. A., Schalk, D., Bealmear, B., Touil, H., Li, R., Muirhead, G. & Bar-Or, A. B cells from patients with multiple sclerosis induce cell death via apoptosis in neurons in vitro. *Journal of neuroimmunology* **309**, 88-99 (2017).
113 Bar-Or, A., Fawaz, L., Fan, B., Darlington, P. J., Rieger, A., Ghorayeb, C., Calabresi, P. A., Waubant, E., Hauser, S. L., Zhang, J. & Smith, C. H. Abnormal B-cell cytokine responses a trigger of T-cell–mediated disease in MS? *Annals of neurology* **67**, 452-461 (2010).
114 Li, R., Rezk, A., Miyazaki, Y., Hilgenberg, E., Touil, H., Shen, P., Moore, C. S., Michel, L., Althekair, F., Rajasekharan, S., Gommerman, J. L., Prat, A., Fillatreau, S. & Bar-Or, A. Proinflammatory GM-CSF-producing B cells in multiple sclerosis and B cell depletion therapy. *Science translational medicine* **7**, 310ra166 (2015).
115 Palanichamy, A., Jahn, S., Nickles, D., Derstine, M., Abounasr, A., Hauser, S. L., Baranzini, S. E., Leppert, D. & von Büdingen, H.-C. Rituximab Efficiently Depletes Increased CD20-Expressing T Cells in Multiple Sclerosis Patients. *The Journal of Immunology* **193**, 580-586 (2014).
116 Wilk, E., Witte, T., Marquardt, N., Horvath, T., Kalippke, K., Scholz, K., Wilke, N., Schmidt, R. E. & Jacobs, R. Depletion of functionally active CD20+ T cells by rituximab treatment. *Arthritis & Rheumatism* **60**, 3563-3571 (2009).
117 Schuh, E., Berer, K., Mulazzani, M., Feil, K., Meinl, I., Lahm, H., Krane, M., Lange, R., Pfannes, K., Subklewe, M., Gürkov, R., Bradl, M., Hohlfeld, R., Kümpfel, T., Meinl, E. & Krumbholz, M. Features of Human CD3⁺CD20⁺ T Cells. *The Journal of Immunology* **197**, 1111-1117 (2016).
118 Kappos, L., Hartung, H.-P., Freedman, M. S., Boyko, A., Radü, E. W., Mikol, D. D., Lamarine, M., Hyvert, Y., Freudensprung, U., Plitz, T. & van Beek, J. Atacicept in multiple sclerosis (ATAMS): a randomised, placebo-controlled, double-blind, phase 2 trial. *The Lancet Neurology* **13**, 353-363 (2014).
119 Hartung, H.-P. & Kieseier, B. C. Atacicept: targeting B cells in multiple sclerosis. *Therapeutic Advances in Neurological Disorders* **3**, 205-216 (2010).
120 Pender, M. P. & Burrows, S. R. Epstein–Barr virus and multiple sclerosis: potential opportunities for immunotherapy. *Clinical & Translational Immunology* **3**, e27 (2014).
121 Fernández-Menéndez, S., Fernández-Morán, M., Fernández-Vega, I., Pérez-Álvarez, A. & Villafani-Echazú, J. Epstein–Barr virus and multiple sclerosis. From evidence to therapeutic strategies. *Journal of the neurological sciences* **361**, 213-219 (2016).
122 Pakpoor, J., Disanto, G., Gerber, J. E., Dobson, R., Meier, U. C., Giovannoni, G. & Ramagopalan, S. V. The risk of developing multiple sclerosis in individuals seronegative for Epstein-Barr virus: a meta-analysis. *Multiple Sclerosis Journal* **19**, 162-166 (2013).
123 Ascherio, A. & Munch, M. Epstein-Barr Virus and Multiple Sclerosis. *Epidemiology* **11**, 220-224 (2000).

124 Márquez, A. C. & Horwitz, M. S. The Role of Latently Infected B Cells in CNS Autoimmunity. *Frontiers in immunology* **6** (2015).
125 Thacker, E. L., Mirzaei, F. & Ascherio, A. Infectious mononucleosis and risk for multiple sclerosis: A meta-analysis. *Annals of neurology* **59**, 499-503 (2006).
126 Belbasis, L., Bellou, V., Evangelou, E., Ioannidis, J. P. A. & Tzoulaki, I. Environmental risk factors and multiple sclerosis: an umbrella review of systematic reviews and meta-analyses. *The Lancet Neurology* **14**, 263-273 (2015).
127 Pender, M. P., Csurhes, P. A., Lenarczyk, A., Pfluger, C. M. M. & Burrows, S. R. Decreased T cell reactivity to Epstein–Barr virus infected lymphoblastoid cell lines in multiple sclerosis. *Journal of Neurology, Neurosurgery & Psychiatry* **80**, 498-505 (2009).
128 Owens, G. P. & Bennett, J. L. Trigger, pathogen, or bystander: the complex nexus linking Epstein–Barr virus and multiple sclerosis. *Multiple Sclerosis Journal* **18**, 1204-1208 (2012).
129 Lindsey, J. W. & Hatfield, L. M. Epstein-Barr virus and multiple sclerosis: Cellular immune response and cross-reactivity. *Journal of neuroimmunology* **229**, 238-242 (2010).
130 Ulvestad, E., Williams, K., Bø, L., Trapp, B., Antel, J. & Mørk, S. HLA class II molecules (HLA-DR, -DP, -DQ) on cells in the human CNS studied in situ and in vitro. *Immunology* **82**, 535-541 (1994).
131 Peferoen, L. A. N., Vogel, D. Y. S., Ummenthum, K., Breur, M., Heijnen, P. D. A. M., Gerritsen, W. H., Peferoen-Baert, R. M. B., van der Valk, P., Dijkstra, C. D. & Amor, S. Activation Status of Human Microglia Is Dependent on Lesion Formation Stage and Remyelination in Multiple Sclerosis. *Journal of Neuropathology & Experimental Neurology* **74**, 48-63 (2015).
132 Sharief, M. K. & Hentges, R. Association between Tumor Necrosis Factor-α and Disease Progression in Patients with Multiple Sclerosis. *New England Journal of Medicine* **325**, 467-472 (1991).
133 TNF neutralization in MS: results of a randomized, placebo-controlled multicenter study. The Lenercept Multiple Sclerosis Study Group and The University of British Columbia MS/MRI Analysis Group. *Neurology* **53**, 457-465 (1999).
134 van Oosten, B. W., Barkhof, F., Truyen, L., Boringa, J. B., Bertelsmann, F. W., von Blomberg, B. M., Woody, J. N., Hartung, H. P. & Polman, C. H. Increased MRI activity and immune activation in two multiple sclerosis patients treated with the monoclonal anti-tumor necrosis factor antibody cA2. *Neurology* **47**, 1531-1534 (1996).
135 Panitch, H., Haley, A., Hirsch, R. & Johnson, K. EXACERBATIONS OF MULTIPLE SCLEROSIS IN PATIENTS TREATED WITH GAMMA INTERFERON. *The Lancet* **329**, 893-895 (1987).
136 Reboldi, A., Coisne, C., Baumjohann, D., Benvenuto, F., Bottinelli, D., Lira, S., Uccelli, A., Lanzavecchia, A., Engelhardt, B. & Sallusto, F. C-C chemokine receptor 6-regulated entry of TH-17 cells into the CNS through the choroid plexus is required for the initiation of EAE. *Nature immunology* **10**, 514-523 (2009).
137 Yamazaki, T., Yang, X. O., Chung, Y., Fukunaga, A., Nurieva, R., Pappu, B., Martin-Orozco, N., Kang, H. S., Ma, L., Panopoulos, A. D., Craig, S., Watowich, S. S., Jetten, A. M., Tian, Q. & Dong, C. CCR6 regulates the migration of inflammatory and regulatory T cells. *Journal of immunology (Baltimore, Md. : 1950)* **181**, 8391-8401 (2008).
138 Kara, E. E., McKenzie, D. R., Bastow, C. R., Gregor, C. E., Fenix, K. A., Ogunniyi, A. D., Paton, J. C., Mack, M., Pombal, D. R., Seillet, C., Dubois, B., Liston, A., MacDonald, K. P., Belz, G. T., Smyth, M. J., Hill, G. R., Comerford, I. & McColl, S. R. CCR2 defines in vivo development and homing of IL-23-driven GM-CSF-producing Th17 cells. *Nat Commun* **6**, 8644 (2015).
139 Ambrosini, E., Remoli, M. E., Giacomini, E., Rosicarelli, B., Serafini, B., Lande, R., Aloisi, F. & Coccia, E. M. Astrocytes produce dendritic cell-attracting chemokines in vitro and in multiple sclerosis lesions. *Journal of neuropathology and experimental neurology* **64**, 706-715 (2005).
140 Kivisakk, P., Trebst, C., Liu, Z., Tucky, B. H., Sorensen, T. L., Rudick, R. A., Mack, M. & Ransohoff, R. M. T-cells in the cerebrospinal fluid express a similar repertoire of inflammatory chemokine receptors in the absence or presence of CNS inflammation: implications for CNS trafficking. *Clinical and experimental immunology* **129**, 510-518 (2002).

141 Ambrosini, E., Columba-Cabezas, S., Serafini, B., Muscella, A. & Aloisi, F. Astrocytes are the major intracerebral source of macrophage inflammatory protein-3alpha/CCL20 in relapsing experimental autoimmune encephalomyelitis and in vitro. *Glia* **41**, 290-300 (2003).
142 Dogan, R. N., Elhofy, A. & Karpus, W. J. Production of CCL2 by central nervous system cells regulates development of murine experimental autoimmune encephalomyelitis through the recruitment of TNF- and iNOS-expressing macrophages and myeloid dendritic cells. *Journal of immunology (Baltimore, Md. : 1950)* **180**, 7376-7384 (2008).
143 Szczucinski, A. & Losy, J. CCL5, CXCL10 and CXCL11 chemokines in patients with active and stable relapsing-remitting multiple sclerosis. *Neuroimmunomodulation* **18**, 67-72 (2011).
144 Rottman, J. B., Slavin, A. J., Silva, R., Weiner, H. L., Gerard, C. G. & Hancock, W. W. Leukocyte recruitment during onset of experimental allergic encephalomyelitis is CCR1 dependent. *European journal of immunology* **30**, 2372-2377 (2000).
145 Ubogu, E. E., Callahan, M. K., Tucky, B. H. & Ransohoff, R. M. Determinants of CCL5-driven mononuclear cell migration across the blood-brain barrier. Implications for therapeutically modulating neuroinflammation. *Journal of neuroimmunology* **179**, 132-144 (2006).
146 Columba-Cabezas, S., Serafini, B., Ambrosini, E. & Aloisi, F. Lymphoid chemokines CCL19 and CCL21 are expressed in the central nervous system during experimental autoimmune encephalomyelitis: implications for the maintenance of chronic neuroinflammation. *Brain pathology (Zurich, Switzerland)* **13**, 38-51 (2003).
147 Krumbholz, M., Theil, D., Steinmeyer, F., Cepok, S., Hemmer, B., Hofbauer, M., Farina, C., Derfuss, T., Junker, A., Arzberger, T., Sinicina, I., Hartle, C., Newcombe, J., Hohlfeld, R. & Meinl, E. CCL19 is constitutively expressed in the CNS, up-regulated in neuroinflammation, active and also inactive multiple sclerosis lesions. *Journal of neuroimmunology* **190**, 72-79 (2007).
148 Kivisakk, P., Mahad, D. J., Callahan, M. K., Sikora, K., Trebst, C., Tucky, B., Wujek, J., Ravid, R., Staugaitis, S. M., Lassmann, H. & Ransohoff, R. M. Expression of CCR7 in multiple sclerosis: implications for CNS immunity. *Annals of neurology* **55**, 627-638 (2004).
149 Alt, C., Laschinger, M. & Engelhardt, B. Functional expression of the lymphoid chemokines CCL19 (ELC) and CCL 21 (SLC) at the blood-brain barrier suggests their involvement in G-protein-dependent lymphocyte recruitment into the central nervous system during experimental autoimmune encephalomyelitis. *European journal of immunology* **32**, 2133-2144 (2002).
150 Sorensen, T. L., Tani, M., Jensen, J., Pierce, V., Lucchinetti, C., Folcik, V. A., Qin, S., Rottman, J., Sellebjerg, F., Strieter, R. M., Frederiksen, J. L. & Ransohoff, R. M. Expression of specific chemokines and chemokine receptors in the central nervous system of multiple sclerosis patients. *The Journal of clinical investigation* **103**, 807-815 (1999).
151 Wilson, E. H., Weninger, W. & Hunter, C. A. Trafficking of immune cells in the central nervous system. *The Journal of clinical investigation* **120**, 1368-1379 (2010).
152 Carlson, T., Kroenke, M., Rao, P., Lane, T. E. & Segal, B. The Th17-ELR+ CXC chemokine pathway is essential for the development of central nervous system autoimmune disease. *The Journal of experimental medicine* **205**, 811-823 (2008).
153 Muller, M., Carter, S. L., Hofer, M. J., Manders, P., Getts, D. R., Getts, M. T., Dreykluft, A., Lu, B., Gerard, C., King, N. J. & Campbell, I. L. CXCR3 signaling reduces the severity of experimental autoimmune encephalomyelitis by controlling the parenchymal distribution of effector and regulatory T cells in the central nervous system. *Journal of immunology (Baltimore, Md. : 1950)* **179**, 2774-2786 (2007).
154 Graham, G. J., Locati, M., Mantovani, A., Rot, A. & Thelen, M. The biochemistry and biology of the atypical chemokine receptors. *Immunology Letters* **145**, 30-38 (2012).
155 Nibbs, R. J. B. & Graham, G. J. Immune regulation by atypical chemokine receptors. *Nature reviews. Immunology* **13**, 815-829 (2013).
156 Cancellieri, C., Caronni, N., Vacchini, A., Savino, B., Borroni, E. M., Locati, M. & Bonecchi, R. Review: Structure-function and biological properties of the atypical chemokine receptor D6. *Molecular immunology* **55**, 87-93 (2013).
157 Liu, L., Graham, G. J., Damodaran, A., Hu, T., Lira, S. A., Sasse, M., Canasto-Chibuque, C., Cook, D. N. & Ransohoff, R. M. Cutting edge: the silent chemokine receptor D6 is required for generating T cell responses that mediate experimental autoimmune encephalomyelitis. *Journal of immunology (Baltimore, Md. : 1950)* **177**, 17-21 (2006).

158 Hansell, C. A., MacLellan, L. M., Oldham, R. S., Doonan, J., Chapple, K. J., Anderson, E. J., Linington, C., McInnes, I. B., Nibbs, R. J. & Goodyear, C. S. The atypical chemokine receptor ACKR2 suppresses Th17 responses to protein autoantigens. *Immunology and cell biology* **93**, 167-176 (2015).

159 Murphy, P. M. in *Clinical Immunology (Fifth Edition)* (eds Robert R. Rich *et al.*) 157-170.e151 (Content Repository Only!, 2019).

160 Nibbs, R. J., Kriehuber, E., Ponath, P. D., Parent, D., Qin, S., Campbell, J. D., Henderson, A., Kerjaschki, D., Maurer, D., Graham, G. J. & Rot, A. The beta-chemokine receptor D6 is expressed by lymphatic endothelium and a subset of vascular tumors. *The American journal of pathology* **158**, 867-877 (2001).

161 Madigan, J., Freeman, D. J., Menzies, F., Forrow, S., Nelson, S. M., Young, A., Sharkey, A., Moffett, A., Graham, G. J., Greer, I. A., Rot, A. & Nibbs, R. J. Chemokine scavenger D6 is expressed by trophoblasts and aids the survival of mouse embryos transferred into allogeneic recipients. *Journal of immunology (Baltimore, Md. : 1950)* **184**, 3202-3212 (2010).

162 McKimmie, C. S., Fraser, A. R., Hansell, C., Gutierrez, L., Philipsen, S., Connell, L., Rot, A., Kurowska-Stolarska, M., Carreno, P., Pruenster, M., Chu, C. C., Lombardi, G., Halsey, C., McInnes, I. B., Liew, F. Y., Nibbs, R. J. & Graham, G. J. Hemopoietic cell expression of the chemokine decoy receptor D6 is dynamic and regulated by GATA1. *Journal of immunology (Baltimore, Md. : 1950)* **181**, 8171-8181 (2008).

163 McKimmie, C. S. & Graham, G. J. Leucocyte expression of the chemokine scavenger D6. *Biochemical Society transactions* **34**, 1002-1004 (2006).

164 Lee, K. M., Nibbs, R. J. B. & Graham, G. J. D6: the 'crowd controller' at the immune gateway. *Trends in Immunology* **34**, 7-12 (2013).

165 Lee, K. M., McKimmie, C. S., Gilchrist, D. S., Pallas, K. J., Nibbs, R. J., Garside, P., McDonald, V., Jenkins, C., Ransohoff, R., Liu, L., Milling, S., Cerovic, V. & Graham, G. J. D6 facilitates cellular migration and fluid flow to lymph nodes by suppressing lymphatic congestion. *Blood* **118**, 6220-6229 (2011).

166 Jamieson, T., Cook, D. N., Nibbs, R. J., Rot, A., Nixon, C., McLean, P., Alcami, A., Lira, S. A., Wiekowski, M. & Graham, G. J. The chemokine receptor D6 limits the inflammatory response in vivo. *Nature immunology* **6**, 403-411 (2005).

167 Di Liberto, D., Locati, M., Caccamo, N., Vecchi, A., Meraviglia, S., Salerno, A., Sireci, G., Nebuloni, M., Caceres, N., Cardona, P. J., Dieli, F. & Mantovani, A. Role of the chemokine decoy receptor D6 in balancing inflammation, immune activation, and antimicrobial resistance in Mycobacterium tuberculosis infection. *The Journal of experimental medicine* **205**, 2075-2084 (2008).

168 Martinez de la Torre, Y., Locati, M., Buracchi, C., Dupor, J., Cook, D. N., Bonecchi, R., Nebuloni, M., Rukavina, D., Vago, L., Vecchi, A., Lira, S. A. & Mantovani, A. Increased inflammation in mice deficient for the chemokine decoy receptor D6. *European journal of immunology* **35**, 1342-1346 (2005).

169 Mantovani, A., Bonecchi, R. & Locati, M. Tuning inflammation and immunity by chemokine sequestration: decoys and more. *Nature reviews. Immunology* **6**, 907-918 (2006).

170 Heinzel, K., Benz, C. & Bleul, C. C. A silent chemokine receptor regulates steady-state leukocyte homing in vivo. *Proceedings of the National Academy of Sciences of the United States of America* **104**, 8421-8426 (2007).

171 Townson, J. R. & Nibbs, R. J. Characterization of mouse CCX-CKR, a receptor for the lymphocyte-attracting chemokines TECK/mCCL25, SLC/mCCL21 and MIP-3beta/mCCL19: comparison to human CCX-CKR. *European journal of immunology* **32**, 1230-1241 (2002).

172 Bryce, S. A., Wilson, R. A. M., Tiplady, E. M., Asquith, D. L., Bromley, S. K., Luster, A. D., Graham, G. J. & Nibbs, R. J. B. ACKR4 on Stromal Cells Scavenges CCL19 To Enable CCR7-Dependent Trafficking of APCs from Inflamed Skin to Lymph Nodes. *The Journal of Immunology* **196**, 3341-3353 (2016).

173 Comerford, I., Nibbs, R. J., Litchfield, W., Bunting, M., Harata-Lee, Y., Haylock-Jacobs, S., Forrow, S., Korner, H. & McColl, S. R. The atypical chemokine receptor CCX-CKR scavenges homeostatic chemokines in circulation and tissues and suppresses Th17 responses. *Blood* **116**, 4130-4140 (2010).

174 Baldassari, L. E. & Fox, R. J. Therapeutic Advances and Challenges in the Treatment of Progressive Multiple Sclerosis. *Drugs* (2018).
175 Dörr, J. & Paul, F. The Transition From First-Line to Second-Line Therapy in Multiple Sclerosis. *Curr Treat Options Neurol* **17**, 1-12 (2015).
176 Paty, D. W. & Li, D. K. B. Interferon beta-1b is effective in relapsing-remitting multiple sclerosis. *II. MRI analysis results of a multicenter, randomized, double-blind, placebo-controlled trial* **43**, 662-662 (1993).
177 Goodin, D. S., Reder, A. T., Ebers, G. C., Cutter, G., Kremenchutzky, M., Oger, J., Langdon, D., Rametta, M., Beckmann, K., DeSimone, T. M. & Knappertz, V. Survival in MS. *A randomized cohort study 21 years after the start of the pivotal IFNβ-1b trial* **78**, 1315-1322 (2012).
178 Ebers, G. C. Randomised double-blind placebo-controlled study of interferon β-1a in relapsing/remitting multiple sclerosis. *The Lancet* **352**, 1498-1504 (1998).
179 Li, D. K. B., Paty, D. W., Group, U. M. M. A. R. & Group, t. P. S. Magnetic resonance imaging results of the PRISMS trial: A randomized, double-blind, placebo-controlled study of interferon-β1a in relapsing-remitting multiple sclerosis. *Annals of neurology* **46**, 197-206 (1999).
180 Kozovska, M. E., Hong, J., Zang, Y. C. Q., Li, S., Rivera, V. M., Killian, J. M. & Zhang, J. Z. Interferon beta induces T-helper 2 immune deviation in MS. *Neurology* **53**, 1692-1692 (1999).
181 Vandenbark, A. A., Huan, J., Agotsch, M., La Tocha, D., Goelz, S., Offner, H., Lanker, S. & Bourdette, D. Interferon-beta-1a treatment increases CD56bright natural killer cells and CD4+CD25+ Foxp3 expression in subjects with multiple sclerosis. *Journal of neuroimmunology* **215**, 125-128 (2009).
182 Hall, G. L., Compston, A. & Scolding, N. J. Beta-interferon and multiple sclerosis. *Trends in Neurosciences* **20**, 63-67 (1997).
183 Kieseier, B. C. The Mechanism of Action of Interferon-β in Relapsing Multiple Sclerosis. *CNS Drugs* **25**, 491-502 (2011).
184 Comi, G., Radaelli, M. & Soelberg Sørensen, P. Evolving concepts in the treatment of relapsing multiple sclerosis. *The Lancet* **389**, 1347-1356 (2017).
185 Kuerten, S., Jackson, L. J., Kaye, J. & Vollmer, T. L. Impact of Glatiramer Acetate on B Cell-Mediated Pathogenesis of Multiple Sclerosis. *CNS Drugs* (2018).
186 Basile, E., Gibbs, E., Aziz, T. & Oger, J. During 3 years treatment of primary progressive multiple sclerosis with glatiramer acetate, specific antibodies switch from IgG1 to IgG4. *Journal of neuroimmunology* **177**, 161-166 (2006).
187 Bomprezzi, R., Schaefer, R., Reese, V., Misra, A., Vollmer, T. L. & Kala, M. Glatiramer Acetate-Specific Antibody Titres in Patients with Relapsing/Remitting Multiple Sclerosis and in Experimental Autoimmune Encephalomyelitis. *Scandinavian Journal of Immunology* **74**, 219-226 (2011).
188 Sellebjerg, F., Hedegaard, C., Krakauer, M., Hesse, D., Lund, H., Nielsen, C., Søndergaard, H. & Sørensen, P. Glatiramer acetate antibodies, gene expression and disease activity in multiple sclerosis. *Multiple Sclerosis Journal* **18**, 305-313 (2012).
189 Jackson, L., Selva, S., Niedzielko, T. & Vollmer, T. B Cell Receptor Recognition Of Glatiramer Acetate Is Required For Efficacy In Experimental Autoimmune Encephalomyelitis And Results In Differential Cytokine Production In MS Patients (P1.210). *Neurology* **82**, P1.210 (2014).
190 Ireland, S. J., Guzman, A. A., O'Brien, D. E., Hughes, S., Greenberg, B., Flores, A., Graves, D., Remington, G., Frohman, E. M., Davis, L. S. & Monson, N. L. The Effect of Glatiramer Acetate Therapy on Functional Properties of B Cells From Patients With Relapsing-Remitting Multiple Sclerosis. *JAMA Neurology* **71**, 1421-1428 (2014).
191 Carrieri, P. B., Carbone, F., Perna, F., Bruzzese, D., La Rocca, C., Galgani, M., Montella, S., Petracca, M., Florio, C., Maniscalco, G. T., Spitaleri, D. L. A., Iuliano, G., Tedeschi, G., Corte, M. D., Bonavita, S. & Matarese, G. Longitudinal assessment of immuno-metabolic parameters in multiple sclerosis patients during treatment with glatiramer acetate. *Metabolism* **64**, 1112-1121 (2015).
192 Linker, R. A., Lee, D.-H., Ryan, S., van Dam, A. M., Conrad, R., Bista, P., Zeng, W., Hronowsky, X., Buko, A., Chollate, S., Ellrichmann, G., Brück, W., Dawson, K., Goelz, S., Wiese, S., Scannevin, R. H., Lukashev, M. & Gold, R. Fumaric acid esters exert neuroprotective effects in

neuroinflammation via activation of the Nrf2 antioxidant pathway. *Brain : a journal of neurology* **134**, 678-692 (2011).

193 Scannevin, R. H., Chollate, S., Jung, M.-y., Shackett, M., Patel, H., Bista, P., Zeng, W., Ryan, S., Yamamoto, M., Lukashev, M. & Rhodes, K. J. Fumarates Promote Cytoprotection of Central Nervous System Cells against Oxidative Stress via the Nuclear Factor (Erythroid-Derived 2)-Like 2 Pathway. *Journal of Pharmacology and Experimental Therapeutics* **341**, 274-284 (2012).

194 Gold, R., Kappos, L., Arnold, D. L., Bar-Or, A., Giovannoni, G., Selmaj, K., Tornatore, C., Sweetser, M. T., Yang, M., Sheikh, S. I. & Dawson, K. T. Placebo-Controlled Phase 3 Study of Oral BG-12 for Relapsing Multiple Sclerosis. *New England Journal of Medicine* **367**, 1098-1107 (2012).

195 O'Connor, P., Wolinsky, J. S., Confavreux, C., Comi, G., Kappos, L., Olsson, T. P., Benzerdjeb, H., Truffinet, P., Wang, L., Miller, A. & Freedman, M. S. Randomized Trial of Oral Teriflunomide for Relapsing Multiple Sclerosis. *New England Journal of Medicine* **365**, 1293-1303 (2011).

196 Torkildsen, Ø., Myhr, K.-M. & Bø, L. Disease-modifying treatments for multiple sclerosis – a review of approved medications. *European Journal of Neurology* **23**, 18-27 (2016).

197 Shirani, A. & Stüve, O. Natalizumab for Multiple Sclerosis: A Case in Point for the Impact of Translational Neuroimmunology. *The Journal of Immunology* **198**, 1381 (2017).

198 Voge, N. V. & Alvarez, E. Monoclonal Antibodies in Multiple Sclerosis: Present and Future. *Biomedicines* **7** (2019).

199 Hauser, S. L., Chan, J. R. & Oksenberg, J. R. Multiple sclerosis: Prospects and promise. *Annals of neurology* **74**, 317-327 (2013).

200 Polman, C. H., O'Connor, P. W., Havrdova, E., Hutchinson, M., Kappos, L., Miller, D. H., Phillips, J. T., Lublin, F. D., Giovannoni, G., Wajgt, A., Toal, M., Lynn, F., Panzara, M. A. & Sandrock, A. W. A Randomized, Placebo-Controlled Trial of Natalizumab for Relapsing Multiple Sclerosis. *New England Journal of Medicine* **354**, 899-910 (2006).

201 Orthmann-Murphy, J. & Calabresi, P. Therapeutic Application of Monoclonal Antibodies in Multiple Sclerosis. *Clinical Pharmacology & Therapeutics* **101**, 52-64 (2017).

202 Cohen, J. A., Coles, A. J., Arnold, D. L., Confavreux, C., Fox, E. J., Hartung, H.-P., Havrdova, E., Selmaj, K. W., Weiner, H. L., Fisher, E., Brinar, V. V., Giovannoni, G., Stojanovic, M., Ertik, B. I., Lake, S. L., Margolin, D. H., Panzara, M. A. & Compston, D. A. S. Alemtuzumab versus interferon beta 1a as first-line treatment for patients with relapsing-remitting multiple sclerosis: a randomised controlled phase 3 trial. *The Lancet* **380**, 1819-1828 (2012).

203 Havrdova, E., Horakova, D. & Kovarova, I. Alemtuzumab in the treatment of multiple sclerosis: key clinical trial results and considerations for use. *Therapeutic advances in neurological disorders* **8**, 31-45 (2015).

204 Singer, B. A. Fingolimod for the treatment of relapsing multiple sclerosis. *Expert Review of Neurotherapeutics* **13**, 589-602 (2013).

205 Kappos, L., Radue, E. W., O'Connor, P., Polman, C., Hohlfeld, R., Calabresi, P., Selmaj, K., Agoropoulou, C., Leyk, M., Zhang-Auberson, L. & Burtin, P. A placebo-controlled trial of oral fingolimod in relapsing multiple sclerosis. *N Engl J Med* **362**, 387-401 (2010).

206 Hartung, H.-P., Gonsette, R., Konig, N., Kwiecinski, H., Guseo, A., Morrissey, S. P., Krapf, H. & Zwingers, T. Mitoxantrone in progressive multiple sclerosis: a placebo-controlled, double-blind, randomised, multicentre trial. *The Lancet* **360**, 2018-2025 (2002).

207 Ragonese, P., Aridon, P., Realmuto, S., Vazzoler, G., Alessi, S., Portera, E., Bianchi, A., Triolo, F., Mazzola, M. A., D'Amelio, M., Savettieri, G. & Salemi, G. Cardiovascular comorbidity in multiple sclerosis patients treated with Mitoxantrone therapy: a cohort study. *Multiple Sclerosis and Demyelinating Disorders* **2**, 12 (2017).

208 Marriott, J. J., Miyasaki, J. M., Gronseth, G. & O'Connor, P. W. Evidence Report: The efficacy and safety of mitoxantrone (Novantrone) in the treatment of multiple sclerosis: Report of the Therapeutics and Technology Assessment Subcommittee of the American Academy of Neurology. *Neurology* **74**, 1463-1470 (2010).

209 Sedal, L., Winkel, A., Laing, J., Law, L. Y. & McDonald, E. Current concepts in multiple sclerosis therapy. *Degener Neurol Neuromuscul Dis* **7**, 109-125 (2017).

210 Muraro, P. A., Pasquini, M., Atkins, H. L., Bowen, J. D., Farge, D., Fassas, A., Freedman, M. S., Georges, G. E., Gualandi, F., Hamerschlak, N., Havrdova, E., Kimiskidis, V. K., Kozak, T.,

Mancardi, G. L., Massacesi, L., Moraes, D. A., Nash, R. A., Pavletic, S., Ouyang, J., Rovira, M., Saiz, A., Simoes, B., Trneny, M., Zhu, L., Badoglio, M., Zhong, X., Sormani, M. P. & Saccardi, R. Long-term Outcomes After Autologous Hematopoietic Stem Cell Transplantation for Multiple Sclerosis. *JAMA Neurol* **74**, 459-469 (2017).

211 Dargahi, N., Katsara, M., Tselios, T., Androutsou, M. E., de Courten, M., Matsoukas, J. & Apostolopoulos, V. Multiple Sclerosis: Immunopathology and Treatment Update. *Brain Sci* **7** (2017).

212 Herberts, C. A., Kwa, M. S. G. & Hermsen, H. P. H. Risk factors in the development of stem cell therapy. *Journal of translational medicine* **9**, 29-29 (2011).

213 Kim, H. J. & Park, J.-S. Usage of Human Mesenchymal Stem Cells in Cell-based Therapy: Advantages and Disadvantages. *Development & reproduction* **21**, 1-10 (2017).

214 Friedenstein, A. J., Chailakhjan, R. K. & Lalykina, K. S. The development of fibroblast colonies in monolayer cultures of guinea-pig bone marrow and spleen cells. *Cell Tissue Kinet* **3** (1970).

215 Pittenger, M. F., Mackay, A. M., Beck, S. C., Jaiswal, R. K., Douglas, R., Mosca, J. D., Moorman, M. A., Simonetti, D. W., Craig, S. & Marshak, D. R. Multilineage potential of adult human mesenchymal stem cells. *Science (New York, N.Y.)* **284**, 143-147 (1999).

216 Kuhn, N. Z. & Tuan, R. S. Regulation of stemness and stem cell niche of mesenchymal stem cells: Implications in tumorigenesis and metastasis. *Journal of cellular physiology* **222**, 268-277 (2010).

217 da Silva Meirelles, L., Chagastelles, P. C. & Nardi, N. B. Mesenchymal stem cells reside in virtually all post-natal organs and tissues. *J Cell Sci* **119** (2006).

218 Dominici, M., Le Blanc, K., Mueller, I., Slaper-Cortenbach, I., Marini, F., Krause, D., Deans, R., Keating, A., Prockop, D. & Horwitz, E. Minimal criteria for defining multipotent mesenchymal stromal cells. The International Society for Cellular Therapy position statement. *Cytotherapy* **8**, 315-317 (2006).

219 Strioga, M., Viswanathan, S., Darinskas, A., Slaby, O. & Michalek, J. Same or not the same? Comparison of adipose tissue-derived versus bone marrow-derived mesenchymal stem and stromal cells. *Stem cells and development* **21**, 2724-2752 (2012).

220 Lemos, D. R. & Duffield, J. S. Tissue-resident mesenchymal stromal cells: Implications for tissue-specific antifibrotic therapies. *Science translational medicine* **10** (2018).

221 Lv, F. J., Tuan, R. S., Cheung, K. M. & Leung, V. Y. Concise review: the surface markers and identity of human mesenchymal stem cells. *Stem cells (Dayton, Ohio)* **32**, 1408-1419 (2014).

222 Sacchetti, B., Funari, A., Remoli, C., Giannicola, G., Kogler, G., Liedtke, S., Cossu, G., Serafini, M., Sampaolesi, M., Tagliafico, E., Tenedini, E., Saggio, I., Robey, P. G., Riminucci, M. & Bianco, P. No Identical "Mesenchymal Stem Cells" at Different Times and Sites: Human Committed Progenitors of Distinct Origin and Differentiation Potential Are Incorporated as Adventitial Cells in Microvessels. *Stem cell reports* **6**, 897-913 (2016).

223 Hass, R., Kasper, C., Böhm, S. & Jacobs, R. Different populations and sources of human mesenchymal stem cells (MSC): A comparison of adult and neonatal tissue-derived MSC. *Cell communication and signaling : CCS* **9**, 12-12 (2011).

224 Kwon, A., Kim, Y., Kim, M., Kim, J., Choi, H., Jekarl, D. W., Lee, S., Kim, J. M., Shin, J.-C. & Park, I. Y. Tissue-specific Differentiation Potency of Mesenchymal Stromal Cells from Perinatal Tissues. *Scientific reports* **6**, 23544 (2016).

225 Vasandan, A. B., Shankar, S. R., Prasad, P., Sowmya Jahnavi, V., Bhonde, R. R. & Jyothi Prasanna, S. Functional differences in mesenchymal stromal cells from human dental pulp and periodontal ligament. *Journal of Cellular and Molecular Medicine* **18**, 344-354 (2014).

226 Li, L. & Clevers, H. Coexistence of Quiescent and Active Adult Stem Cells in Mammals. *Science (New York, N.Y.)* **327**, 542 (2010).

227 Crisan, M., Yap, S., Casteilla, L., Chen, C. W., Corselli, M., Park, T. S., Andriolo, G., Sun, B., Zheng, B., Zhang, L., Norotte, C., Teng, P. N., Traas, J., Schugar, R., Deasy, B. M., Badylak, S., Buhring, H. J., Giacobino, J. P., Lazzari, L., Huard, J. & Peault, B. A perivascular origin for mesenchymal stem cells in multiple human organs. *Cell stem cell* **3**, 301-313 (2008).

228 Shi, S. & Gronthos, S. Perivascular niche of postnatal mesenchymal stem cells in human bone marrow and dental pulp. *J Bone Miner Res* **18** (2003).

229 Zannettino, A. C., Paton, S., Arthur, A., Khor, F., Itescu, S., Gimble, J. M. & Gronthos, S. Multipotential human adipose-derived stromal stem cells exhibit a perivascular phenotype in vitro and in vivo. *Journal of cellular physiology* **214**, 413-421 (2008).

230 Corselli, M., Chen, C. W., Crisan, M., Lazzari, L. & Peault, B. Perivascular ancestors of adult multipotent stem cells. *Arterioscler Thromb Vasc Biol* **30**, 1104-1109 (2010).

231 Corselli, M., Chen, C. W., Sun, B., Yap, S., Rubin, J. P. & Peault, B. The tunica adventitia of human arteries and veins as a source of mesenchymal stem cells. *Stem cells and development* **21**, 1299-1308 (2012).

232 Zhao, H., Feng, J., Seidel, K., Shi, S., Klein, O., Sharpe, P. & Chai, Y. Secretion of Shh by a Neurovascular Bundle Niche Supports Mesenchymal Stem Cell Homeostasis in the Adult Mouse Incisor. *Cell stem cell* **14**, 160-173 (2014).

233 Guimarães-Camboa, N., Cattaneo, P., Sun, Y., Moore-Morris, T., Gu, Y., Dalton, N. D., Rockenstein, E., Masliah, E., Peterson, K. L., Stallcup, W. B., Chen, J. & Evans, S. M. Pericytes of Multiple Organs Do Not Behave as Mesenchymal Stem Cells In Vivo. *Cell stem cell* **20**, 345-359.e345 (2017).

234 da Silva Meirelles, L., Caplan, A. I. & Nardi, N. B. In Search of the In Vivo Identity of Mesenchymal Stem Cells. *Stem cells (Dayton, Ohio)* **26**, 2287-2299 (2008).

235 Kolf, C. M., Cho, E. & Tuan, R. S. Mesenchymal stromal cells: Biology of adult mesenchymal stem cells: regulation of niche, self-renewal and differentiation. *Arthritis Research & Therapy* **9**, 204 (2007).

236 Su, J., Chen, X., Huang, Y., Li, W., Li, J., Cao, K., Cao, G., Zhang, L., Li, F., Roberts, A. I., Kang, H., Yu, P., Ren, G., Ji, W., Wang, Y. & Shi, Y. Phylogenetic distinction of iNOS and IDO function in mesenchymal stem cell-mediated immunosuppression in mammalian species. *Cell death and differentiation* **21**, 388-396 (2014).

237 Ren, G., Su, J., Zhang, L., Zhao, X., Ling, W., L'Huillie, A., Zhang, J., Lu, Y., Roberts, A. I., Ji, W., Zhang, H., Rabson, A. B. & Shi, Y. Species variation in the mechanisms of mesenchymal stem cell-mediated immunosuppression. *Stem cells (Dayton, Ohio)* **27**, 1954-1962 (2009).

238 English, K., Barry, F. P., Field-Corbett, C. P. & Mahon, B. P. IFN-gamma and TNF-alpha differentially regulate immunomodulation by murine mesenchymal stem cells. *Immunol Lett* **110**, 91-100 (2007).

239 Krampera, M., Cosmi, L., Angeli, R., Pasini, A., Liotta, F., Andreini, A., Santarlasci, V., Mazzinghi, B., Pizzolo, G., Vinante, F., Romagnani, P., Maggi, E., Romagnani, S. & Annunziato, F. Role for interferon-gamma in the immunomodulatory activity of human bone marrow mesenchymal stem cells. *Stem cells (Dayton, Ohio)* **24**, 386-398 (2006).

240 Zhang, B., Liu, R., Shi, D., Liu, X., Chen, Y., Dou, X., Zhu, X., Lu, C., Liang, W., Liao, L., Zenke, M. & Zhao, R. C. Mesenchymal stem cells induce mature dendritic cells into a novel Jagged-2-dependent regulatory dendritic cell population. *Blood* **113**, 46-57 (2009).

241 Nauta, A. J., Kruisselbrink, A. B., Lurvink, E., Willemze, R. & Fibbe, W. E. Mesenchymal stem cells inhibit generation and function of both CD34+-derived and monocyte-derived dendritic cells. *Journal of immunology (Baltimore, Md. : 1950)* **177**, 2080-2087 (2006).

242 Djouad, F., Charbonnier, L. M., Bouffi, C., Louis-Plence, P., Bony, C., Apparailly, F., Cantos, C., Jorgensen, C. & Noel, D. Mesenchymal stem cells inhibit the differentiation of dendritic cells through an interleukin-6-dependent mechanism. *Stem cells (Dayton, Ohio)* **25**, 2025-2032 (2007).

243 Li, Y. P., Paczesny, S., Lauret, E., Poirault, S., Bordigoni, P., Mekhloufi, F., Hequet, O., Bertrand, Y., Ou-Yang, J. P., Stoltz, J. F., Miossec, P. & Eljaafari, A. Human mesenchymal stem cells license adult CD34+ hemopoietic progenitor cells to differentiate into regulatory dendritic cells through activation of the Notch pathway. *Journal of immunology (Baltimore, Md. : 1950)* **180**, 1598-1608 (2008).

244 Liu, X., Qu, X., Chen, Y., Liao, L., Cheng, K., Shao, C., Zenke, M., Keating, A. & Zhao, R. C. Mesenchymal stem/stromal cells induce the generation of novel IL-10-dependent regulatory dendritic cells by SOCS3 activation. *Journal of immunology (Baltimore, Md. : 1950)* **189**, 1182-1192 (2012).

245 Chen, L., Zhang, W., Yue, H., Han, Q., Chen, B., Shi, M., Li, J., Li, B., You, S., Shi, Y. & Zhao, R. C. Effects of human mesenchymal stem cells on the differentiation of dendritic cells from CD34+ cells. *Stem cells and development* **16**, 719-731 (2007).

246 Xu, C., Fu, F., Li, X. & Zhang, S. Mesenchymal stem cells maintain the microenvironment of central nervous system by regulating the polarization of macrophages/microglia after traumatic brain injury. *Int J Neurosci* **127**, 1124-1135 (2017).

247 Jaimes, Y., Naaldijk, Y., Wenk, K., Leovsky, C. & Emmrich, F. Mesenchymal Stem Cell-Derived Microvesicles Modulate Lipopolysaccharides-Induced Inflammatory Responses to Microglia Cells. *Stem cells (Dayton, Ohio)* **35**, 812-823 (2017).

248 Najar, M., Raicevic, G., Boufker, H. I., Fayyad Kazan, H., De Bruyn, C., Meuleman, N., Bron, D., Toungouz, M. & Lagneaux, L. Mesenchymal stromal cells use PGE2 to modulate activation and proliferation of lymphocyte subsets: Combined comparison of adipose tissue, Wharton's Jelly and bone marrow sources. *Cellular immunology* **264**, 171-179 (2010).

249 Ryan, J. M., Barry, F., Murphy, J. M. & Mahon, B. P. Interferon-gamma does not break, but promotes the immunosuppressive capacity of adult human mesenchymal stem cells. *Clinical and experimental immunology* **149**, 353-363 (2007).

250 Tse, W. T., Pendleton, J. D., Beyer, W. M., Egalka, M. C. & Guinan, E. C. Suppression of allogeneic T-cell proliferation by human marrow stromal cells: implications in transplantation. *Transplantation* **75**, 389-397 (2003).

251 Meisel, R., Zibert, A., Laryea, M., Gobel, U., Daubener, W. & Dilloo, D. Human bone marrow stromal cells inhibit allogeneic T-cell responses by indoleamine 2,3-dioxygenase-mediated tryptophan degradation. *Blood* **103**, 4619-4621 (2004).

252 Aggarwal, S. & Pittenger, M. F. Human mesenchymal stem cells modulate allogeneic immune cell responses. *Blood* **105**, 1815-1822 (2005).

253 Szabo, E., Fajka-Boja, R., Kriston-Pal, E., Hornung, A., Makra, I., Kudlik, G., Uher, F., Katona, R. L., Monostori, E. & Czibula, A. Licensing by Inflammatory Cytokines Abolishes Heterogeneity of Immunosuppressive Function of Mesenchymal Stem Cell Population. *Stem cells and development* **24**, 2171-2180 (2015).

254 Ren, G., Zhang, L., Zhao, X., Xu, G., Zhang, Y., Roberts, A. I., Zhao, R. C. & Shi, Y. Mesenchymal stem cell-mediated immunosuppression occurs via concerted action of chemokines and nitric oxide. *Cell stem cell* **2**, 141-150 (2008).

255 Rozenberg, A., Rezk, A., Boivin, M. N., Darlington, P. J., Nyirenda, M., Li, R., Jalili, F., Winer, R., Artsy, E. A., Uccelli, A., Reese, J. S., Planchon, S. M., Cohen, J. A. & Bar-Or, A. Human Mesenchymal Stem Cells Impact Th17 and Th1 Responses Through a Prostaglandin E2 and Myeloid-Dependent Mechanism. *Stem cells translational medicine* (2016).

256 Ghannam, S., Pène, J., Torcy-Moquet, G., Jorgensen, C. & Yssel, H. Mesenchymal Stem Cells Inhibit Human Th17 Cell Differentiation and Function and Induce a T Regulatory Cell Phenotype. *The Journal of Immunology* **185**, 302-312 (2010).

257 Bai, L., Lennon, D. P., Eaton, V., Maier, K., Caplan, A. I., Miller, S. D. & Miller, R. H. Human bone marrow-derived mesenchymal stem cells induce Th2-polarized immune response and promote endogenous repair in animal models of multiple sclerosis. *Glia* **57**, 1192-1203 (2009).

258 English, K., Ryan, J. M., Tobin, L., Murphy, M. J., Barry, F. P. & Mahon, B. P. Cell contact, prostaglandin E2 and transforming growth factor beta 1 play non-redundant roles in human mesenchymal stem cell induction of CD4+CD25Highforkhead box P3+ regulatory T cells. *Clinical & Experimental Immunology* **156**, 149-160 (2009).

259 Ge, W., Jiang, J., Arp, J., Liu, W., Garcia, B. & Wang, H. Regulatory T-cell generation and kidney allograft tolerance induced by mesenchymal stem cells associated with indoleamine 2,3-dioxygenase expression. *Transplantation* **90**, 1312-1320 (2010).

260 Tasso, R., Ilengo, C., Quarto, R., Cancedda, R., Caspi, R. R. & Pennesi, G. Mesenchymal stem cells induce functionally active T-regulatory lymphocytes in a paracrine fashion and ameliorate experimental autoimmune uveitis. *Investigative ophthalmology & visual science* **53**, 786-793 (2012).

261 Akiyama, K., Chen, C., Wang, D., Xu, X., Qu, C., Yamaza, T., Cai, T., Chen, W., Sun, L. & Shi, S. Mesenchymal-stem-cell-induced immunoregulation involves FAS-ligand-/FAS-mediated T cell apoptosis. *Cell stem cell* **10**, 544-555 (2012).

262 Duffy, M. M., Pindjakova, J., Hanley, S. A., McCarthy, C., Weidhofer, G. A., Sweeney, E. M., English, K., Shaw, G., Murphy, J. M., Barry, F. P., Mahon, B. P., Belton, O., Ceredig, R. & Griffin, M. D. Mesenchymal stem cell inhibition of T-helper 17 cell- differentiation is triggered by cell-cell contact and mediated by prostaglandin E2 via the EP4 receptor. *European journal of immunology* **41**, 2840-2851 (2011).

263 Martinet, L., Fleury-Cappellesso, S., Gadelorge, M., Dietrich, G., Bourin, P., Fournie, J. J. & Poupot, R. A regulatory cross-talk between Vgamma9Vdelta2 T lymphocytes and mesenchymal stem cells. *European journal of immunology* **39**, 752-762 (2009).

264 Lim, J. H., Kim, J. S., Yoon, I. H., Shin, J. S., Nam, H. Y., Yang, S. H., Kim, S. J. & Park, C. G. Immunomodulation of delayed-type hypersensitivity responses by mesenchymal stem cells is associated with bystander T cell apoptosis in the draining lymph node. *Journal of immunology (Baltimore, Md. : 1950)* **185**, 4022-4029 (2010).

265 Luz-Crawford, P., Kurte, M., Bravo-Alegria, J., Contreras, R., Nova-Lamperti, E., Tejedor, G., Noel, D., Jorgensen, C., Figueroa, F., Djouad, F. & Carrion, F. Mesenchymal stem cells generate a CD4+CD25+Foxp3+ regulatory T cell population during the differentiation process of Th1 and Th17 cells. *Stem cell research & therapy* **4**, 65 (2013).

266 Schena, F., Gambini, C., Gregorio, A., Mosconi, M., Reverberi, D., Gattorno, M., Casazza, S., Uccelli, A., Moretta, L., Martini, A. & Traggiai, E. Interferon-gamma-dependent inhibition of B cell activation by bone marrow-derived mesenchymal stem cells in a murine model of systemic lupus erythematosus. *Arthritis and rheumatism* **62**, 2776-2786 (2010).

267 Augello, A., Tasso, R., Negrini, S. M., Amateis, A., Indiveri, F., Cancedda, R. & Pennesi, G. Bone marrow mesenchymal progenitor cells inhibit lymphocyte proliferation by activation of the programmed death 1 pathway. *European journal of immunology* **35**, 1482-1490 (2005).

268 Corcione, A., Benvenuto, F., Ferretti, E., Giunti, D., Cappiello, V., Cazzanti, F., Risso, M., Gualandi, F., Mancardi, G. L., Pistoia, V. & Uccelli, A. Human mesenchymal stem cells modulate B-cell functions. *Blood* **107**, 367-372 (2006).

269 Rafei, M., Hsieh, J., Fortier, S., Li, M., Yuan, S., Birman, E., Forner, K., Boivin, M. N., Doody, K., Tremblay, M., Annabi, B. & Galipeau, J. Mesenchymal stromal cell-derived CCL2 suppresses plasma cell immunoglobulin production via STAT3 inactivation and PAX5 induction. *Blood* **112**, 4991-4998 (2008).

270 Youd, M., Blickarz, C., Woodworth, L., Touzjian, T., Edling, A., Tedstone, J., Ruzek, M., Tubo, R., Kaplan, J. & Lodie, T. Allogeneic mesenchymal stem cells do not protect NZB × NZW F1 mice from developing lupus disease. *Clinical & Experimental Immunology* **161**, 176-186 (2010).

271 Rasmusson, I., Le Blanc, K., Sundberg, B. & Ringden, O. Mesenchymal stem cells stimulate antibody secretion in human B cells. *Scand J Immunol* **65**, 336-343 (2007).

272 Tabera, S., Perez-Simon, J. A., Diez-Campelo, M., Sanchez-Abarca, L. I., Blanco, B., Lopez, A., Benito, A., Ocio, E., Sanchez-Guijo, F. M., Canizo, C. & San Miguel, J. F. The effect of mesenchymal stem cells on the viability, proliferation and differentiation of B-lymphocytes. *Haematologica* **93**, 1301-1309 (2008).

273 Asari, S., Itakura, S., Ferreri, K., Liu, C. P., Kuroda, Y., Kandeel, F. & Mullen, Y. Mesenchymal stem cells suppress B-cell terminal differentiation. *Experimental hematology* **37**, 604-615 (2009).

274 Choi, E. W., Shin, I. S., Park, S. Y., Park, J. H., Kim, J. S., Yoon, E. J., Kang, S. K., Ra, J. C. & Hong, S. H. Reversal of serologic, immunologic, and histologic dysfunction in mice with systemic lupus erythematosus by long-term serial adipose tissue-derived mesenchymal stem cell transplantation. *Arthritis and rheumatism* **64**, 243-253 (2012).

275 Zhou, K., Zhang, H., Jin, O., Feng, X., Yao, G., Hou, Y. & Sun, L. Transplantation of human bone marrow mesenchymal stem cell ameliorates the autoimmune pathogenesis in MRL/lpr mice. *Cellular & molecular immunology* **5**, 417-424 (2008).

276 Ge, W., Jiang, J., Baroja, M. L., Arp, J., Zassoko, R., Liu, W., Bartholomew, A., Garcia, B. & Wang, H. Infusion of mesenchymal stem cells and rapamycin synergize to attenuate alloimmune responses and promote cardiac allograft tolerance. *Am J Transplant* **9**, 1760-1772 (2009).

277 Karussis, D., Karageorgiou, C., Vaknin-Dembinsky, A., Gowda-Kurkalli, B., Gomori, J. M., Kassis, I., Bulte, J. W., Petrou, P., Ben-Hur, T., Abramsky, O. & Slavin, S. Safety and immunological

effects of mesenchymal stem cell transplantation in patients with multiple sclerosis and amyotrophic lateral sclerosis. *Archives of neurology* **67**, 1187-1194 (2010).

278 Mohyeddin Bonab, M., Mohajeri, M., Sahraian, M. A., Yazdanifar, M., Aghsaie, A., Farazmand, A. & Nikbin, B. Evaluation of cytokines in multiple sclerosis patients treated with mesenchymal stem cells. *Archives of medical research* **44**, 266-272 (2013).

279 Yamout, B., Hourani, R., Salti, H., Barada, W., El-Hajj, T., Al-Kutoubi, A., Herlopian, A., Baz, E. K., Mahfouz, R., Khalil-Hamdan, R., Kreidieh, N. M., El-Sabban, M. & Bazarbachi, A. Bone marrow mesenchymal stem cell transplantation in patients with multiple sclerosis: a pilot study. *Journal of neuroimmunology* **227**, 185-189 (2010).

280 Connick, P., Kolappan, M., Crawley, C., Webber, D. J., Patani, R., Michell, A. W., Du, M. Q., Luan, S. L., Altmann, D. R., Thompson, A. J., Compston, A., Scott, M. A., Miller, D. H. & Chandran, S. Autologous mesenchymal stem cells for the treatment of secondary progressive multiple sclerosis: an open-label phase 2a proof-of-concept study. *Lancet neurology* **11**, 150-156 (2012).

281 Liang, J., Zhang, H., Hua, B., Wang, H., Wang, J., Han, Z. & Sun, L. Allogeneic mesenchymal stem cells transplantation in treatment of multiple sclerosis. *Multiple sclerosis (Houndmills, Basingstoke, England)* **15**, 644-646 (2009).

282 Lublin, F. D., Bowen, J. D., Huddlestone, J., Kremenchutzky, M., Carpenter, A., Corboy, J. R., Freedman, M. S., Krupp, L., Paulo, C., Hariri, R. J. & Fischkoff, S. A. Human placenta-derived cells (PDA-001) for the treatment of adults with multiple sclerosis: A randomized, placebo-controlled, multiple-dose study. *Mult Scler Relat Disord* **3**, 696-704 (2014).

283 Mohajeri, M., Farazmand, A., Mohyeddin Bonab, M., Nikbin, B. & Minagar, A. FOXP3 gene expression in multiple sclerosis patients pre- and post mesenchymal stem cell therapy. *Iranian journal of allergy, asthma, and immunology* **10**, 155-161 (2011).

284 Marin-Banasco, C., Benabdellah, K., Melero-Jerez, C., Oliver, B., Pinto-Medel, M. J., Hurtado-Guerrero, I., de Castro, F., Clemente, D., Fernandez, O., Martin, F., Leyva, L. & Suardiaz, M. Gene therapy with mesenchymal stem cells expressing IFN-ss ameliorates neuroinflammation in experimental models of multiple sclerosis. *Br J Pharmacol* **174**, 238-253 (2017).

285 Zhang, X., Huang, W., Chen, X., Lian, Y., Wang, J., Cai, C., Huang, L., Wang, T., Ren, J. & Xiang, A. P. CXCR5-Overexpressing Mesenchymal Stromal Cells Exhibit Enhanced Homing and Can Decrease Contact Hypersensitivity. *Molecular therapy : the journal of the American Society of Gene Therapy* **25**, 1434-1447 (2017).

286 Ma, T., Luan, S.-L., Huang, H., Sun, X.-K., Yang, Y.-M., Zhang, H., Han, W.-d., Li, H. & Han, Y. Upregulation of CC Chemokine Receptor 7 (CCR7) Enables Migration of Xenogeneic Human Adipose-Derived Mesenchymal Stem Cells to Rat Secondary Lymphoid Organs. *Medical Science Monitor : International Medical Journal of Experimental and Clinical Research* **22**, 5206-5217 (2016).

287 Lee, H. J., Kim, S. N., Jeon, M. S., Yi, T. & Song, S. U. ICOSL expression in human bone marrow-derived mesenchymal stem cells promotes induction of regulatory T cells. *Scientific reports* **7**, 44486 (2017).

288 Tang, J., Yang, R., Lv, L., Yao, A., Pu, L., Yin, A., Li, X., Yu, Y., Nyberg, S. L. & Wang, X. Transforming growth factor-beta-Expressing Mesenchymal Stem Cells Induce Local Tolerance in a Rat Liver Transplantation Model of Acute Rejection. *Stem cells (Dayton, Ohio)* **34**, 2681-2692 (2016).

289 Kim, J. Y., Kim, D. H., Kim, J. H., Lee, D., Jeon, H. B., Kwon, S. J., Kim, S. M., Yoo, Y. J., Lee, E. H., Choi, S. J., Seo, S. W., Lee, J. I., Na, D. L., Yang, Y. S., Oh, W. & Chang, J. W. Soluble intracellular adhesion molecule-1 secreted by human umbilical cord blood-derived mesenchymal stem cell reduces amyloid-beta plaques. *Cell death and differentiation* **19**, 680-691 (2012).

290 Wang, Z., Yao, W., Deng, Q., Zhang, X. & Zhang, J. Protective effects of BDNF overexpression bone marrow stromal cell transplantation in rat models of traumatic brain injury. *Journal of molecular neuroscience : MN* **49**, 409-416 (2013).

291 Jeong, C. H., Kim, S. M., Lim, J. Y., Ryu, C. H., Jun, J. A. & Jeun, S. S. Mesenchymal stem cells expressing brain-derived neurotrophic factor enhance endogenous neurogenesis in an ischemic stroke model. *Biomed Res Int* **2014**, 129145 (2014).

292 Gransee, H. M., Zhan, W. Z., Sieck, G. C. & Mantilla, C. B. Localized delivery of brain-derived neurotrophic factor-expressing mesenchymal stem cells enhances functional recovery following cervical spinal cord injury. *J Neurotrauma* **32**, 185-193 (2015).

293 Pollock, K., Dahlenburg, H., Nelson, H., Fink, K. D., Cary, W., Hendrix, K., Annett, G., Torrest, A., Deng, P., Gutierrez, J., Nacey, C., Pepper, K., Kalomoiris, S., Anderson, J. D., McGee, J., Gruenloh, W., Fury, B., Bauer, G., Duffy, A., Tempkin, T., Wheelock, V. & Nolta, J. A. Human Mesenchymal Stem Cells Genetically Engineered to Overexpress Brain-derived Neurotrophic Factor Improve Outcomes in Huntington's Disease Mouse Models. *Molecular therapy : the journal of the American Society of Gene Therapy* **24**, 965-977 (2016).

294 Uchida, S., Hayakawa, K., Ogata, T., Tanaka, S., Kataoka, K. & Itaka, K. Treatment of spinal cord injury by an advanced cell transplantation technology using brain-derived neurotrophic factor-transfected mesenchymal stem cell spheroids. *Biomaterials* **109**, 1-11 (2016).

295 Lee, S. H., Kim, Y., Rhew, D., Kim, A., Jo, K. R., Yoon, Y., Choi, K. U., Jung, T., Kim, W. H. & Kweon, O. K. Impact of local injection of brain-derived neurotrophic factor-expressing mesenchymal stromal cells (MSCs) combined with intravenous MSC delivery in a canine model of chronic spinal cord injury. *Cytotherapy* (2016).

296 Hei, W. H., Almansoori, A. A., Sung, M. A., Ju, K. W., Seo, N., Lee, S. H., Kim, B. J., Kim, S. M., Jahng, J. W., He, H. & Lee, J. H. Adenovirus vector-mediated ex vivo gene transfer of brain-derived neurotrophic factor (BDNF) tohuman umbilical cord blood-derived mesenchymal stem cells (UCB-MSCs) promotescrush-injured rat sciatic nerve regeneration. *Neurosci Lett* **643**, 111-120 (2017).

297 Zhang, L., Zhou, Y., Sun, X., Zhou, J. & Yang, P. CXCL12 overexpression promotes the angiogenesis potential of periodontal ligament stem cells. *Scientific reports* **7**, 10286 (2017).

298 Zhang, H., Kot, A., Lay, Y. E., Fierro, F. A., Chen, H., Lane, N. E. & Yao, W. Acceleration of Fracture Healing by Overexpression of Basic Fibroblast Growth Factor in the Mesenchymal Stromal Cells. *Stem cells translational medicine* **6**, 1880-1893 (2017).

299 Gronthos, S., Mankani, M., Brahim, J., Robey, P. G. & Shi, S. Postnatal human dental pulp stem cells (DPSCs) in vitro and in vivo. *Proceedings of the National Academy of Sciences of the United States of America* **97**, 13625-13630 (2000).

300 Miletich, I. & Sharpe, P. T. Neural crest contribution to mammalian tooth formation. *Birth Defects Research Part C: Embryo Today: Reviews* **72**, 200-212 (2004).

301 Kaukua, N., Shahidi, M. K., Konstantinidou, C., Dyachuk, V., Kaucka, M., Furlan, A., An, Z., Wang, L., Hultman, I., Ährlund-Richter, L., Blom, H., Brismar, H., Lopes, N. A., Pachnis, V., Suter, U., Clevers, H., Thesleff, I., Sharpe, P., Ernfors, P., Fried, K. & Adameyko, I. Glial origin of mesenchymal stem cells in a tooth model system. *Nature* **513**, 551 (2014).

302 Pierdomenico, L., Bonsi, L., Calvitti, M., Rondelli, D., Arpinati, M., Chirumbolo, G., Becchetti, E., Marchionni, C., Alviano, F., Fossati, V., Staffolani, N., Franchina, M., Grossi, A. & Bagnara, G. P. Multipotent mesenchymal stem cells with immunosuppressive activity can be easily isolated from dental pulp. *Transplantation* **80**, 836-842 (2005).

303 Alge, D. L., Zhou, D., Adams, L. L., Wyss, B. K., Shadday, M. D., Woods, E. J., Gabriel Chu, T. M. & Goebel, W. S. Donor-matched comparison of dental pulp stem cells and bone marrow-derived mesenchymal stem cells in a rat model. *Journal of Tissue Engineering and Regenerative Medicine* **4**, 73-81 (2010).

304 Kumar, A., Kumar, V., Rattan, V., Jha, V. & Bhattacharyya, S. Secretome Cues Modulate the Neurogenic Potential of Bone Marrow and Dental Stem Cells. *Molecular Neurobiology*, 1-11 (2016).

305 Arthur, A., Rychkov, G., Shi, S., Koblar, S. A. & Gronthos, S. Adult human dental pulp stem cells differentiate toward functionally active neurons under appropriate environmental cues. *Stem cells (Dayton, Ohio)* **26**, 1787-1795 (2008).

306 Kanafi, M., Majumdar, D., Bhonde, R. & Datta, I. Midbrain Cues Dictate Differentiation of Human Dental Pulp Stem Cells Towards Functional Dopaminergic Neurons. *Journal of cellular physiology* (2014).

307 Chun, S. Y., Soker, S., Jang, Y. J., Kwon, T. G. & Yoo, E. S. Differentiation of Human Dental Pulp Stem Cells into Dopaminergic Neuron-like Cells in Vitro. *Journal of Korean medical science* **31**, 171-177 (2016).

308 Ganapathy, K., Datta, I. & Bhonde, R. Astrocyte-Like Cells Differentiated from Dental Pulp Stem Cells Protect Dopaminergic Neurons Against 6-Hydroxydopamine Toxicity. *Mol Neurobiol* **56**, 4395-4413 (2019).

309 Singh, M., Kakkar, A., Sharma, R., Kharbanda, O. P., Monga, N., Kumar, M., Chowdhary, S., Airan, B. & Mohanty, S. Synergistic Effect of BDNF and FGF2 in Efficient Generation of Functional Dopaminergic Neurons from human Mesenchymal Stem Cells. *Scientific reports* **7**, 10378 (2017).

310 Ullah, I., Subbarao, R. B., Kim, E.-J., Bharti, D., Jang, S.-J., Park, J.-S., Shivakumar, S. B., Lee, S.-L., Kang, D., Byun, J.-H., Park, B.-W. & Rho, G.-J. In vitro comparative analysis of human dental stem cells from a single donor and its neuronal differentiation potential evaluated by electrophysiology. *Life Sciences* **154**, 39-51 (2016).

311 Leong, W. K., Henshall, T. L., Arthur, A., Kremer, K. L., Lewis, M. D., Helps, S. C., Field, J., Hamilton-Bruce, M. A., Warming, S., Manavis, J., Vink, R., Gronthos, S. & Koblar, S. A. Human adult dental pulp stem cells enhance poststroke functional recovery through non-neural replacement mechanisms. *Stem cells translational medicine* **1**, 177-187 (2012).

312 Arthur, A., Shi, S., Zannettino, A. C., Fujii, N., Gronthos, S. & Koblar, S. A. Implanted adult human dental pulp stem cells induce endogenous axon guidance. *Stem cells (Dayton, Ohio)* **27**, 2229-2237 (2009).

313 Zhao, Y., Wang, L., Jin, Y. & Shi, S. Fas ligand regulates the immunomodulatory properties of dental pulp stem cells. *Journal of dental research* **91**, 948-954 (2012).

314 Yi, Q., Liu, O., Yan, F., Lin, X., Diao, S., Wang, L., Jin, L., Wang, S., Lu, Y. & Fan, Z. Analysis of Senescence-Related Differentiation Potentials and Gene Expression Profiles in Human Dental Pulp Stem Cells. *Cells Tissues Organs* **203**, 1-11 (2017).

315 Wu, W., Zhou, J., Xu, C. T., Zhang, J., Jin, Y. J. & Sun, G. L. Derivation and growth characteristics of dental pulp stem cells from patients of different ages. *Mol Med Rep* **12**, 5127-5134 (2015).

316 Spaggiari, G. M., Abdelrazik, H., Becchetti, F. & Moretta, L. MSCs inhibit monocyte-derived DC maturation and function by selectively interfering with the generation of immature DCs: central role of MSC-derived prostaglandin E2. *Blood* **113**, 6576-6583 (2009).

317 Francois, M., Romieu-Mourez, R., Li, M. & Galipeau, J. Human MSC suppression correlates with cytokine induction of indoleamine 2,3-dioxygenase and bystander M2 macrophage differentiation. *Molecular therapy : the journal of the American Society of Gene Therapy* **20**, 187-195 (2012).

318 Lee, R. H., Pulin, A. A., Seo, M. J., Kota, D. J., Ylostalo, J., Larson, B. L., Semprun-Prieto, L., Delafontaine, P. & Prockop, D. J. Intravenous hMSCs Improve Myocardial Infarction in Mice because Cells Embolized in Lung Are Activated to Secrete the Anti-inflammatory Protein TSG-6. *Cell stem cell* **5**, 54-63 (2009).

319 Jiang, X. X., Zhang, Y., Liu, B., Zhang, S. X., Wu, Y., Yu, X. D. & Mao, N. Human mesenchymal stem cells inhibit differentiation and function of monocyte-derived dendritic cells. *Blood* **105**, 4120-4126 (2005).

320 Bai, L., Lennon, D. P., Caplan, A. I., DeChant, A., Hecker, J., Kranso, J., Zaremba, A. & Miller, R. H. Hepatocyte growth factor mediates mesenchymal stem cell-induced recovery in multiple sclerosis models. *Nature neuroscience* **15**, 862-870 (2012).

321 Kemp, K., Gray, E., Mallam, E., Scolding, N. & Wilkins, A. Inflammatory cytokine induced regulation of superoxide dismutase 3 expression by human mesenchymal stem cells. *Stem cell reviews* **6**, 548-559 (2010).

322 Bonab, M. M., Sahraian, M. A., Aghsaie, A., Karvigh, S. A., Hosseinian, S. M., Nikbin, B., Lotfi, J., Khorramnia, S., Motamed, M. R., Togha, M., Harirchian, M. H., Moghadam, N. B., Alikhani, K., Yadegari, S., Jafarian, S. & Gheini, M. R. Autologous mesenchymal stem cell therapy in progressive multiple sclerosis: an open label study. *Current stem cell research & therapy* **7**, 407-414 (2012).

323 Mohyeddin Bonab, M., Yazdanbakhsh, S., Lotfi, J., Alimoghaddom, K., Talebian, F., Hooshmand, F., Ghavamzadeh, A. & Nikbin, B. Does mesenchymal stem cell therapy help multiple sclerosis patients? Report of a pilot study. *Iranian journal of immunology : IJI* **4**, 50-57 (2007).

324 Li, J. F., Zhang, D. J., Geng, T., Chen, L., Huang, H., Yin, H. L., Zhang, Y. Z., Lou, J. Y., Cao, B. & Wang, Y. L. The potential of human umbilical cord-derived mesenchymal stem cells as a novel cellular therapy for multiple sclerosis. *Cell transplantation* **23 Suppl 1**, S113-122 (2014).

325 Llufriu, S., Sepulveda, M., Blanco, Y., Marin, P., Moreno, B., Berenguer, J., Gabilondo, I., Martinez-Heras, E., Sola-Valls, N., Arnaiz, J. A., Andreu, E. J., Fernandez, B., Bullich, S., Sanchez-

Dalmau, B., Graus, F., Villoslada, P. & Saiz, A. Randomized placebo-controlled phase II trial of autologous mesenchymal stem cells in multiple sclerosis. *PloS one* **9**, e113936 (2014).

326 Wagner, W., Wein, F., Seckinger, A., Frankhauser, M., Wirkner, U., Krause, U., Blake, J., Schwager, C., Eckstein, V., Ansorge, W. & Ho, A. D. Comparative characteristics of mesenchymal stem cells from human bone marrow, adipose tissue, and umbilical cord blood. *Experimental hematology* **33**, 1402-1416 (2005).

327 Miao, Z., Jin, J., Chen, L., Zhu, J., Huang, W., Zhao, J., Qian, H. & Zhang, X. Isolation of mesenchymal stem cells from human placenta: Comparison with human bone marrow mesenchymal stem cells. *Cell Biology International* **30**, 681-687 (2006).

328 Bara, J. J., Richards, R. G., Alini, M. & Stoddart, M. J. Concise Review: Bone Marrow-Derived Mesenchymal Stem Cells Change Phenotype Following In Vitro Culture: Implications for Basic Research and the Clinic. *Stem cells (Dayton, Ohio)* **32**, 1713-1723 (2014).

329 Bruder, S. P., Jaiswal, N. & Haynesworth, S. E. Growth kinetics, self-renewal, and the osteogenic potential of purified human mesenchymal stem cells during extensive subcultivation and following cryopreservation. *Journal of cellular biochemistry* **64**, 278-294 (1997).

330 Bonab, M. M., Alimoghaddam, K., Talebian, F., Ghaffari, S. H., Ghavamzadeh, A. & Nikbin, B. Aging of mesenchymal stem cell in vitro. *BMC Cell Biol* **7**, 14 (2006).

331 Yang, Y.-H. K., Ogando, C. R., Wang See, C., Chang, T.-Y. & Barabino, G. A. Changes in phenotype and differentiation potential of human mesenchymal stem cells aging in vitro. *Stem cell research & therapy* **9**, 131 (2018).

332 Zaim, M., Karaman, S., Cetin, G. & Isik, S. Donor age and long-term culture affect differentiation and proliferation of human bone marrow mesenchymal stem cells. *Annals of Hematology* **91**, 1175-1186 (2012).

333 Kim, J., Kang, J. W., Park, J. H., Choi, Y., Choi, K. S., Park, K. D., Baek, D. H., Seong, S. K., Min, H.-K. & Kim, H. S. Biological characterization of long-term cultured human mesenchymal stem cells. *Archives of Pharmacal Research* **32**, 117-126 (2009).

334 Chen, Y., Langrish, C. L., McKenzie, B., Joyce-Shaikh, B., Stumhofer, J. S., McClanahan, T., Blumenschein, W., Churakovsa, T., Low, J., Presta, L., Hunter, C. A., Kastelein, R. A. & Cua, D. J. Anti–IL-23 therapy inhibits multiple inflammatory pathways and ameliorates autoimmune encephalomyelitis. *The Journal of clinical investigation* **116**, 1317-1326 (2006).

335 Yu, R. Y. & Gallagher, G. A naturally occurring, soluble antagonist of human IL-23 inhibits the development and in vitro function of human Th17 cells. *Journal of immunology (Baltimore, Md. : 1950)* **185**, 7302-7308 (2010).

336 Aggarwal, S., Ghilardi, N., Xie, M. H., de Sauvage, F. J. & Gurney, A. L. Interleukin-23 promotes a distinct CD4 T cell activation state characterized by the production of interleukin-17. *The Journal of biological chemistry* **278**, 1910-1914 (2003).

337 Liu, J., Yu, F., Sun, Y., Jiang, B., Zhang, W., Yang, J., Xu, G.-T., Liang, A. & Liu, S. Concise Reviews: Characteristics and Potential Applications of Human Dental Tissue-Derived Mesenchymal Stem Cells. *Stem cells (Dayton, Ohio)* **33**, 627-638 (2015).

338 Lan, X., Sun, Z., Chu, C., Boltze, J. & Li, S. Dental Pulp Stem Cells: An Attractive Alternative for Cell Therapy in Ischemic Stroke. *Front Neurol* **10**, 824 (2019).

339 Luo, L., He, Y., Wang, X., Key, B., Lee, B. H., Li, H. & Ye, Q. Potential Roles of Dental Pulp Stem Cells in Neural Regeneration and Repair. *Stem Cells Int* **2018**, 1731289 (2018).

340 Ketterl, N., Brachtl, G., Schuh, C., Bieback, K., Schallmoser, K., Reinisch, A. & Strunk, D. A robust potency assay highlights significant donor variation of human mesenchymal stem/progenitor cell immune modulatory capacity and extended radio-resistance. *Stem cell research & therapy* **6**, 236-236 (2015).

341 Payne, N. L., Dantanarayana, A., Sun, G., Moussa, L., Caine, S., McDonald, C., Herszfeld, D., Bernard, C. C. & Siatskas, C. Early intervention with gene-modified mesenchymal stem cells overexpressing interleukin-4 enhances anti-inflammatory responses and functional recovery in experimental autoimmune demyelination. *Cell adhesion & migration* **6**, 179-189 (2012).

342 Payne, N. L., Sun, G., McDonald, C., Layton, D., Moussa, L., Emerson-Webber, A., Veron, N., Siatskas, C., Herszfeld, D., Price, J. & Bernard, C. C. Distinct immunomodulatory and migratory

mechanisms underpin the therapeutic potential of human mesenchymal stem cells in autoimmune demyelination. *Cell transplantation* **22**, 1409-1425 (2013).

343 Perry, V. H. & Holmes, C. Microglial priming in neurodegenerative disease. *Nature Reviews Neurology* **10**, 217 (2014).

344 Sinha, S., Boyden, A. W., Itani, F. R., Crawford, M. P. & Karandikar, N. J. CD8(+) T-Cells as Immune Regulators of Multiple Sclerosis. *Frontiers in immunology* **6**, 619 (2015).

345 Salou, M., Nicol, B., Garcia, A. & Laplaud, D.-A. Involvement of CD8+ T Cells in Multiple Sclerosis. *Frontiers in immunology* **6** (2015).

346 Ong, W. K. & Sugii, S. Adipose-derived stem cells: Fatty potentials for therapy. *The International Journal of Biochemistry & Cell Biology* **45**, 1083-1086 (2013).

347 Cao, W., Yang, Y., Wang, Z., Liu, A., Fang, L., Wu, F., Hong, J., Shi, Y., Leung, S., Dong, C. & Zhang, J. Z. Leukemia inhibitory factor inhibits T helper 17 cell differentiation and confers treatment effects of neural progenitor cell therapy in autoimmune disease. *Immunity* **35**, 273-284 (2011).

348 Mor, F., Quintana, F. J. & Cohen, I. R. Angiogenesis-Inflammation Cross-Talk: Vascular Endothelial Growth Factor Is Secreted by Activated T Cells and Induces Th1 Polarization. *The Journal of Immunology* **172**, 4618-4623 (2004).

349 Gavalas, N. G., Tsiatas, M., Tsitsilonis, O., Politi, E., Ioannou, K., Ziogas, A. C., Rodolakis, A., Vlahos, G., Thomakos, N., Haidopoulos, D., Terpos, E., Antsaklis, A., Dimopoulos, M. A. & Bamias, A. VEGF directly suppresses activation of T cells from ascites secondary to ovarian cancer via VEGF receptor type 2. *British Journal Of Cancer* **107**, 1869 (2012).

350 Macrin, D., Alghadeer, A., Zhao, Y. T., Miklas, J. W., Hussein, A. M., Detraux, D., Robitaille, A. M., Madan, A., Moon, R. T., Wang, Y., Devi, A., Mathieu, J. & Ruohola-Baker, H. Metabolism as an early predictor of DPSCs aging. *Scientific reports* **9**, 2195 (2019).

351 Alraies, A., Alaidaroos, N. Y., Waddington, R. J., Moseley, R. & Sloan, A. J. Variation in human dental pulp stem cell ageing profiles reflect contrasting proliferative and regenerative capabilities. *BMC Cell Biol* **18**, 12 (2017).

352 Yang, C., Li, X., Sun, L., Guo, W. & Tian, W. Potential of human dental stem cells in repairing the complete transection of rat spinal cord. *Journal of neural engineering* **14**, 026005 (2017).

353 Mead, B., Hill, L. J., Blanch, R. J., Ward, K., Logan, A., Berry, M., Leadbeater, W. & Scheven, B. A. Mesenchymal stromal cell–mediated neuroprotection and functional preservation of retinal ganglion cells in a rodent model of glaucoma. *Cytotherapy* **18**, 487-496 (2016).

354 Hung, C.-N., Mar, K., Chang, H.-C., Chiang, Y.-L., Hu, H.-Y., Lai, C.-C., Chu, R.-M. & Ma, C. M. A comparison between adipose tissue and dental pulp as sources of MSCs for tooth regeneration. *Biomaterials* **32**, 6995-7005 (2011).

355 Gandia, C., Armiñan, A., García-Verdugo, J. M., Lledó, E., Ruiz, A., Miñana, M. D., Sanchez-Torrijos, J., Payá, R., Mirabet, V., Carbonell-Uberos, F., Llop, M., Montero, J. A. & Sepúlveda, P. Human Dental Pulp Stem Cells Improve Left Ventricular Function, Induce Angiogenesis, and Reduce Infarct Size in Rats with Acute Myocardial Infarction. *Stem cells (Dayton, Ohio)* **26**, 638-645 (2008).

356 Guo, Y., Chan, K. H., Lai, W. H., Siu, C. W., Kwan, S. C., Tse, H. F., Wing-Lok Ho, P. & Wing-Man Ho, J. Human mesenchymal stem cells upregulate CD1dCD5(+) regulatory B cells in experimental autoimmune encephalomyelitis. *Neuroimmunomodulation* **20**, 294-303 (2013).

357 Kassis, I., Petrou, P., Halimi, M. & Karussis, D. Mesenchymal stem cells (MSC) derived from mice with experimental autoimmune encephalomyelitis (EAE) suppress EAE and have similar biological properties with MSC from healthy donors. *Immunol Lett* **154**, 70-76 (2013).

358 Jo, Y.-Y., Lee, H.-J., Kook, S.-Y., Choung, H.-W., Park, J.-Y., Chung, J.-H., Choung, Y.-H., Kim, E.-S., Yang, H.-C. & Choung, P.-H. Isolation and Characterization of Postnatal Stem Cells from Human Dental Tissues. *Tissue engineering* **13**, 767-773 (2007).

359 Constantin, G., Marconi, S., Rossi, B., Angiari, S., Calderan, L., Anghileri, E., Gini, B., Bach, S. D., Martinello, M., Bifari, F., Galie, M., Turano, E., Budui, S., Sbarbati, A., Krampera, M. & Bonetti, B. Adipose-derived mesenchymal stem cells ameliorate chronic experimental autoimmune encephalomyelitis. *Stem cells (Dayton, Ohio)* **27**, 2624-2635 (2009).

360 Rossato, C., Brandao, W. N., Castro, S. B. R., de Almeida, D. C., Maranduba, C. M. C., Camara, N. O. S., Peron, J. P. S. & Silva, F. S. Stem cells from human-exfoliated deciduous teeth reduce tissue-

infiltrating inflammatory cells improving clinical signs in experimental autoimmune encephalomyelitis. *Biologicals* **49**, 62-68 (2017).

361 Shimojima, C., Takeuchi, H., Jin, S., Parajuli, B., Hattori, H., Suzumura, A., Hibi, H., Ueda, M. & Yamamoto, A. Conditioned Medium from the Stem Cells of Human Exfoliated Deciduous Teeth Ameliorates Experimental Autoimmune Encephalomyelitis. *Journal of immunology (Baltimore, Md. : 1950)* **196**, 4164-4171 (2016).

362 Kolar, M. K., Itte, V. N., Kingham, P. J., Novikov, L. N., Wiberg, M. & Kelk, P. The neurotrophic effects of different human dental mesenchymal stem cells. *Scientific reports* **7**, 12605 (2017).

363 Hiremath, M. M., Chen, V. S., Suzuki, K., Ting, J. P. Y. & Matsushima, G. K. MHC class II exacerbates demyelination in vivo independently of T cells. *Journal of neuroimmunology* **203**, 23-32 (2008).

364 Kellner, M., Steindorff, M. M., Strempel, J. F., Winkel, A., Kuhnel, M. P. & Stiesch, M. Differences of isolated dental stem cells dependent on donor age and consequences for autologous tooth replacement. *Archives of oral biology* **59**, 559-567 (2014).

365 Crisostomo, P. R., Wang, M., Wairiuko, G. M., Morrell, E. D., Terrell, A. M., Seshadri, P., Nam, U. H. & Meldrum, D. R. High passage number of stem cells adversely affects setm cell activation and myocardial protection. *Shock* **26**, 575-580 (2006).

366 Salkin, H., Gonen, Z. B., Ergen, E., Bahar, D. & Cetin, M. Effects of TGF-beta1 Overexpression on Biological Characteristics of Human Dental Pulp-derived Mesenchymal Stromal Cells. *Int J Stem Cells* **12**, 170-182 (2019).

367 Rani, S., Ryan, A. E., Griffin, M. D. & Ritter, T. Mesenchymal Stem Cell-derived Extracellular Vesicles: Toward Cell-free Therapeutic Applications. *Molecular Therapy* **23**, 812-823 (2015).

368 Sheng, W., Yang, F., Zhou, Y., Yang, H., Low, P. Y., Kemeny, D. M., Tan, P., Moh, A., Kaplan, M. H., Zhang, Y. & Fu, X. Y. STAT5 programs a distinct subset of GM-CSF-producing T helper cells that is essential for autoimmune neuroinflammation. *Cell research* **24**, 1387-1402 (2014).

369 Stephens, L. A., Gray, D. & Anderton, S. M. CD4⁺CD25⁺ regulatory T cells limit the risk of autoimmune disease arising from T cell receptor crossreactivity. *Proceedings of the National Academy of Sciences of the United States of America* **102**, 17418-17423 (2005).

370 Ohshima, M., Yamahara, K., Ishikane, S., Harada, K., Tsuda, H., Otani, K., Taguchi, A., Miyazato, M., Katsuragi, S., Yoshimatsu, J., Kodama, M., Kangawa, K. & Ikeda, T. Systemic transplantation of allogenic fetal membrane-derived mesenchymal stem cells suppresses Th1 and Th17 T cell responses in experimental autoimmune myocarditis. *Journal of Molecular and Cellular Cardiology* **53**, 420-428 (2012).

371 Chen, M., Su, W., Lin, X., Guo, Z., Wang, J., Zhang, Q., Brand, D., Ryffel, B., Huang, J., Liu, Z., He, X., Le, A. D. & Zheng, S. G. Adoptive Transfer of Human Gingiva-Derived Mesenchymal Stem Cells Ameliorates Collagen-Induced Arthritis via Suppression of Th1 and Th17 Cells and Enhancement of Regulatory T Cell Differentiation. *Arthritis & Rheumatism* **65**, 1181-1193 (2013).

372 Goodwin, M., Sueblinvong, V., Eisenhauer, P., Ziats, N. P., LeClair, L., Poynter, M. E., Steele, C., Rincon, M. & Weiss, D. J. Bone marrow-derived mesenchymal stromal cells inhibit Th2-mediated allergic airways inflammation in mice. *Stem cells (Dayton, Ohio)* **29**, 1137-1148 (2011).

373 Selleri, S., Dieng, M. M., Nicoletti, S., Louis, I., Beausejour, C., Le Deist, F. & Haddad, E. Cord-Blood-Derived Mesenchymal Stromal Cells Downmodulate CD4+ T-Cell Activation by Inducing IL-10-Producing Th1 Cells. *Stem cells and development* **22**, 1063-1075 (2012).

374 Qu, X., Liu, X., Cheng, K., Yang, R. & Zhao, R. C. H. Mesenchymal stem cells inhibit Th17 cell differentiation by IL-10 secretion. *Experimental hematology* **40**, 761-770 (2012).

375 Kessler, M., Hoffmann, K., Fritsche, K., Brinkmann, V., Mollenkopf, H.-J., Thieck, O., Teixeira da Costa, A. R., Braicu, E. I., Sehouli, J., Mangler, M., Berger, H. & Meyer, T. F. Chronic Chlamydia infection in human organoids increases stemness and promotes age-dependent CpG methylation. *Nature Communications* **10**, 1194 (2019).

376 Younis, A. J., Lerer-Serfaty, G., Stav, D., Sabbah, B., Shochat, T., Kessler-Icekson, G., Zahalka, M. A., Shachar-Goldenberg, M., Ben-Haroush, A., Fisch, B. & Abir, R. Extracellular-like matrices and leukaemia inhibitory factor for in vitro culture of human primordial follicles. *Reprod Fertil Dev* **29**, 1982-1994 (2017).

377 Glenn, J. D., Smith, M. D., Calabresi, P. A. & Whartenby, K. A. Mesenchymal stem cells differentially modulate effector CD8+ T cell subsets and exacerbate experimental autoimmune encephalomyelitis. *Stem cells (Dayton, Ohio)* (2014).

378 Peron, J. P., Jazedje, T., Brandao, W. N., Perin, P. M., Maluf, M., Evangelista, L. P., Halpern, S., Nisenbaum, M. G., Czeresnia, C. E., Zatz, M., Camara, N. O. & Rizzo, L. V. Human endometrial-derived mesenchymal stem cells suppress inflammation in the central nervous system of EAE mice. *Stem cell reviews* **8**, 940-952 (2012).

379 Cobo, M., Anderson, P., Benabdellah, K., Toscano, M. G., Munoz, P., Garcia-Perez, A., Gutierrez, I., Delgado, M. & Martin, F. Mesenchymal stem cells expressing vasoactive intestinal peptide ameliorate symptoms in a model of chronic multiple sclerosis. *Cell transplantation* **22**, 839-854 (2013).

380 Zhao, F., Zhang, Y. F., Liu, Y. G., Zhou, J. J., Li, Z. K., Wu, C. G. & Qi, H. W. Therapeutic Effects of Bone Marrow-Derived Mesenchymal Stem Cells Engraftment on Bleomycin-Induced Lung Injury in Rats. *Transplantation Proceedings* **40**, 1700-1705 (2008).

381 Tögel, F., Hu, Z., Weiss, K., Isaac, J., Lange, C. & Westenfelder, C. Administered mesenchymal stem cells protect against ischemic acute renal failure through differentiation-independent mechanisms. *American Journal of Physiology-Renal Physiology* **289**, F31-F42 (2005).

382 Ezquer, F., Ezquer, M., Contador, D., Ricca, M., Simon, V. & Conget, P. The Antidiabetic Effect of Mesenchymal Stem Cells Is Unrelated to Their Transdifferentiation Potential But to Their Capability to Restore Th1/Th2 Balance and to Modify the Pancreatic Microenvironment. *Stem cells (Dayton, Ohio)* **30**, 1664-1674 (2012).

383 Kraitchman, D. L., Tatsumi, M., Gilson, W. D., Ishimori, T., Kedziorek, D., Walczak, P., Segars, W. P., Chen, H. H., Fritzges, D., Izbudak, I., Young, R. G., Marcelino, M., Pittenger, M. F., Solaiyappan, M., Boston, R. C., Tsui, B. M., Wahl, R. L. & Bulte, J. W. Dynamic imaging of allogeneic mesenchymal stem cells trafficking to myocardial infarction. *Circulation* **112**, 1451-1461 (2005).

384 de Witte, S. F. H., Luk, F., Sierra Parraga, J. M., Gargesha, M., Merino, A., Korevaar, S. S., Shankar, A. S., O'Flynn, L., Elliman, S. J., Roy, D., Betjes, M. G. H., Newsome, P. N., Baan, C. C. & Hoogduijn, M. J. Immunomodulation By Therapeutic Mesenchymal Stromal Cells (MSC) Is Triggered Through Phagocytosis of MSC By Monocytic Cells. *Stem cells (Dayton, Ohio)* **36**, 602-615 (2018).

385 Beggs, K. J., Lyubimov, A., Borneman, J. N., Bartholomew, A., Moseley, A., Dodds, R., Archambault, M. P., Smith, A. K. & McIntosh, K. R. Immunologic consequences of multiple, high-dose administration of allogeneic mesenchymal stem cells to baboons. *Cell transplantation* **15**, 711-721 (2006).

386 Oliveira, R., #x00E9, Linhares, g., Chagastelles, P. C., Sesterheim, P., #x00ED, cia & Pranke, P. In Vivo Immunogenic Response to Allogeneic Mesenchymal Stem Cells and the Role of Preactivated Mesenchymal Stem Cells Cotransplanted with Allogeneic Islets. *Stem Cells International* **2017**, 12 (2017).

387 Nauta, A. J., Westerhuis, G., Kruisselbrink, A. B., Lurvink, E. G., Willemze, R. & Fibbe, W. E. Donor-derived mesenchymal stem cells are immunogenic in an allogeneic host and stimulate donor graft rejection in a nonmyeloablative setting. *Blood* **108**, 2114-2120 (2006).

388 Eliopoulos, N., Stagg, J., Lejeune, L., Pommey, S. & Galipeau, J. Allogeneic marrow stromal cells are immune rejected by MHC class I- and class II-mismatched recipient mice. *Blood* **106**, 4057-4065 (2005).

389 Najar, M., Fayyad-Kazan, M., Meuleman, N., Bron, D., Fayyad-Kazan, H. & Lagneaux, L. Immunological impact of Wharton's Jelly mesenchymal stromal cells and natural killer cell co-culture. *Mol Cell Biochem* (2018).

390 Schu, S., Nosov, M., O'Flynn, L., Shaw, G., Treacy, O., Barry, F., Murphy, M., O'Brien, T. & Ritter, T. Immunogenicity of allogeneic mesenchymal stem cells. *J Cell Mol Med* **16**, 2094-2103 (2012).

391 Franquesa, M., Herrero, E., Torras, J., Ripoll, E., Flaquer, M., Gomà, M., Lloberas, N., Anegon, I., Cruzado, J. M., Grinyó, J. M. & Herrero-Fresneda, I. Mesenchymal Stem Cell Therapy Prevents Interstitial Fibrosis and Tubular Atrophy in a Rat Kidney Allograft Model. *Stem cells and development* **21**, 3125-3135 (2012).